Anna Fankhauser, BSc

A data-driven statistical evaluation and characterization of in-situ measurements

MASTER'S THESIS

to achieve the university degree of

Diplomingenieur

submitted to

Graz University of Technology

Supervisors

Ass.Prof. Dipl.-Ing. Dr.techn. Franz Tschuchnigg

Univ.-Prof. Dipl.-Ing. Dr.techn. Roman Marte

Institute of Soil Mechanics, Foundation Engineering and Computational Geotechnics

Co-Supervisor

Dipl.-Ing. Simon Oberhollenzer

Graz, January 2020

Statutory declaration

I declare that I have authored this thesis independently, that I have not used other than the declared sources/resources, and that I have explicitly marked all material which has been quoted either literally or by content from the used sources. The text document uploaded to TUGRAZonline is identical to the present master's thesis.

…… date

…… signature

Abstract

In the course of this master's thesis, given data of penetration tests (CPT, CPTu, SCPT, DMT and SDMT) performed in Austria is investigated and evaluated by means of different aspects. In-situ measured test data as the tip resistance, the sleeve friction, the friction ratio and the shear wave velocity are plotted over depth. Hereby statements can be made regarding local differences within Austria, especially within the basin of Salzburg, the basin of Zell and the region of Flachgau. A comparison of the in-situ measured values was also performed based on the grain-size distribution. Therefore, the information of over 200 core drillings served as a base for a division into six soil groups with respect to the grain size. Furthermore, these six soil groups were used for data presentation by means of box-plots and violin- plots. As a last step, the penetration test data was investigated with the help of soil behaviour type charts according to Robertson (2009) and Robertson (2016). In addition to that, a method after Robertson (2016) was used for the detection of possible microstructure. In all investigations, special attention was paid to silt-dominated soils, as these often prove to be problematic in Austria. Silt-dominated soils show the occurrence of partial drainage and microstructure, two effects that can both influence the mechanical behaviour of soil and therefore still need to be further investigated.

Kurzfassung

Im Zuge dieser Masterarbeit werden die vorliegenden Daten von in Österreich durchgeführten Penetrationstests (CPT, CPTu, SCPT, DMT und SDMT) analysiert und unter verschiedenen Aspekten ausgewertet. In-situ Messwerte wie der Spitzenwiderstand, die Mantelreibung, das Reibungsverhältnis und die Scherwellengeschwindigkeit werden über die Tiefe dargestellt. Dadurch können Aussagen über lokale Unterschiede innerhalb Österreichs, insbesondere im Salzburger Becken, im Zeller Becken und im Flachgau getroffen werden. Ebenfalls wird ein Vergleich der in-situ-Messwerte anhand der Korngrößenverteilung durchgeführt. Es werden Auswertungen von mehr als 200 Kernbohrungen herangezogen, um eine Einteilung der unterschiedlichen Bodenansprachen in sechs Bodengruppen vorzunehmen. In weiterer Folge werden diese sechs Bodengruppen verwendet, um die in-situ Messwerte mittels Box-Plot und Violin-Plot darzustellen. In einem letzten Schritt werden die Daten der Drucksondierungen mit Hilfe von Bodenverhaltensdiagrammen nach Robertson (2009), Robertson (2016) und Schneider (2008) analysiert. Darüber hinaus wird eine Methode nach Robertson (2016) zur Detektion von Mikrostruktur betrachtet und diskutiert. Bei allen Untersuchungen wird besonderes Augenmerk auf Schluff-dominierte Böden gelegt, da sich diese in Österreich oft als problematisch erweisen. Diese Schluff-dominierten Böden zeigen das Auftreten von Teildrainage und Mikrostruktur, zwei Effekte, die das mechanische Verhalten des Bodens beeinflussen können und daher in weiterer Folge noch intensiver erforscht werden müssen.

Acknowledgement

At first, I would like to express my sincere gratitude to all those who have contributed to the success of this thesis.

In particular I want to thank Prof. Franz Tschuchnigg for giving me the opportunity to write a master's thesis at the Institute of Soil Mechanics, Foundation Engineering and Computational Geotechnics. I am grateful for your guidance and support, especially when we reached the point where this thesis went into a slightly different direction.

A big thank you also to Prof. Roman Marte, whose input was a substantial enrichment for this thesis. I would also like to thank Dipl.-Ing. Georg Erharter for giving me useful programming advice.

However, the greatest thanks go to my co-supervisor Dipl.-Ing. Simon Oberhollenzer. I greatly appreciate our good collaboration and your exceptional support. You were always there with advice, no matter if I had technical, organizational or personal questions. Thank you for taking so much time for all the meetings we had and emails we wrote. Grazie di tutto, Simon!

I also want to thank my friends and two families who are the greatest enrichment in my life and make it full of joy and happiness. I must especially emphasize my parents, who have always been very supportive of my education. To quote Johann Wolfgang von Goethe, they have given me both on my path of life: roots and wings.

Finally, my deepest heartfelt appreciation goes to my husband Nikolaus. I am so thankful for your support, your encouragement and your positive words, not only during the time of my studies and the months of writing this thesis, but throughout the whole time we've been together. Without you, I wouldn't be standing where I am today!

Contents

List of Figures

List of Tables

1 Introduction

This chapter of the master's thesis intends to give the reader a better understanding of the topic. The problem of in-situ ground investigations in fine-grained sediments is shortly introduced, the aim of this thesis is explained, and an overview of the thesis' structure is given.

1.1 Motivation

Performing a statistical evaluation and characterization of in-situ measurements aims a better understanding of the use and application of penetration tests, in the case of this master's thesis with special regard to fine-grained sediments. Geotechnical engineers in Austria often have to deal with postglacial sedimented soils, especially in basins that are mostly located within valleys of the Alps. These basins formed about 10'000 years ago. Through the progressive melting of the former glaciers, huge amounts of water were trapped within those basins and large lakes developed. Fine sediments filled the basins over thousands of years and settled to ground, causing thick layers of those sediments. From a geological point of view, these soils are declared as young, generally normally or slightly under consolidated. This under-consolidation can be explained by the still incomplete consolidation process of the sediments, i.e. there are still very small ongoing settlement processes happening in these fine sedimented soils. A well-known example is the city of Salzburg with its delicate soil, the so called "Salzburger Seeton". Postglacial sedimented soils, such as the Salzburger Seeton, generally are fine-grained soft soils that show a shallow ground water table and low stiffness and strength properties. These characteristics tend to be very challenging when it comes to foundation and construction works. For numerous projects, those soils have caused time delays and have led to highly (often unforeseen) increased costs due to necessary ground improvements. Especially in the city of Salzburg, the soft subsoil conditions within the basin of Salzburg are responsible for settlements of one to two millimetres of the whole city every year. This can be especially observed when it comes to differential settlements that cause cracks in facades and walls, as parts of the buildings are founded on stable rocks, whereas other parts are standing on the soft Salzburger Seeton (as shown in Fig. 1). (Oberhollenzer, et al., 2020), (derStandard, 2018)

Fig. 1: Salzburger Seeton (iCgroup, 2020)

In order to avoid expensive remediation works, thorough planning needs to be done upfront in which careful and comprehensive soil investigations are an essential part. Robertson (2009) claims that depending on the geotechnical risk, different types of soil investigations are necessary. For low-risk projects, simple cone penetration tests in combination with simple conservative design criteria are often sufficient, while for medium-risk projects the above should be supplemented with the measurement of seismic shear waves and porewater pressures (SCPTu). For high-risk projects, cone penetration tests can help with the identification of critical soil stratigraphy where core drillings and high-quality soil sampling should be performed, followed by advanced laboratory testing. Over the past 40 years the cone penetration test has gained popularity because of its advantages over traditional methods. It is fast, repeatable and economical. In addition to that, near continuous data over depth is provided. This has led to a steady increase in the use of the CPT with a continuous development of different correlations for parameter determination and soil type classification. (Robertson, 2010)

Correlations that have been developed so far for the derivation of soil parameters from CPT-data, provide satisfactory results for sands and clays, i.e. soils with either drained or undrained behaviour, respectively. However, silt-dominated soils, that occur in Austrian's postglacial sedimented soils, show partially drained conditions. In addition to that, it was observed that such soils often show unexpected low settlements under static loading on shallow foundations while sudden high settlements occur when it comes to deep foundations or soil improvement works. This different mechanical behaviour of fine-sedimented soils may be explained by the presence of microstructural bonds which are acting in between soil particles and increase the stiffness and strength properties of the soil. They can be caused by different factors such as secondary compression, thixotropy, cementation, cold welding or aging (Robertson, 2016). Compared to soils without microstructural bonds (unstructured soils), structured soils tend to have a higher yield stress and small strain stiffness, up to a certain point where the microstructural bonds suddenly fail due to large strains, weathering or large dynamic loads (i.e. soil improvements). (Robertson, 2016), (Oberhollenzer, et al., 2020)

Apparently, there is a great need for research on silt dominated soils to improve the characterization of those sensitive soils where results are influenced by effects of partial drainage and microstructure. Therefore, the research project PITS "Parameter identification by means of in-situ testing in silty soils" was started by the 'Austrian Chamber of Architects and chartered Engineering Consultants' in cooperation with the institutes of 'Soil Mechanics, Foundation Engineering and Computational Geotechnics' and 'Applied Geosciences' of Graz University of Technology. This master's thesis should serve as a first step to provide information about the evaluation and investigation of existing CPT data collected within Austria.

1.2 Aim

Based on the previous stated reasons, the aim of this thesis is to elaborate the following points:

- An overall comparison of in-situ tests in Austria
- A statistical comparison of in-situ measurements for different basins and valleys within Austria
- The detection of regional differences and heterogeneities within the basins and valleys
- A comparison of basins by means of "soil behaviour type charts" in combination with an evaluation of accuracy of the SBTn charts (especially for silt-dominated soils)
- Discussion of a method for the detection of possible microstructure

1.3 Structure of the thesis

Chapter 1: This chapter gives an introduction into the topic and the contents of each chapter are briefly listed.

Chapter 2: The most common types of in-situ tests are presented together with their procedure and outcome.

Chapter 3: A chronological overview of different approaches of soil classification systems based on cone penetration tests is given.

Chapter 4: The QGIS Database with its design and structure is presented in this section. Additionally, the data preparation and evaluation procedure are explained, the python codes are shortly introduced and the results of a first analysis of the database is presented.

Chapter 5: This chapter intends to refresh the knowledge of fundamental statistical terms that are needed for the chapters 6 and 7.

Chapter 6: Chapter 6 represents the core of this master's thesis. It deals with the comparison of in-situ measurements. Various representations are chosen to describe regional differences and thus heterogeneities within different basins. Secondly comparisons based on the grain size distributions are performed with the help of box-plots and violin-plots. Last but not least, different soil type distributions over depth are discussed.

Chapter 7: In this chapter the comparison of in-situ measurements is performed by means of soil behaviour type charts. Therefore, approaches according to Robertson (2009, 2016) and Schneider (2008) are used. A last important point is the detection of possible microstructure in fine sedimented soils.

Chapter 8: The last chapter summarizes the most important findings. A conclusion and possible measures for improvement are presented.

Appendices: Important additional information as well as a CD with the complete Python code is attached to the Appendix of this master's thesis.

2 In-situ testing

A careful investigation of the subsoil should be carried out before the beginning of any construction project. There are numerous forms of soil investigations that can be performed. Sampling and laboratory testing should also be included. However, the difficulty of an undisturbed soil sample recovery, not only of gravelly soils but also of fine-grained soft soils, complicates a correct determination of soil parameters in the laboratory as those tests are often carried out on disturbed samples. This is one of many more reasons why in-situ testing gets more and more popular in geotechnical engineering. In this chapter two of the most common in-situ investigation methods are shortly introduced: the cone penetration test and the flat dilatometer test.

2.1 Cone penetration test (CPT and CPTu)

The cone penetration test (CPT) is one of the most popular in-situ investigation methods. Its rapid, repeatable and continuous way of measuring data over depth makes it a very useful and cost-effective tool for soil profiling, site characterization and identification of present materials. Over the years, many different correlations have been developed to facilitate the determination of constitutive parameters based on the in-situ measurements. (Schnaid, 2009)

2.1.1 Equipment and procedure

A cone as it can be seen in Fig. 2, with the standard dimensions of a diameter of 35.7 mm and an apex angle of 60° is pushed under a constant rate of 20 ± 5 mm/s into the ground. Standardly, the cone has a cross-sectional area of 10 cm², but can reach up to 15 cm² when more robust cones with a higher-load pushing equipment are used. (Schnaid, 2009)

While penetrating the soil, continuous or recurrent measurements of the resistance to the penetration process are made. The total force that is acting on the cone, Q_c, is divided by the projected area of the cone, A_c, to determine the cone resistance q_c. The total force F_s, which is acting on the friction sleeve of the cone, is divided by the surface area of the friction sleeve, A_s, and represents the sleeve friction f_s. When performing a CPTu test, a piezocone with porous elements is used as a penetrometer. In this case, additionally to the tip resistance and the sleeve friction, pore water pressures can be measured either on the cone (u_1), behind the cone (u_2) or behind the friction sleeve (u_3). The three different positions of these pore pressure measurements can be seen in Fig. 2. (Lunne, et al., 1997)

There are three main groups of existing CPT systems:

- Mechanical cone penetrometers: measurement of the resistance of the cone on the surface through the mechanical transfer of resistance passed on by the rods.
- Electric cone penetrometers: measurement of tip resistance q_c and sleeve friction f_s directly at the cone via electrically instrumented load cells.
- Piezocone penetrometers: in addition to the electrical measurements of q_c and f_s, pore water pressures u, generated while driving, can be recorded. (Schnaid, 2009)

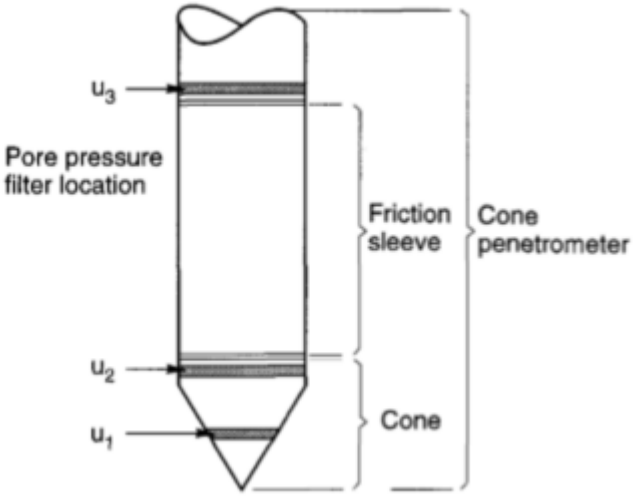

Fig. 2: Terminology for cone penetrometers (Lunne, et al., 1997)

There is a great variety of different pushing equipment. Generally hydraulic jacks are used to create the pressure for the penetration process. The cone penetration test shows a very wide range of its applicability. Off-shore rigs and drill ships make CPT testing even in near-shore but also in deep water conditions possible, facilitating the construction of e.g. structures for ports, oil and gas industry or wind turbines. For the on-shore application, trucks, rigs or caterpillars with weights from 10 to 20 t can build up the reaction system to the hydraulic jacks. As an illustration the in-situ testing truck from the company Geo-Pro is shown in Fig. 3. (Schnaid, 2009)

Fig. 3: Heavy-duty truck for in-situ testing from Geo-Pro

In Fig. 4 the typical interior of an in-situ testing truck is shown. The steel beam between the two vertical hydraulic jacks is, depending on the position of the hydraulic clamp, either pushing or pulling the driving rods by moving up and down. To achieve the recommended penetration rate of 20 ± 5 mm/s a flow rate valve is used as a control instrument. The driving steel rods have a length of 1m each. Consequently, the penetration process is interrupted at each meter as the next rod needs to be installed. (Schnaid, 2009)

Fig. 4: Interior of an in-situ testing truck

Lightweight rigs make it possible to perform the cone penetration test even in inaccessible and difficult locations. The main disadvantage is that the required reaction force cannot be achieved by weight of the installation. Therefore, back anchoring is necessary, which tends to be challenging when it comes to gravely or soft soils. (Schnaid, 2009)

2.1.2 Test results

In order to be able to compare results that are obtained with different equipment, a standardization of the test was implemented by the ISSMGE. Certain recommendations regarding dimensions of cones, procedures, inclination of rods etc. make the test results comparable. (Schnaid, 2009)

In the standard CPTu test, the tip resistance q_c, the sleeve friction f_s and the pore water pressure u are continuously measured over depth. Due to geometry of the cone, porewater pressures acting in between the joints of the penetrometer can affect the measured values of tip resistance. According to Campanella et al. (1982) this effect is often referred to as the unequal end-area effect. With the use of equal end-area friction sleeves, there is no need for correction of the sleeve friction f_s (Robertson, 2009). However, the unequal end-area effect is always present for the tip resistance q_c, which can be considered by introducing the corrected tip resistance q_t as follows: (Schnaid, 2009)

$$q_t = q_c + (1 - a)u_2 \tag{1}$$

where

q_t = cone resistance corrected for water effects
q_c = measured cone resistance
a = cone area ratio, typically around 0.8
u_2 = penetration pore pressure at shoulder of cone (Robertson, 2016)

For sands, q_c is relatively large compared to the pore pressure u_2 and hence, $q_c \sim q_t$. This means that the correction for coarse grained soils is of minor importance. However, for fine grained undrained soils the correction for pore water effects on the cone can be significant where q_c is relatively low compared to the high pore pressures u_2. (Robertson, 2009)

Two other important parameters for the classification of soil are the friction ratio R_f and the pore pressure ratio B_q: (Schnaid, 2009)

$$R_f = \frac{f_s}{q_c} * 100\ [\%] \tag{2}$$

$$B_q = \frac{(u_2 - u_0)}{q_t - \sigma_{v0}} * 100\ [\%] \tag{3}$$

where

B_q = pore pressure ratio
q_t = cone resistance corrected for water effects
u_2 = penetration pore water pressure at shoulder of cone

u_0 = in-situ pore water pressure
σ_{v0} = total vertical stress

More on the topic of soil classification using CPT-measurements will be presented in chapter 3.

2.2 Flat dilatometer test (DMT)

While the first tests with cone penetrometers were already performed in the 1930s (Lunne, et al., 1997), the DMT is a comparatively young testing method. Silviano Marchetti developed it in 1980, primarily to establish a reliable constrained modulus for the problem of laterally loaded piles. (Schnaid, 2009) The CPT test was criticized that its cone shaped probe would massively disturb the ground while penetrating. For this reason, Marchetti decided to develop a spade-shaped probe that would be pushed into the ground and disturb the soil less.

By performing a flat dilatometer test, a stainless-steel plate with a circular steel membrane in the middle of one side of the plate (see Fig. 5) is pushed into the ground at a constant rate. Hold is made at every 20 cm and a test is performed by inflating the membrane and taking pressure readings at specified displacements. (Schnaid, 2009)

2.2.1 Equipment and procedure

The dilatometer blade standardly has a width of 95 mm and a thickness of 15 mm. The cutting edge to penetrate the soil, ranges between 24° to 32°. The steel membrane has a diameter of 60 mm, is around 0.2 mm thick and is connected to the blade by a retaining ring fixed through 8 slotted screws. (Schnaid, 2009)

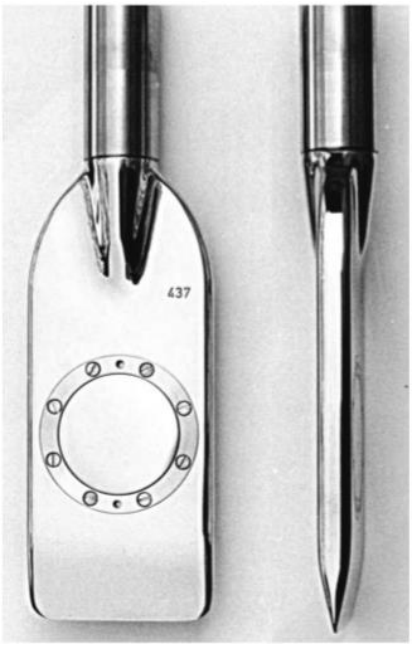

Fig. 5: Flat Dilatometer blade (Schnaid, 2009)

When performing the test, the blade is pushed into the ground at a constant rate (20 ± 5 mm/s). Every 20 cm the penetration procedure is interrupted for the following pressure readings:

- A-pressure: the membrane starts to expand.
- B-pressure: the centre of the membrane is pushed 1.1mm against the soil.
- C-pressure (optional): pressure of the deflating membrane. For drained soils this pressure can represent the pore water pressure u_0.

When performing this test, a continuous sound signal shows the operator when to take readings for pressure A and pressure B. At the beginning, the inner sensing disc in the blade is in contact with the steel membrane. As the membrane starts to expand, the electrical contact gets lost. As soon as the 1.1 mm of expansion are reached, the electrical contact is back again. This de- and reactivation of the sound signal marks the points for the A and B pressure readings respectively. Once the membrane is deflated again, the probe is pushed down for another 20 cm and the testing can be repeated. (Schnaid, 2009)

2.2.2 Test results

As the CPT test, the DMT test is not only characterized by the simplicity of its application, but also through the high reproducibility of its test results. To obtain correct test results, calibrations for the membrane stiffness are necessary before test execution, as this has a great influence on the soil parameters that are derived from the pressure results. Therefore, the two calibration factors ΔA and ΔB are established to correct the A-reading and B-reading respectively. With that, the pressures p_0 and p_1 can be calculated as follows:

$$p_0 = 1.05\ (A - Z_m + \Delta A) - 0.05(B - Z_m - \Delta B) \quad (4)$$

$$p_1 = B - Z_m - \Delta B \quad (5)$$

where *„Z_m is the gauge zero offset when vented to atmospheric pressure"*. (Schnaid, 2009) The p_0 pressure is related to the in-situ horizontal effective stress and therefore it represents an indication for the preconsolidation pressure. The difference between p_0 and p_1 is related to the soil compressibility. For detailed information reference is made to Schnaid (2009).

With existing correlations, these DMT parameters can later be related to soil types, soil unit weight, coefficient of earth pressure at rest (K_0), overconsolidation ratio (OCR), constrained modulus (M), undrained shear strength (s_u) and friction angle (φ'). Given the fact that those correlations are empirical, caution should be made when applying, as site-specific differences are inevitable. (Schnaid, 2009)

2.3 Seismic tests

An enhancement in in-situ testing presents the possibility of adding seismic measurements either to the cone penetration test or the flat dilatometer test. By simply adding geophones in the rods of the CPT or DMT, the seismic test has become a very fast and cost-effective way of measuring shear wave velocities in different depth intervals. Based on the shear wave velocity and the density of the soil, the small stain shear modulus G_0 can be calculated (see chapter 2.3.1). (Schnaid, 2009)

2.3.1 Procedure and results

The whole test procedure is graphically pictured in Fig. 7. In 0.5 m steps, the penetration process comes to hold and a seismic test is performed. Therefore, seismic waves are generated on the surface induced by hammer blows on a steel beam that is held to ground by the CPT truck or any other heavy weight (see Fig. 6).

Fig. 6: Hammer and steel beam for seismic test (geotechnik, 2013)

Above the CPT or DMT probe, two geophones in a distance of 0.5 m are installed. The shear wave velocity V_s can be determined by the two different arrival times of the shear wave at the geophones:

$$V_s = \frac{S_1 - S_2}{\Delta t} \tag{6}$$

where S_1 and S_2 are the distances between the geophones and the steel beam (see Fig. 7). Δt represents the time lag. Further on, the small strain shear modulus G_0 can be calculated by:

$$G_0 = \rho\,(V_s^{\,2}) \tag{7}$$

where ρ is the soil density and V_s the shear wave velocity. With the G_0, the seismic behaviour as well as the liquefaction potential of soils during earthquakes or any other dynamic loading can be determined. Additionally, Robertson (2016) developed a method for the detection of microstructure based on G_0. (Schnaid, 2009)

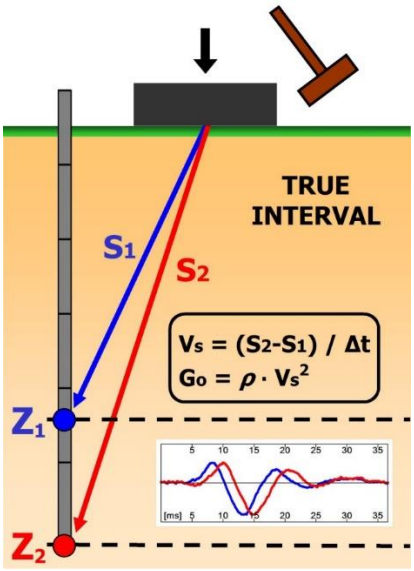

Fig. 7: Test procedure of seismic penetration tests (Marchetti, 2016)

2.4 Piezocone dissipation test

Dissipation tests can be carried out as part of penetration tests with the piezocone. The penetration is stopped at selected depths and the decay of penetration generated pore pressures (u_2) can be recorded with time.

In fine-grained, cohesive soils excessive pore water pressures are generated while in coarser grained, non-cohesive soils the measured pore water pressures correspond approximately to the hydrostatic in-situ water pressure conditions. With the knowledge of the pore water pressure distributions, the coefficients of consolidation C_v and C_h can be determined with the use of different other parameters like the dimensionless excess pore pressure dissipation U, the time for 50% dissipation $u_{50\%}$ or the dimensionless time factor for the consolidation process T*. In addition to that also permeability parameters K can be correlated. Dissipation tests as well as variable rate penetration tests can ease the interpretation of CPTu data when partial consolidation (i.e. partial drainage) occurs during the penetration process. (Schnaid, 2009)

3 Soil classification based on cone penetration tests

The in-situ measurements of cone penetration tests - the tip resistance and the sleeve friction - allow a classification of soil types. Generally, high tip resistances and high sleeve frictions classify coarse grained and rather stiff soils, whereas small tip resistances and sleeve frictions stand for fine grained, softer soils. With that knowledge, rather a determination of soil layer boundaries than an exact soil type classification is possible and a nearby core drilling is still inevitable to verify the different soil types. But there are several published methods which try to provide a solution to that shortcoming. They are presented chronologically in this section. Over time, the cones have developed progressively: from mechanical cones, over electrical cones to piezocones. Consequently, also the reliability of the soil type classification has improved. (Fellenius & Eslami, 2000)

3.1 Soil classification based on CPT measurements

3.1.1 Begemann (1965)

Begemann (1965) was the first who stated that soil profiling from CPT data is not either a function of the tip resistance q_c or the sleeve friction f_s, but a combination of the two. A first graph showing the relationship between q_c and f_s is shown in Fig. 8. The friction ratio R_f is the inclination of the fanned lines. (Fellenius & Eslami, 2000) (Begemann, 1965)

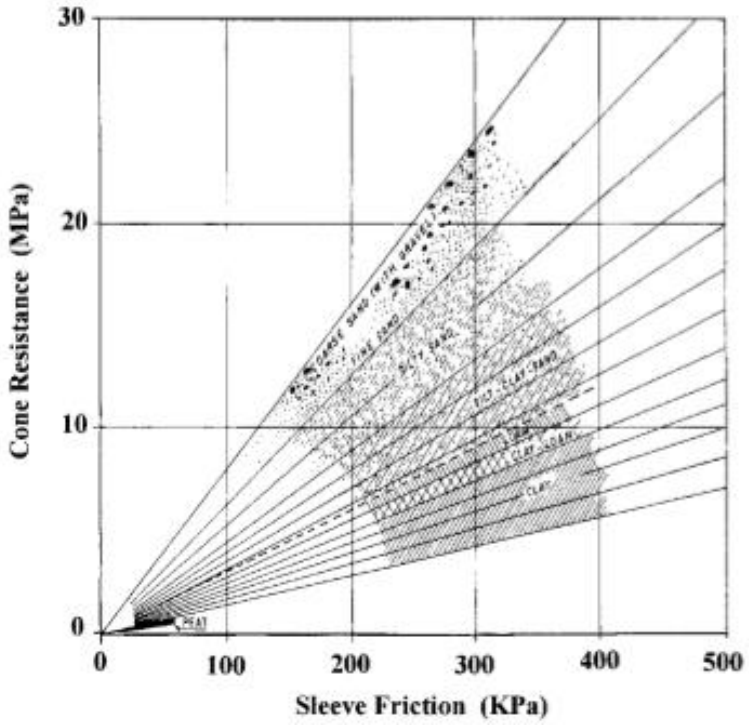

Fig. 8: Soil classification according to Begemann (1965)

According to Begemann (1965), each soil type is characterized by a range of the friction ratio R_f, presented in Tab. 1.

Tab. 1: Soil classification based on the friction ratio R_f, (Begemann, 1965)

Soil type as a function of friction ratio			
Coarse sand with gravel through fine sand	1.2 %	-	1.6 %
Silty sand	1.6 %	-	2.2 %
Silty sandy clayey soils	2.2 %	-	3.2 %
Clay and Loam, and loam soils	3.2 %	-	4.1 %
Clay	4.1 %	-	7.0 %
Peat	1.6 %	-	> 7 %

Begemann (1965) states that his chart is based on 250 CPT tests performed all over the Netherlands and is therefore only a site-specific approach for the characterization of soils in that area. However, the chart presents a first rough estimation of soil types. (Fellenius & Eslami, 2000) (Begemann, 1965)

3.1.2 Schmertmann (1978)

The soil profiling chart as Schmertmann (1978) proposed it, is shown in Fig. 9. This chart represents the correlation between soil type and CPT data, based on mechanical cone data performed in Florida. It incorporates CPT data from Begemann (1965), as similar soil types are present.

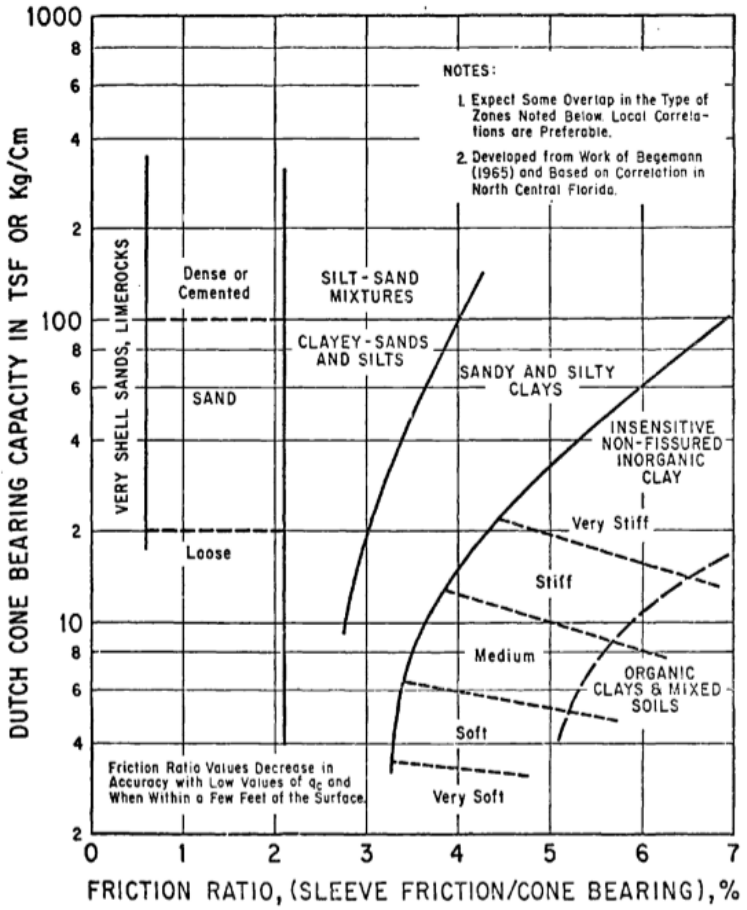

Fig. 9: Soil classification according to Schmertmann (1978)

Schmertmann (1978) notes that local correlation is needed for a correct interpretation of the chart when used elsewhere. It can be seen that the Schmertmann (1978) chart shows a plot of cone resistance q_c vs. friction ratio R_f, which means that the data is plotted against their inverse itself as q_c is contained in R_f. Fellenius & Eslami (2000) state, that caution should be made at these methods. (Fellenius & Eslami, 2000)

3.1.3 Douglas and Olsen (1981)

Douglas and Olsen (1981) were the first ones who developed a soil classification chart based on electrical cone penetrometer tests. The chart primarily shows three zones of different soil behaviour types: non-cohesive coarse-grained soils (sands), cohesive fine-grained soils (clays) and mixed soils. The chart also shows trends for the liquidity index, the earth pressure coefficient and the grain size.

When comparing this chart (Fig. 10) and the one after Schmertmann (1978) (Fig. 9), similar areas for sands and clays can be seen, although the soil type envelopes curve differently. (Fellenius & Eslami, 2000)

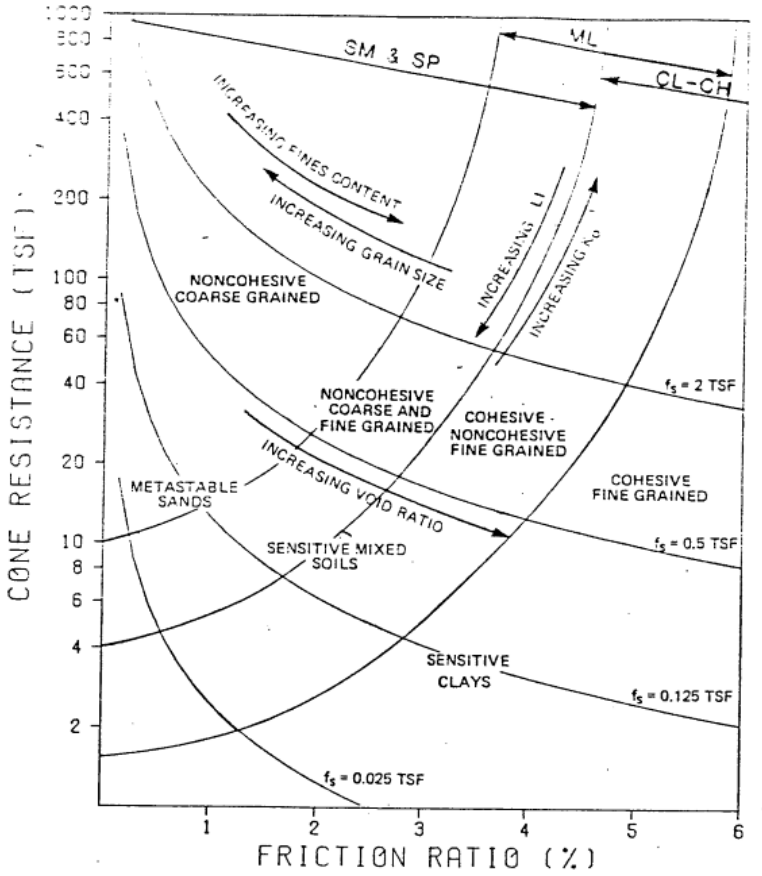

Fig. 10: Soil behaviour type chart according to Douglas and Olsen (1981)

3.2 Soil classification based on CPTu measurements

3.2.1 Eslami and Fellenius (1997)

In 1997, Eslami and Fellenius developed a soil classification chart while investigating pile design using cone penetration tests. Therefore, a database of CPT and CPTu data from 20 different sites in 5 different countries was organized. The test data was accompanied by results of borings, samplings and laboratory testing. CPT tests without pore water pressure measurements were performed in sandy soils. Hence, the assumption was made that the u_2 value for these tests is equal to the hydrostatic pore water pressure u_0. With that assumption Eslami and Fellenius (1997) developed five soil type groups as follows:

1. Sensitive and collapsible clay and/or silt
2. Clay and/or silt
3. Silty clay and/or clayey silt
4. Sandy silt and/or silty sand
5. Sand and/or sandy gravel (Fellenius & Eslami, 2000)

As it can be seen in Fig. 11, the profiling chart according to Eslami and Fellenius (1997) is based on the Begemann (1965) format, because on the x-axis the sleeve friction f_s is applied instead of the friction ratio R_f. Consequently, Eslami and

Fellenius (1997) did not to plot the tip resistance against its own inverse. On the y-axis an "effective" cone resistance is applied, which can be calculated as follows:

$$q_E = q_t - u_2 \tag{8}$$

where

q_t = cone resistance corrected for water effects Eq.*(1)*
u_2 = penetration pore pressure at shoulder of cone.

Robertson (1990) states that the pore water pressure is a function of where it is measured. It should be noted that q_E is not a measure of effective stress in the conventional sense. It is more an approximation to account for the generated excess pore water pressure. Such an approximation was not performed for the sleeve friction. According to Eslami and Fellenius (1997) the q_E value for coarse grained soils is similar to the tip resistance q_t. For fine grained soils on the other hand, q_E can be significantly smaller as greater excess pore pressures develop. (Fellenius & Eslami, 2000)

This soil behaviour type chart is simple and quick in its application since no steps are necessary to normalize the data. The chart is primarily intended for the soil type profiling with CPTu data. One shortcoming of the chart is that only five main soil groups are available, which makes it difficult to classify soils with contents other than the main soil fraction. Another shortcoming of the chart is that the effective cone resistance q_E suffers from lack of accuracy in soft fine-grained soils, which is shown by Robertson (2009).

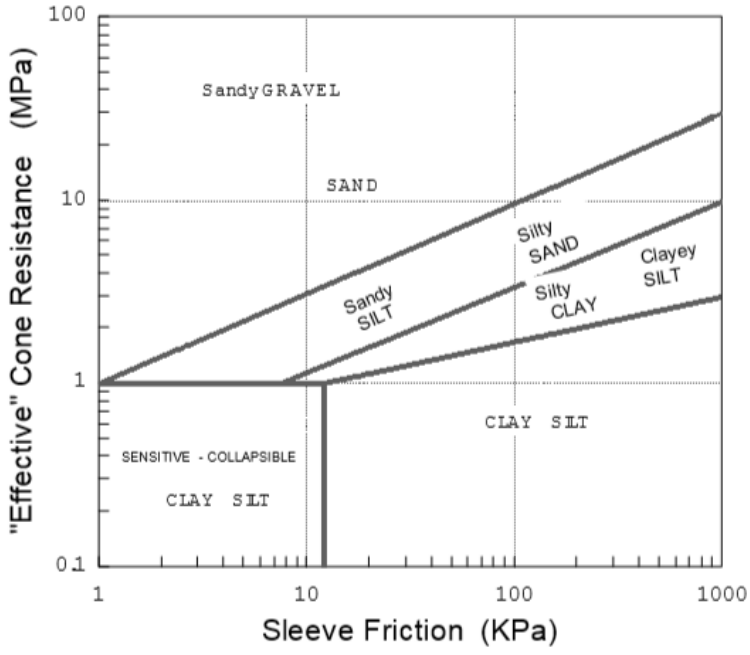

Fig. 11: Soil behaviour type chart according to Eslami & Fellenius (1997)

3.2.2 Robertson et al. (1986)

In Robertson et al. (1986), the first time a soil behaviour type chart was presented that is based on CPTu data, so tests that were performed with the piezocone. Robertson et al. (1986) states that pore water pressures generated during the penetration process can influence the measured cone resistance q_c and sleeve friction f_s. Therefore, they should be corrected using *Eq.(1)* for the cone resistance. A correction of the sleeve friction data is of minor importance when a cone with an equal end area friction sleeve is used. (Robertson, et al., 1986)

Several charts, developed on the basis of basic CPT measurements, show similar tendencies: sandy soils generally show high cone bearings with low friction ratios whereas clayey soils show low cone bearings with rather high friction ratios. Robertson et al. (1986) makes aware of the fact that the measurement of the sleeve friction is sometimes less reliable than the cone resistance because of the different designs of friction sleeves as well as unequal end areas. To overcome this problem of the sleeve friction and because Robertson et al. (1986) were the first ones who used the measurement of pore pressures with the piezocone, two charts for soil classification were developed in 1986. One, plotting the cone resistance corrected for water effects q_t against the friction ratio R_f, and another plotting q_t against the pore pressure ratio B_q. The definition of B_q can be taken from *Eq.(3).* According to Robertson et al. (1986), the identification of soil should be done using all three pieces of data q_t, B_q and R_f: (Robertson, et al., 1986)

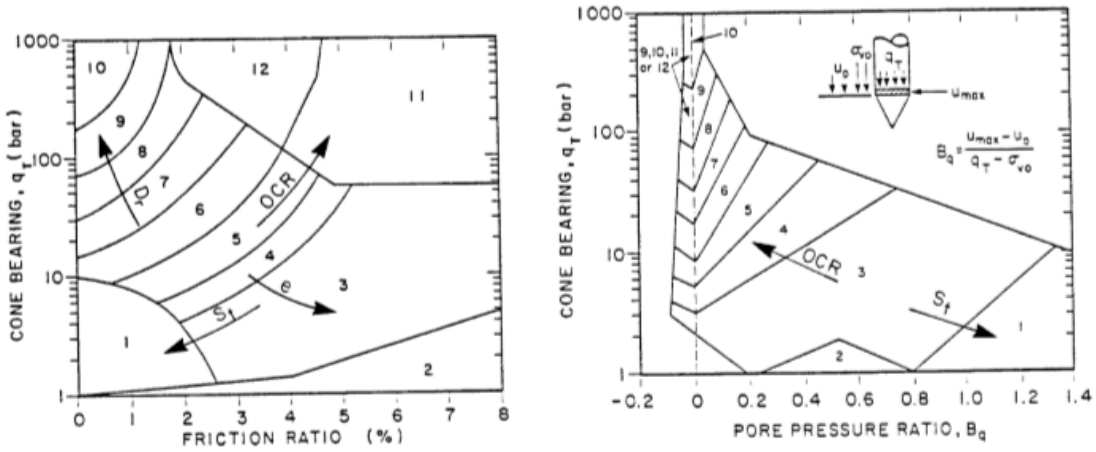

Fig. 12: Soil behaviour type charts according to Robertson et al. (1986): (a) q_t - R_f and (b) q_t - B_q

Fig. 12 identifies twelve zones of different soil types as follows:

1. Sensitive fine-grained soil
2. Organic soil
3. Clay
4. Silty clay to clay
5. Clayey silt to silty clay
6. Sandy silt to clayey silt

7. Silty sand to sandy silt
8. Sand to silty sand
9. Sand
10. Sand to gravelly sand
11. Very stiff fine-grained soil*
12. Sand to clayey sand*

*heavily over-consolidated or cemented

Within the zones 3 to 9 of the chart, a very detailed separation between soil types is made, going from a fine-grained to a coarse-grained soil. If such a detailed separation of soil types can be made in reality, stays questionable. The B_q chart (Fig. 12b) shows zones where pore pressures u_2 can become smaller than the static pore pressure (u_0) and therefore become negative during the penetration process, resulting in negative B_q values. This can appear in very permeable or dilative soils where the excess pore pressure u_2 dissipates very quickly. However, the approach according to Robertson et al. (1986) with the creation of a soil type classification chart based on B_q is rather an additional approach to the q_t - R_f chart than an independent solution. Plotting CPTu data in both charts (a) and (b) of Fig. 12, may result in the appearance of data in different soil-type zones. Therefore, Robertson et al. (1986) recommend measuring the pore pressure dissipation rate in dissipation tests. Depending on this information, a decision can be made which chart applies better to the data to be examined. Robertson (1986) gives the example of a soil with in-situ measured parameters that would classify as clay on the q_t - R_f chart and as clayey silt to silty clay on the q_t - B_q chart. However, with the knowledge of the rate of dissipation, the soil could be correctly identified as a slow rate of dissipation would stand for the clay while a more rapid dissipation rate (t_{50}<60sec) would imply a classification of clayey silt to silty clay. (Robertson, et al., 1986)

Fellenius and Eslami (2000) state that in Robertson et al. (1986) both parameters R_f and B_q are inverse functions of the tip resistance q_t. Both plots in Fig. 12 represent the data as a function of their inverse, which stands generally in conflict with data representation principles. However, the soil classification according to Robertson et al. (1986) has the big advantage of real time use and soil type evaluation since the basic CPT measurements serve as input parameters. (Fellenius & Eslami, 2000) (Robertson, 2010)

3.3 Normalized soil behaviour type charts

3.3.1 Robertson (1990)

In 1990, Robertson did a refinement of his proposed soil profiling charts from 1986, by using normalized CPTu data. In Fig. 13, on the one side a normalized cone resistance is plotted against a normalized friction ratio and on the other side the normalized cone resistance is plotted against the pore pressure ratio B_q. The pore pressure ratio B_q stayed the same as in the approach of 1986 described by

Eq.(3). The newly introduced normalized cone resistance Q_t and normalized friction factor F_r are defined by *Eq.(9)* and *Eq. (10):*

$$Q_t = \frac{(q_t - \sigma_v)}{\sigma_v'} \tag{9}$$

$$F_r = \frac{f_s}{(q_t - \sigma_v)} * 100\ [\%] \tag{10}$$

where

q_t = cone resistance corrected for water effects *Eq.(1)*
σ_v = total vertical stress
σ_v' = effective vertical stress
f_s = sleeve friction (Robertson, 1990)

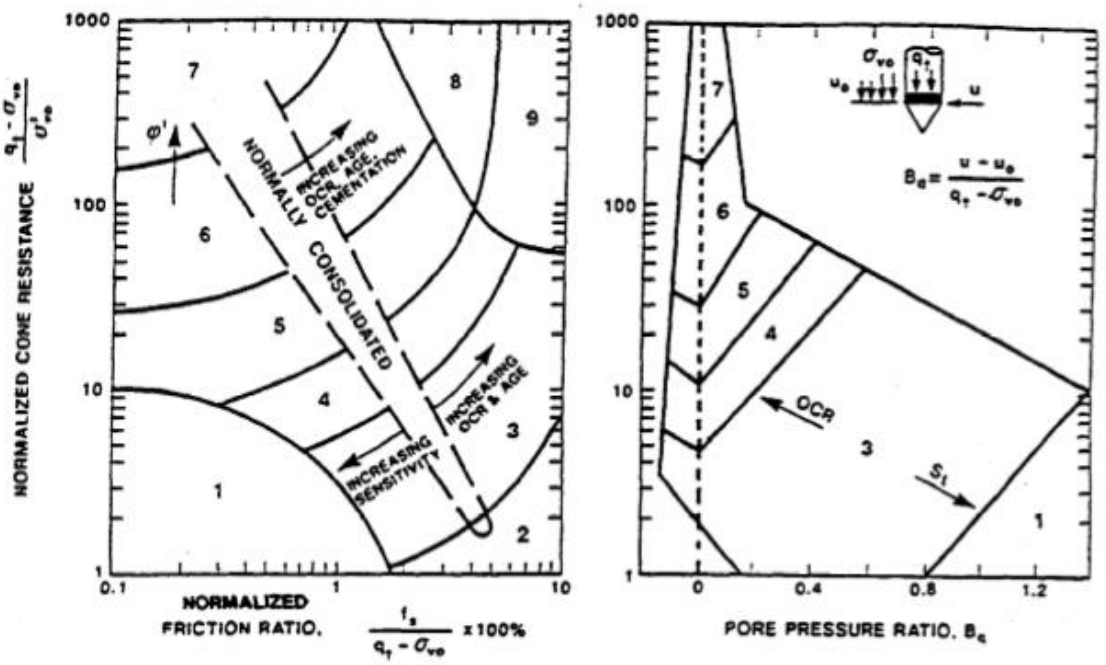

Fig. 13: Soil behaviour type charts according to Robertson (1990): (a) Q_t - F_r and (b) Q_t - B_q

In the approach of 1990, the soil type zones reduced to a number of 9, which are:

1. Sensitive, fine-grained soil
2. Organic soils – peats
3. Clays (clay to silty clay)
4. Silt mixtures (clayey silt to silty clay)
5. Sand mixtures (silty sand to sandy silt)
6. Sand (clean sand to silty sand)
7. Gravelly sand to sand
8. Very stiff sand to clayey sand*
9. Very stiff fine-grained soil*

*heavily over-consolidated or cemented

The first two and last two soil groups stayed the same as those from 1986, whereas the former soil groups 3 to 10 are reduced to soil groups 3 to 7. Robertson (1990) has used normalized input parameters to compensate for the overburden stresses, which influence the magnitude of tip resistance and sleeve friction. Especially deep CPTu soundings require a normalization of data, otherwise the data cannot be applied to the soil profiling charts which are mainly developed for shallow soundings. On the other hand, Fellenius and Eslami (2000) state that for very shallow CPTu data, the proposed normalization of data may lift the data in the chart, which could lead to a coarser soil classification than actually apparent. The non-normalized soil behaviour type charts (SBT) according to Robertson et al. (1986) and normalized soil behaviour type charts (SBTn) according to Robertson (1990) have extensively been applied in geotechnical engineering. (Fellenius & Eslami, 2000)

3.3.2 Robertson (2009)

In 2009, Robertson presented an effort to link CPT interpretation to soil type in a more unified way. Based on his normalized soil behaviour type charts (SBTn-charts) from 1990, Robertson proposed an update in 2009 on the normalization process for the normalized dimensionless cone resistance Q_t. In 1990 the normalized and dimensionless resistance parameters Q_{t1}, F_r and B_q were:

$$Q_{t1} = \frac{(q_t - \sigma_{v0})}{\sigma_{v0}'} = \frac{q_{cnet}}{\sigma_{v0}'} \tag{11}$$

$$F_r = \frac{f_s}{(q_t - \sigma_{v0})} * 100\ [\%] \tag{12}$$

$$B_q = \frac{u_2 - u_0}{q_t - \sigma_{v0}} = \frac{\Delta u_2}{q_t - \sigma_{v0}} \tag{13}$$

In the original paper from Robertson (1990), the normalized cone resistance was defined as Q_t, but in the approach of 2009 the term Q_{t1} is used for the normalized cone resistance of 1990, where the ‘t’ stands for the use of the corrected cone resistance q_t, and the ‘1’ implies that the stress exponent for stress normalization is 1.0. (Robertson, 2009)

Robertson and Wride (1998) and Zhang et al. (2002) suggested an update on the normalization process of the tip resistance using a variable stress exponent n:

$$Q_{tn} = \frac{(q_t - \sigma_{v0})}{p_a} * \left(\frac{p_a}{\sigma_{v0}'}\right)^n \tag{14}$$

where $(q_t - \sigma_{v0})/p_a$ is the dimensionless net cone resistance, $(p_a/\sigma_{v0}')^n$ is the stress normalization factor, p_a is the atmospheric pressure and n is the stress exponent that varies with the normalized Soil Behaviour Type (SBTn). Zhang et al. (2002) stated that n should be estimated from the soil behaviour type Index I_c, which was first identified by Jeffries and Davies (1993) and then further modified by Robertson and Wride (1998) to apply to the Robertson (1990) Q_{t1}-F_r chart:

$$I_c = [(3.47 - logQ_{t1})^2 + (logF_r + 1.22)^2]^{0.5} \quad (15)$$

I_c is the radius of concentric circles that define the boundaries of the soil types in the SBTn zones. Based on several thoughts that can be read in Robertson (2009), he recommended the use of *Eq.(16)* for an updated normalization process to allow for a variation of the stress exponent n with both, the I_c and effective overburden stress:

$$n = 0.381(I_c) - 0.05\left(\frac{\sigma_{v0}'}{p_a}\right) - 0.15 \quad (16)$$

where n≤1.0.

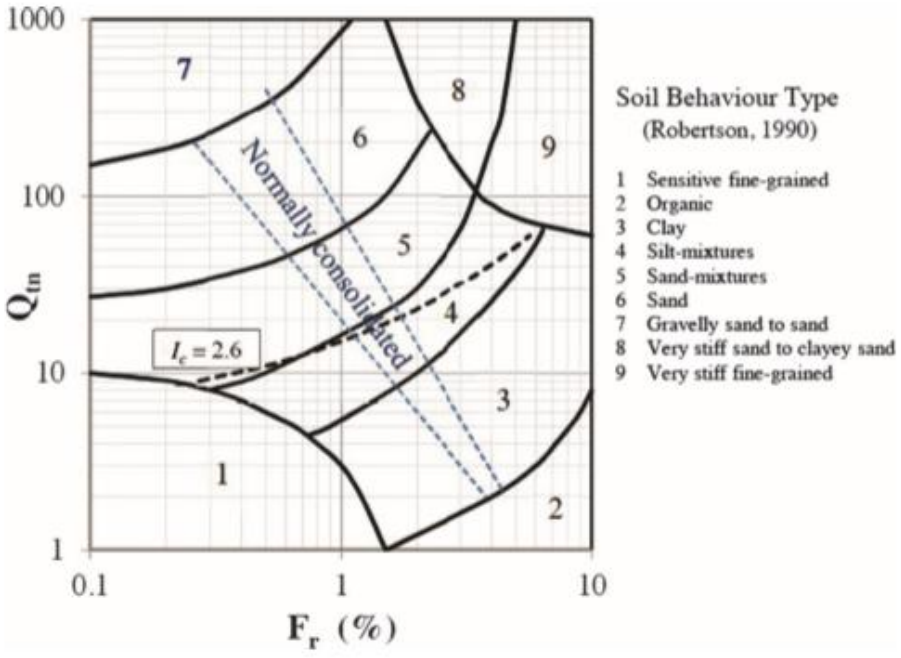

Fig. 14: Soil classification chart according to Robertson (2009)

3.3.3 Robertson (2016)

Most existing soil classification systems are based on the grain-size distribution and plasticity, so simply physical (textural) characteristics. In addition to that, the classification of soils in geotechnical engineering should provide a description of soil behaviour characteristics, which ideally could provide knowledge of the in-situ behaviour of soils. Robertson (2016) states that many natural soils show the

occurrence of microstructure, a certain bonding between soil particles, caused by cementation. Soils with microstructure tend to show a different in-situ behaviour than ideal, unstructured soils. Based on these thoughts, Robertson (2016) provided additional SBTn classification charts with behaviour-based descriptions for each soil group (see Fig. 15). Robertson (2016) distinguishes between four behaviour characteristics: contractive or dilative behaviour and sand-like or clay-like behaviour. In the middle of the chart a small transition zone is provided that should cover soils that don't strictly show one or another behaviour. According to Robertson (2016), the boundary between contractive and dilative (CD) behaviour is defined as:

$$CD = 70 = (Q_{tn} - 11)(1 + 0.06F_r)^{17} \quad (17)$$

If CD>70, soils show a more likely dilative behaviour at large shear strains. In Fig. 15 the SBTn boundary lines after Robertson (1990, 2009) are shaded in grey. The two lines I_B =22 and I_B = 32 are the upper and lower boundaries for clay-like and sand-like soils, respectively. I_B-values in between those two lines define a transition zone between clay-like and sand-like soils. According to Robertson (2016) these transitional soils are characterized by partially drained conditions during test execution. The soil behaviour type charts after Robertson (2009) and (2016) were primarily developed for unstructured soils, i.e. soils with no or rather weak microstructure.

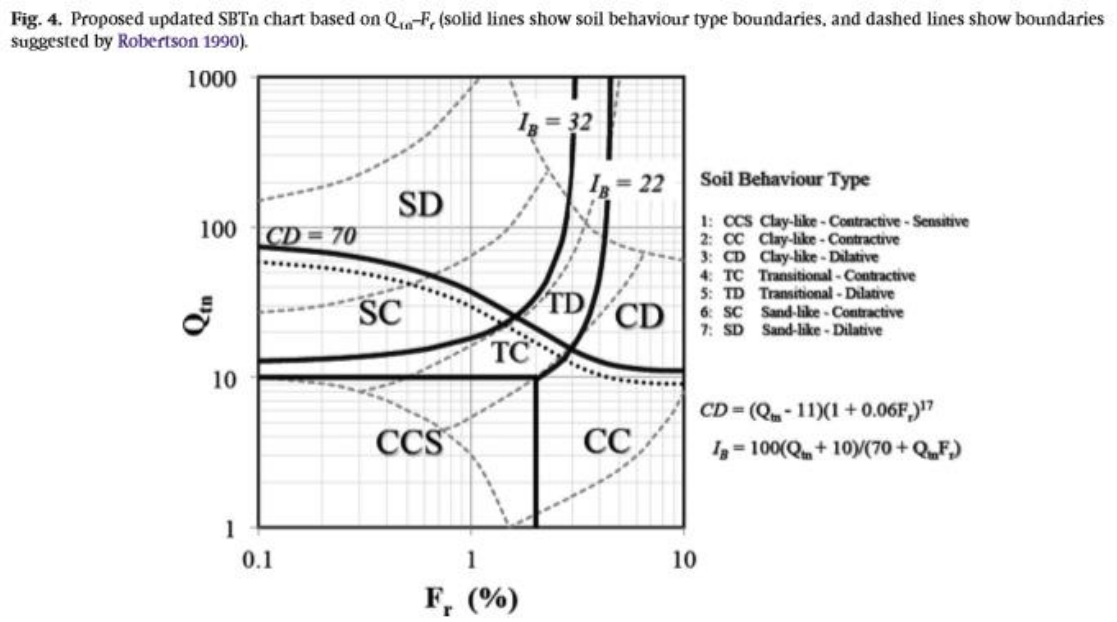

Fig. 15: SBTn chart after Robertson (2016)

Therefore, Robertson (2016) advises that before using a soil classification system, it is of great importance to detect if soils show significant microstructure, as this can have great influence on the behaviour of soil and therefore the effectiveness of the soil type classification. Using the results of seismic cone penetration tests, the small stain shear modulus G_0 can be determined by applying *Eq.(7)*. Since aging

and bonding of soil particles tend to increase G_0 significantly more than the large-strain strength of a soil (reflected in Q_{tn} and q_t), Robertson (2016) proposed Fig. 16 for the determination of possible microstructure. The input parameters for this chart are the normalized dimensionless cone resistance Q_{tn} (see *Eq.(14)*) on the y-axis and the small-strain rigidity index I_G on the x-axis. I_G can be calculated as follows:

$$I_G = \frac{G_0}{q_n} \tag{18}$$

where $q_n = (q_t - \sigma_{v0})$. (Robertson, 2016)

Based on the empirical parameter K_G, as suggested by Schneider and Moss (2011), Robertson (2016) introduced K_G^* to detect microstructure for a wider range of soils:

$$K_G^* = \frac{G_0}{q_n} (Q_{tn})^{0.75} \tag{19}$$

According to Robertson (2016), if soils have $K_G^* < 300$, they are rather young and uncemented, i.d. have little or no microstructure, while soils with $K_G^* > 300$, show significant microstructure and therefore should be interpreted with caution as traditional correlations may not apply. As a conclusion it can be said, that these soil classification charts should be used in addition to textural-based classification systems (e.g. USCS). (Robertson, 2016)

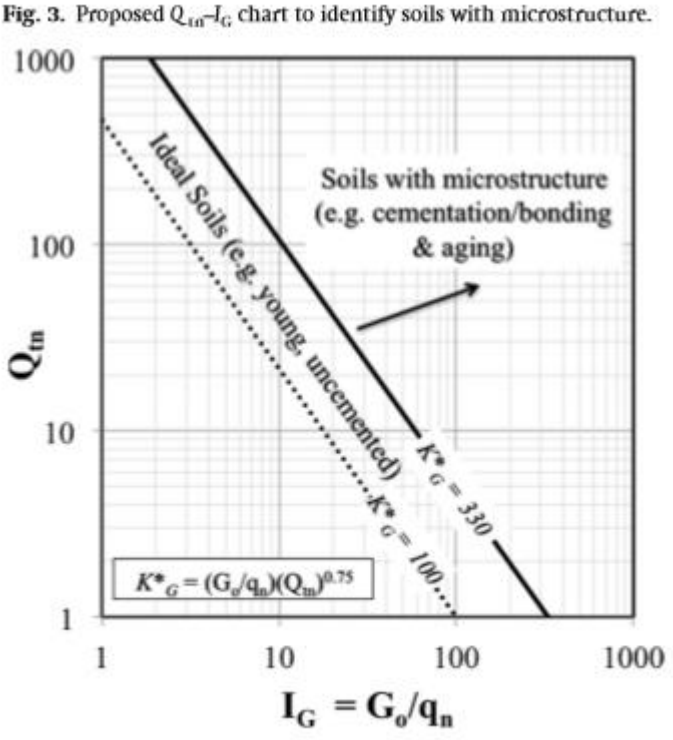

Fig. 16: Proposed Q_{tn}-I_G chart for microstructure identification

3.3.1 Schneider et al. (2008)

Schneider et al. (2008) state that correlations for design parameters based on piezocone penetration testing are relatively reliable for soils like sands and clays, where penetration and the design process typically are under a fully drained or undrained condition, respectively. Correlations for design approaches are rather inadequate when it comes to so called "transitional soils", such as clayey sands and silts and mixed soils, as CPTu tests performed in those soils mainly are conducted under partially drained conditions. Hence, there is a significant uncertainty in the influence of pore pressures on the cone resistance and consequently in the assessment of correlated soil properties for design approaches when partially drained conditions prevail. (Schneider, et al., 2008)

For a correct soil classification, Schneider et al. (2008) pay special attention to the normalization process of parameters. To account for the overburden stress, this normalization of parameters is necessary. The most practical option to do so is to normalize to the initial vertical effective stresses. According to Schneider et. al. (2008) there are insufficiencies in the normalization process regarding the overconsolidation ratio (OCR), having a great influence on the vertical effective stress. Therefore, Schneider et al. (2008) proposed different ways for normalizing the input parameters that incorporate the OCR depending on the soil type. Furthermore, trendlines regarding the OCR are included in the charts (see Fig. 17). In addition to the OCR, the normalization of the cone resistance *Q* and the excess pore water pressure is discussed with regard to whether the penetration is drained, undrained or partially drained. Schneider et al. (2008) state that during fully undrained penetration, the cone tip resistance q_t is primarily controlled by the undrained shear strength c_u and proposed therefore the normalization of the cone tip resistance by c_u for undrained soils as follows:

$$N_{kt} = \frac{q_t - \sigma_{v0}}{c_u} = \frac{q_{cnet}}{c_u} \tag{20}$$

where

N_{kt} = normalized cone tip resistance
q_t = cone resistance corrected for water effects from *Eq.(1)*
q_{cnet} = net cone tip resistance
σ_{v0} = total vertical stress

Neither the undrained shear strength c_u nor the OCR are available as complete profiles over depth, which makes these types of normalization not usable in practice. Therefore, the normalization of cone tip resistance is still based on the most practical option according to Robertson (1990): (Schneider, et al., 2008)

$$Q = \frac{(q_t - \sigma_{v0})}{\sigma_{v0}'} = \frac{q_{cnet}}{\sigma_{v0}'} \tag{21}$$

where

σ_{v0}' = effective vertical stress
Q = normalized cone tip resistance.

To gather information whether the penetration process is drained, undrained or partially drained, penetration tests on variable rates can provide help (Schneider, et al., 2008). Typical soil classification charts, like the ones after Robertson (1990), use the normalized pore pressure ratio B_q which is already stated in *Eq.(2)* but for completeness is recited here again:

$$B_q = \frac{u_2 - u_0}{q_t - \sigma_{v0}} = \frac{\Delta u_2}{q_{cnet}} \tag{22}$$

where

B_q = pore pressure ratio
u_2 = penetration pore pressure at shoulder of cone
u_0 = in-situ pore pressure
Δu_2 = excess pore water pressure

Alternatively, Schneider et al. (2008) introduced new classification charts making direct use of the excess pore water pressure Δu_2 by normalizing it with the effective vertical stress σ_{v0}'. Consequently, the charts were created within the Q-B_q and Q-$\Delta u_2/\sigma_{v0}'$ space. The three charts can be seen in Fig. 17. They are in three different formats and according to Schneider et al. (2008), depending on the type of soil, one of the three graphs should be used. Fig. 17(a) is in the log Q-$\Delta u_2/\sigma_{v0}'$ space and best fits to clays, clayey silts, silts, sandy silts and sands with no negative penetration pore pressures. Fig. 17(b) is in the semi log Q-$\Delta u_2/\sigma_{v0}'$ space which is applicable for sands and transitional soils with small negative excess penetration pore pressures. Fig. 17(c) is in the semi log Q-B_q space and is best applicable for clay soils with large negative excess pore pressures, so the undrained case. (Schneider, et al., 2008)

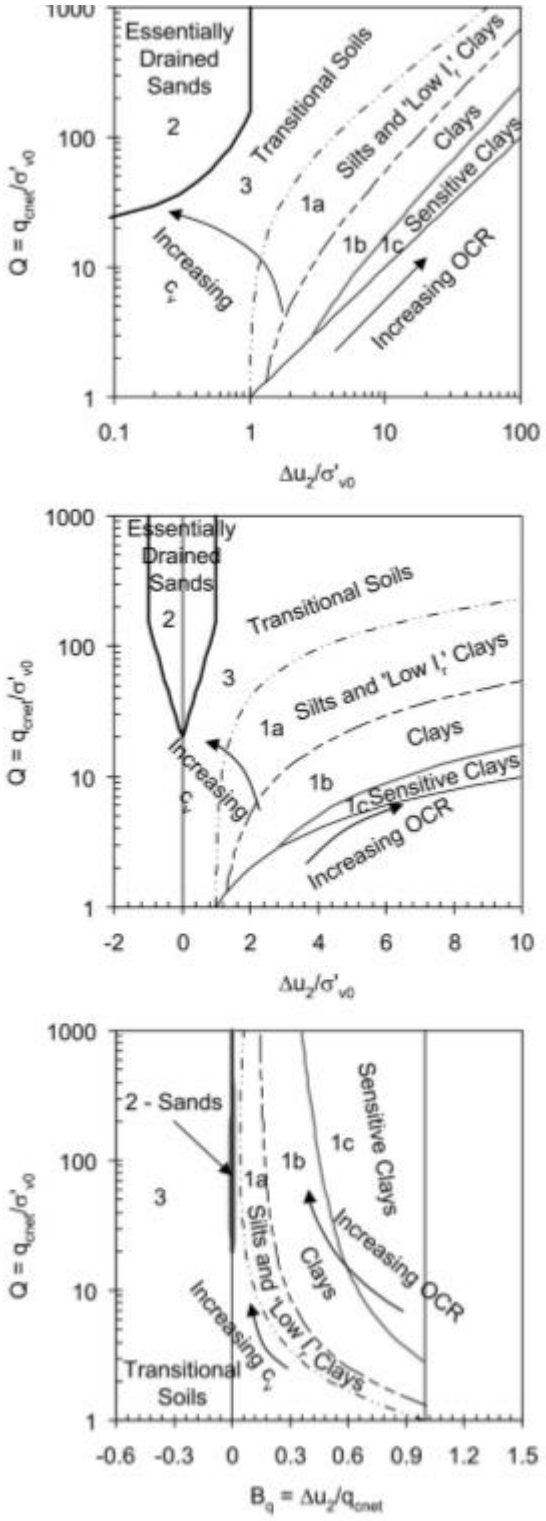

Zone	Soil Type
1a	SILTS and 'Low I_r' CLAYS
1b	CLAYS
1c	Sensitive CLAYS
2	Essentially drained SANDS
3	Transitional soils

Fig. 17: Soil behaviour type charts according to Schneider et al. (2008)

4 QGIS Database

The following chapter gives the reader an overview of the available data that was used for further processing and evaluation. The necessary preparation of the data was carried out with different software packages, which are also briefly introduced.

4.1 Data basis

Because of the wide range of applicability, the cost-effectiveness and the high repeatability of results, a steady increase in use and application of the cone penetration test all over the world could be observed over the past years. (Robertson, 2009) This statement is also valid for Austria. Intensive in-situ testing, by means of CPT, CPTu and SCPT tests, has been performed over the past 10 years by the Premstaller Geotechnik ZT GmbH all over Austria but with the main emphasis on the state of Salzburg. As it can be seen in Fig. 18, 1468 tests that were conducted and provided by Premstaller Geotechnik ZT GmbH, form the fundamental groundwork of this master's thesis. Based on the 757 CPT, 612 CPTu, 2 DMT and 97 seismic penetration tests (SCPT, SCPTu, SDMT), this statistical evaluation of in-situ measurements could be performed.

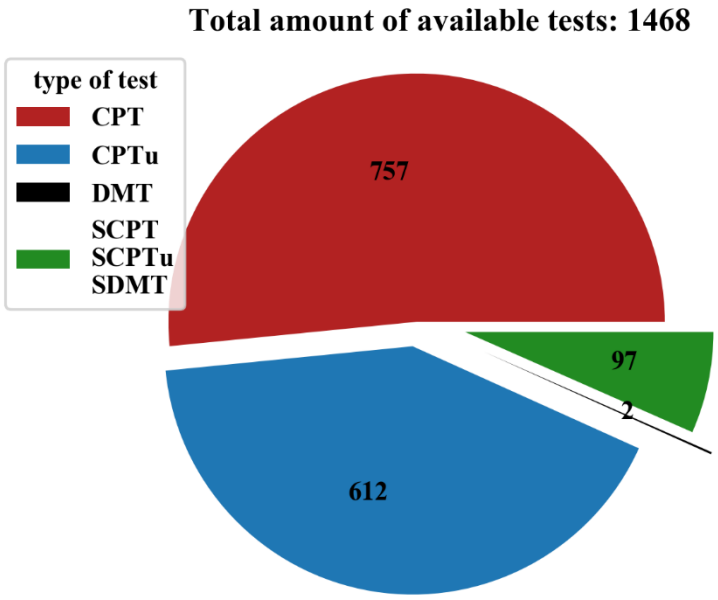

Fig. 18: Distribution of available test data in Austria depending on the test type

In addition to the results of penetration tests, a total amount of 282 core drillings founded the basis of the characterization of in-situ measurements by means of the grain size distribution, which can be read in chapter 6.3. Premstaller Geotechnik ZT GmbH as well as the geo information system of the state Salzburg provided the core drillings.

4.2 Data base design

All the provided test data was implemented into a QGIS Database. QGIS is an open source geographic information system that was used to create a large database in which all in-situ tests and core drillings could coordinatively correctly be placed and archived. Fig. 19 shows a screenshot of the implemented datapoints into the software within Austria. Five differently coloured layers served as a distinction between the different types of data:

Layer 1 (red markers): CPT data
Layer 2 (blue markers): CPTu data
Layer 3 (yellow markers): DMT data
Layer 4 (green markers): SCPT, SCPTu and SDMT data
Layer 5 (pink markers): core drillings

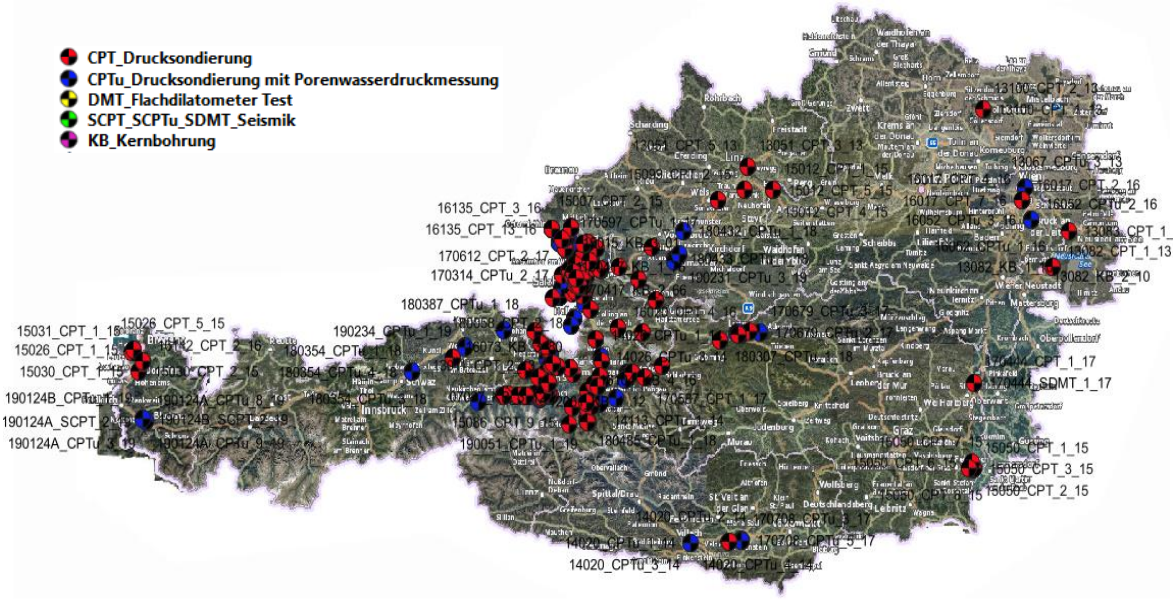

Fig. 19: QGIS Database: Overview of layers within Austria

To store important categorizing information of each in-situ test or core drilling, five attribute tables, one for each layer, were established. For a better understanding, an extract from such an attribute table is shown in Fig. 20. Within one attribute table, the following attributes were assigned to each test:

- a consecutive ID number
- the company's name that executed the test
- the project number
- the project name
- the exact location of the test regarding the city, the state, the cadastral community and the property number
- the basin or valley the test was executed in
- a declaration about whether fine sediments have been found (i.e. if the test was executed deeper than 3 m)

- the year of test execution
- a declaration if any other core drilling, DMT test or seismic test was executed right next to the test.
- additional space for annotations

For the CPTu attribute table, additional attributes were placed to the ones mentioned above:

- the number of dissipation tests performed
- a declaration about the pore water pressure distribution (for further information see chapter 4.3.1, section about flawed CPTu tests)

In the attribute table for the core drillings, several columns where provided in which the allocated penetration tests were namely entered.

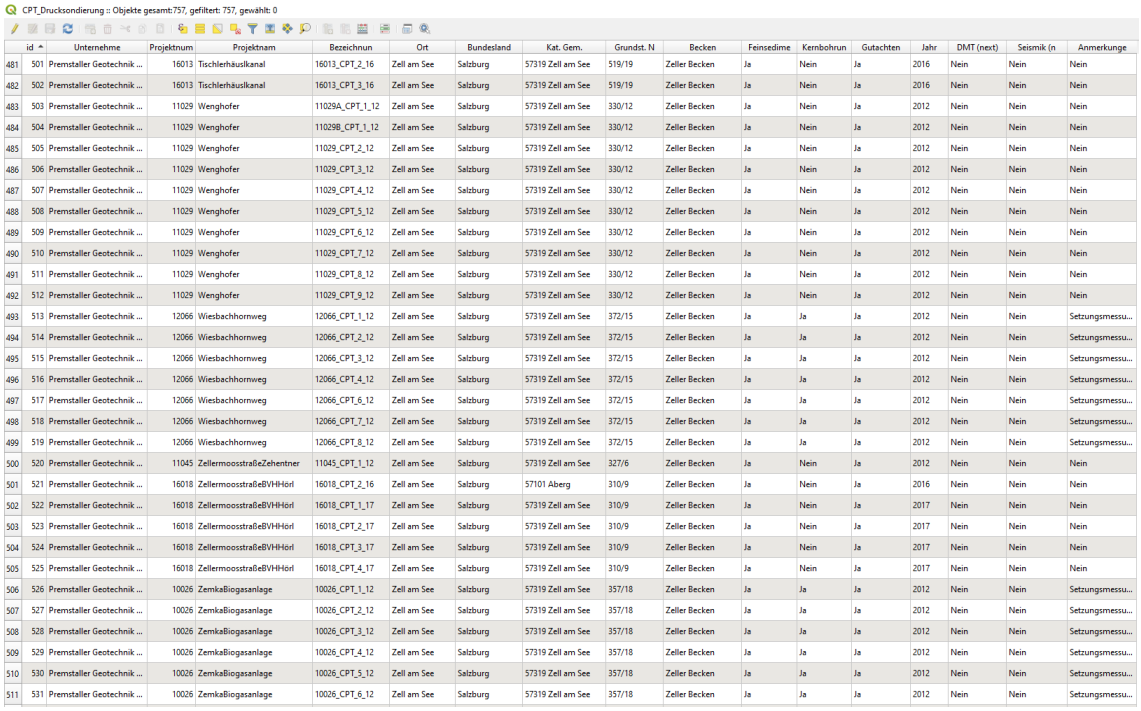
CPT_Drucksondierung :: Objekte gesamt:757, gefiltert: 757, gewählt: 0

	id	Unternehme	Projektnum	Projektnam	Bezeichnun	Ort	Bundesland	Kat. Gem.	Grundst. N	Becken	Feinsedime	Kernbohrun	Gutachten	Jahr	DMT (next)	Seismik (n	Anmerkunge
481	501	Premstaller Geotechnik ...	16013	Tischlerhäuslkanal	16013_CPT_2_16	Zell am See	Salzburg	57319 Zell am See	519/19	Zeller Becken	Ja	Nein	Ja	2016	Nein	Nein	Nein
482	502	Premstaller Geotechnik ...	16013	Tischlerhäuslkanal	16013_CPT_3_16	Zell am See	Salzburg	57319 Zell am See	519/19	Zeller Becken	Ja	Nein	Ja	2016	Nein	Nein	Nein
483	503	Premstaller Geotechnik ...	11029	Wenghofer	11029A_CPT_1_12	Zell am See	Salzburg	57319 Zell am See	330/12	Zeller Becken	Ja	Nein	Ja	2012	Nein	Nein	Nein
484	504	Premstaller Geotechnik ...	11029	Wenghofer	11029B_CPT_1_12	Zell am See	Salzburg	57319 Zell am See	330/12	Zeller Becken	Ja	Nein	Ja	2012	Nein	Nein	Nein
485	505	Premstaller Geotechnik ...	11029	Wenghofer	11029_CPT_2_12	Zell am See	Salzburg	57319 Zell am See	330/12	Zeller Becken	Ja	Nein	Ja	2012	Nein	Nein	Nein
486	506	Premstaller Geotechnik ...	11029	Wenghofer	11029_CPT_3_12	Zell am See	Salzburg	57319 Zell am See	330/12	Zeller Becken	Ja	Nein	Ja	2012	Nein	Nein	Nein
487	507	Premstaller Geotechnik ...	11029	Wenghofer	11029_CPT_4_12	Zell am See	Salzburg	57319 Zell am See	330/12	Zeller Becken	Ja	Nein	Ja	2012	Nein	Nein	Nein
488	508	Premstaller Geotechnik ...	11029	Wenghofer	11029_CPT_5_12	Zell am See	Salzburg	57319 Zell am See	330/12	Zeller Becken	Ja	Nein	Ja	2012	Nein	Nein	Nein
489	509	Premstaller Geotechnik ...	11029	Wenghofer	11029_CPT_6_12	Zell am See	Salzburg	57319 Zell am See	330/12	Zeller Becken	Ja	Nein	Ja	2012	Nein	Nein	Nein
490	510	Premstaller Geotechnik ...	11029	Wenghofer	11029_CPT_7_12	Zell am See	Salzburg	57319 Zell am See	330/12	Zeller Becken	Ja	Nein	Ja	2012	Nein	Nein	Nein
491	511	Premstaller Geotechnik ...	11029	Wenghofer	11029_CPT_8_12	Zell am See	Salzburg	57319 Zell am See	330/12	Zeller Becken	Ja	Nein	Ja	2012	Nein	Nein	Nein
492	512	Premstaller Geotechnik ...	11029	Wenghofer	11029_CPT_9_12	Zell am See	Salzburg	57319 Zell am See	330/12	Zeller Becken	Ja	Nein	Ja	2012	Nein	Nein	Nein
493	513	Premstaller Geotechnik ...	12066	Wiesbachhornweg	12066_CPT_1_12	Zell am See	Salzburg	57319 Zell am See	372/15	Zeller Becken	Ja	Ja	Ja	2012	Nein	Nein	Setzungsmessu...
494	514	Premstaller Geotechnik ...	12066	Wiesbachhornweg	12066_CPT_2_12	Zell am See	Salzburg	57319 Zell am See	372/15	Zeller Becken	Ja	Ja	Ja	2012	Nein	Nein	Setzungsmessu...
495	515	Premstaller Geotechnik ...	12066	Wiesbachhornweg	12066_CPT_3_12	Zell am See	Salzburg	57319 Zell am See	372/15	Zeller Becken	Ja	Ja	Ja	2012	Nein	Nein	Setzungsmessu...
496	516	Premstaller Geotechnik ...	12066	Wiesbachhornweg	12066_CPT_4_12	Zell am See	Salzburg	57319 Zell am See	372/15	Zeller Becken	Ja	Ja	Ja	2012	Nein	Nein	Setzungsmessu...
497	517	Premstaller Geotechnik ...	12066	Wiesbachhornweg	12066_CPT_6_12	Zell am See	Salzburg	57319 Zell am See	372/15	Zeller Becken	Ja	Ja	Ja	2012	Nein	Nein	Setzungsmessu...
498	518	Premstaller Geotechnik ...	12066	Wiesbachhornweg	12066_CPT_7_12	Zell am See	Salzburg	57319 Zell am See	372/15	Zeller Becken	Ja	Ja	Ja	2012	Nein	Nein	Setzungsmessu...
499	519	Premstaller Geotechnik ...	12066	Wiesbachhornweg	12066_CPT_8_12	Zell am See	Salzburg	57319 Zell am See	372/15	Zeller Becken	Ja	Ja	Ja	2012	Nein	Nein	Setzungsmessu...
500	520	Premstaller Geotechnik ...	11045	ZellermoosstraßeZehentner	11045_CPT_1_12	Zell am See	Salzburg	57319 Zell am See	327/6	Zeller Becken	Ja	Nein	Ja	2012	Nein	Nein	Nein
501	521	Premstaller Geotechnik ...	16018	ZellermoosstraßeBVHHörl	16018_CPT_2_16	Zell am See	Salzburg	57101 Aberg	310/9	Zeller Becken	Ja	Nein	Ja	2016	Nein	Nein	Nein
502	522	Premstaller Geotechnik ...	16018	ZellermoosstraßeBVHHörl	16018_CPT_1_17	Zell am See	Salzburg	57319 Zell am See	310/9	Zeller Becken	Ja	Nein	Ja	2017	Nein	Nein	Nein
503	523	Premstaller Geotechnik ...	16018	ZellermoosstraßeBVHHörl	16018_CPT_2_17	Zell am See	Salzburg	57319 Zell am See	310/9	Zeller Becken	Ja	Nein	Ja	2017	Nein	Nein	Nein
504	524	Premstaller Geotechnik ...	16018	ZellermoosstraßeBVHHörl	16018_CPT_3_17	Zell am See	Salzburg	57319 Zell am See	310/9	Zeller Becken	Ja	Nein	Ja	2017	Nein	Nein	Nein
505	525	Premstaller Geotechnik ...	16018	ZellermoosstraßeBVHHörl	16018_CPT_4_17	Zell am See	Salzburg	57319 Zell am See	310/9	Zeller Becken	Ja	Nein	Ja	2017	Nein	Nein	Nein
506	526	Premstaller Geotechnik ...	10026	ZemkaBiogasanlage	10026_CPT_1_12	Zell am See	Salzburg	57319 Zell am See	357/18	Zeller Becken	Ja	Ja	Ja	2012	Nein	Nein	Setzungsmessu...
507	527	Premstaller Geotechnik ...	10026	ZemkaBiogasanlage	10026_CPT_2_12	Zell am See	Salzburg	57319 Zell am See	357/18	Zeller Becken	Ja	Ja	Ja	2012	Nein	Nein	Setzungsmessu...
508	528	Premstaller Geotechnik ...	10026	ZemkaBiogasanlage	10026_CPT_3_12	Zell am See	Salzburg	57319 Zell am See	357/18	Zeller Becken	Ja	Ja	Ja	2012	Nein	Nein	Setzungsmessu...
509	529	Premstaller Geotechnik ...	10026	ZemkaBiogasanlage	10026_CPT_4_12	Zell am See	Salzburg	57319 Zell am See	357/18	Zeller Becken	Ja	Ja	Ja	2012	Nein	Nein	Setzungsmessu...
510	530	Premstaller Geotechnik ...	10026	ZemkaBiogasanlage	10026_CPT_5_12	Zell am See	Salzburg	57319 Zell am See	357/18	Zeller Becken	Ja	Ja	Ja	2012	Nein	Nein	Setzungsmessu...
511	531	Premstaller Geotechnik ...	10026	ZemkaBiogasanlage	10026_CPT_6_12	Zell am See	Salzburg	57319 Zell am See	357/18	Zeller Becken	Ja	Ja	Ja	2012	Nein	Nein	Setzungsmessu...

Fig. 20: Extract from the CPT attribute table

4.3 Analysis of data base

For an investigation of the whole database, time-consuming data preparation and data homogenisation was necessary. This subchapter provides an insight into the work done.

4.3.1 Data preparation and evaluation procedure

In order not to lose the overview of data, a uniform nomenclature was introduced for each penetration test and core drilling consisting of the project number, a consecutive number and the year of execution. E.g. a seismic cone penetration test

that was performed in the year 2016 shows the following structure: 170021_SCPT_1_16.

Flawed CPTu tests:

At this point it should be mentioned that a certain amount of CPTu tests showed an incorrect distribution of the excess pore water pressure u_2. This can be explained by the performance of these tests on the construction site. Before each CPTu test, the piezocone needs to be saturated either with water or for better results with an oily liquid. Because the information of one CPTu test per site is usually sufficient and therefore to save time, the probe is saturated only once before the first test and the same probe is then used for all following tests. As a result, the distribution of the excess pore water pressure is only accurate for the first test and flawed excess pore water distributions are created for the other tests. In order not to lose the important information about tip resistances and sleeve frictions, these flawed CPTU tests are treated as normal CPT tests where the pore water pressure is ignored, but are incorrectly listed as CPTu tests.

Allocation of core drillings to in-situ tests:

Core drillings that were found within a range of a maximum distance of 100 m to the test site were allocated to surrounding penetration tests. Therefore, a large Excel database was set up, including the information of all core drillings with their soil genesis. By comparing the soil layers that were given by the core drillings with the distribution of in-situ measured resistance values next to each other, the soil layers could more or less correctly be identified. The corresponding soil genesis according to the core drilling was then assigned to its appearing depth for each test. A correct allocation of core drilling to test was not always possible when e.g. distances were too large or the soil layers could not be identified within the distribution of measured in-situ values. In this case they were neglected. An extract of this database can be found in Appendix A. How this data from the core drillings was further used for data processing can be read in chapter 6.3.1.

Determination of parameters with Geologismiki:

CPeT-IT is a software for the interpretation of (piezo-)cone penetration test data, which was developed by Geologismiki in collaboration with the Gregg Drilling & Testing Inc. and Professor Peter K. Robertson. The raw data of each penetration test was imported into CPeT-IT. With the use of this software, the following parameters could be automatically calculated over depth:

- the corrected tip resistance q_t from *Eq.(1)*
- the friction ratio R_f from *Eq.(2)*
- the normalized friction ratio F_r according to *Eq.(12)*
- the normalized pore pressure ratio according to *Eq.(13)*

- the dimensionless normalized tip resistance according to *Eq.(14)* with the soil boundaries I_c and the stress exponent n according to *Eq.(15)* and *Eq.(16)*, respectively.

Especially the last parameters are needed in chapter 7 for the interpretation of data by means of normalized soil behaviour type charts.

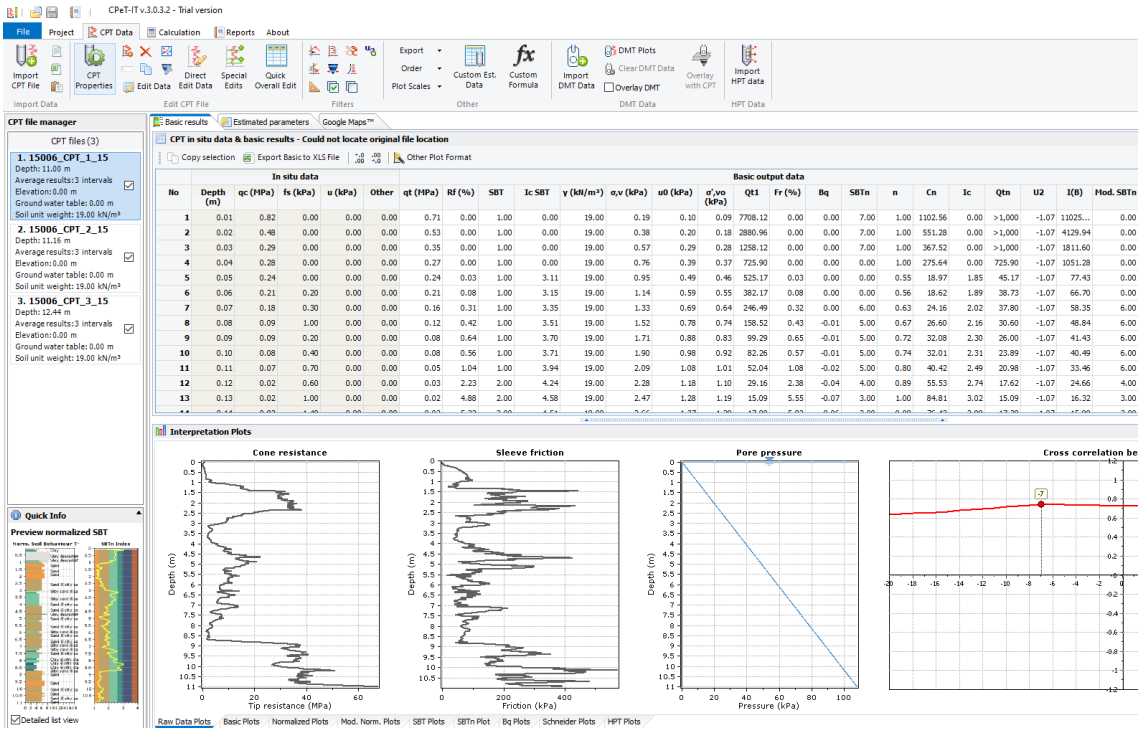

Fig. 21: Screenshot out of CPeT-IT

Data processing with Python:

Due to the large amount of data, the programming language Python was chosen for the further processing of the in-situ tests. With the help of several codes created in Python, all statistical investigations and evaluations from chapters 4, 6 and 7 were performed. Due to the large number of different codes, only selected codes will be listed in the appendices, in order to save space. The Python codes for this chapter, so the first analysis of the database, can be found in Appendix B. Selected Python codes for chapters 6 and 7 can be found in the Appendix E and the Appendix F, respectively. A collection of all Python codes that were written for this master's thesis is included after the appendices on a CD.

4.3.2 Results

In a first step the whole data base was analysed with regard to the distribution of the in-situ tests. Fig. 18 gave an overview of the total amount of available data depending on the test type. Fig. 22 clearly shows that the majority of all tests were performed in the state of Salzburg. This can be related to the high density of soft to very soft soils within this federal state, which make increasing soil sampling and

in-situ testing necessary. In Fig. 23 one can see how the 1468 available penetration tests are distributed over the basins and valleys they were conducted in. It is immediately apparent that the most tests, to be precise 569, 323 and 151 tests, were carried out within the basin of Salzburg, the basin of Zell and the region of Flachgau, respectively. This is the reason why these three regions are used in the course of this master's thesis when it comes to more precise investigations, as the most data is available there.

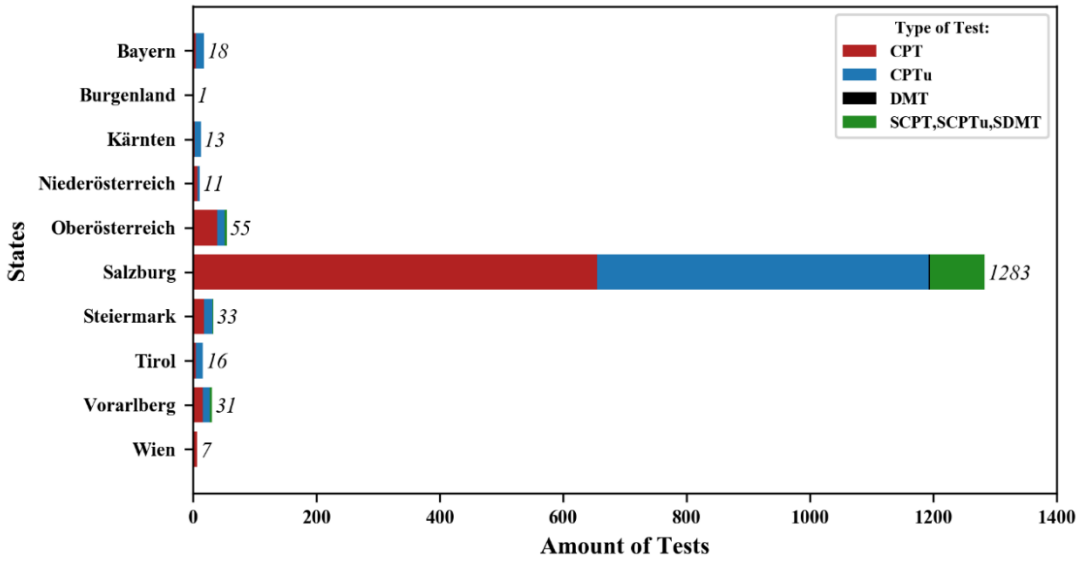

Fig. 22: Overview of database: Comparison of the federal states

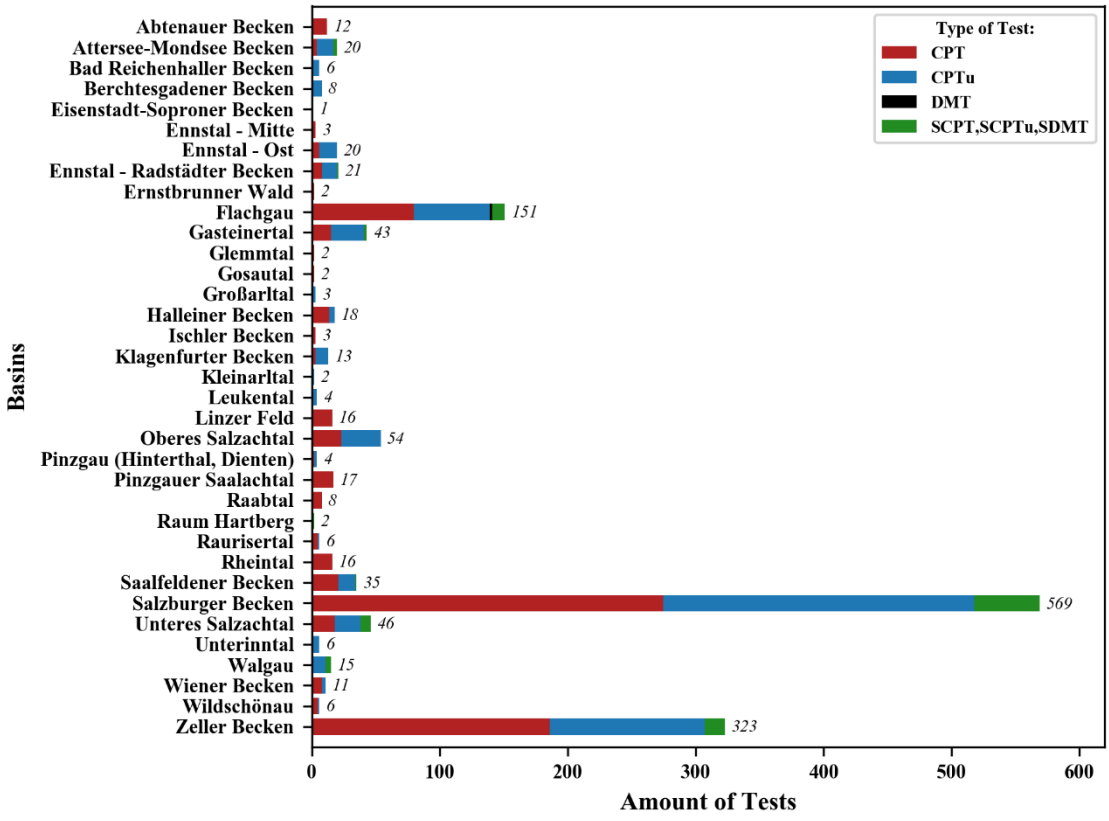

Fig. 23: Overview of database: Comparison of valleys and basins

5 Statistical basis

For a better understanding of chapters 6 and 7, important statistical terms are presented and explained in the following subchapters.

5.1 Fundamental terms

5.1.1 Frequency distribution

In statistics, the frequency distribution of data, also known as empirical distribution (based on real data), gives a first insight into the structure of data.
The frequency distribution shows how often a particular characteristic size occurs in a sample. Due to statistical processes, different sizes can turn into different values. These values are called random variables. A distinction is made between discrete random variables (e.g. coin toss, roulette) and continuous random variables. The latter are typically the result of a measurement or experiment. For this master's thesis the in-situ measured data represents continuous random variables. (Feindt & Kerzel, 2015)

5.1.2 Arithmetic mean

In statistics, there are different ways to describe the expected value μ. For a normal distribution, an average value is the most appropriate way to describe the expected valueμ. The most common average value which provides the most useful results is the arithmetic mean $\bar{x}$. It can be calculated as follows:

$$\bar{x} = \frac{1}{n} \sum_{i=1}^{n} x_i \tag{23}$$

where

$\bar{x}$ = mean value
x_i = i-th measured value
n = amount of measured values (Hemmerich, 2011)

It is the sum of all measured values divided by the total amount of measured values. Generally, one should not use the arithmetic mean if:

- values with a high scatter and therefor a large standard deviation are present,
- the average of the average is to be calculated. If several averages have already been determined, the arithmetic mean is only conditionally suitable for calculating an average value from these values,
- the data is not normally distributed. For skewed or multimodal distributions, other approaches than the calculation of the arithmetic

mean should be preferred to determine the expected value μ. In such a case, the median or the modus are a better representation. (Hemmerich, 2011)

5.1.3 Median

The median value, or just median, is mainly used when data is present that diverges widely, i.e. data with a high scatter. Data that disperses highly is characterized by values that are extremely high or extremely low, and therefore shift the arithmetic mean in either direction, which leads to a wrong result if one is aiming for an expected value μ. A descriptive example of the wrong use of the arithmetic mean would be the calculation of income of one million people, where one person earns 1 million euros and the rest nothing at all. The arithmetic mean would give an average income of 1000 euros per person, which is not representative for the population. Therefore, the median income is used, as this is more realistic. (Hemmerich, 2011)

For the calculation of the median, all measured values need to be sorted from small to large. The median value is the value that lies in the middle of this sorting. *Eq.(24)* describes the mathematical procedure:

$$\tilde{x} = \begin{cases} x_{\frac{n+1}{2}} & for\ n\ is\ uneven \\ \frac{1}{2}\left(x_{\frac{n}{2}} + x_{\frac{n}{2}+1}\right) & for\ n\ is\ even \end{cases} \tag{24}$$

where

$\tilde{x}$ = median value
n = amount of measured values (Hemmerich, 2011)

Depending on whether the total amount of measured values n is even or uneven, the calculation process is different. For an uneven number, the median simply represents the middle value:

$$1,\ 3,\quad 5,\quad 7,\ 9$$

$$\rightarrow \tilde{x} = 5$$

If n is an even number, the median is calculated by the arithmetic mean of the two in the middle lying values: (Hemmerich, 2011)

$$1,\ 3,\ \ 5,\ \ 7,\ \ 9,\ \ 11$$

$$\rightarrow \tilde{x} = \frac{5+7}{2} = 6$$

5.1.4 Mode

The modal value, or simply the mode, is the value that occurs most frequently in a frequency distribution. It is considered as the value x at which the frequency distribution has a locally maximum value. Consequently, any peak is a mode. There can be two or more modes if several values occur equally frequently in a frequency distribution. In the case of a skewed or multimodal distribution of data, the mode may be a better way of determining the expected value μ. However, the mode is a special value that can be used additionally to the mean and median value, but is not used very often in mathematical calculations. (Hemmerich, 2011)

5.1.5 Normal distribution

The normal distribution assumes a symmetrical distribution form of data. It is also known as the Gaussian bell curve or the Gaussian normal distribution – named after the German mathematician Carl Friedrich Gauss. The normal distribution is a statistical distribution model. Its curve is symmetrical, i.e. the median value and the arithmetic mean are identical and both represent the expected value μ. The distribution shows a skewness of 0. See Fig. 24 for a graphical explanation of the normal distribution. (Statista, 2019)

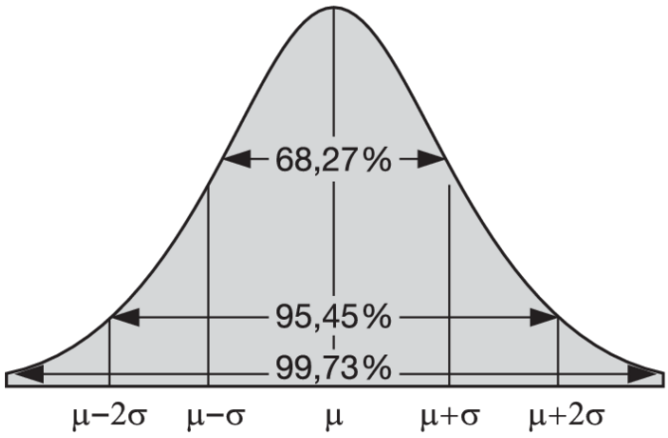

Fig. 24: Normal distribution (Kamps, 2019)

Around the expected value of a distribution the measured values show a scatter. Information on this dispersion of data can be gained via the standard deviation σ.

For the normal distribution, about two-thirds (68.27 %) of all measured values lie within the distance of one time the standard deviation from the mean value $\bar{x}$. With the distance of two times the standard deviation, already over 95 % of all measured values are included. 99.73 % of all measured values lie within a distance of three times the standard deviation. The standard deviation σ is calculated using the square root of the variance (Statista, 2019):

$$\sigma = \sqrt{Var(x)} = \sqrt{\frac{\sum_{i=1}^{n}(x_i - \bar{x})^2}{n}} \quad (25)$$

where

x_i = i-th measured value
$\bar{x}$ = mean value
n = amount of measured values

The standard deviation is either a positive number or zero; it can never get negative. A smaller standard deviation usually indicates that the measured values are lying close to the mean value $\bar{x}$, while a lager standard deviation indicates a larger scatter of data. (Statista, 2019)

5.1.6 Skewness

The skewness is a measure of the symmetry of a frequency distribution. The highest point of the distribution represents the mode. As explained in chapter 5.1.4, the mode on the x-axis marks the value that occurs the most. Skewness means that a distribution rises steeper on one side of the mode than on the other – it is asymmetric. Fig. 25 shows that a distribution is right-skewed if it rises steeper on the left side than it decreases on the right side. Left- skewness is exactly the other way around, the distribution rises more slowly on the left side of the mode than it decreases on the right side of this mode. (Statista, 2019)

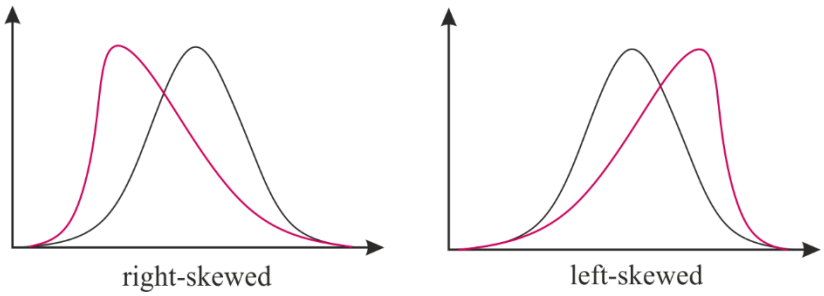

Fig. 25: Right- and left-skewed distribution

The skewness of a distribution is caused by extreme outliers which lead to an asymmetry of the normal distribution. For an asymmetric distribution, the use of the standard deviation as a measure of the scatter of a distribution is not applicable anymore. By using the standard deviation, one would over-or underestimate the amount of measured values that are lying within the range of the standard deviation. This is illustrated in Fig. 26. To overcome this problem, a better parameter to describe the dispersion of a distribution is introduced - the quantile.

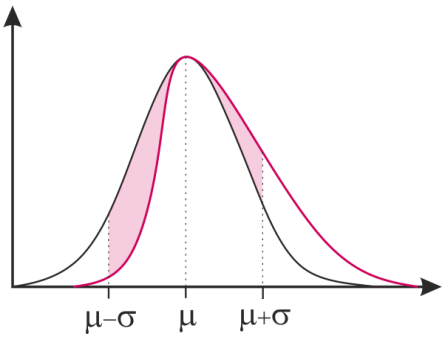

Fig. 26: Over- and underestimation of standard deviation

5.1.7 Quantile

A quantile defines a certain part of a data set. This means that a quantile determines how many values of a distribution are above or below a certain limit. Special quantiles are the quartile (a quarter), the quintile (a fifth) or the percentile (a hundredth). Those are the most common quantiles used in statistics. In the course of this master's thesis, the 25 % and 75 % quartiles are chosen to give information about the dispersion of the data presented. (Statista, 2019)

In Fig. 27, it can be seen that the 25% quartile indicates the limit below which 25% of the measured data is situated. Below the 75% quartile, three-quarters of the measured values are situated. The median value is at the same time the 50% quartile, as this value represents exactly the middle value of all values. This means that 50 % of the data lies above and the other 50 % of data below the median value. The 25%, 50% and 75% quartiles can also be called the 1st, 2nd and 3rd quartile or lower quartile, median and upper quartile.

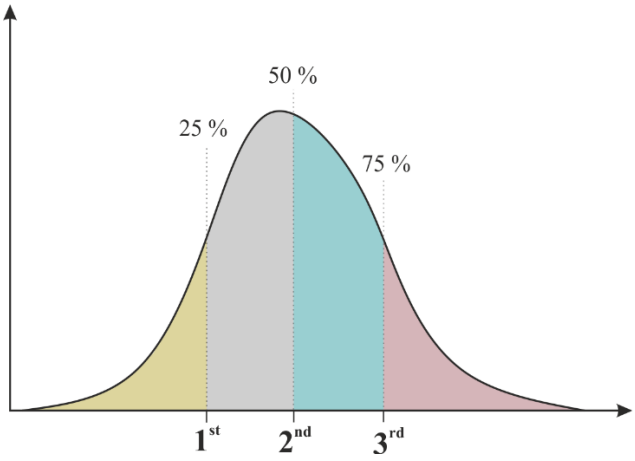

Fig. 27: Quartile values

5.1.8 Bimodal frequency distribution

A unimodal frequency distribution (e.g. the normal distribution) is characterized by the appearance of one peak, which, depending on the underlying distribution function, either represents the mean, the median or modal value.

In the case of a bimodal frequency distribution two peaks with two different modal values occur. Multimodal frequency distributions may even show multiple peaks. Bimodal frequency distributions can be both, symmetrical and asymmetrical. However, the bimodality often indicates that the sample is inhomogeneous and the observed values belong to two mutually overlapping distributions, which shows that two sub groups of data may be present. Sometimes the appearance of more than one peak in a frequency distribution can be an indication of problems in the measurement procedure (e.g. calibration problems in natural sciences). (StatSoft, 2019)

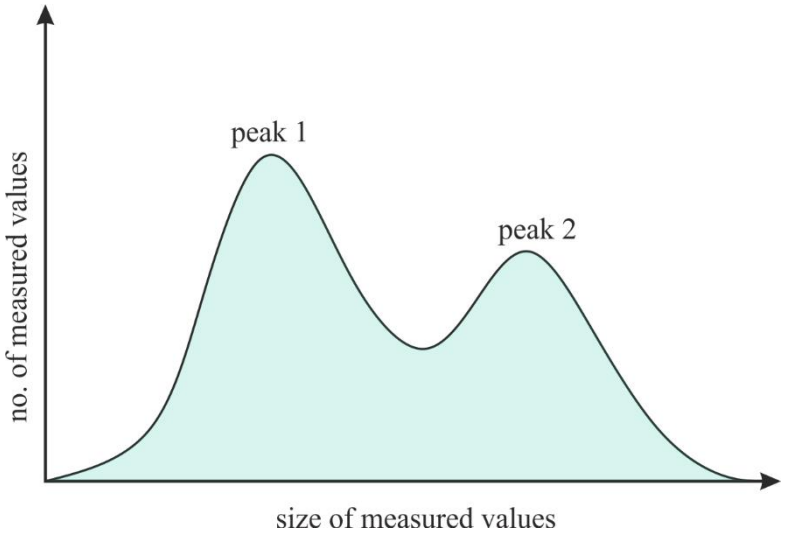

Fig. 28: Bimodal frequency distribution

5.2 Box-Whisker-Plot

The Box-Whisker-Plot, also called Boxplot (in German “Kastengrafik”), is a common diagram type which contains five characteristic values: the minimum, the maximum, the 1st quartile, the median and the 3rd quartile. The special thing about this method of data presentation is that no assumptions of the underlying frequency distribution is necessary. This means that in the case of a skewed distribution, the Box-Whisker-Plot is a very useful tool to illustrate data. (Hemmerich, 2011)

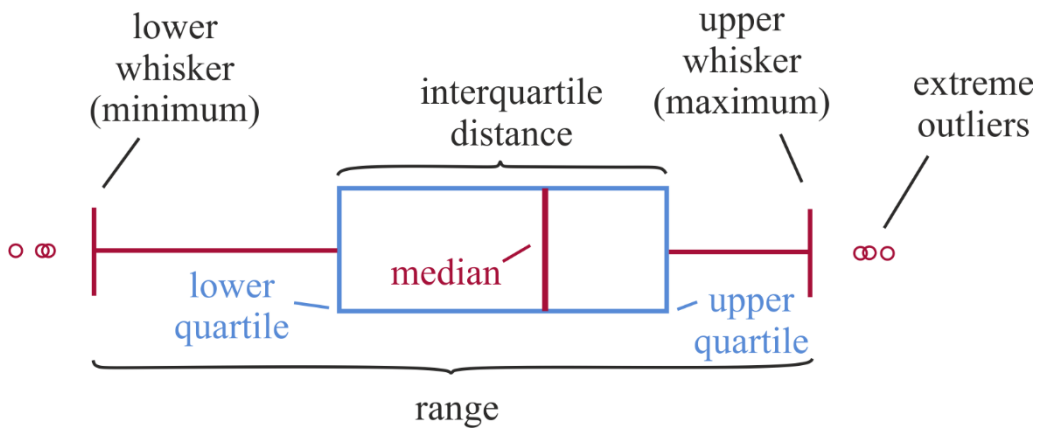

Fig. 29: Box-Whisker-Plot

In addition to the above mentioned five characteristic values, further properties of the data can be read from Fig. 29: the interquartile distance, the range *R* and the skewness. The interquartile distance represents the area in which 50 % of all measured data is situated. The range *R* gives an overview of the distance between the minimum and maximum value. Together with the size of the interquartile distance it is a first and very simple measure of dispersion of data. Large interquartile distances indicate a high dispersion while small interquartile distances mean that the measured data lie close to the median value. (Hemmerich, 2011)

The whiskers, sometimes also called the “antennas”, are not always used. In this case the diagrams are only called box plots. In general, the whiskers represent the minimum and maximum values, although there is no uniform regulation. Hence, the whiskers sometimes refer to the interquartile distance. Data points that are classified as extreme outliers can be plotted separately in the form of little asterisks (see Fig. 29).

5.2.1 Skewness in box-plot

The skewness of the distribution function can be determined from the position of the median within the box. Fig. 30(b) shows that if the median is exactly in the middle of the box, the underlying frequency distribution is symmetrical, otherwise it is asymmetrical. If the median is rather on the left side of the box, the distribution of data is right-skewed (see Fig. 30(a)). On the other hand, if the median is rather on the right side of the box, a left-skewed distribution is present (see Fig. 30(c)). However, these statements are only valid for unimodal distributions, i.e. distributions that only show one peak. In the case of bimodal (or even multimodal) distributions, a violin plot (see chapter 5.3) for data illustration should be preferred.

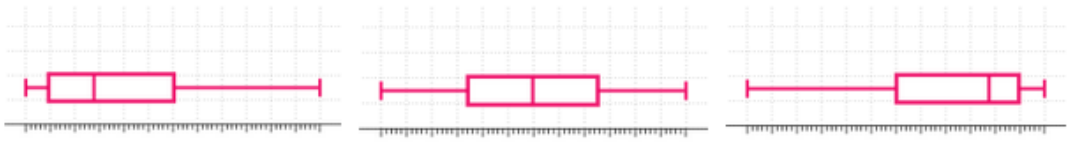

Fig. 30: Box-Whisker-Plot for skewed distribution functions (Hemmerich, 2011)

5.3 Violin Plot

The violin plot is a very useful tool for data analysis and illustration. As shown in Fig. 31, it combines the box plot with its density trace into one diagram. This means that additionally to medians, minimum and maximum values, also information about the density of data values is given. (Hintze & Nelson, 1998)

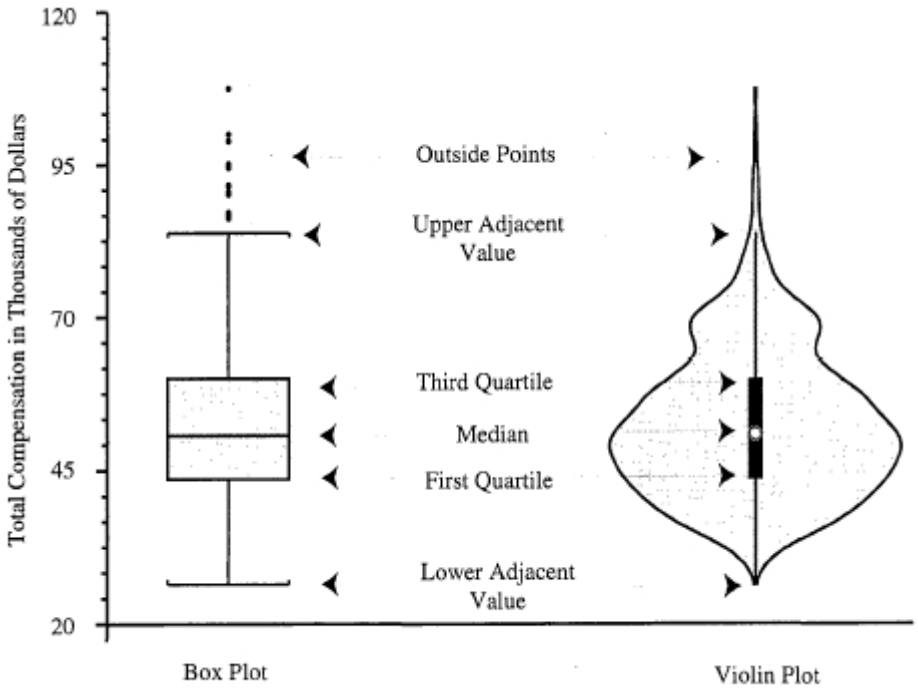

Fig. 31: Comparison Box plot to Violin plot (Hintze & Nelson, 1998)

There are different modifications for the violin plot, e.g. extreme outliers are not identified by individual symbols as it is done for box plots, which facilitates the quick readability of violin plots. The main advantage of violin plots is the additional information gain about the distribution of data. By the shape of the violin, it is easy to tell if the data is unimodal or bimodal distributed or if any skewness is apparent. (Hintze & Nelson, 1998)

6 Comparison of in-situ measurements

From Fig. 18 one can see that a total amount of 1468 penetration tests executed within Austria are available for data interpretation. It is important to mention that tests, that were only conducted to depths less than 3 m were neglected, as they don't show the appearance of fine sediments and therefore can't provide any interesting information about the deeper situated (fine sedimented) soil layers. After neglecting all those tests, the data of 1299 available tests remain. Fig. 32 gives a similar overview as Fig. 23, but this time only tests that were performed deeper than 3 m are included.

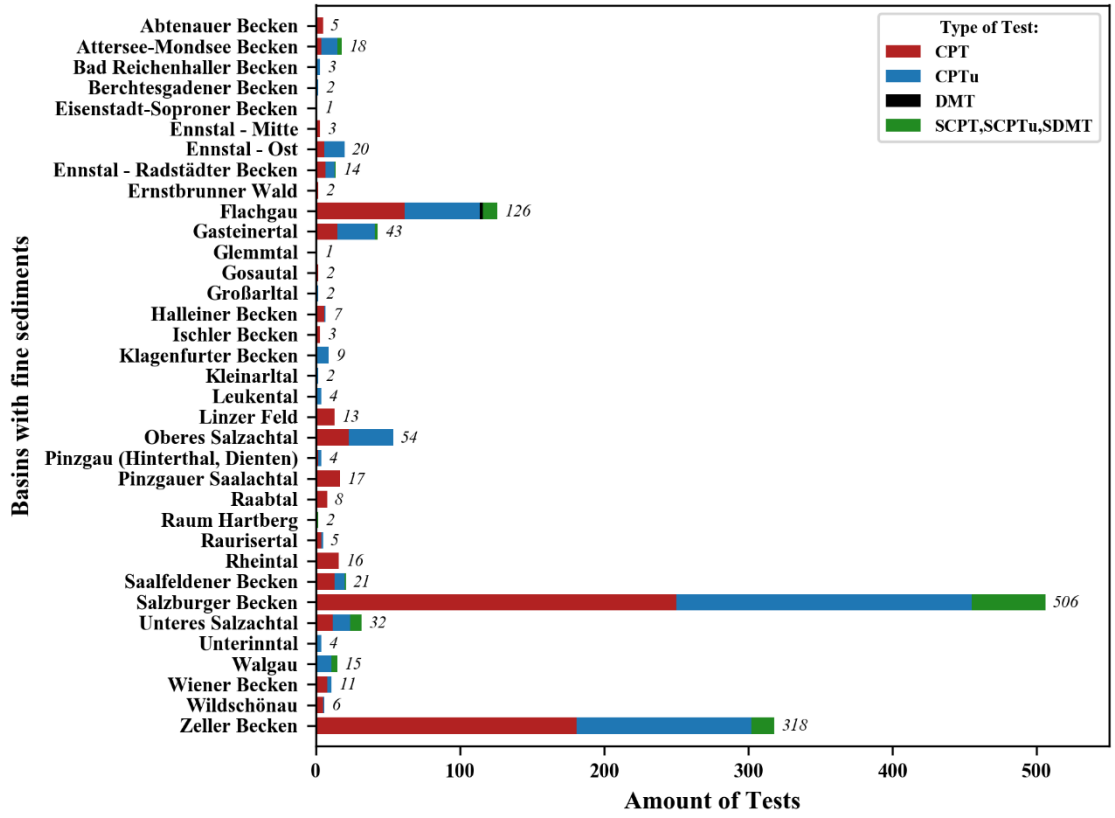

Fig. 32: Overview of in-situ tests for data interpretation

In this chapter, the in-situ measurements of the database are investigated regarding different aspects. First, chapter 6.1 gives a comparison of the in-situ measurements over depth for all basins. In chapter 6.2 regional differences within one basin are discussed using the examples of Salzburg, Zell and Flachgau because those are the three regions with the greatest amount of test data. In chapter 6.3 a comparison of in-situ measurements is performed based on the grain-size distribution. Chapter 6.4 discusses the soil type distribution over depth by means of density plots, histograms and horizontal stacked percentage bar charts.

6.1 Comparison of in-situ measurements

In the following, several graphs are presented that show the distribution of the tip resistance q_c, the sleeve friction f_s, the friction ratio R_f and the shear wave velocity V_s that are measured within the basin of Salzburg, Zell am See as well as the region of Flachgau. Only a small number of tests were executed deeper than 25 m, which is why the results of in-situ measured values is only presented up to this depth. In later sections of this thesis it gets obvious that the measured data is not normally distributed. This is the reason why calculating the median values of all in-situ measured values over depth is chosen over the calculation of mean values. Consequently, not the standard deviation but the 25% and 75% quartiles were used as a measure of the dispersion of data. In Fig. 33, the in-situ measured data over depth is shown for the basin of Salzburg. The red lines represent the median, the grey shadow shows the range between the first and third quartile and the dashed lines the range between minimum and maximum value for certain depths. The same graphs are presented for the basin of Zell and the region of Flachgau in Fig. 34 and Fig. 35, respectively.

All three figures show similar tendencies: higher tip resistances and sleeve frictions near the surface and decreasing resistances with increasing depth. In accordance to that the friction ratio is slightly increasing where the tip resistance and sleeve friction are decreasing. The exact values on which Fig. 33, Fig. 34 and Fig. 35 are based on, can be found in Excel Files that are included on the attached CD.

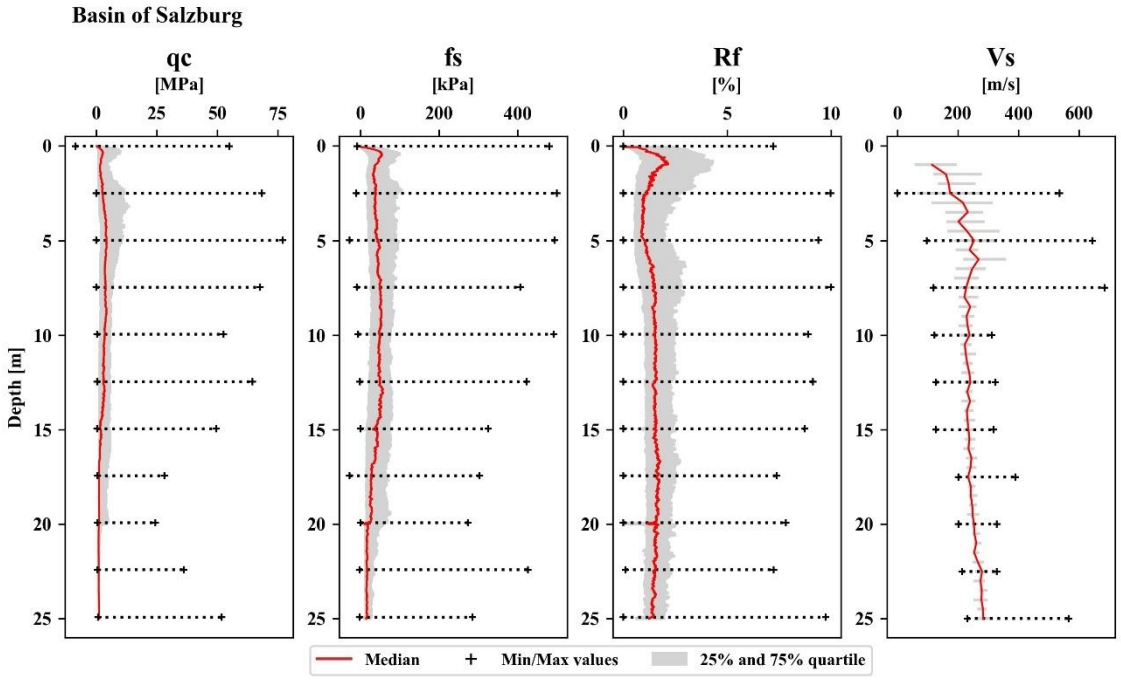

Fig. 33: In-situ measurements within the basin of Salzburg

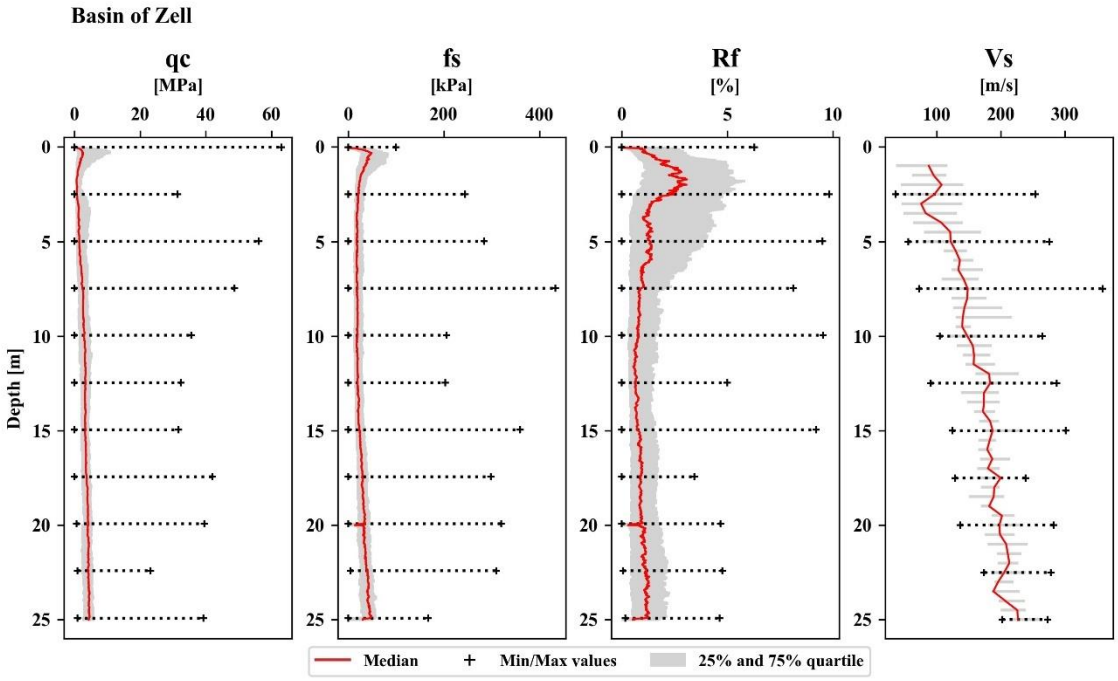

Fig. 34: In-situ measurements within the basin of Zell

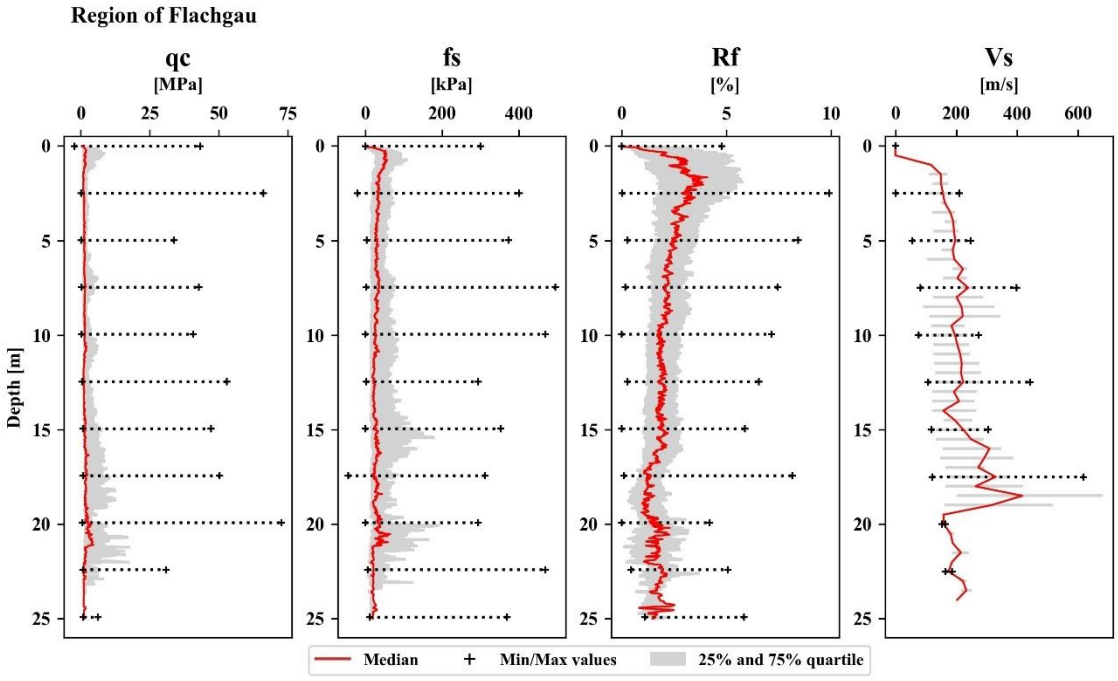

Fig. 35: In-situ measurements within the region of Flachgau

According to Douglas and Olsen (1981), higher friction ratios (ratio between sleeve friction and tip resistance) indicate softer soils with a higher fines content. These results are in good agreement with reality as we know that in Salzburg the so-called “Salzburger Seeton”, a very soft fine-grained soil, prevails in depths between -10 to -25m. It can also be seen that the range within the 25% and 75% quartile decreases with increasing depth. This again is proof for an increasing homogeneity and therefore increasing fines content with depth especially within

the basin of Salzburg. The basin of Zell shows a rather small scatter for the tip resistance and the sleeve friction when looking at the quartiles. The latter is pretty high when it comes to the friction ratio R_f. The region of Flachgau also shows a higher scatter of data with increasing depth. This leads to the conclusion that the basin of Zell and the region of Flachgau show a greater heterogeneity within their region.

Within basins local differences can occur. Hence, an overall comparison of an entire basin is not the best approach. Consequently, a separation of areas within one basin should be preferred to work out those regional differences. This elaboration can be found in chapter 6.2.

In general, it can be said once again that the basin of Salzburg, the basin of Zell and the region of Flachgau, all three show an increasing fines content with increasing depth. As a comparison to that, results for the Pinzgauer Saalachtal are shown in Fig. 36. It can be seen that the values for the tip resistance q_c and sleeve friction f_s are higher and the friction ratio R_f is lower than for the previous regions. The exact values are again included via an Excel File on the attached CD. No shear wave velocity measurements are present for this valley. However, the distribution, as it is shown in Fig. 36, clearly states the presence of a coarser grain size distribution within the Pinzgauer Saalachtal.
This leads to the conclusion that valleys consist of coarser-grained soils while in basins finer-grained soils prevail. To prove latter statement, Fig. 37 was elaborated. This figure contains all distributions of median values of q_c, f_s and R_f for all basins and valleys for which data was available in Austria. All red lines represent medians for regions that were declared as valleys, while the green lines represent medians from all basins. It can be seen that for the tip resistance q_c and the sleeve friction f_s the red lines, so the valleys, show higher median values over depth while the friction ratio R_f is lower for valleys. For the basin it is generally the other way around. Of course, slight deviations are evident. It should be noted that small basins within valleys are possible, which can cause those deviations. Therefore, the division into basin and valley is not too strict. Nevertheless, the tendency of coarser-grained soils occurring in valleys can be proven by Fig. 37. The distribution of in-situ measurements over depth for all other available basins and valleys, can be found in Appendix C.

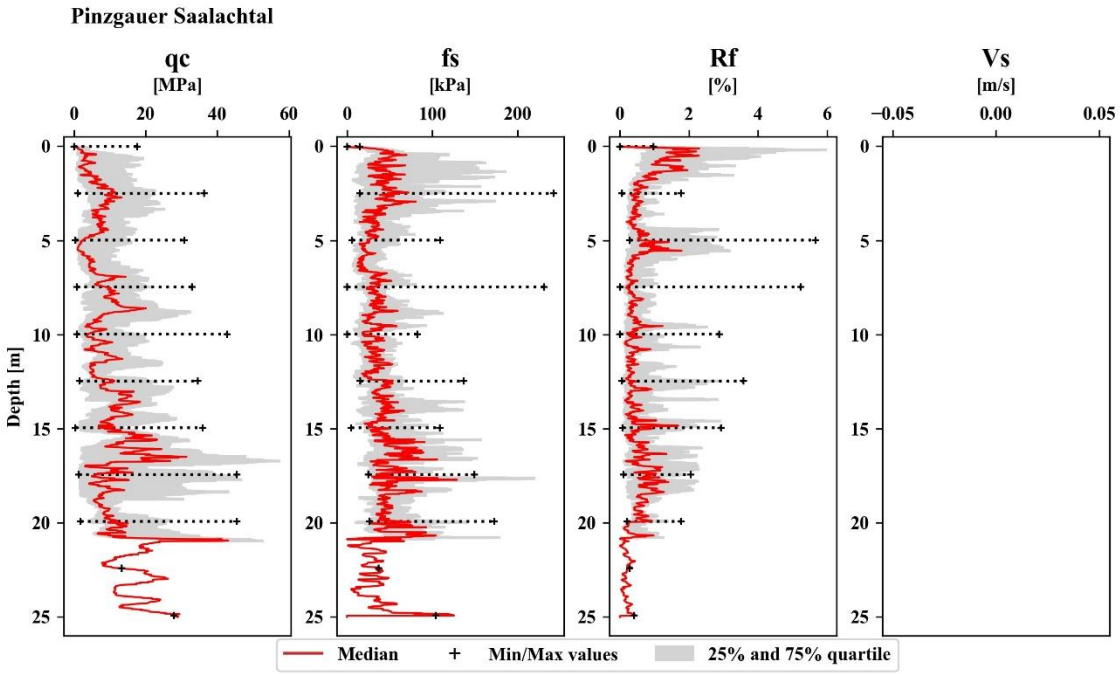

Fig. 36: In-situ measurements for the Pinzgauer Saalachtal

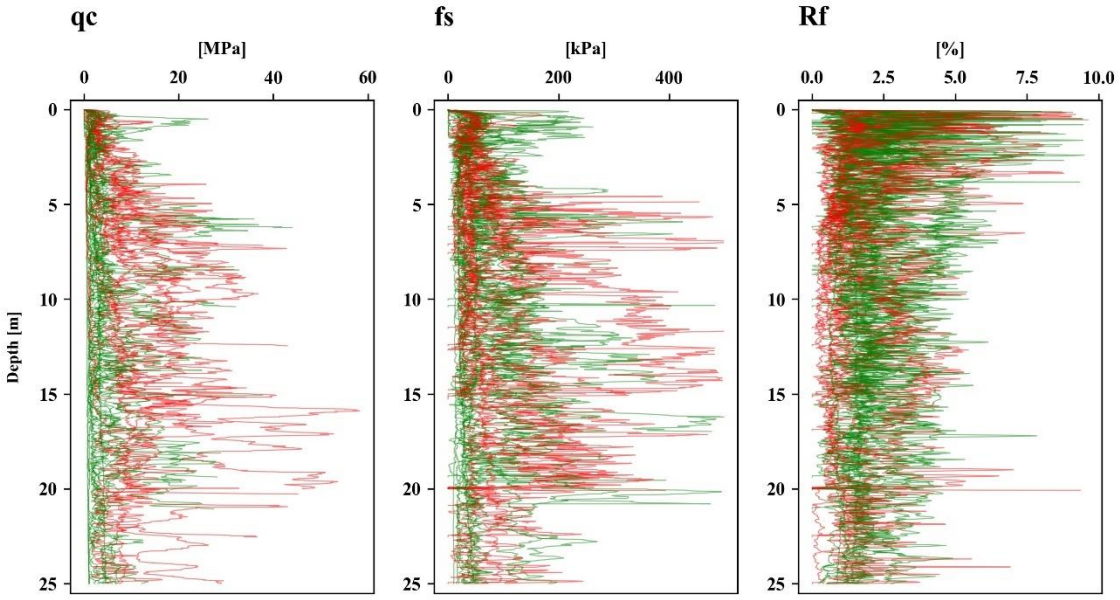

Fig. 37: Comparison of in-situ measurements for basins (green) and valleys (red) using the median values

6.2 Heterogeneities within basins

Due to different physical, chemical and environmental formation processes within a basin, it appears that regional differences regarding soil layering and stratigraphy may occur. In the following chapter, these local differences within one basin are worked out by comparing the cadastral communities within the basin. This is done for the basin of Salzburg, the basin of Zell and the region of Flachgau. For the other basins and valleys there isn't enough data present for general statements. At the beginning of each chapter, a graph of all existing cadastral communities within the region is presented. It intends to give an overview of the type of available test data and its amount.

6.2.1 Basin of Salzburg

In the basin of Salzburg, a total amount of 506 tests was used for a comparison of all in-situ measured values. The four cadastral communities Salzburg, Gnigl, Voggenberg and Liefering II were chosen for further investigation as those were the ones with the most data available according to Fig. 38.

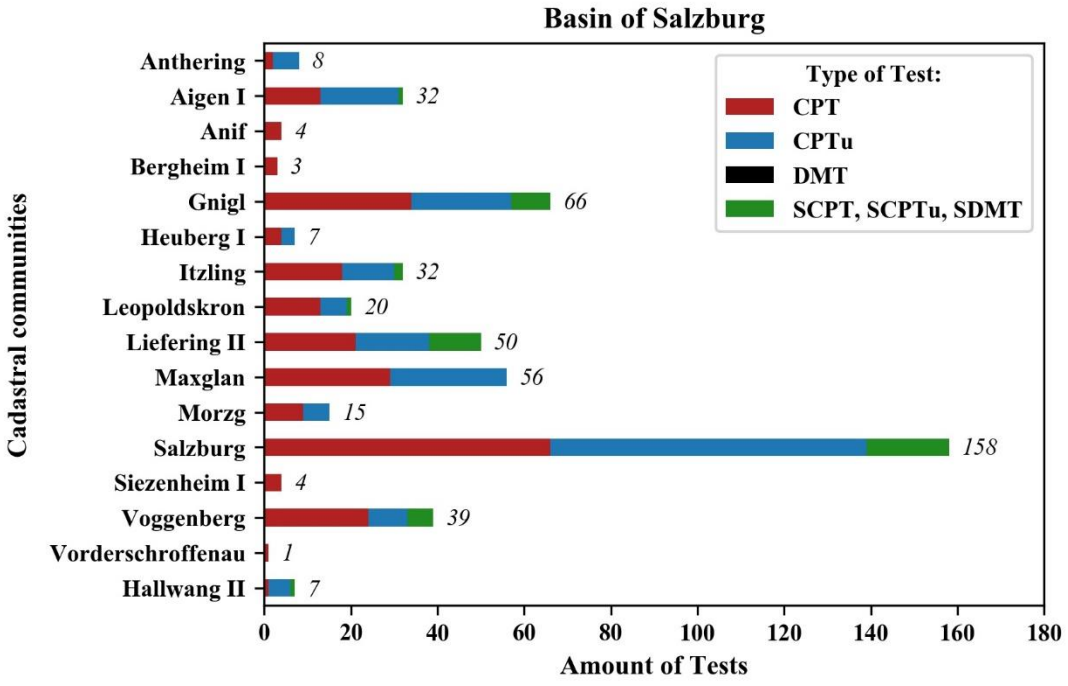

Fig. 38: Overview of in-situ tests executed within the basin of Salzburg

In Fig. 39 the geographic location of the four cadastral communities within the basin of Salzburg is shown. It can be seen that Salzburg and Gnigl represent the city centre of Salzburg, while Voggenberg and Liefering II are located in the more northern part of the basin of Salzburg.

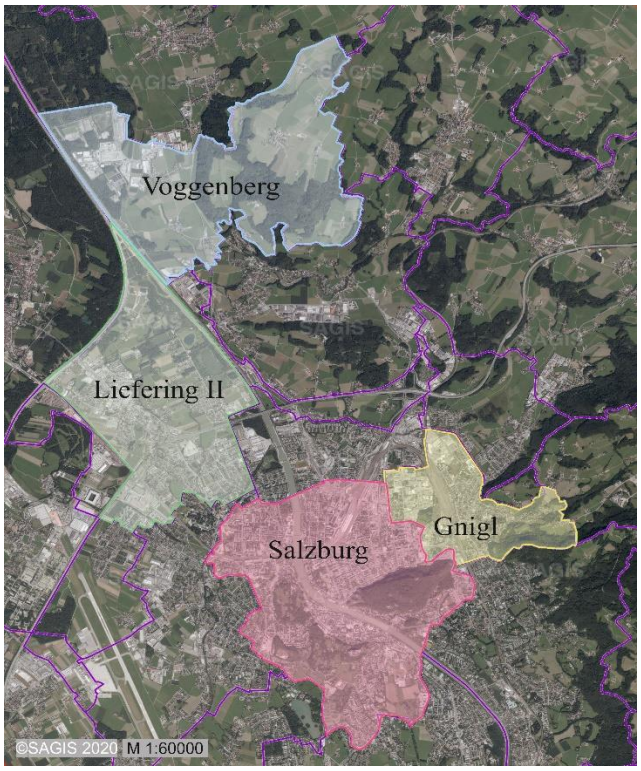

Fig. 39: Location of cadastral communities within the basin of Salzburg

Fig. 40 shows median values and the first and third quartile over depth for the tip resistance q_c, the friction ratio R_f and the shear wave velocity V_s. It can be seen that the tip resistance decreases with increasing depth for all four cadastral communities while the friction ratio increases. They all show the same tendency but it is obvious that the distribution is different for all four. Salzburg and Gnigl generally show lower tip resistances, especially after a depth of - 15m. The very low resistances in Gnigl, especially between depths of -2m to -5m, lead to the conclusion that softer, very fine-grained soil prevails which is in good agreement with observations made in Gnigl, as they often have problems with constructions regarding settlements. Very differently to that, high tip resistances with a large scatter (grey shadow) appear in Voggenberg within the first 7 meters. Consequently, it can be concluded that soils are coarser grained in Voggenberg. Nevertheless, in a depth of about -20m all four communities show values for q_c in the same range of about 1-3 MPa. So, with increasing depth the values converge. The measured shear wave velocities slightly increase with depth which can be explained by the increase of vertical in-situ stress.

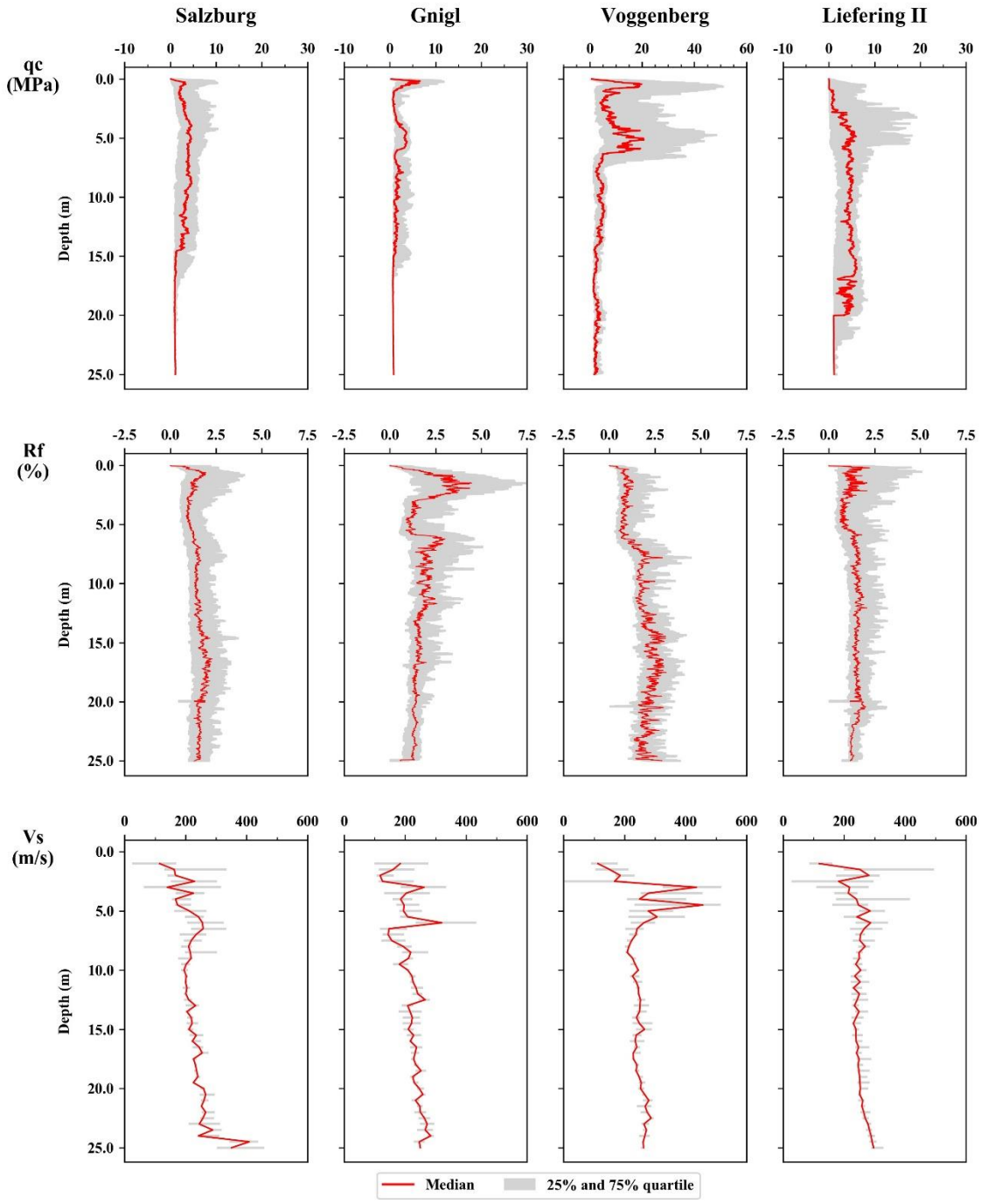

Fig. 40: Comparison of in-situ measurements for the cadastral communities Salzburg, Gnigl, Voggenberg and Liefering II

6.2.2 Basin of Zell

For the basin of Zell, 318 in-situ tests are available for data interpretation. The four cadastral communities Kaprun, Bruck, Bruckberg and Zell am See were chosen for the comparison of in-situ measurements in Fig. 43. It should be noted that both villages ‘Zell am See’ and ‘Schüttdorf’ belong to the cadastral community Zell am See. These two villages can differ in their characteristics due to their location. This is explained more precisely in chapter 6.4.2. However, this was ignored in the following, which can have influence on the results.

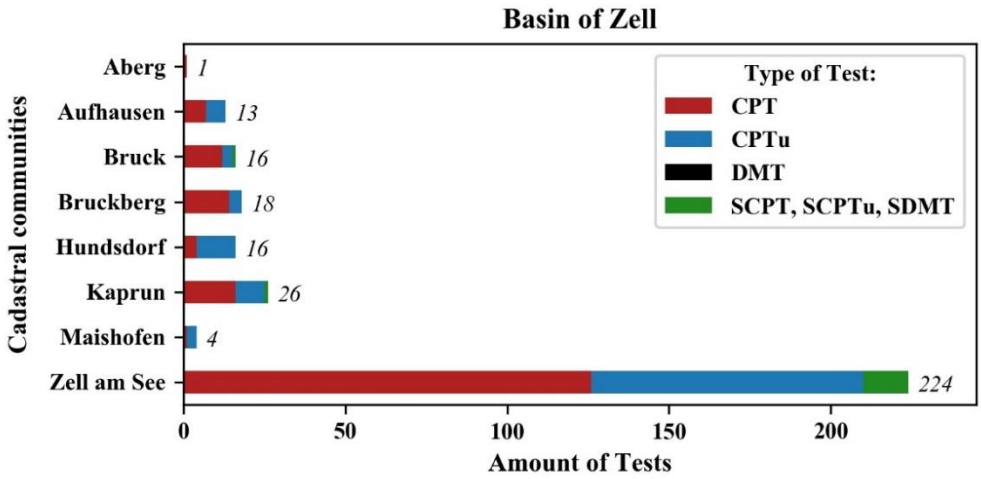

Fig. 41: Overview of in-situ tests executed within the basin of Zell

It gets immediately obvious that the basin of Zell is characterized by a higher heterogeneity within the basin, because the first two cadastral communities (Kaprun, Bruck) show very high tip resistances with a large scatter, whereas Bruckberg and Zell am See show low tip resistances with a smaller scatter. Furthermore, from the higher values of the friction ratio in Bruckberg, it can be concluded that very fine-grained soil predominates. The fact that there are 224 tests in Zell am See and only about 20 tests for each of the other cadastral communities, smears the overall result for the whole basin of Zell, which gave the impression of a very heterogenous basin (Fig. 34). In addition to that, it becomes obvious that with increasing number of tests, the distribution of in-situ measured values gets smoother and more homogeneous. These are all reasons why it is so important to take a closer look at the individual cadastral communities to show that Zell actually has a higher heterogeneity within its basin as thought.

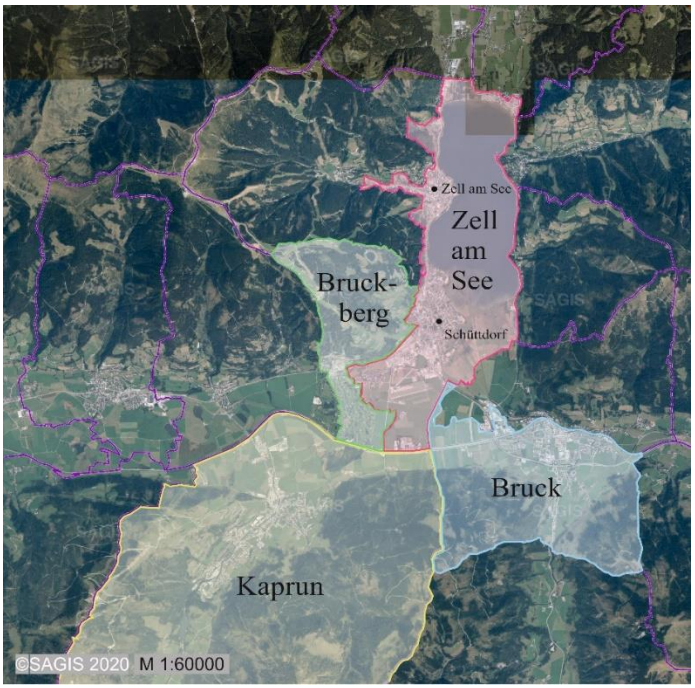

Fig. 42: Location of cadastral communities within the basin of Zell

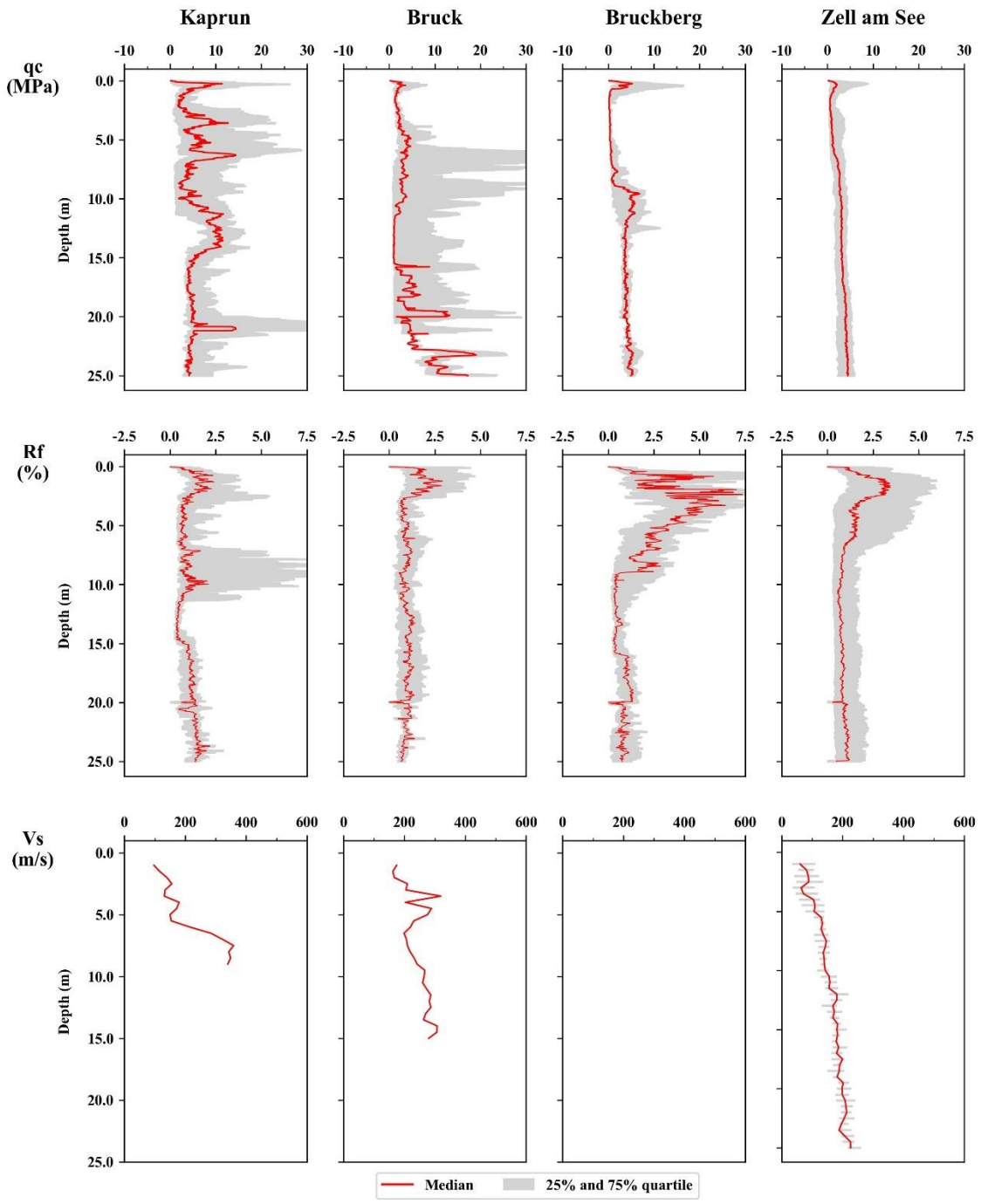

Fig. 43: Comparison of in-situ measurements for the cadastral communities Kaprun, Bruck, Bruckberg and Zell am See

6.2.3 Region of Flachgau

For the region of Flachgau 126 available tests were the basis for an investigation within this area. The four cadastral communities Oberndorf, Bürmoos, Weitwörth and Obertrum were chosen for elaboration of the regional differences.

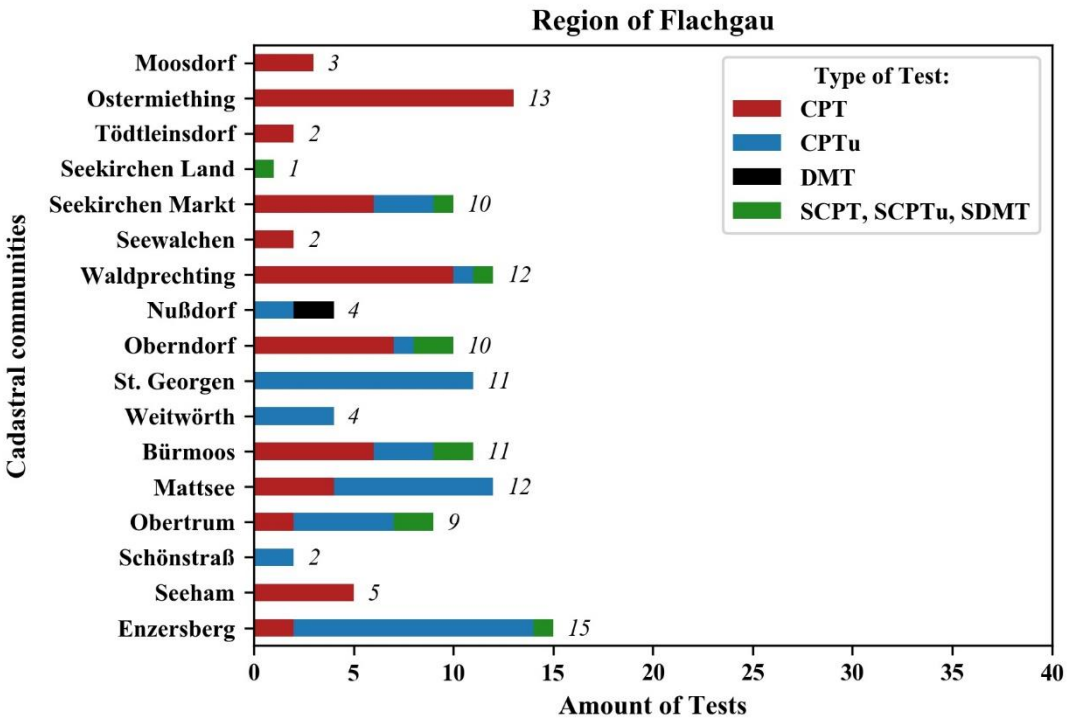

Fig. 44: Overview of in-situ tests executed within the region of Flachgau

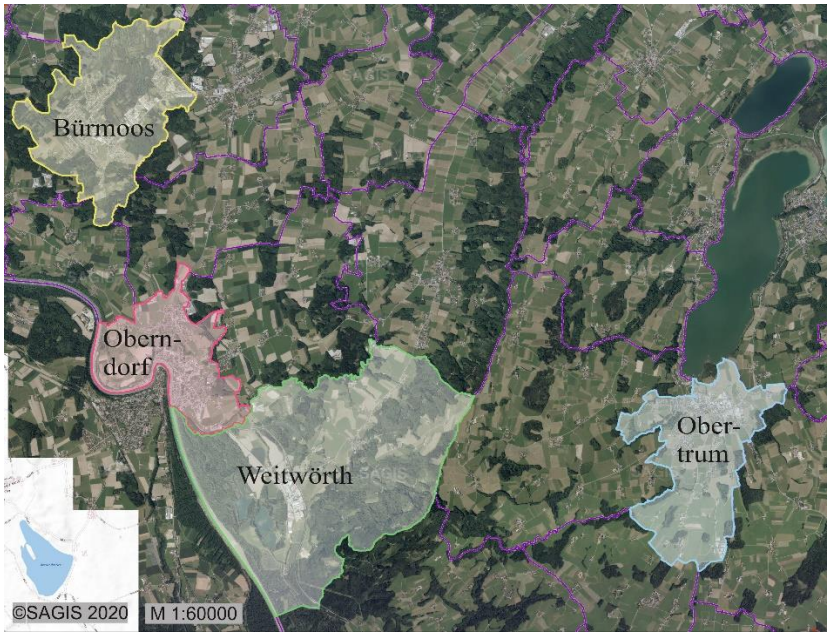

Fig. 45: Location of cadastral communities within the region of Flachgau

Fig. 46 shows that Oberndorf is characterized by small tip resistances with a very small scatter down to a depth of about -18 m, where the sudden increase of q_c as well as V_s clearly implies the appearance of a coarser soil layer (probably river gravel). A similar distribution shows the cadastral community Bürmoos although the top layer shows a slightly higher scatter and at a depth of about -10m a thin coarse interlayer appears. In contrary to that, the cadastral communities Weitwörth and Obertrum do not show the appearance of river gravel at the depth of -25 m at all. Fine, soft soils prevail in that depth. It can nicely be seen that the latter two

communities show the appearance of coarse soil layers within depths of -7 m to -9 m and between -16 m and -18.5 m. For Weitwörth no seismic tests were available to work out a distribution of V_S. Fig. 46 nicely shows that the distribution of in-situ measurements over depth of the first two and the last two cadastral communities are in good agreement with each other and differ strongly from the other two.

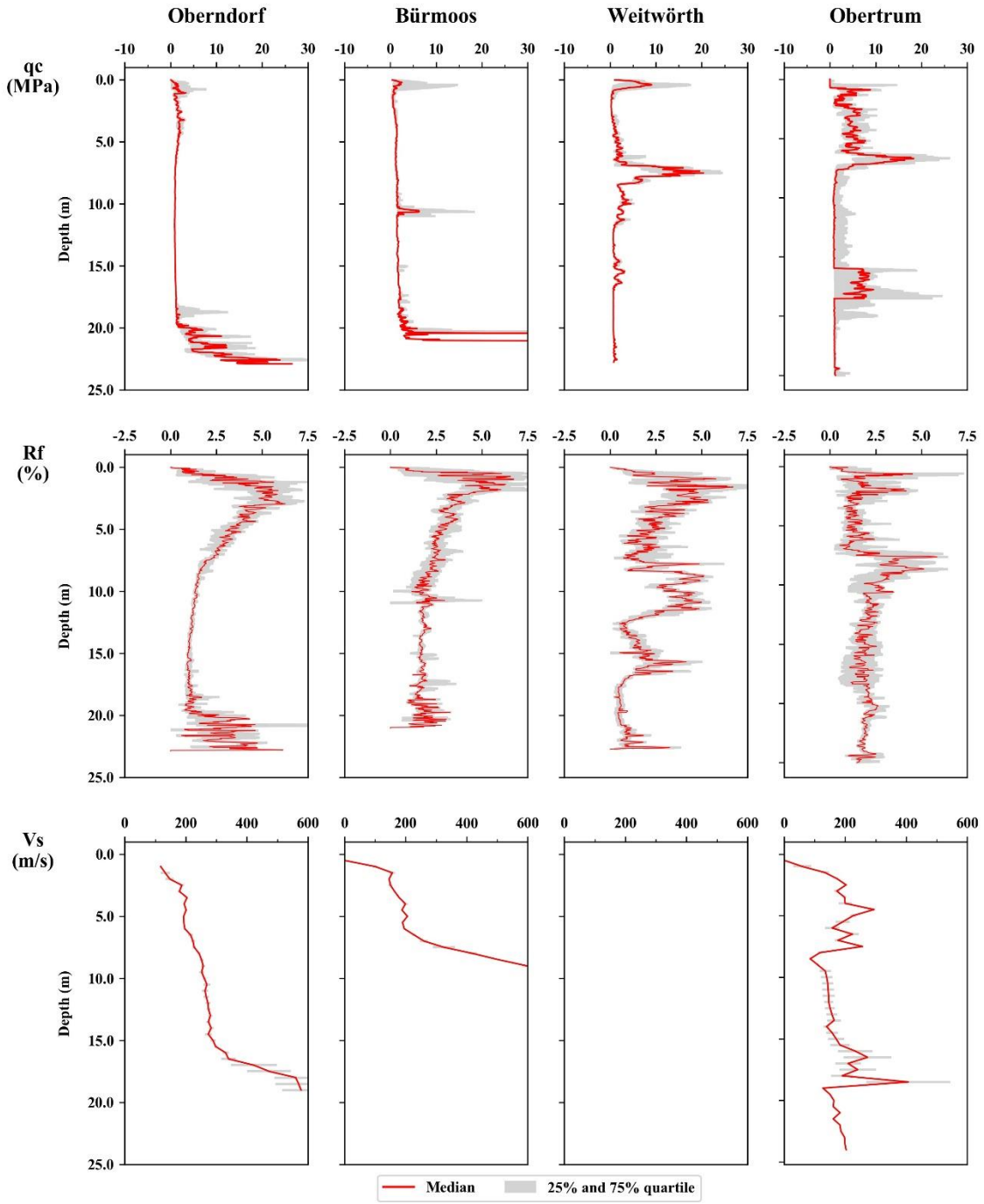

Fig. 46: Comparison of in-situ measurements for the cadastral communities Oberndorf, Bürmoos, Weitwörth and Obertrum

6.2.4 Comparison of Salzburg, Zell and Flachgau

In this section, the heterogeneity of the three basins is evaluated. In a first step, the heterogeneities of Salzburg, Zell and Flachgau are compared in Fig. 47. The thick layer shows the difference between the third (upper) and first (lower) quartile. The coloured shadow in the background shows the original range between the first and third quartile. These values should decrease with increasing homogeneity, which means that large values imply a higher heterogeneity. In Fig. 47 it can be seen that the basin of Salzburg (red) shows the following tendency: higher heterogeneities in the top layers and lower heterogeneities in the deeper layers, where the so called Salzburger Seeton is situated. The region of Flachgau (blue) shows a lower heterogeneity in the upper 15 m for q_c and f_s, while in deeper layers a higher heterogeneity appears. This is due to different appearance depths of the river gravel. In Salzburg, no river gravel appears at all until a depth of -25 m. The basin of Zell (green) is interesting, as the distributions over depth show rather low values which would wrongly lead to the conclusion that within the basin of Zell very homogeneous conditions occur. However, experience has shown that this is not the case. The reason for this deficiency is caused by the large number of tests that are available in the cadastral community of Zell am See (224 tests = 70% of all test data within this basin) which all show a very homogeneous distribution of test results, while the other cadastral communities cannot prove the contrary due to the lack of existing tests.

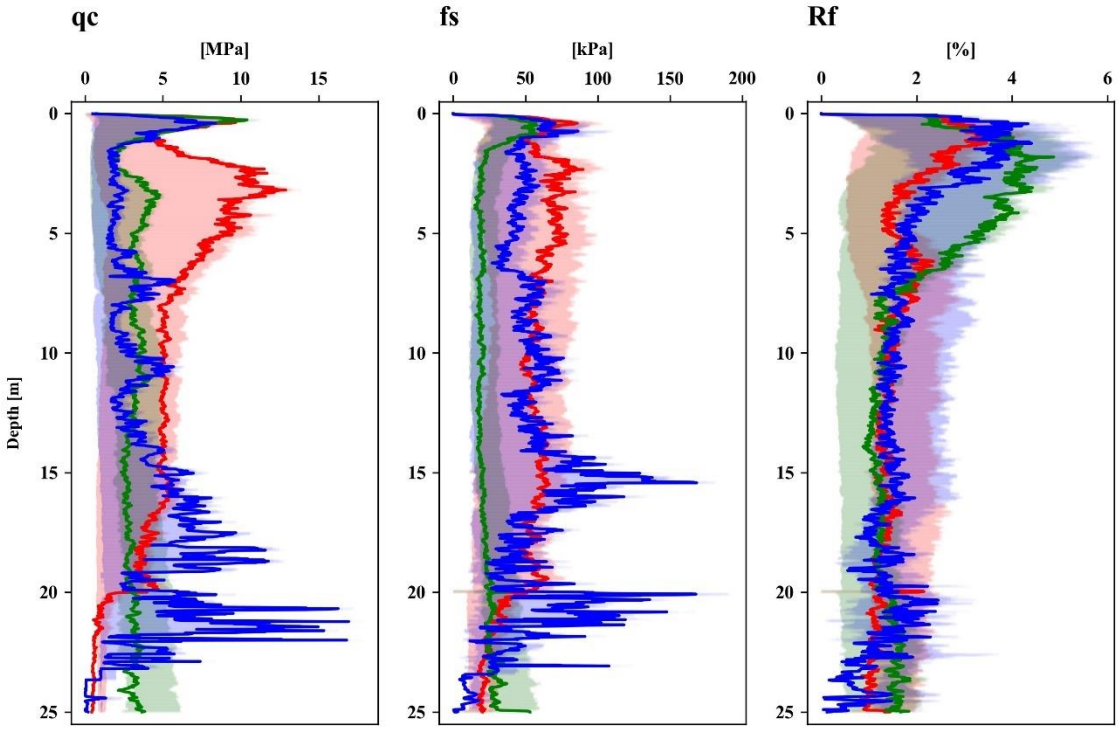

Fig. 47: Comparison of heterogeneity for Salzburg (red), Zell (green) and Flachgau (blue)

Additionally, another chart was elaborated to show that basins are generally characterized by a lower heterogeneity than valleys. In Fig. 48, the different lines

represent the difference between the third and the first quartile. Therefore, higher values stand for a higher heterogeneity, while lower values stand for a lower heterogeneity. All red lines represent the regions that were declared as valleys while the green lines represent the basins. It can be observed that for the tip resistance and the sleeve friction generally the red lines, so the valleys, show higher values and therefore higher heterogeneities than the basins (green lines) do. For the friction ratio it can be seen that the green lines show higher values, which is again proof that in basins finer-grained soils with lower heterogeneities appear.

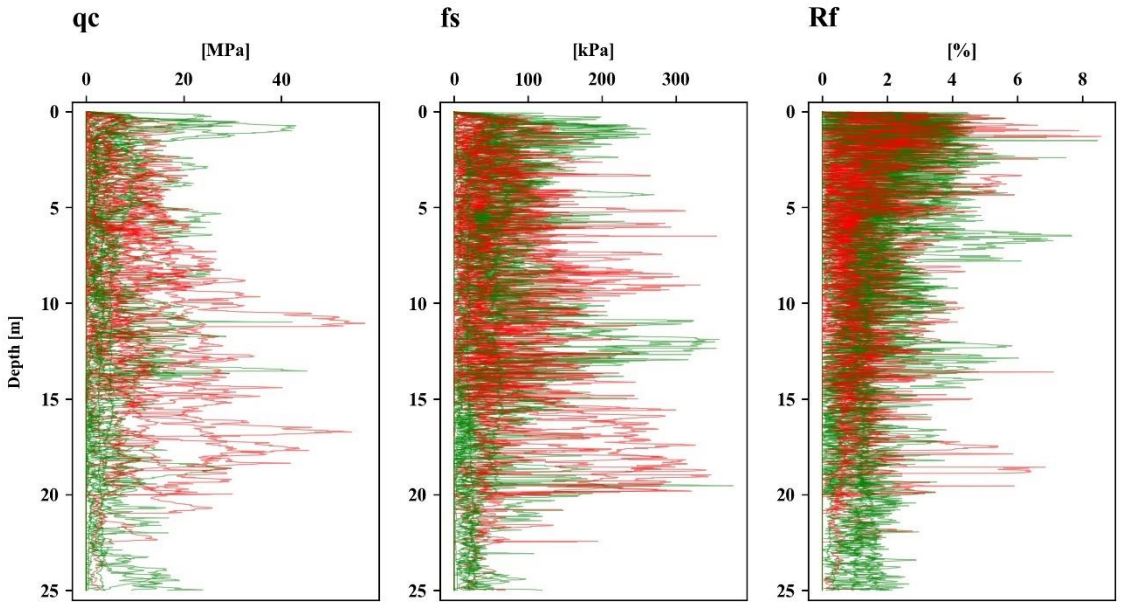

Fig. 48: Comparison of heterogeneity for basins (green) and valleys (red) based on the difference of 75% and 25% quartiles

6.3 Comparison of in-situ measurements based on the grain-size distribution

As discussed in the preceding chapters, soil layering and the transition between different soil layers can vary within a basin and within a cadastral community. Even within several meters, soil layering can strongly differ because of different formation processes that happened ages ago. Furthermore, the absolute altitude was not considered and might influence the result. As a consequence, there is a great risk of comparing different soil types against each other at a given depth when combining all in-situ measured values for one whole region. In order to avoid that, an additional comparison of the in-situ measured values based on the grain size distribution and the soil genesis was performed next to the comparison of the in-situ measured values depending on their location, which was presented in chapters 6.1 and 6.2. In the following chapters, the results of this comparison regarding the tip resistance q_c, the sleeve friction f_s, the friction ratio R_f and the shear wave velocity V_s, based on the grain size distribution is presented.

6.3.1 Soil group classification

Based on the total number of 282 core drillings - executed next to the penetration tests - an allocation of soil type to in-situ test was performed. For the basin of Salzburg, the basin of Zell and the region of Flachgau 168, 35 and 23 core drillings were available, respectively. The remaining 56 core drillings were found in other basins of Austria. As already stated in chapter 4.3.1, a maximum distance of 100 m between the core drilling and the in-situ test was considered in order to correctly allocate soil layers to their appearing depth. All suitable soil types that were found in the core drillings were assigned based on their grain size to one of six main soil groups. The six soil groups are presented in Tab. 2. During the process of grouping, a couple of soil lithologies were found unsuitable for categorization. E.g. a soil lithology classified as "Si, Cl, Sa, Gr, x" (gravelly sandy clayey silt with occurring stones) showed too high grading and could therefore not be clearly assigned to one of the six main soil groups. Soils like these were neglected in the classification process. The detailed listing of the soil lithologies within the soil group classification for the basin of Salzburg, the basin of Zell and the region of Flachgau can be taken from Appendix D.

Tab. 2: Overview of the soil group classification based on the grain size distribution

Soil group	Grain-size distribution	Genesis
1	CSa → Gr	coarse sand → gravel
2	Pt	peat
3	FSa → CSa	fine sand → coarse sand
4	Si, fsa → FSa, si	fine sandy silt → silty fine sand
5	Si, cl- → Si, fsa-	clayey silt → fine sandy silt
6	Si, Cl → Si, cl	Silt, Clay → clayey silt

Last but not least, it is important to note that soil groups 1, 2, and 3 basically represent the rather shallow situated soil layers, while soil groups 4, 5, and 6, represent more likely deeper situated soil layers. Especially in the case of the basin of Salzburg, one can say that soil groups 3 and 4 represent floating sediments which build the upper 'Salzburger Seeton', while soil groups 5 and 6 represent the lower 'Salzburger Seeton', a very homogeneous silty clay layer. Soil group 1 in general represents a very heterogeneous soil layer, mainly occurring in the very top layers. For soil group 2, all soil lithologies with peaty parts were grouped together, not primarily considering the actual grain size. This is why this soil group often shows a large scatter in the results which are presented in the following chapters.

6.3.2 Holistic evaluation

Based on the soil type classification of Tab. 2, a holistic comparison of the four in-situ measurements q_c, f_s, R_f and V_s for the soil lithologies was performed for all penetration tests for which core drillings were available. In Fig. 49, the data is presented as a box-plot. The squared markers represent the median value, while the dashed vertical lines, starting from the median value and directing downwards and upwards, represent the 25% and 75% quartile, respectively. In addition to that, the mean value is plotted in the charts (circled markers). It is immediately noticeable that the data is not normally distributed as the median and the mean value differ greatly from each other. It should be noted that for this kind of comparison all measured values that exceeded a value greater than 500 were deleted because extreme outliers may falsify the result. The reason for these extreme outliers can be shortcomings in the measurement.

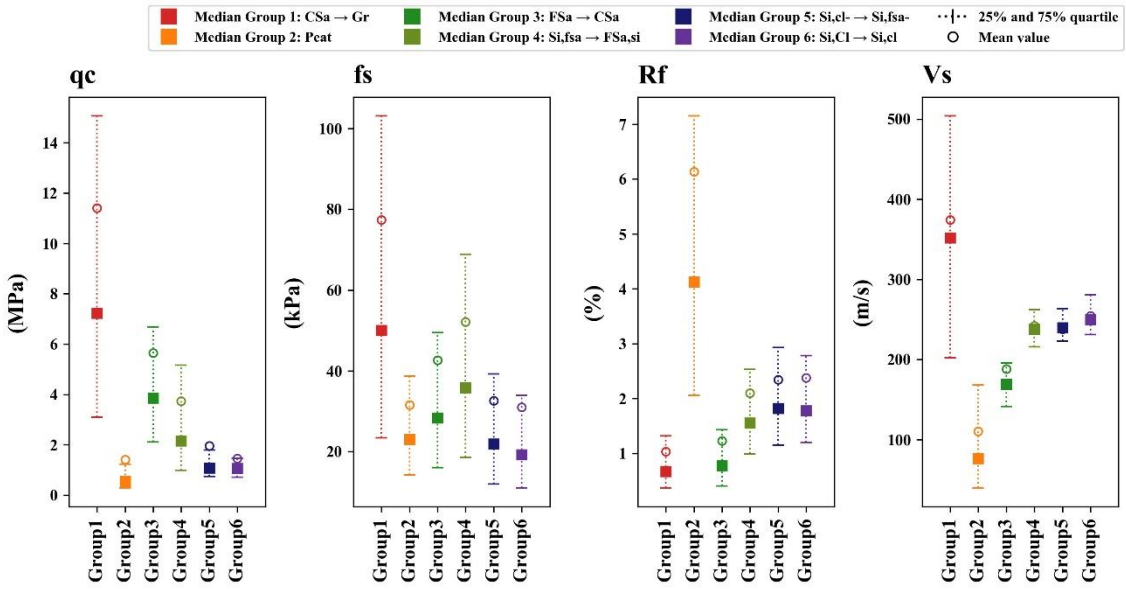

Fig. 49: Box-plot: Holistic evaluation of in-situ measurements based on the grain-size distribution

Tab. 3: Overview of median values: Holistic evaluation of in-situ measurements based on the grain-size distribution

Soil Group	q_c [MPa]	f_s [kPa]	R_f [%]	V_s [m/s]
1	7.23	50	0.67	379
2	0.54	23.1	4.13	85
3	3.86	28.4	0.78	297
4	2.16	35.8	1.56	243
5	1.07	21.9	1.82	240
6	1.06	19.3	1.78	250

For soil group 1, which mainly covers the grain size distributions between coarse sand and gravel, the median values amount to q_c=7.23 MPa, f_s= 50 kPa, R_f=0.67% and V_s=379 m/s. It immediately becomes obvious that soil group 1 mainly consists of coarse-grained soils as the in-situ measured values are way higher than for soil groups 2 to 6. Additionally, the range between the 25% and 75% quartile is higher than for the other soil groups, which can be explained by the strong heterogeneity of this soil group. For soil groups 2 to 6 the individual medians for in-situ measured parameters are given in Tab. 3. The expected tendency, that fine grained soils show lower resistances to the penetration process can be validated by Fig. 49. With increasing fines content, so with increasing soil group numbering, the tip resistance q_c and sleeve friction f_s decrease, while the friction ratio R_f increases. Soil groups 5 and 6 are very fine-grained soils that show similarly low resistances. Also soil group 2, consisting of peaty soils, shows a low tip resistance and a low sleeve friction, while the friction ratio is relatively high. The shear wave velocities V_s for soil groups 4, 5 and 6, show very similar and stable results, as those layers represent more homogeneous soil types.

In addition to the box-plots, the in-situ measurements are compared using a violin plot. The advantage of the violin plot is that beside the median value and the lower and upper quartile, the entire distribution of the data can be shown. In Fig. 50 several violins are plotted for each soil group with respect to the tip resistance q_c, the sleeve friction f_s and the friction ratio R_f. The shear wave velocity V_s could not be plotted because too little number of tests were available and therefore the violins were not representable. Based on the violin plots it is shown that the available data is clearly not normally distributed. Skewed distributions with multiple peaks (bimodal distributions) are apparent.
It is important to note that for the boxplot in Fig. 49, extreme outliers were cut-off at values of ±500. The problem for the violin plot is that a cut-off at values of ±500 is still a very wide range which lead to a distortion of the violins and meaningless results. Therefore, new cut-off criteria for the violin plots were defined, individually for each in-situ measured parameter:

q_c : 0 – 20 MPa
f_s : 0 – 200 kPa
R_f : 0 – 10 %

The consequence of this measure is that the newly calculated median values for the violin plot differ from those for the box plot, because the number of values that lie above the newly defined cut-off criteria cause higher median values for the box-plot. Since higher tip resistances than 20 MPa or higher sleeve frictions than 200 kPa make no sense, the new median values from the violin plot should be used as reference values, as those are probably the more accurate ones. The updated median values are listed in Tab. 4. In Fig. 50, both median values are plotted. The black squared markers with the dashed lines downwards and upwards represent the median, the 25% and the 75% quartile values from Fig. 49, respectively, while

the small horizontal blue line represents the new changed median value. It is obvious that the difference between the original median and the changed median is smaller for soil groups 2,4,5, and 6 which are the more fine-grained soil groups that show a smaller scatter. For soil groups 1 and 3 the difference is much greater since those are the groups with a larger scatter and a larger number of outliers.

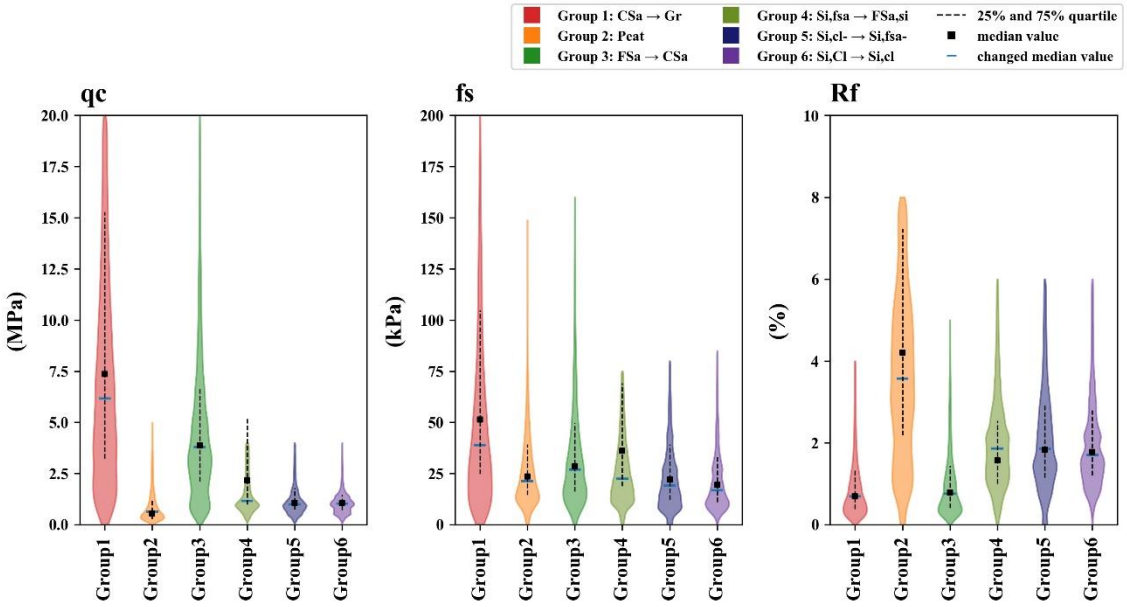

Fig. 50: Violin plot: Holistic evaluation of in-situ measurements based on the grain-size distribution

Thought should be given why measured values can be larger than a tip resistance >20 MPa and a sleeve friction >200 kPa. Individual extreme outliers can be explained through single stones or thin solidified layers that have been crossed during the penetration process. Another important question is how to handle more frequently occurring outliers. Simply cutting them off seems wrong as the tests have given these values and the results should not be manipulated manually. This is why they were considered in the boxplot and can be compared to the changed median values from the violin plot.

Tab. 4: Overview of median values (considering the new limits - see Fig. 50): Holistic evaluation of in-situ measurements based on the grain-size distribution

Soil Group	q_c [MPa]	f_s [kPa]	R_f [%]
1	6.17	38.9	0.69
2	0.63	21.4	3.57
3	3.79	26.9	0.76
4	1.16	22.5	1.86
5	1.0	19.1	1.85
6	1.02	16.9	1.7

For a normal distribution, the median value is situated in the widest area of the violin plot because this is where the most data points are situated (=expected value μ). By considering median values as a measurement for the expected value, this statement is correct for data that doesn't show a large scatter. In the case of the apparent data distribution, the median values do not always (e.g. soil group 1 and 3) coincide with the position where the violin is widest. In fact, even lower values for q_c, f_s and R_f would result if the values from where the violin is widest were taken. This leads to the conclusion that a large dispersion of data points significantly influences the determination of the median value. Consequently, care must be taken when considering the cut-off criteria and determining an expected value μ.

6.3.3 Comparison of Salzburg, Zell and Flachgau

From the previous chapter it can be concluded that with increasing fines content, the resistances to penetration reduces and that the range between the 25% and 75% quartile decreases, which leads to the conclusion that the soil groups get more homogenous with increasing numbering. To elaborate differences between the basins of Salzburg and Zell as well as the region of Flachgau, the box-plots and violin plots are discussed separately in this section.

Basin of Salzburg

In Fig. 51, the in-situ measurements based on the grain size distribution are presented for the basin of Salzburg. When comparing this figure with Fig. 49 (holistic evaluation) a very similar distribution can be observed. This is because most of the data from the holistic comparison originates from the basin of Salzburg. Therefore, when comparing Tab. 3 with Tab. 5, the values in both tables follow the same tendency, with increasing fines content the resistance to penetration reduces while the friction ratio R_f increases. All six values for the shear wave velocity V_s lie in a range between 241.5 [m/s] and 269.5 [m/s]. Thus, they only differ by a maximum value of about 10%. As seismic penetration tests are carried out less frequently, less data is available to compare the shear wave velocities. For the basin of Salzburg, no data corresponding to soil group 3 was available for determining V_s.
The violin plot for the basin of Salzburg is shown in Fig. 52. It follows the same assumptions as for the holistic evaluation regarding the cut-off criteria. Again, it can be seen that soil group 1, the very heterogeneous soil group with a large scatter in data, shows deviations between the original median values and the changed median value. The exact values for the two different medians are listed in Tab. 5 and Tab. 6.

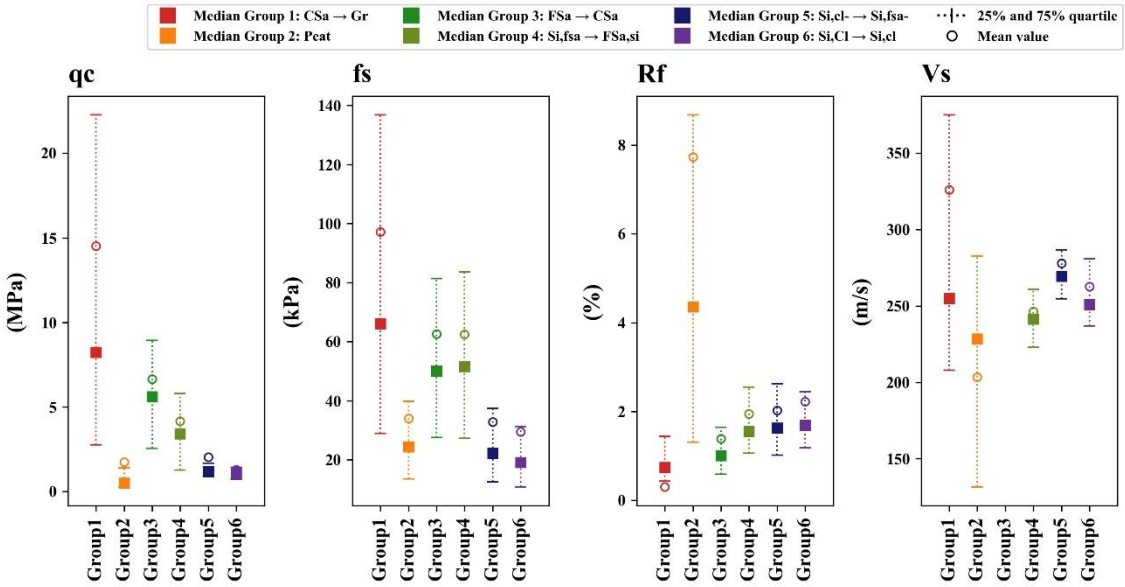

Fig. 51: Boxplot: In-situ measurements from the basin of Salzburg

Tab. 5: Overview of median values: In-situ measurements from the basin of Salzburg

Soil Group	q_c [MPa]	f_s [kPa]	R_f [%]	V_s [m/s]
1	8.23	66.1	0.74	255
2	0.51	24.4	4.36	228.5
3	5.62	50.1	1.01	-
4	3.41	51.6	1.55	241.5
5	1.19	22.3	1.63	269.5
6	1.08	19.2	1.69	251

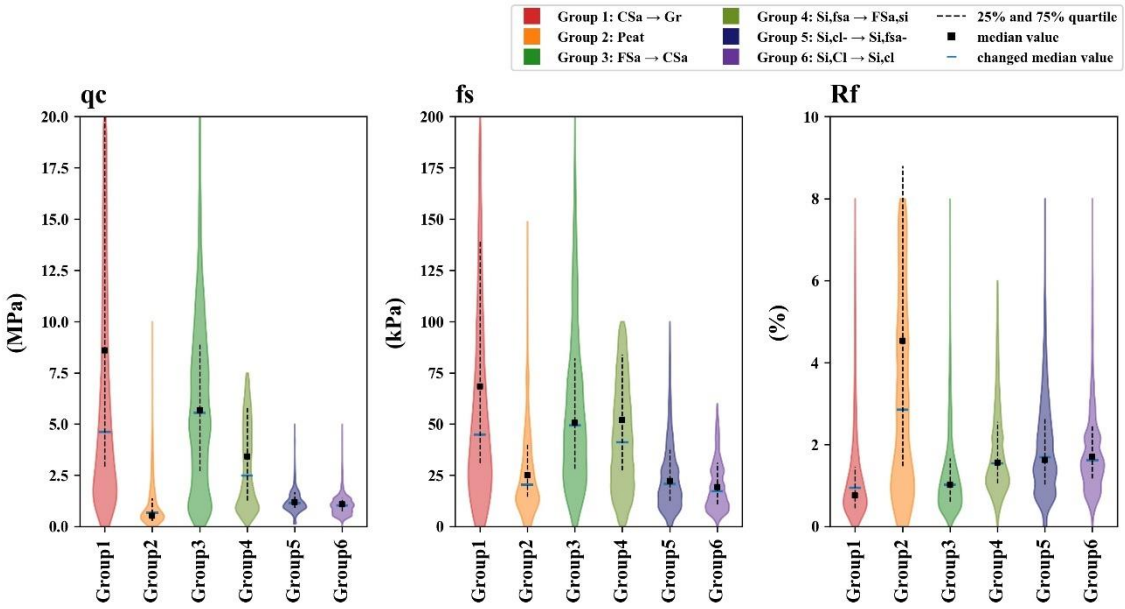

Fig. 52: Violin plot: In-situ measurements from the basin of Salzburg

Tab. 6: Overview of (updated) median values: In-situ measurements from the basin of Salzburg

Soil Group	q_c [MPa]	f_s [kPa]	R_f [%]
1	4.62	44.9	17.2
2	0.6	21.9	0.94
3	5.55	49.4	3.45
4	3.31	48.5	1.02
5	1.14	20.8	1.5
6	1.03	17.2	1.69

Basin of Zell

When performing the same comparison for the basin of Zell, it can be seen that nearly the same tendency is achieved, although in general the values for q_c and f_s are lower than for the basin of Salzburg (Tab. 5) and for the holistic evaluation (Tab. 3). It can also be observed that the sleeve friction for soil group 4 is higher than for soil group 3, as well as soil group 6 compared to soil group 5.
When having a closer look at soil group 5 of the basin of Zell, it can be seen that this soil group shows higher q_c resistance values than soil group 4 of the same basin. This can also be due to the higher stress level as soil group 5 generally occurs at greater depths. In general, when investigating soil group 5 in all three regions, it can be seen that the highest tip resistance of this soil group can be found in Zell with a value of q_c=1.73, while the shear wave velocity is rather low for this soil group in the basin of Zell.
The violin plot in Fig. 54 proves that soil group 5 within this basin has a very wide range of R_f, while soil group 6 regarding R_f within this basin gives a nice example of a bimodal distribution of data. This clearly indicates that two subgroups within soil group 6 exist. This bimodality could either mean that certain grain sizes should be regrouped to soil group 5 or that one core drilling was used for allocation to several penetration tests that showed two main ranges of R_f. Furthermore, it becomes obvious that there is hardly no difference between the original median value and the changed median value after a new cut-off criterion. This leads to the conclusion that within the basin of Zell a smaller number of extreme outliers is apparent. This should be interpreted with caution as section 6.2.2 taught that the results within the basin of Zell are a little distorted due to the imbalanced distribution of tests within this basin, which leads to the wrong impression of a very homogeneous basin.

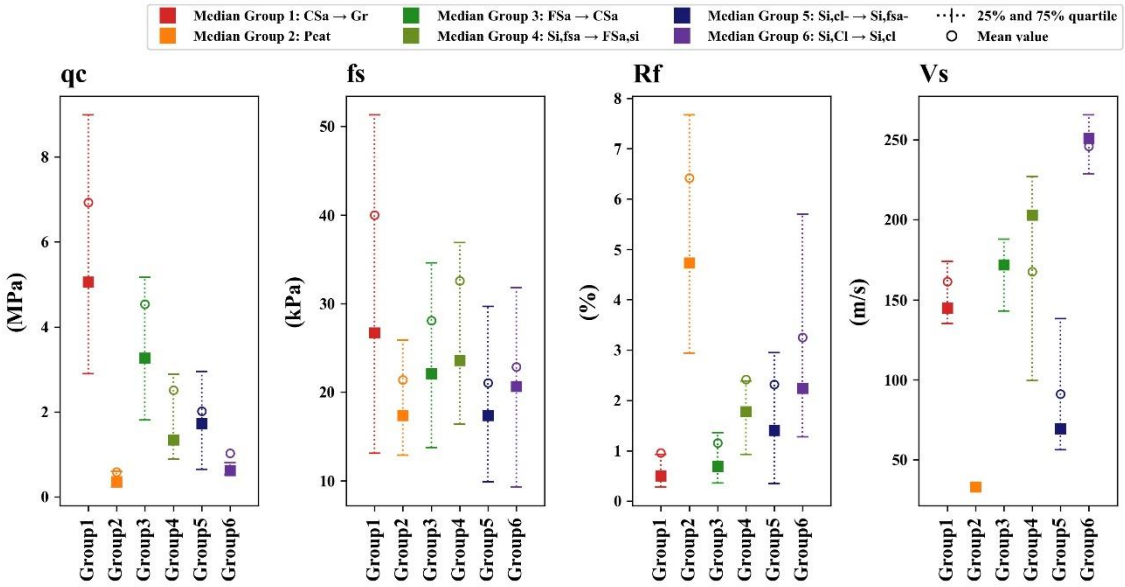

Fig. 53: Boxplot: In-situ measurements from the basin of Zell

Tab. 7: Overview of median values: In-situ measurements from the basin of Zell

Soil Group	q_c [MPa]	f_s [kPa]	R_f [%]	V_s [m/s]
1	5.06	26.7	0.5	145
2	0.36	17.4	4.73	33
3	3.27	22.1	0.69	172
4	1.34	23.6	1.78	203
5	1.73	17.4	1.41	69.5
6	0.62	20.67	2.24	251

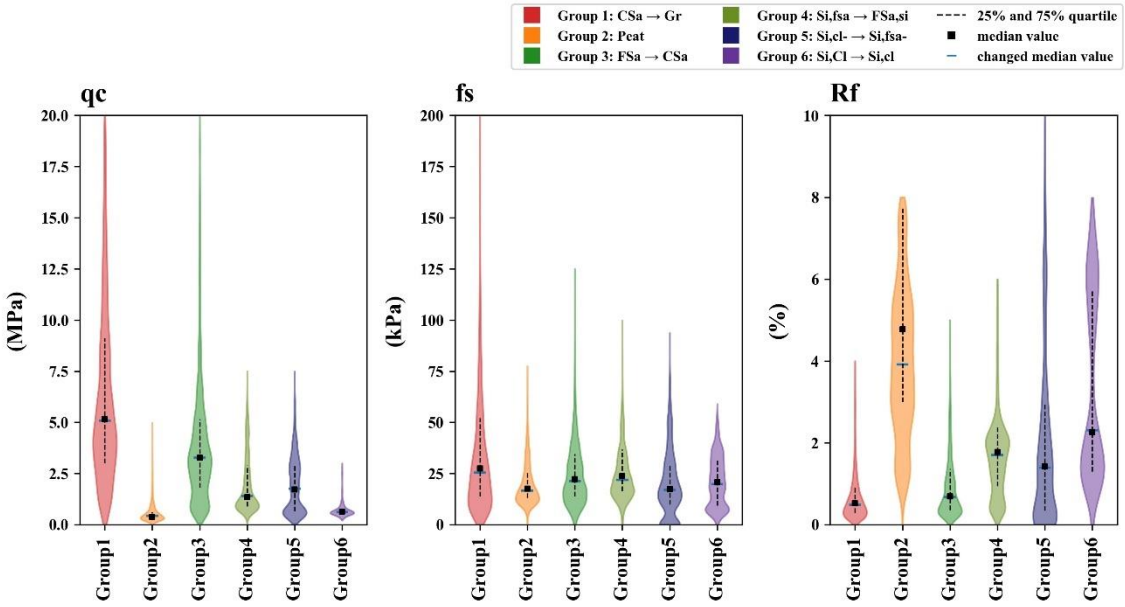

Fig. 54: Violin plot: In-situ measurements from the basin of Zell

Tab. 8: Overview of (updated) median values: In-situ measurements from the basin of Zell

Soil Group	q_c [MPa]	f_s [kPa]	R_f [%]
1	5.09	25.4	0.49
2	0.42	16.9	4.18
3	3.28	21.4	0.67
4	1.41	21.8	1.7
5	1.75	17.0	1.395
6	0.61	20.2	2.35

Region of Flachgau

Comparing the results of q_c and f_s for soil groups 1, 2, and 3 in the region of Flachgau with the same soil groups of the basin of Salzburg and Zell, it can be seen that generally the values for these three soil groups are higher in the region of Flachgau than for the two other basins. To be exact, according to Tab. 9, the tip resistance q_c for the first three soil groups in the region of Flachgau amount to 7.22, 1.76 and 5.7 [MPa], respectively, while for the Basin of Zell those values amount to 5.06, 0.36 and 3.27 [MPa], respectively. The tendency of decreasing resistance values with increasing soil numbering and therefore increasing fines content can be observed, even though the slope is not as smooth as for the basin of Salzburg or the basin of Zell. Generally, it can be seen that the range between the 25% and the 75% quartile is rather high for R_f. This leads to the conclusion that there is a higher heterogeneity within the region of Flachgau for soil groups 1, 2 and 3. For the shear wave velocity, soil group 3 doesn't show any quartile values because only a few tests are available. For soils within soil group 4, no shear wave velocity V_s was determined. When looking at the friction ratio R_f in the violin plot in Fig. 56, high heterogeneities for all soil groups can be observed. Soil group 4 is a nice example for a multimodal distribution of R_f. The original values for the median differ strongly from the changed median values for soil group 1 and soil group 3. For the other soil groups, the values fit way better.

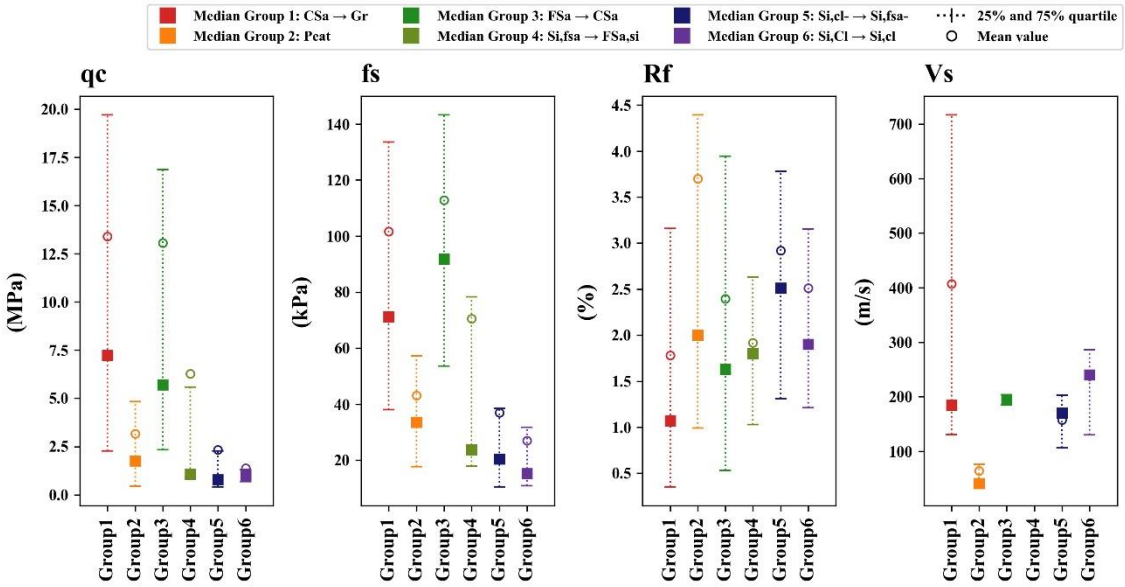

Fig. 55: Boxplot: In-situ measurements from the region of Flachgau

Tab. 9: Overview of median values: In-situ measurements from the region of Flachgau

Soil Group	q_c [MPa]	f_s [kPa]	R_f [%]	V_s [m/s]
1	7.22	71.2	1.07	185
2	1.76	33.55	2	41
3	5.7	91.8	1.63	195
4	1.07	23.7	1.8	-
5	0.78	20.4	2.51	170
6	1.01	15.3	1.9	240.5

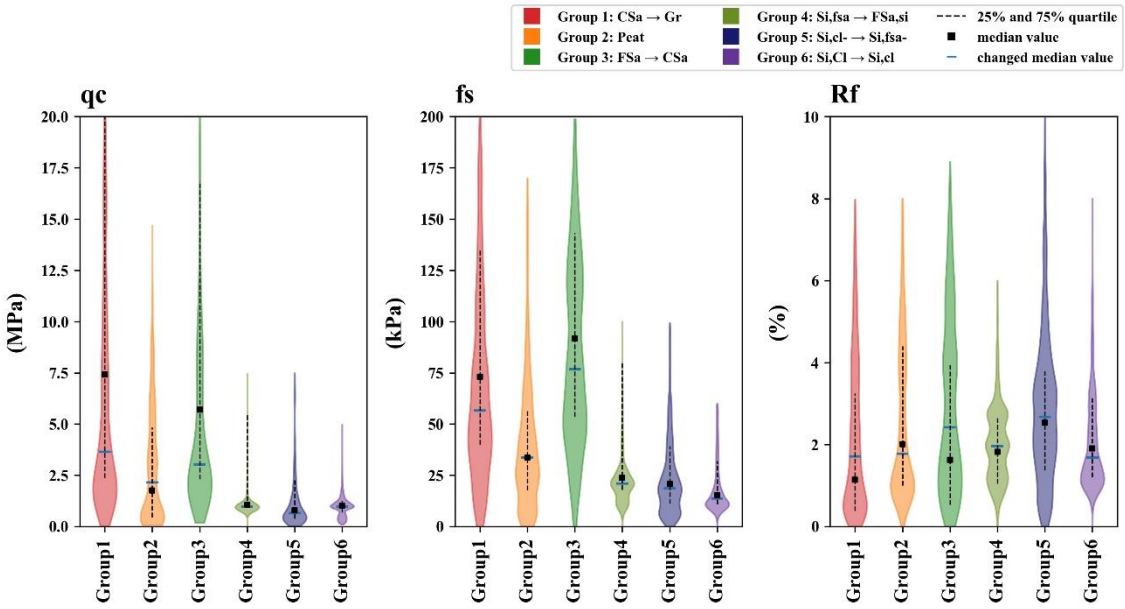

Fig. 56: Violin plot: In-situ measurements from the region of Flachgau

Tab. 10: Overview of (updated) median values: In-situ measurements from the region of Flachgau

Soil Group	q_c [MPa]	f_s [kPa]	R_f [%]
1	3.64	56.7	1.71
2	2.15	33.6	1.78
3	3.025	76.8	2.42
4	0.97	20.9	1.96
5	0.66	18.7	2.67
6	0.98	13.6	1.68

Tab. 11 gives once again an exact comparison of the median values of the in-situ measured parameters for the holistic evaluation, the basin of Salzburg and Zell as well as the region of Flachgau. To summarize the above mentioned, the main differences that were found between the three regions are once again listed here:

- the basin of Salzburg shows a very similar distribution as the holistic evaluation as most of the data originates from the basin of Salzburg
- within the basin of Salzburg, soil groups 3 to 6 show low ranges between the first and third quartile which stands for the homogeneity of these soil groups
- the basin of Zell shows lower resistance values than the basin of Salzburg with lower heterogeneities
- within the basin of Zell, the median value and the changed median value hardly differ from each other
- the results for the basin of Zell should be interpreted with caution as they are falsified due to an uneven distribution of the tests regarding their location
- the region of Flachgau shows higher in-situ measurements with a larger scatter which leads to the conclusion of coarser grain sizes apparent.

Tab. 11: Overview of median values: Comparison of Salzburg, Zell and Flachgau

	Holistic	Basin of Salzburg	Basin of Zell	Flachgau
Soil Group	**q_c [MPa]**	**q_c [MPa]**	**q_c [MPa]**	**q_c [MPa]**
1	7.23	8.23	5.06	7.22
2	0.54	0.51	0.36	1.76
3	3.86	5.62	3.27	5.7
4	2.16	3.41	1.34	1.07
5	1.07	1.19	1.73	0.78
6	1.06	1.08	0.62	1.01
Soil Group	**f_s [kPa]**	**f_s [kPa]**	**f_s [kPa]**	**f_s [kPa]**
1	50	66.1	26.7	71.2
2	23.1	24.4	17.4	33.55
3	28.4	50.1	22.1	91.8
4	35.8	51.6	23.6	23.7
5	21.9	22.3	17.4	20.4
6	19.3	19.2	20.67	15.3
Soil Group	**R_f [%]**	**R_f [%]**	**R_f [%]**	**R_f [%]**
1	0.67	0.74	0.5	1.07
2	4.13	4.36	4.73	2
3	0.78	1.01	0.69	1.63
4	1.56	1.55	1.78	1.8
5	1.82	1.63	1.41	2.51
6	1.78	1.69	2.24	1.9
Soil Group	**V_s [m/s]**	**V_s [m/s]**	**V_s [m/s]**	**V_s [m/s]**
1	379	255	145	185
2	85	228.5	33	41
3	297	-	172	195
4	243	241.5	203	-
5	240	269.5	69.5	170
6	250	251	251	240.5

6.4 Distribution of the soil types over depth

The violin plot is a good way to visualize the distribution of data and to see which values can be expected as medians for the in-situ measurements for the respective soil group. However, a shortcoming of this presentation of data is that all information about the depth, at which the respective soil groups occur, is lost. This is where histograms, density plots and stacked percentage bar charts can be a useful tool for the presentation of data depending on the soil type classification and their occurring depth. The histogram plots the amount of datapoints within a certain depth interval for each soil type, while the density plot is a smoothed, continuous version of a histogram which gives a probability density. Both charts, the histogram and the density plot, fail in the presentation of soil type data used in this thesis because of the overlapping of results which causes incomprehensibility. This is why a horizontal stacked percentage bar chart was chosen for a correct interpretation of the soil type distribution over depth. In the following, these charts are shown and discussed for the three regions: the basin of Salzburg, the basin of Zell and the region of Flachgau.

6.4.1 Basin of Salzburg

At this point, the geographical location of the basin of Salzburg should be shortly explained. It is a slightly elongated rather round basin, which is evenly flat and has the Mönchsberg and the Kapuzinerberg as the only elevations. Today the river Salzach, formerly served as an inflow and outflow of the large lake on the south- and north side, respectively. This lake had developed by the melting of the Salzach glacier. Due to these geographical conditions, the sediments were deposited relatively evenly within the basin, which explains the homogeneity of the basin today.

Fig. 57: Location of the basin of Salzburg

From experience, a typical soil lithology for the basin of Salzburg can be described as follows:

- top layer: a very heterogeneous, coarse grained layer consisting of mostly backfill material with a thickness between 1 to various meters.
- peat layer: peat lenses of thicknesses between 1 to 3m may occur and show very low tip resistances and a large friction ratio
- the upper Salzburger Seeton: mostly floating sediments (silty fine-sands to fine-sandy silts) with a possible inclusion of gravelly lenses
- the lower Salzburger Seeton: a very homogeneous clayey silt with low tip resistances. The transition between the upper and the lower Salzburger Seeton is usually located between 10 to 25 m below ground surface. (Oberhollenzer, et al., 2020)

Based on 168 core drillings that were assigned to the results of penetration tests within the basin of Salzburg, Fig. 58 was elaborated. While on the y-axis of this chart the depth is shown, the x-axis shows 100% of the test data available for each cm on the y-axis.

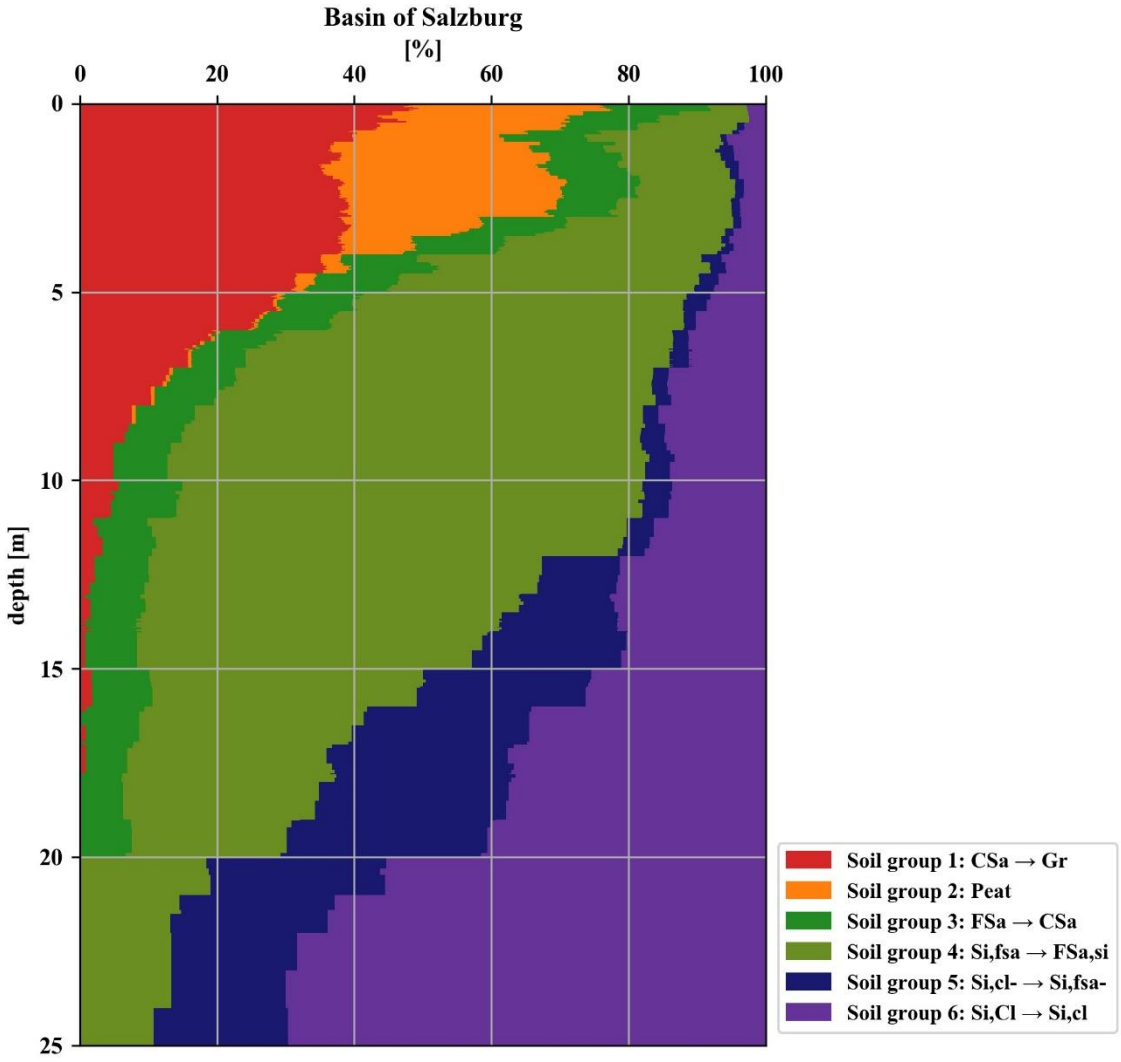

Fig. 58: Horizontal stacked percentage bar chart: Basin of Salzburg

Fig. 58 nicely confirms the before stated typical soil lithology. Within the basin of Salzburg, soil group 1 mainly represents the top layer, while soil group 2 corresponds to the followed peat lenses. Soil groups 3 and 4 can be interpreted as the upper Salzburger Seeton and soil groups 5 and 6 as the lower Salzburger Seeton. It can be seen that with increasing depth the coarse-grained soils decrease and at depths of about -10m below ground surface, nearly 100% of all measured data points only show the appearance of the Salzburger Seeton (upper and lower). Experience has shown that, in general, river gravel is found again in deep layers, below the Salzburger Seeton. For the basin of Salzburg, however, the result shows that this does not occur down to a depth of -25m. This again stands for the mightiness of the Salzburger Seeton.
With increasing depth, data of core drillings and penetration tests get less available. This means that 100% of the data for each cm of the upper layers consists of more datapoints than for the lower depths. Anyhow, the x-axis always represents 100% of the test data available for each cm. This decrease of datapoints could lead to a distortion of the results. However, for the basin of Salzburg, the clear and relatively smooth transitions between the six soil groups over depth can not only be explained by the large number of tests and core drillings that were available for this basin, but also by the fact that these tests and core drillings were carried out to greater depths. Nevertheless, the basin of Salzburg can be characterized as a very homogenous basin as step-like transitions are relatively rare and a clear distribution of the soil types regarding their occurring depth can be seen.

6.4.2 Basin of Zell

The basin of Zell is a bent, elongated basin lying within a trough valley that was formed through the glaciers of the “Glockner group” during the last glacial period.

Fig. 59: Location of the basin of Zell

Because of the melting of the glaciers, the Zeller lake developed and fine-grained soils sedimented. The kink within the basin caused differences in the sedimentation processes before and after. In addition to that, creeks of the surrounding mountains

carry a lot of floating sediments. When those creeks emerge from a mountain into a plain, they are called alluvial fans (“Schwemmfächer” in German) which consist of a coarser grain size and therefore settle quicker especially at the peripheral regions of the basin. To sum it up, the kink and the mountain creeks can be the reasons for a greater heterogeneity and coarser grain-sizes within the basin of Zell.

The same investigation as for the basin of Salzburg, was performed for the basin of Zell, although only 35 core drillings could be assigned to penetration tests within this basin. The result is shown in Fig. 60. For the basin of Zell, it can be seen that the lower number of tests leads to a more step-like distribution of soil types. Especially within depths of -20 m to -25 m, the three steps of soil group 1 and the sudden cut-off of soil groups 4 and 5, lead to the conclusion that at these depths, only a very little number of penetration tests and core drillings could deliver data. It should therefore be interpreted with caution, although it still can be observed that at a depth of -20 m the occurrence of the deep situated river gravel increases and that soil groups 4, 5 and 6 are not present.

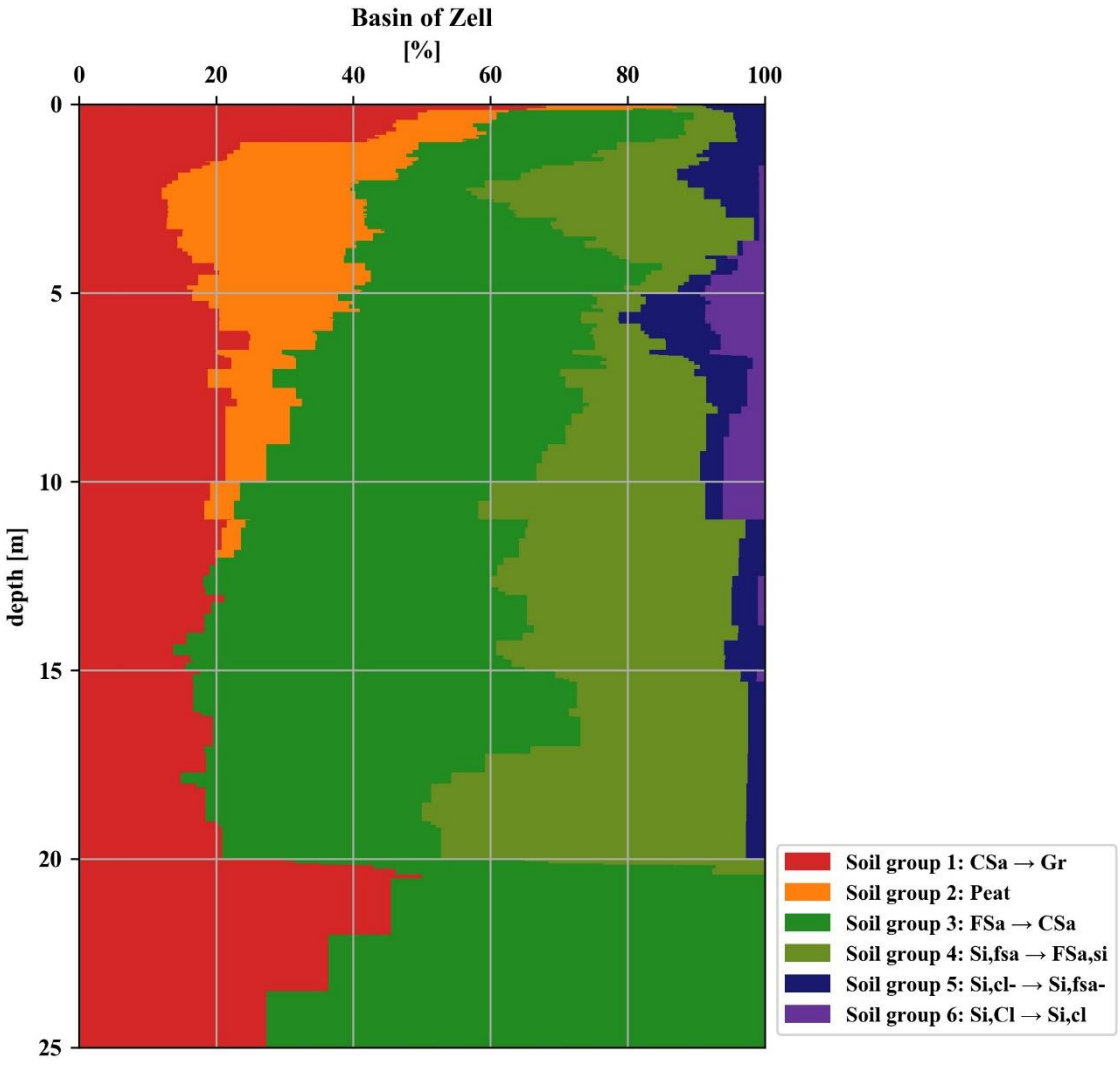

Fig. 60: Horizontal stacked percentage bar chart: Basin of Zell

From the same figure it can be seen that soil groups 5 and 6, so the very fine-grained soil groups, already occur at shallow depths but in a much smaller percentage than, for example, within the basin of Salzburg. Soil groups 3 and 4, consisting of fine-sandy silts to sands, make up the main part of the soil type distribution over depth. The reason for the coarser grain sizes may be explained by the geographical location of the basin and its formation.

6.4.3 Region of Flachgau

The region of Flachgau is a very widespread surrounding area of the city of Salzburg, which is characterized by a hilly landscape with numerous elevations and depressions. Therefore, a distinction should be made if tests were carried out situated in a basin or on a hillside within the region of Flachgau, as soil type distributions over depth may show more fine-grained or coarse-grained results, respectively. Depending on the location of a test, the appearance of soil types can be very differently which leads to the conclusion that the region of Flachgau is characterized by a great heterogeneity.

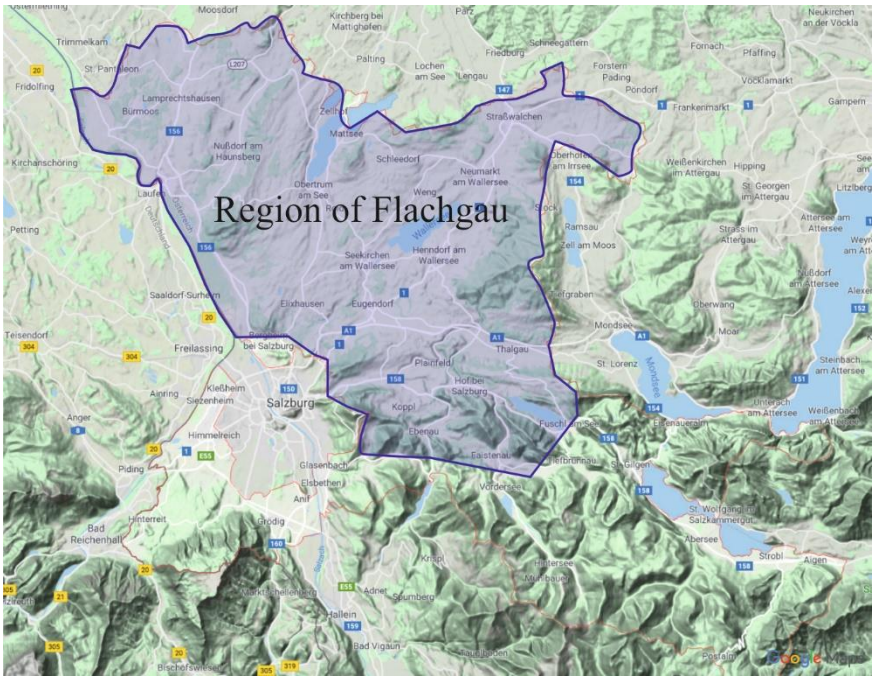

Fig. 61: Location of the region of Flachgau

23 core drillings, allocated to in-situ tests, formed the basis of the soil-type investigation over depth for the region of Flachgau. The result is shown in Fig. 62. It can be observed that soil group 1, consisting of coarse sands and gravels, is mainly occurring in two depth levels. At first in the uppermost layers as a top layer and then increasingly again at a depth of about -16 to -23 m in the form of river gravel. Hence, it can be said that in the region of Flachgau, the deeper situated river gravel generally already occurs earlier and the above lying homogeneous silty clay layers are not as thick as for the basin of Salzburg or the basin of Zell. As for the other two basins, the peat layer again mainly occurs in the first 7 m, which

shows that peat lenses occurring below the top layers are a common thing in all three regions.

Fig. 62 gives the impression that within the region of Flachgau in the first 20m mainly very fine-grained soft soils, i.e. soil groups 5 and 6, occur. This appearance may be explained by two reasons. Firstly, a few core drillings may have shown very fine-grained soils in the uppermost layers, and these core drillings have been assigned to many penetration tests, which can be an explanation for the frequent occurrence of these soils. Secondly, a reason could be the geographical location of Flachgau. From Fig. 62 it can be concluded that more tests were carried out in basin locations than on hillsides due to the high presence of soil groups 5 and 6.

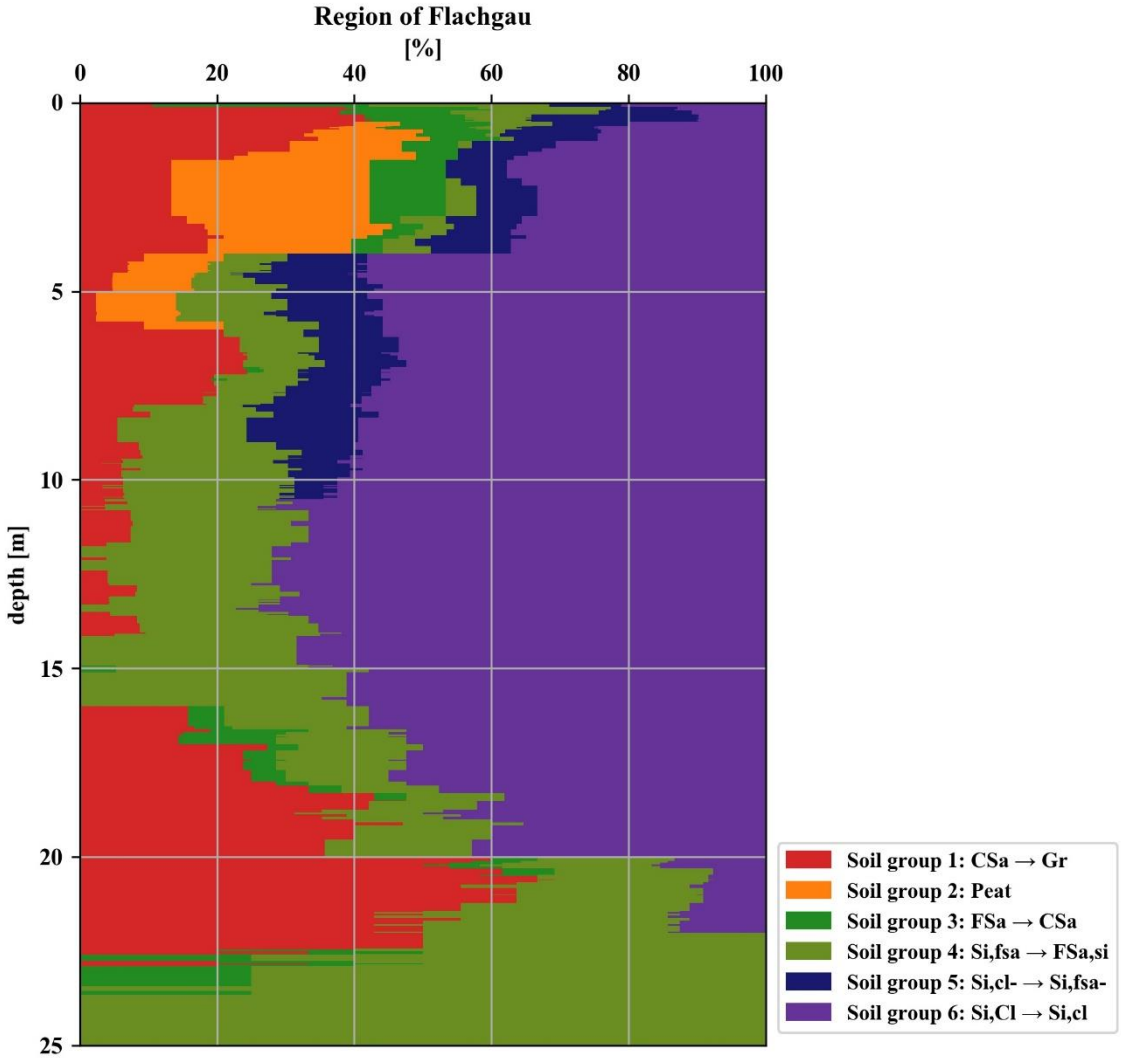

Fig. 62: Horizontal stacked percentage bar chart: Region of Flachgau

7 Comparison of in-situ measurements by means of soil behaviour type charts

By using charts that link in-situ measurements to soil types, the CPT test can be applied for the determination of soil stratigraphy and the identification of different soil types. As it can be read in chapter 3, different approaches have been developed over the past fifty years. Robertson (2010) stresses that CPT-based charts often predict soil behaviour type (SBT) better than other classification systems (e.g. Unified Soil Classification System, USCS) that are based on grain-size distribution and soil plasticity, which use parameters measured on disturbed soil samples. In Robertson (2010) several examples are given where the application of SBT charts is a better way to describe soil types than a classification simply based on grain-size distribution and plasticity. For a geotechnical engineer, a classification based on the knowledge of both approaches is helpful. Since normalized soil behaviour type charts (SBTn) provide more reliable results than non-normalized charts (e.g. Robertson 1986), the results are presented in the following chapter in SBTn charts. In the first part, a holistic comparison of all data is presented by means of the SBTn charts after Robertson (2009, 2016) and Schneider (2008). Further only the data for the basin of Salzburg, the basin of Zell and the region of Flachgau are compared using the mentioned charts. In a last step, the SBTn chart according to Robertson (2016) was used to detect a possible microstructure acting between the soil particles.

7.1 Holistic evaluation

In this section, all in-situ measurements that were executed in Austria are discussed based on the normalized soil behaviour type charts according to Robertson (2009) (see Fig. 63), Robertson (2016) (see Fig. 64) and Schneider (2008) (see Fig. 65).
According to the core drillings, soil group 1 contains soils in the range of course sand to gravel. In Fig. 63 it is shown that Robertson (2009) correctly describes this soil group as sand-mixtures to gravely sands (sections 5 to 7). They are characterized by a sand-like dilative behaviour according to Robertson (2016). Soil group 1 shows a large scatter. This was already proven by the box-plots and violin plots in chapter 6.3, but can once again be seen here as the data points are widely spread. Soil group 2, the peaty soils, do not show that much of a scatter. They are mainly situated in section 3 (clay) in Fig. 63. Consequently, the mentioned peaty soil layers or peat lenses are mostly characterized by fine-grained soils. No assessment regarding the dilative or contractive behaviour of soil group 2 can be made according to Fig. 64 as this soil group plots in both regions. Nevertheless, hardly any data points plot within the region for organic soils (section 2). Therefore, it has to be noted that the chart after Robertson (2009) fails to identify soil group 2 correctly, although of course only a rare amount of data points consists of pure organic soils. They are mostly occurring in combination with other soils,

e.g. gravel, sand or clay. Soil group 3 (FSa→CSa) is mainly situated within sections 5 and 6, so sand-mixtures and sand according to Robertson (2009). However, a tendency of some data points towards the silt-mixtures and clay regions can be detected. This may be explained by thin clayey interlayers within the coarse layers that were not declared as separate lithologies and therefore probably showed low tip resistances and sleeve frictions. When looking at soil group 4, a large scatter of the data points can be observed. This soil group represents fine-sandy silts to silty fine-sands. A reason for the large scatter in results could be thin gravelly interlayers, that were not classified as separate lithologies in the core drillings. Another, very likely reason is that these silt-dominated soils have the problem of partial drainage while penetration testing. This effect of partial drainage can influence the results of penetration tests, although there is still a great need for research to know to what extent this effect really has an influence on the results and how this effect can be correctly considered.

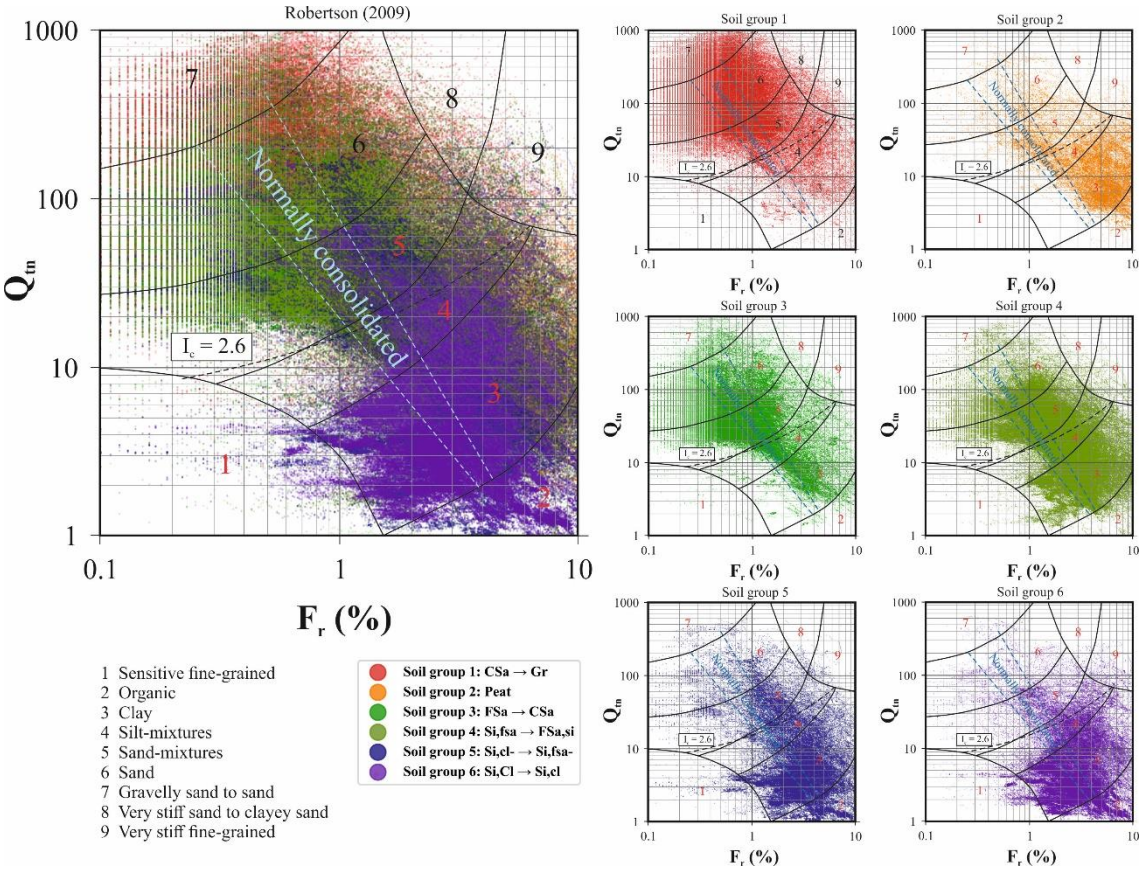

Fig. 63: SBTn chart according to Robertson (2009): Holistic evaluation

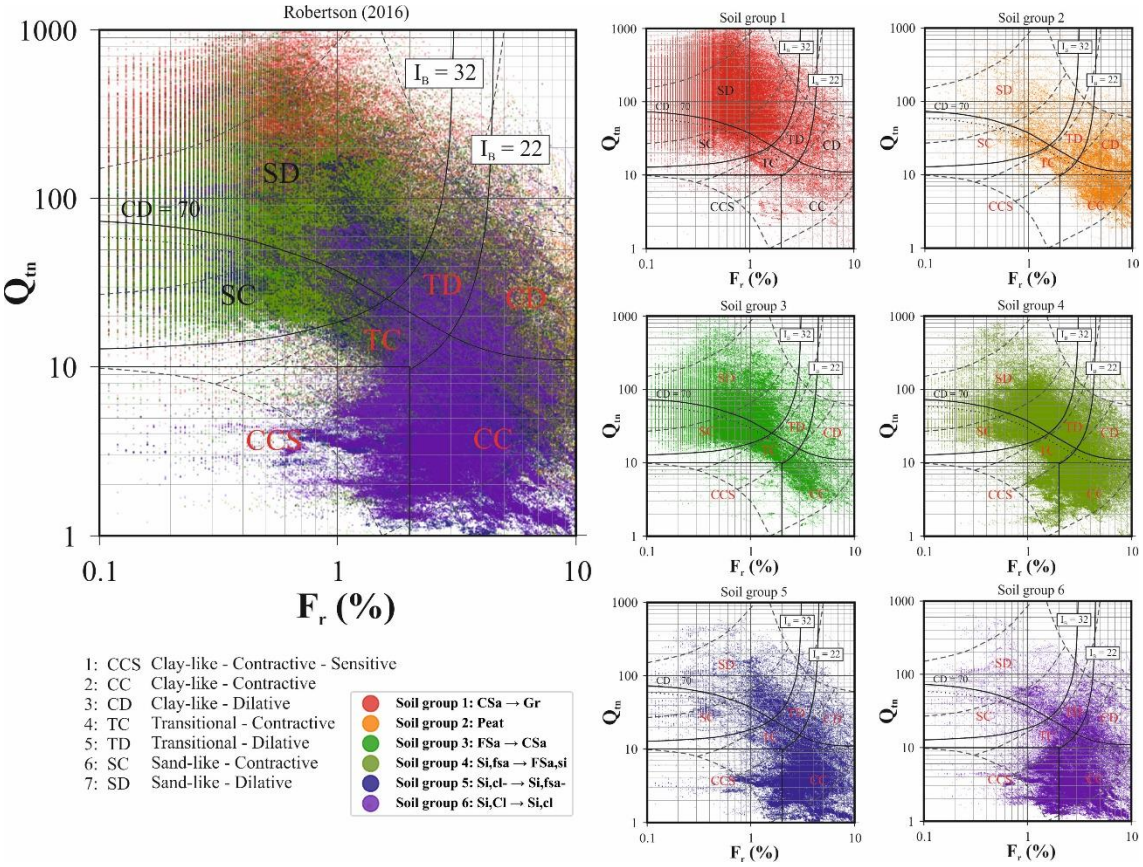

Fig. 64: SBTn chart according to Robertson (2016): Holistic evaluation

The measurements of the very fine-grained, soft soils (soil groups 5 and 6) are in good agreement. Both are mainly (except for a few data points) located within section 3 (clay) according to Robertson (2009) and are characterized by a clay-like contractive behaviour according to the updated soil behaviour type chart after Robertson (2016). The latter statement is in good agreement with the fact that these sediments are classified as slightly under-consolidated and are still undergoing settlement processes.

For the Schneider et al. (2008) soil classification chart it should be noted that only data from CPTu tests can be used, as U_2 depends on the difference between the excess pore water pressure u_2 and the hydrostatic pore water pressure u_0. According to Fig. 65, soil group 1 is again classified as sand-like-dilative and doesn't show that much of a scatter. Soil group 2 and 3 are more scattered and plot in two zones, the sand-like-dilative zone and the transitional – contractive zone. Soil group 4 shows much more of a scatter as this soil group clearly plots in the sand-like, the transitional as well as the clay-like soil zone. The same reasons as mentioned above cause the large scatter in this chart. Soil groups 5 and 6 are for the Schneider et al. (2008) again in good agreement. Both groups are mainly situated in the clay-like contractive region, although still a large number of data points plot in the transitional and sand-like region.

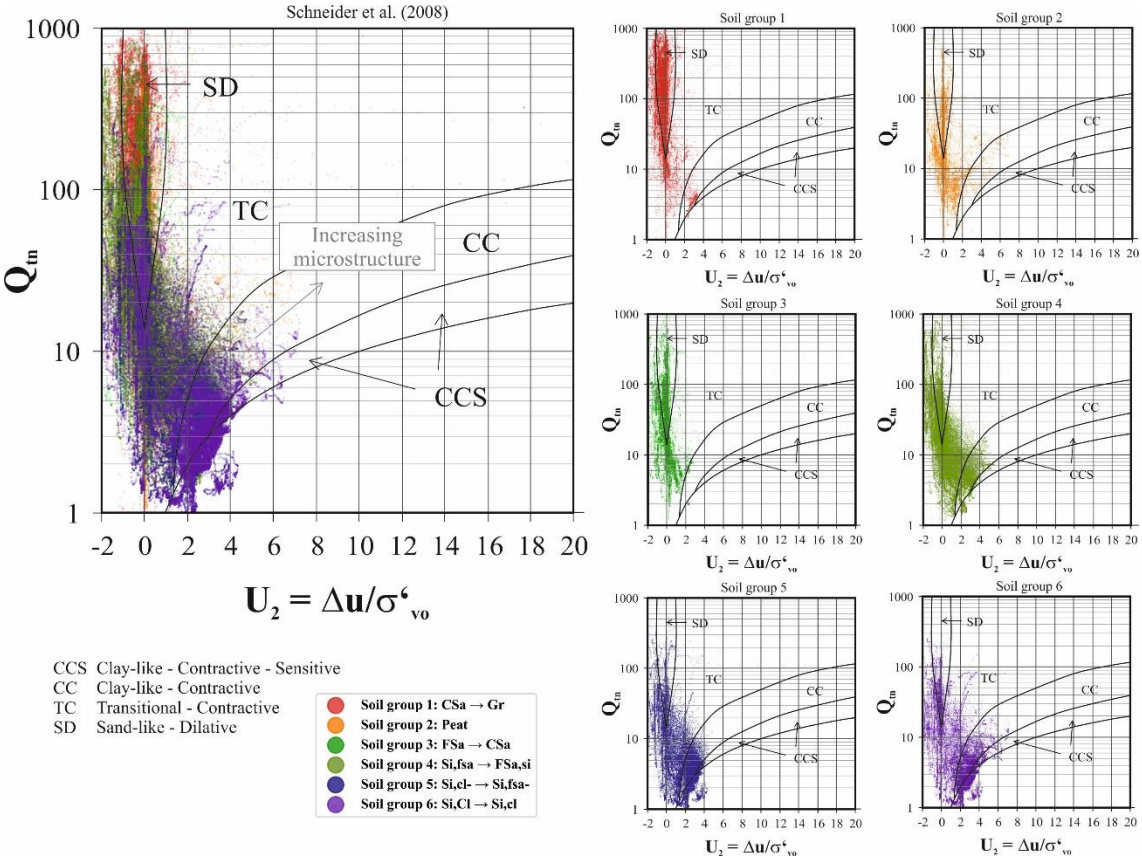

Fig. 65: SBTn chart according to Schneider et al. (2008): Holistic evaluation

7.2 Comparison of Salzburg, Zell and Flachgau

7.2.1 Basin of Salzburg

In this section, a closer look is given to the data points within the basin of Salzburg. They are plotted into the soil behaviour type charts after Robertson (2009), Robertson (2016) and Schneider et al. (2008) which can be seen in Fig. 66, Fig. 67, and Fig. 68, respectively. The same tendencies as in the holistic comparison of the previous section can be observed. This is because most of the data points for the holistic comparison come mainly from the basin of Salzburg. Therefore, everything that was mentioned in the previous section for the holistic comparison also applies to the comparison for the basin of Salzburg. A main difference between the holistic evaluation and the basin of Salzburg can be seen regarding soil group 3. Within the basin of Salzburg this soil group shows a smaller scatter and the main part of this soil group can be classified as sand and sand-mixtures. Also soil groups 5 and 6 show differences when looking at the Schneider et al. (2008) charts (see Fig. 68). They show a smaller scatter and are characterized as clay-like contractive. Only a very small part of data of both soil groups remains in the sand-like dilative section, especially soil group 5 shows a very small scatter.

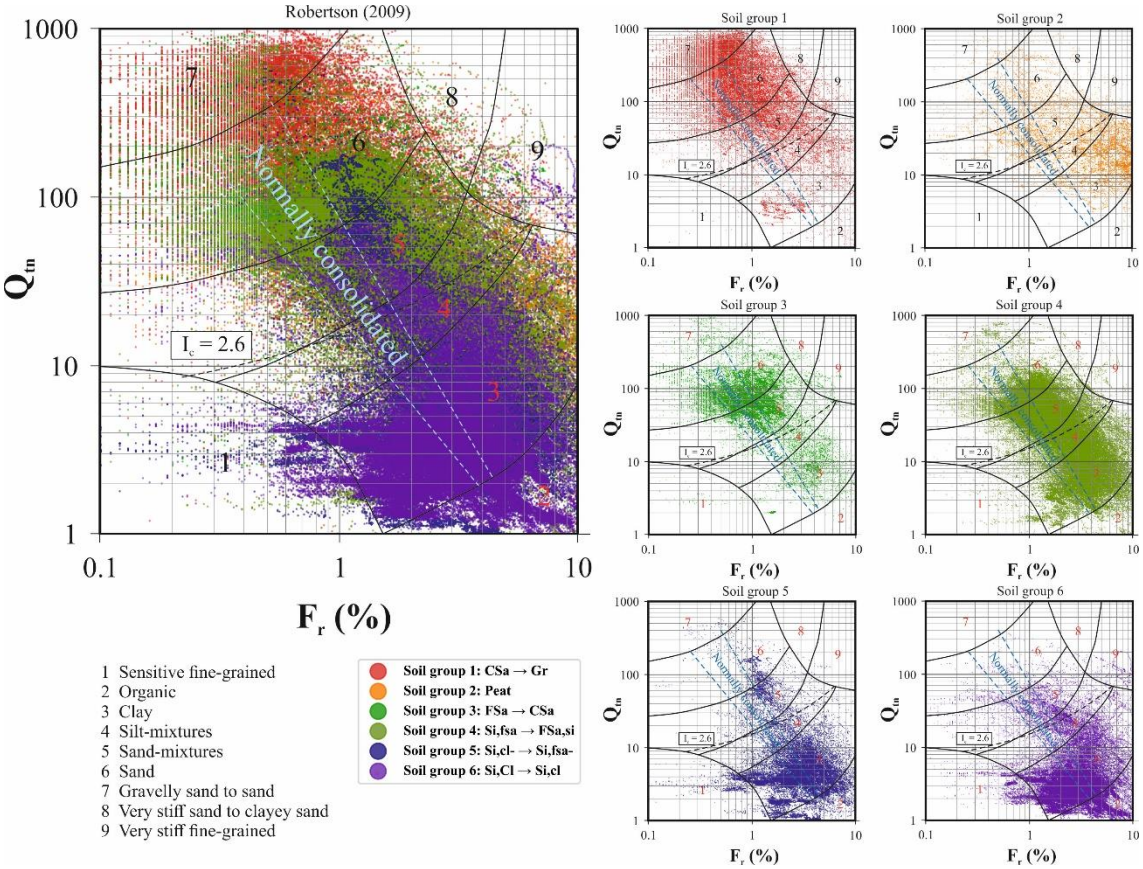

Fig. 66: SBTn chart according to Robertson (2009): Basin of Salzburg

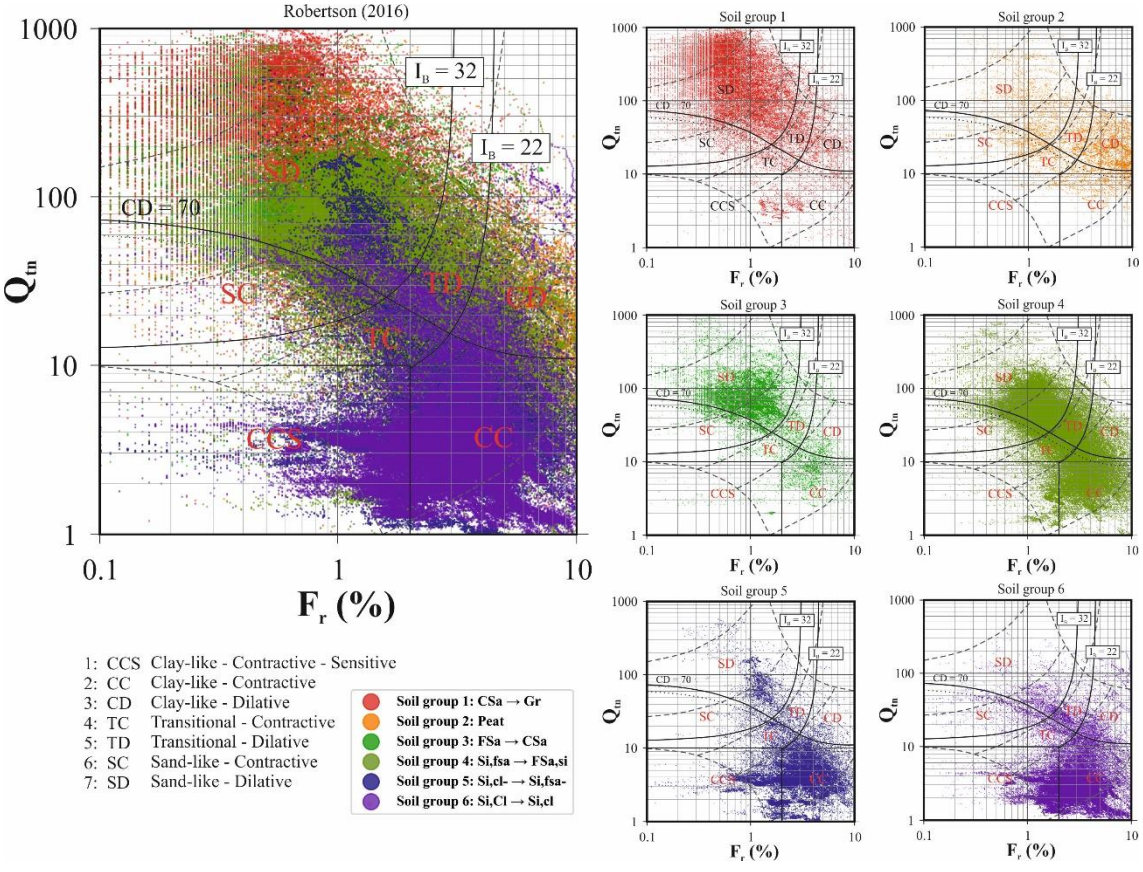

Fig. 67: SBTn chart according to Robertson (2016): Basin of Salzburg

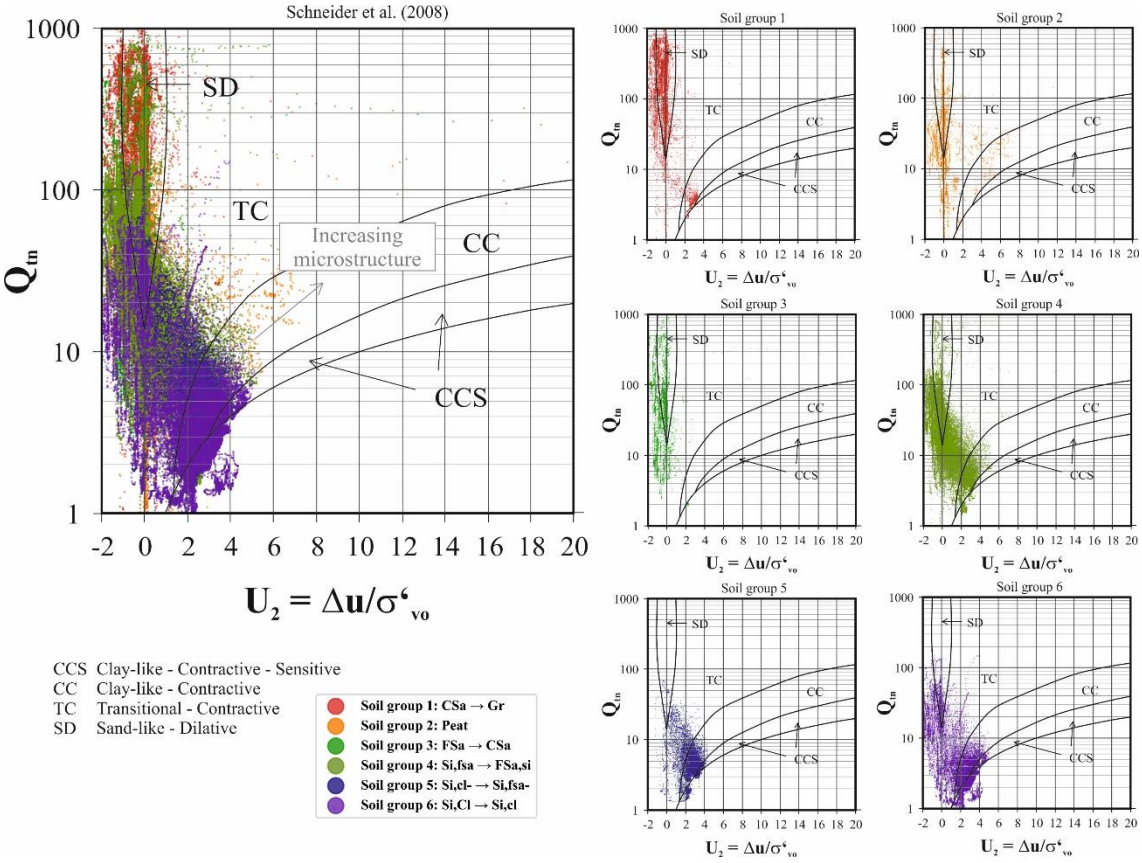

Fig. 68: SBTn chart according to Schneider et al. (2008): Basin of Salzburg

7.2.2 Basin of Zell

In this section, only the data points that were available for the six soils groups within the basin of Zell were picked out and plotted into Fig. 69, Fig. 70 and Fig. 71. For soil groups 1 and 2, the same tendencies as shown above are observed. The main part of the data can be assigned to the soil groups 3 and 4 while for the very fine-grained, soft soils (groups 5 and 6) less data is available.
Soil groups 3 and 4 both show a very similar distribution of the data points, with a rather large scatter. Fig. 70 indicates that both soil groups show a contractive soil behaviour which stands again for loosely layered soils with consolidation processes not yet completed. Soil group 5, the clayey to fine-sandy silts, shows a large scatter. Some parts nicely plot within the silt-mixture zone (Robertson, 2009) and in the transition zone (Robertson, 2016). Some other points are classified as clay-like or sand-like (see Robertson, 2016).
Soil group 6 clearly plots within section 3 (clay – see Robertson, 2009) and is described as a contractive clay to sensitive clay according to Robertson (2016). It shows a rather small scatter.

According to the Schneider et al. (2008) profiling chart, soil group 1 can again be classified as a sand-like dilative soil. Soil group 2 (Peat) is no longer clearly classifiable as it was possible with the Robertson charts. Also soil group 3 shows

a large scatter within the Schneider et al (2008) chart and no correct classification can be performed. For soil groups 4 and 5, however, the chart works perfectly fine as these soil groups are clearly identified as transitional dilative soil types. For soil group 6, not enough data is available to make a correct assessment, although a small data cloud can be observed in the clay-like contractive region.

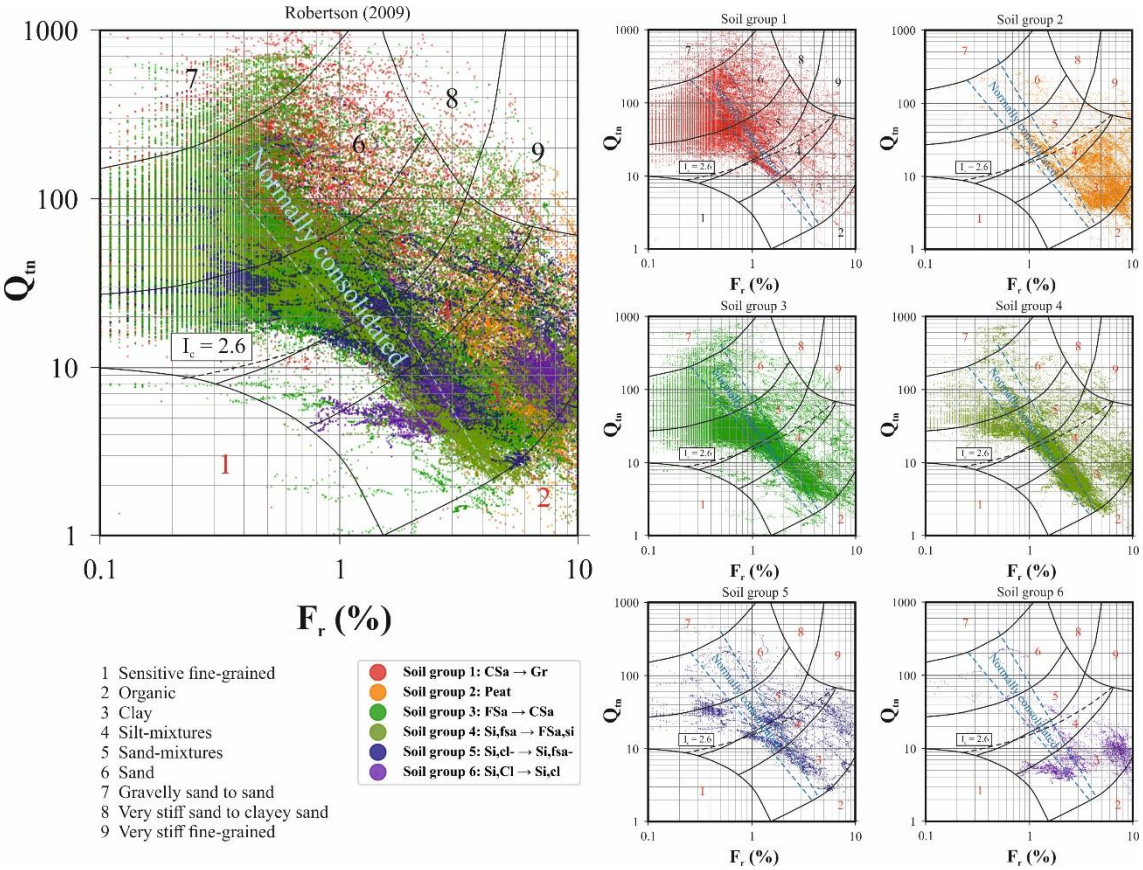

Fig. 69: SBTn chart according to Robertson (2009): Basin of Zell

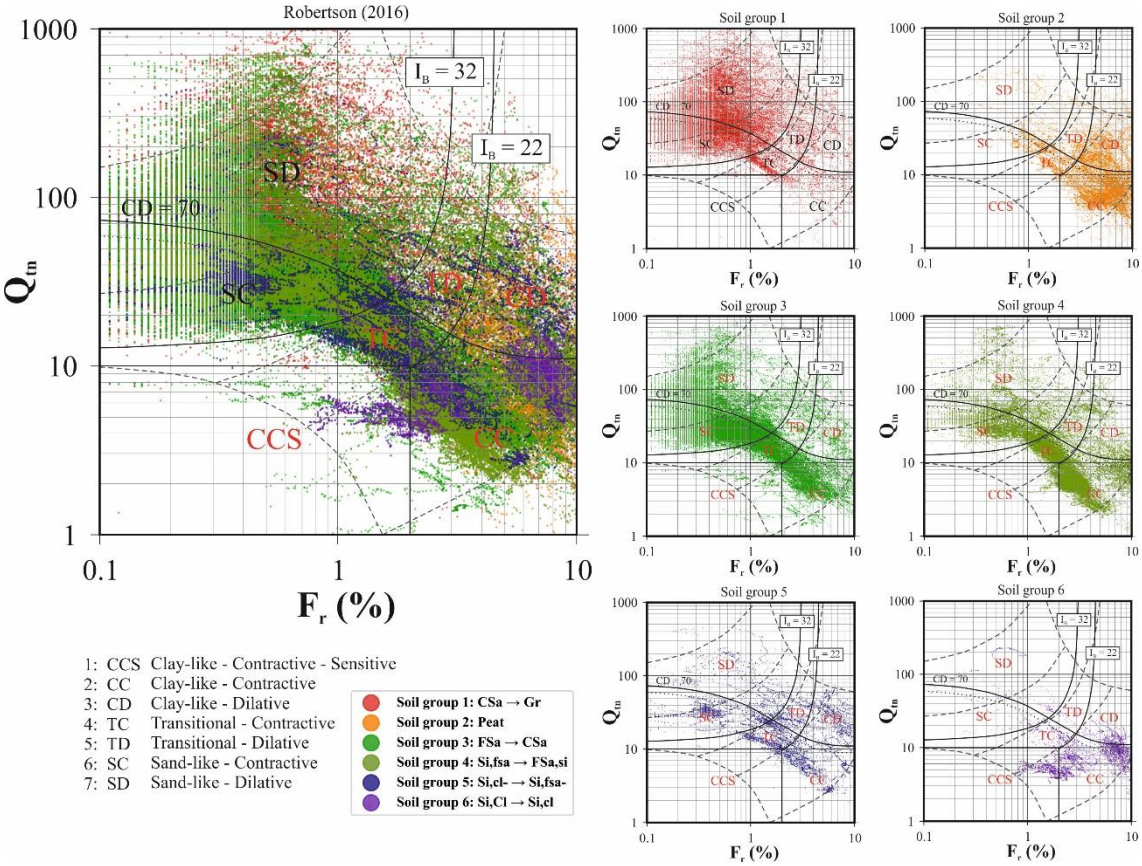

Fig. 70: SBTn chart according to Robertson (2016): Basin of Zell

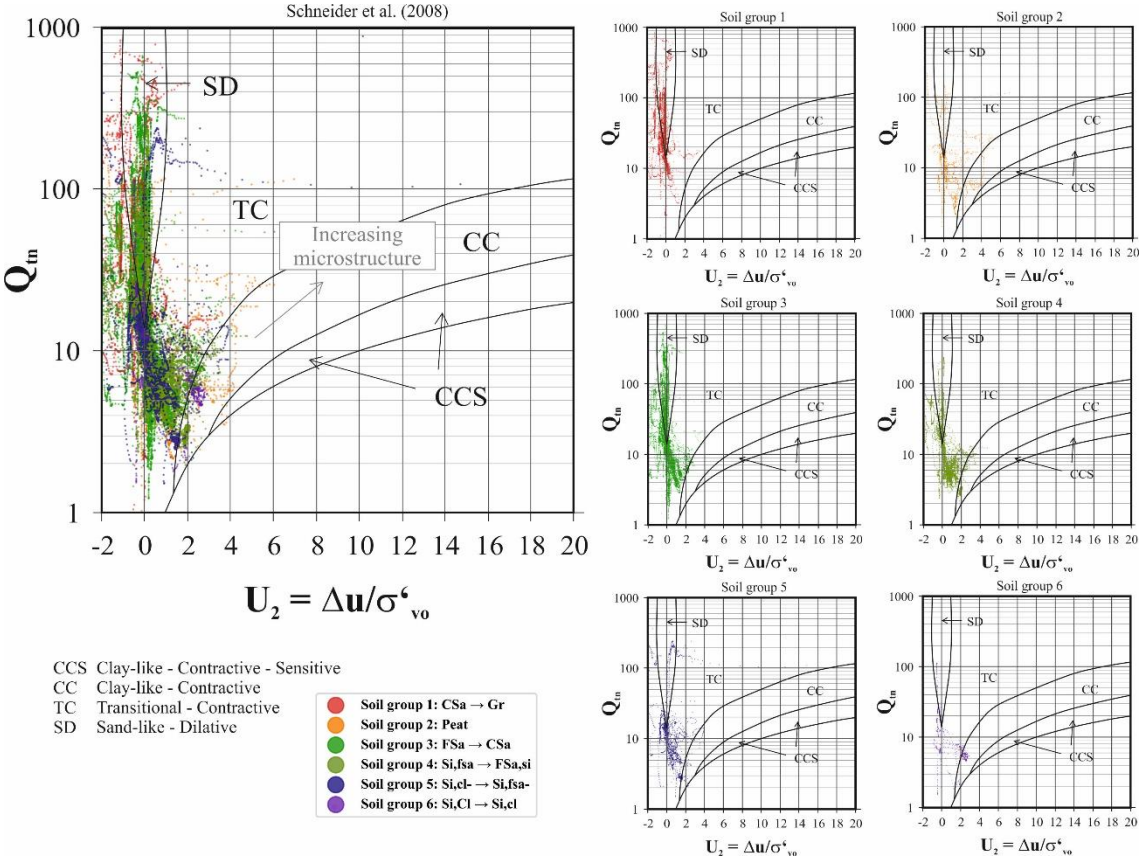

Fig. 71: SBTn chart according to Schneider et al. (2008): Basin of Zell

7.2.3 Region of Flachgau

For the region of Flachgau, only a few data points are available. Nevertheless, it becomes obvious that the data plotted within the soil behaviour type charts after Robertson (2009) (see Fig. 72), Robertson (2016) (see Fig. 73) and Schneider et al. (2008) (see Fig. 75) show a large scatter for all soil groups.
When looking at soil groups 1 and 2, no soil type classification can be made with the help of the Robertson (2009) or Robertson (2016) classification chart, as the scatter is too high. Especially for soil group 2 it cannot be said anymore that peaty soils are mostly characterized by fine-grained soils, as data is plotted within sections 2 to 6 in Fig. 72. However, when using the profiling chart according to Schneider et al. (2008), both soil groups can be classified as sand-like dilative, although this contradicts the previous statement that soil group 2 is generally characterized by a fine-grained soft transitional to clay-like soil.
According to Robertson (2009), soil group 3 plots within regions 5 to 7, so sand mixtures to gravelly sand. Still some parts plot within the silty zones, which implies silty components. Soil group 4 shows two clusters. In Fig. 73 numerous data points plot within the sand regions (dilative regions). Another point cloud can be observed in the clay region (contractive) of this figure. These two clusters can also be observed in the Schneider et al. (2008) chart in Fig. 74 where one part of the data plots in the uppermost region of the chart which can be characterized as sand-like dilative, while the other part of the data is classified as transitional contractive. Nevertheless, inconsistencies are visible, as Robertson (2009) classifies the lower point cloud clearly as clay while Schneider et al. (2008) classifies this point cloud as transitional soil. This proves again the difficult distinction within silt-dominated soils. Soil group 5 shows such a strong scatter, that not really any statement can be made according to Robertson (2009,2016). For Fig. 74, no data of soil group 5 is available at all. Soil group 6 is classified as clay (see Fig. 72), but also shows the presence of silty mixtures.
As an overall conclusion it can be stated that a contractive behaviour for the silt-dominated, fine-grained soils could be observed within the basin of Salzburg and the basin of Zell according to Robertson (2016). This is not valid for region of Flachgau as no assessment regarding the dilative or contractive behaviour for soil groups 5 and 6 can be made in this region (see Fig. 73).

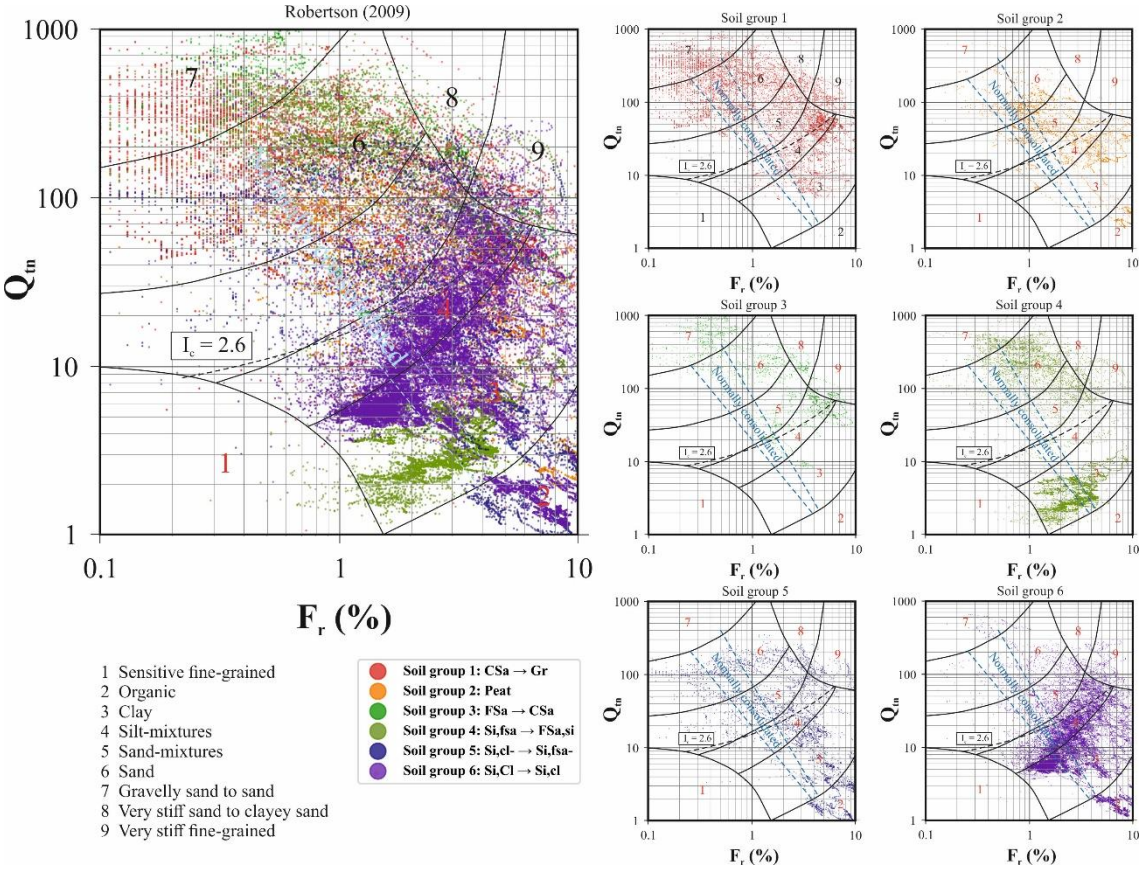

Fig. 72: SBTn chart according to Robertson (2009): Region of Flachgau

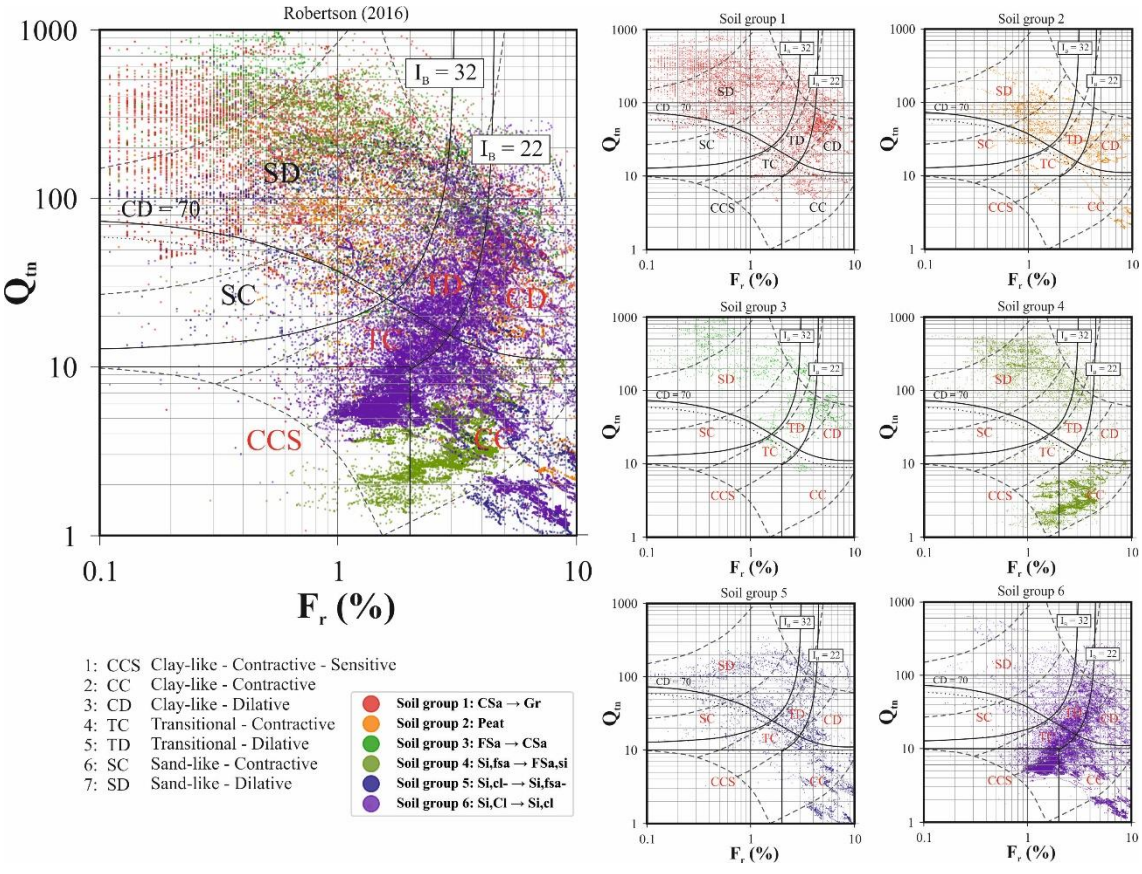

Fig. 73: SBTn chart according to Robertson (2016): Region of Flachgau

As already discussed in chapter 6.4.3, care should be taken if a test conducted in the region of Flachgau is situated within a basin or on the hill side. This dependency on the location can also be an explanation for the two resulting clusters for soil group 4 where it could be assumed that datapoints from tests performed on the hill side result in the sandy regions, while datapoints from basins plot in the contractive clay regions.

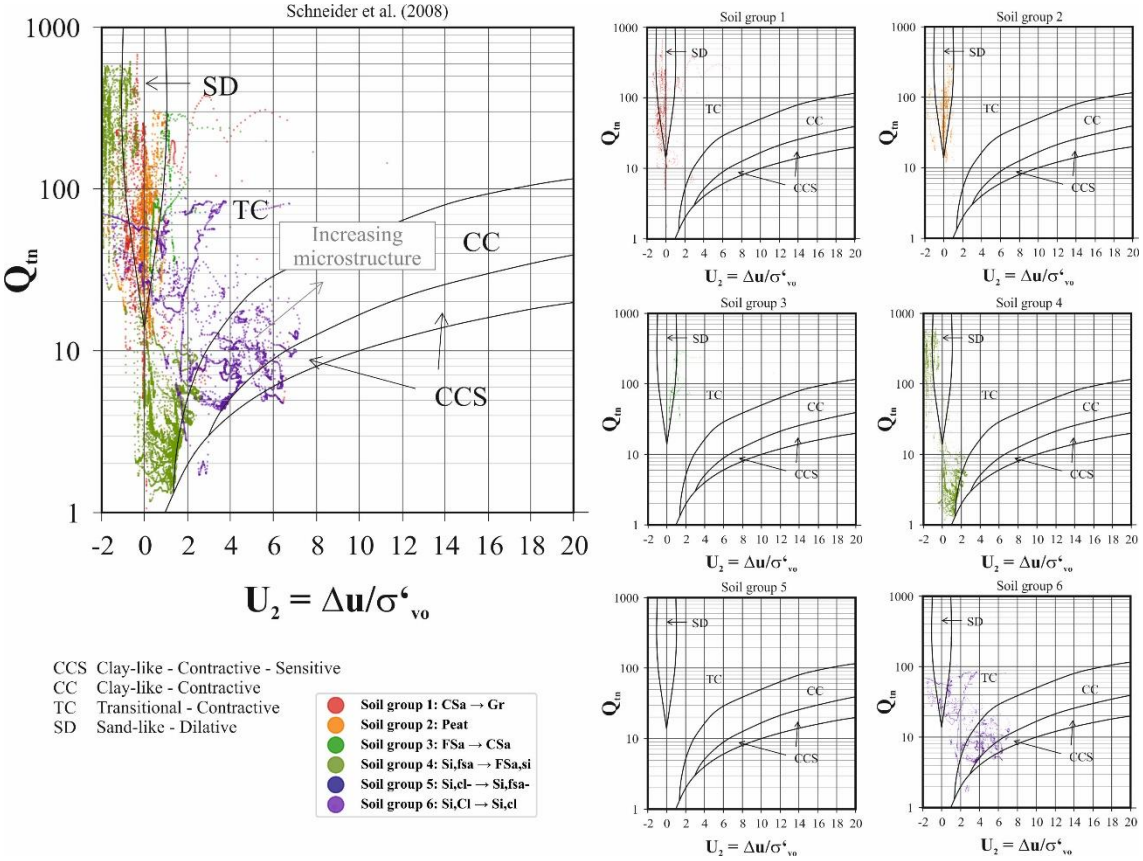

Fig. 74: SBTn chart according to Schneider et al. (2008): Region of Flachgau

7.3 Detection of microstructure based on Robertson (2016)

Last but not least an investigation regarding the detection of possible microstructure was performed. This was done with the approach after Robertson (2016). Only a few data points were available for this kind of investigation, as seismic tests are performed less frequently. However, these are necessary to provide information about the seismic shear wave velocity which is further used for the calculation of the small strain shear modulus G_0 from *Eq.(7)* and the small strain rigidity index I_G from *Eq.(18)*. The results of the SBTn chart according to Robertson (2016) are shown in Fig. 75. Only the results for soil groups 4 to 6 are presented, as the other two groups are not of main interest. The data points within the Q_{tn}-I_G space imply the presence of microstructure for all four soil groups.

In order to make a specific statement about the individual basins, all three regions are plotted separately in Fig. 76. It is immediately apparent that the most data points originate from the basin of Salzburg. Consequently, all four soil groups within the basin of Salzburg show the presence of microstructure according to Robertson (2016). The data points within the basin of Zell are characterized by a large scatter. Therefore, no statement is possible regarding the presence of a microstructure. According to Robertson (2016), soil groups 5 and 6 within the region of Flachgau are characterized by microstructural bonds, as K_G* is clearly greater than 330. Although there is still a cluster of data points lying below the K_G* = 330 boundary line.

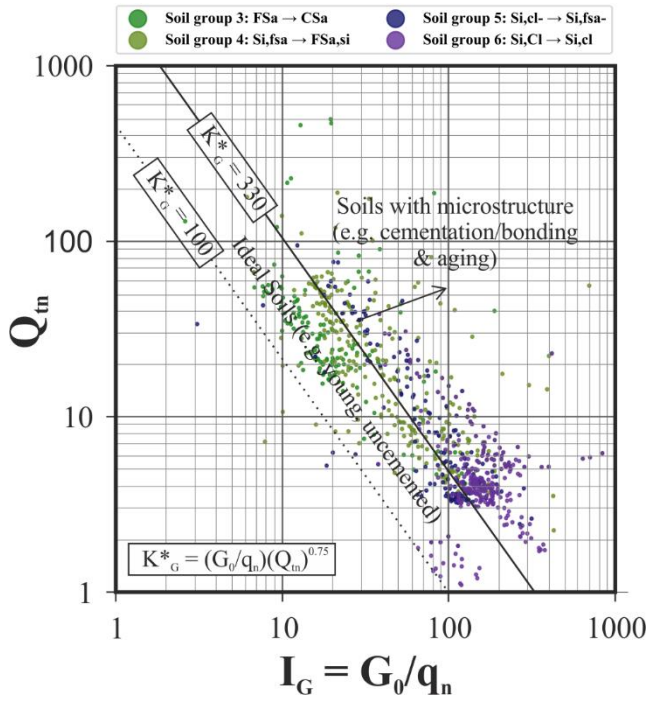

Fig. 75: Q_{tn} I_G chart (Robertson 2016): Holistic evaluation

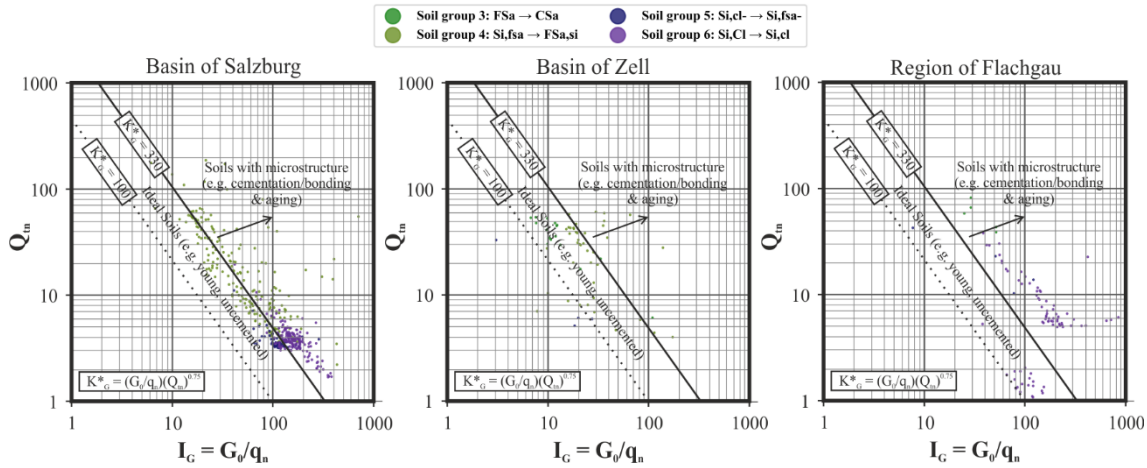

Fig. 76: Q_{tn} I_G chart (Robertson 2016): Comparison of Salzburg, Zell and Flachgau

8 Conclusion and Outlook

A large data set of penetration tests (CPT, CPTu, SCPT and DMT) and core drillings conducted in Austria was investigated and evaluated in the course of this master's thesis. This last chapter intends to summarize the most important findings for chapter 6 and 7 and to present possible measures for improvement.

8.1 Chapter 6

In chapter 6, a comparison of in-situ measurements was performed. At first, all basins and valleys where data was available were investigated. It was shown that basins are generally characterized by a greater fines content with lower heterogeneities than valleys. However, soil properties within a basin can still vary significantly. This was shown in chapter 6.2 where the basin of Salzburg, the basin of Zell and the region of Flachgau were investigated by means of a subdivision into smaller regions, the so-called cadastral communities. For all three regions the same tendency could be observed: increasing homogeneity with increasing depth as the dispersion of data decreases (see decreasing quartile values). In addition to that, the resistances to penetration decrease with increasing depth as the fines-content increases. Furthermore, it was shown that within the basin of Salzburg the deeper situated river gravel occurs at depths below -25m while in the basin of Zell and the region of Flachgau this river gravel already appears at smaller depths. However, differences within the cadastral communities of all three regions showed that the basin of Salzburg is characterized by a more homogeneous pattern while the basin of Zell and the region of Flachgau are characterized by a greater heterogeneity as the in-situ measurements show different distributions over depth.

A comparison of the in-situ measurements based on the grain-size distribution was performed by means of box-plots and violin-plots (see chapter 6.3). Therefor the data from nearby core drillings was divided into six different soil groups. It was shown that extreme outliers occur, and that the data is not normally distributed. Changing the cut-off criteria for the in-situ measured values for the violin-plots compared to the ones for the box-plots, showed how sensitive this parameter is, as not only the mean values but even the median values changed extremely. Further investigations should be performed on the high number of outliers, how they can be avoided and how they should be considered in order to reach correct median values. The example of Zell showed that imbalances can occur when a large number of tests is performed next to each other and only fewer tests are performed at other locations. This proves that actual heterogeneities cannot be determined when doing a holistic evaluation without investigating separate regions. An improvement therefore would definitely be to delete too many identical tests in order not to falsify the results. In general, it can be said that more area-wide tests with core-drillings right next to them can give more reliable results. Additionally,

a limit should be set on how often one core drilling can be allocated to several cone penetration tests as this may also lead to a distortion of results.

The horizontal stacked percentage bar charts from chapter 6.4 showed that the distribution of soil types over depth are different for Salzburg, Zell and Flachgau. While the basin of Salzburg shows an increase of soil groups 5 and 6 (silt-dominated soils) with increasing depth, the basin of Zell is characterized by the appearance of coarser soil groups (mainly soil groups 3 and 4). These differences are explained by the geographical location of the basins. Especially in the region of Flachgau it was shown that attention should be paid if a penetration test is conducted in a basin or on the hillside as the soil type distribution then gives more fine-grained or coarse-grained results, respectively.

As a conclusion of chapter 6 it can be stated that although basins can be characterized as rather homogeneous, it is very difficult to predict soil lithologies without performing CPT tests, because the probability of local differences is too high. A generalized statement for a whole basin or a whole region is extremely complicated, simply because of the large number of unknowns and assumptions that need to be made which can lead to enormous inaccuracies.

8.2 Chapter 7

In chapter 7, in-situ measurements were investigated by means of normalized soil behaviour type charts with respect to the six soil groups. It was shown that the approaches according to Robertson (2009, 2016) and Schneider (2008) yield good results for Austrian sands, i.e. soils that show a sand-like dilative behaviour with fully drained conditions while penetration. However, all three approaches show shortcomings in the classification when it comes to silt-dominated soils (soil groups 4 to 6). These are often wrongly characterized as clays. Especially soil group 4 (fine-sandy silts to silty fine-sands) shows a large scatter in the soil behaviour type charts according to Robertson (2009, 2016). Pure silts practically never occur. They are always in combination with other soil types, which makes a classification of them very complicated. Especially the example of the basin of Zell showed that a separation between soil groups 3 and 4 (sands and sands with silty constituents) is very difficult, as both groups plot in the same regions with a very large scatter according to Robertson (2009, 2016). Other reasons for the large dispersion of data can be thin interlayers of clay, sand or gravel that were not individually classified within the core drillings but cause large scatters. They could be identified by regrouping single soil lithologies to see which are actually responsible for the large scatter. In addition to that, silt dominated soils are characterized by partial drained conditions during the penetration process. This effect can also be an explanation for the large scatter. In order to detect to which extent partial drainage influences the results, further research is needed, especially on the methods of how partial drainage can be considered. The investigation of data with the soil behaviour type chart according to Schneider (2008) also showed

shortcomings for the classification of silt-dominated soils. Although it should be noted that, as mentioned in chapter 3, Schneider (2008) introduced his soil classification charts in three different scales, depending on the soil type to be investigated. However, a distinction of these charts was neglected within this thesis and all six soil types were investigated by the same soil classification chart. A disadvantage of the soil classification charts according to Schneider (2008) is the need for CPTu data, which is less available than simple CPT data. Additionally, Schneider (2008) only provides four different soil types which leaves the classification of soil very inaccurate. These facts leave the approaches according to Robertson (2009, 2016) more applicable in practice, although it needs to be stated that those give too little room for silty soils, i.e. transitional soils according to Robertson (2009, 2016).

The detection of microstructure according to Robertson (2016) showed that all soil groups imply the presence of microstructure, although the results for Zell and Flachgau are not as clear as those for the basin of Salzburg. A closer look at the empirical value K_G* of 330 should be taken, as this value should probably be adjusted for Austrian silt-dominated soils. In addition, further research is needed for a deeper understanding of the microstructural bonds acting and influencing the mechanical behaviour of soils. This leaves the approaches after Robertson (2009, 2016) and Schneider (2008) questionable in their application, at least for Austrian silt-dominated soils.

Bibliography

Apriyono, A., Yanto, S. P. B. & Sumiyanto, 2018. *Soil classification based on cone penetration test (CPT) data in Western Central Java,*. Engineering International Conference (EIC2017), AIP Conference Proceedings.

Begemann, H. K. S., 1965. *The friction jacket cone as an aid in determining the soil profile.* Montreal, Proceedings of the 6th International Conference on Soil Mechanics and Foundation Engineering, ICSMFE, September 8 - 15, Vol. 2.

Campanella, R., Roberston, P. K. & Gillespie, D., 1982. *Pore pressures during cone penetration testing.* Amsterdam, in: Proceedings of the 2nd European Symposium on Penetration Testing, ESPOT II, 24-27 May 1982.

derStandard, 2018. *STANDARD Verlagsgesellschaft m.b.H.*. [Online] Available at: https://www.derstandard.at/story/2000071496231/die-salzburger-altstadt-sinkt-langsam-ab [Accessed 27 12 2019].

Douglas, B. J. & Olsen, R. S., 1981. *Soil classification using electric cone penetrometer.* St. Louis, American Society of Civil Engineers, ASCE, Proceedings of Conference on Cone Penetration Testing and Experience, October 26 - 30, pp. 209 – 227.

Eslami, A. & Fellenius, B. H., 1997. Pile capacity by direct CPT and CPTu methods applied to 102 case histories. *Canadian Geotechnical Journal, Vol. 34, No. 6,* pp. 880 - 898.

Feindt, M. & Kerzel, U., 2015. *Prognosen bewerten - Statistische Grundlagen und praktische Tipps.* [Ebook] ed. Berlin, Heidelberg: Springer Verlag.

Fellenius, B. H. & Eslami, A., 2000. *Soil Profile Interpeted from CPTu Data.* Bangkok, Thailand, Asian Institute of Technology, "Year 2000 Geotechnics" Geotechnical Engineering Conference, November 27 - 30, 2000, p. 18.

Geologismiki, 2018. *Geologismiki: CPeT-IT-Software.* [Online] Available at: https://geologismiki.gr/products/cpet-it/ [Accessed 27 12 2019].

geotechnik, 2013. *DocPlayer.org - Drucksondiertechnik nach DIN EN ISO 22476 Teil 1.* [Online]

Available at: https://docplayer.org/64803396-Drucksondiertechnik-nach-din-en-iso-teil-1-oktober-2013.html
[Accessed 07 01 2020].

Hemmerich, W., 2011. *Mathe Guru.* [Online]
Available at: https://matheguru.com/stochastik
[Accessed 09 12 2019].

Hintze, J. & Nelson, R., 1998. Statistical Computing and Graphics - Violin Plots: A Box-Plot Density Trace Synergism. *The American Statistician, Vol 52*.

iCgroup, 2020. *iC consulenten Ziviltechniker GesmbH.* [Online]
Available at: https://www.google.com/search?q=Salzburger+Seeton&client=firefox-b-d&sxsrf=ACYBGNSIHJHR7CgwiQzokMq9U8zjrXY_uw:1578648269866&source=lnms&tbm=isch&sa=X&ved=2ahUKEwiG1-aK2_jmAhUSU1AKHVPkC4EQ_AUoAnoECAwQBA&biw=1920&bih=966#imgrc=qLKgRu0zmT99-M:
[Accessed 10 01 2020].

Jefferies, M. G. & Davies, M. P., 1993. Use of CPTu to Estimate Equivalent SPT N60. *Geotechnical Testing Journal, Vol. 16, No. 4*, pp. 458-468.

Kamps, U., 2019. *Gabler Wirtschaftslexikon - Springer Fachmedien Wiesbaden GmbH.* [Online]
Available at: https://wirtschaftslexikon.gabler.de/definition/normalverteilung-39769
[Accessed 09 12 2019].

Lunne, T., Robertson, P. K. & Powell, J. J., 1997. *Cone Penetration Testin in Geotechnical Practice.* England, London: Taylor and Francis Group.

Marchetti, 2016. *Marchetti Dilatometer.* [Online]
Available at: http://www.marchetti-dmt.it/seismic-dilatometer-sdmt/
[Zugriff am 07 01 2020].

Oberhollenzer, S. et al., 2020. *Characterization of microstructure in silt-dominated sediments.* Budapest, Hungary, 6th International Conference on Geotechnical and Geophysical Site Characterization, [paper in review].

Roberston, P. K. & Wride, C. E., 1998. Evaluating cyclic liquefaction potential using the cone penetration test. *Canadian Geotechnical Journal, Vol. 35*, pp. 442-459.

Robertson, P. K., 1990. Soil classification using the cone penetration test. *Canadian Geotechnical Journal, Vol. 27, No. 1*, pp. 151 - 158.

Robertson, P. K., 2009. Interpretation of cone penetration tests - a unified approach. *Canadian Geotechnical Journal, Vol. 46*, pp. 1337-1355.

Robertson, P. K., 2010. *Soil Behaviour Type from the CPT- An Update,* Signal Hill, California, USA: Gregg Drilling & Testing Inc..

Robertson, P. K., 2016. Cone penetration test (CPT) - based soil behaviour type (SBT) classification system – an update. *Canadian Geotechnical Journal, Vol. 53*, pp. 1910-1927.

Robertson, P. K., Camanella, R. G., Gillespie, D. & Greig, J., 1986. *Use of piezometer cone data.* s.l., in: Proceedings of American Society of Civil Engineers, ASCE, In-Situ 86 Specialty Conference, Edited by S. Clemence, Blacksburg, June 23 - 25, Geotechnical Special Publication.

Schmertmann, J. H., 1978. *Guidelines for cone penetration test (Performance and Design),* Washington: U.S. Department of Transportation, Federal Highway Administration, Report FHWA-TS-78209.

Schnaid, F., 2009. *In Situ Testin in Geomechanics - The main tests.* 1st edition ed. England, London: Taylor and Francis Group.

Schneider, J. A. & Moss, R. E., 2011. Linking cyclic stress and cyclic strain based methods for assessment of cyclic liquefaction triggering in sands. *Geotechnique Letters 1, Institute of Civil Engineers, U.K.*, pp. 31-36.

Schneider, J. A., Randolph, M. F., Mayne, P. W. & Ramsey, N. R., 2008. Analysis of Factors Influencing Soil Classification Using Normalized Piezocone Tip Resistance and Pore Pressure Parameters. *Journal of Geotechnical and Geoenvironmental Engineering, Vol 134, No.11*.

Statista, 2019. *Statistik Lexikon - Statista GmbH.* [Online]
Available at:
https://de.statista.com/statistik/lexikon/definition/11/statistik_fuer_anfaenger_einfuehrung_in_die_statistik/
[Accessed 09 12 2019].

StatSoft, 2019. *StatSoft Europe GmbH.* [Online]
Available at:
https://www.statsoft.de/glossary/B/BimodalDistribution.htm
[Accessed 10 12 2019].

Zhang, G., Robertson, P. K. & Brachmann, R. W., 2002. Estimating liquefaction-induced ground settlements from CPT for level ground. *Canadian Geotechnical Journal, Vol. 39*, pp. 1168-1180.

Appendices

Appendix A:

Allocation of core drillings to in-situ tests

A-Tab. 1.: Extract from Excel-File: allocation of core drillings to in-situ tests

Projektnummer	Projektname	Bezeichnung	KB	Kat. Gem.	Becken	L1_Genese	L1_BA	L1_Tiefe	L2_Genese	L2_BA	L2_Tiefe	L3_Genese	L3_BA	L3_Tiefe
12031	CDKPflegezentrum	12031_CPTu_2_12	12031_KB_1_12	56531 Maxglan	Salzburger Becken	Auffüllung	A	-2	Schotter	G,s,u-	-7	Seeton	fS,u	-10
12031	CDKPflegezentrum	12031_CPTu_10_12	12031_KB_1_12	56531 Maxglan	Salzburger Becken	Auffüllung	A	-1	Schotter	G,s,u-	-4	Seeton	fS,u	-10
12031	CDKPflegezentrum	12031_CPTu_6_12	12031_KB_2_12	56531 Maxglan	Salzburger Becken	Auffüllung	A	-2	Schotter	G,s,u-	-4,5	Seeton	fS,u	-12
12031	CDKPflegezentrum	12031_CPTu_5_12	12031_KB_2_12	56531 Maxglan	Salzburger Becken	Auffüllung	A	-1	Schotter	G,s,u-	-6,5	Seeton	fS,u	-8,5
12086	Robinigstraße	12086_CPTu_6_13	12086_KB_1_12	56513 Gnigl	Salzburger Becken	Anschüttung	A	-0,5	Torf	H	2,5	XY	fS,mS,u-,g	-6
12086	Robinigstraße	12086_CPT_5_12	12086_KB_2_12	56513 Gnigl	Salzburger Becken	Anschüttung	A,G	-1	Torf	H	-3	XY	fS,U,mS	-8
12086	Robinigstraße	12086_CPT_8_12	12086_KB_2_12	56513 Gnigl	Salzburger Becken	Anschüttung	A,G	-1	Torf	H	-3	XY	fS,U,mS	-15
12086	Robinigstraße	12086_CPTu_4_12	12086_KB_2_12	56513 Gnigl	Salzburger Becken	Anschüttung	A,G	-1	Torf	H	-3	XY	fS,U,mS	-16
12086	Robinigstraße	12086_CPTu_2_13	12086_KB_3_12	56513 Gnigl	Salzburger Becken	Anschüttung	A,G,S,x,u-	-1,5	Torf	H	-4	XY	fS,mS	-6,5
12086	Robinigstraße	12086_CPTu_5_13	12086_KB_1_13	56513 Gnigl	Salzburger Becken	Anschüttung	G,s,u+	-1	Torf	H	-3	Schwemms	S,u	-7
12086	Robinigstraße	12086_CPTu_3_13	12086_KB_1_13	56513 Gnigl	Salzburger Becken	Anschüttung	G,s,u+	-1,2	Torf	H	-3	Schwemms	S,u	-6,5
12086	Robinigstraße	12086_CPT_6_12	12086_KB_2_13	56513 Gnigl	Salzburger Becken	Anschüttung	G,s,u+	-1	Torf	H	-4	Schwemms	S,u	-8
12087	SteinbruchstraßeKanal	12087_CPT_10_12	12087_KB_2148_11	56537 Salzburg	Salzburger Becken	Anschüttung	A,s,g,x	-0,5	Schotter	G,s,x	-1	Schwemms	U,fs	-7
12087	SteinbruchstraßeKanal	12087_CPT_1_12	12087_KB_2151_11	56537 Salzburg	Salzburger Becken	Anschüttung	A,s,g,x	-1	Torf	H	-3	Seeton	U,fs	-6
12087	SteinbruchstraßeKanal	12087_CPT_4_12	12087_KB_2156_11	56537 Salzburg	Salzburger Becken	Anschüttung	A,s,g,x	-0,8	Seeton	U,s	-7			
12087	SteinbruchstraßeKanal	12087_CPTu_2_13	12087_KB_2156_11	56537 Salzburg	Salzburger Becken	Anschüttung	A,s,g,x	-1	Seeton	U,s	-9			
12087	SteinbruchstraßeKanal	12087_CPT_5_12	12087_KB_2152_11	56537 Salzburg	Salzburger Becken	Anschüttung	A,s,g,x	-0,45	Schotter	S,g,x	-0,9	Torf	H	-3,45
12087	SteinbruchstraßeKanal	12087_CPTu_1_14	12087_KB_2152_11	56537 Salzburg	Salzburger Becken	Anschüttung	A,s,g,x	-0,45	Schotter	S,g,x	-2	Torf	H	-3,45
12087	SteinbruchstraßeKanal	12087_CPTu_2_14	12087_KB_2153_11	56537 Salzburg	Salzburger Becken	Anschüttung	A,s,g,x	-0,5	Schotter	S,g,x	-1,5	Torf	H	-4
12087	SteinbruchstraßeKanal	12087_CPT_9_12	12087_KB_2150_11	56537 Salzburg	Salzburger Becken	Anschüttung	A,s,g,x	-1	Torf	H	-2	Seeton	U,fs	-8
12095	StrubergasseBaufeldB	12095_CPT_1_13	12095_KB_1_13	56537 Salzburg	Salzburger Becken	Anschüttung	A,g,s,u	-0,8	Ausediment	S,u-	-2,5	Schotter	G,s,u-	-6
12095	StrubergasseBaufeldB	12095_CPTu_2_13	12095_KB_2_13	56537 Salzburg	Salzburger Becken	Anschüttung	A,g,s	-0,8	Ausediment	S,u-	-2	Schotter	G,s,u-	-6
12095	StrubergasseBaufeldB	12095_CPT_5_13	12095_KB_2_13	56537 Salzburg	Salzburger Becken	Anschüttung	A,g,s	-0,8	Ausediment	S,u-	-2	Schotter	G,s,u-	-7
12095	StrubergasseBaufeldB	12095_CPT_4_13	12095_KB_2_13	56537 Salzburg	Salzburger Becken	Anschüttung	A,g,s	-0,8	Ausediment	S,u-	-2	Schotter	G,s,u-	-8
12095	StrubergasseBaufeldB	12095_CPT_6_13	12095_KB_3_13	56537 Salzburg	Salzburger Becken	Anschüttung	A,g,s,u-	-0,5	Ausediment	S,u-	-1	Schotter	G,s,u-	-8
12095	StrubergasseBaufeldB	12095_CPT_3_13	12095_KB_3_13	56537 Salzburg	Salzburger Becken	Anschüttung	A,g,s,u-	-0,5	Ausediment	S,u-	-1	Schotter	G,s,u-	-5
12095	StrubergasseBaufeldB	12095_CPT_8_13	12095_KB_4_13	56537 Salzburg	Salzburger Becken	Anschüttung	A,g,s	-0,7	Ausediment	S,u	-2	Schotter	G,s,u-	-5
12095	StrubergasseBaufeldB	12095_CPT_7_13	12095_KB_4_13	56537 Salzburg	Salzburger Becken	Anschüttung	A,g,s	-0,7	Ausediment	S,u	-1	Schotter	G,s,u-	-4,5
13069	VinzenzMariaSüßstraße	13069_CPT_1_13	13069_KB_2039_04	56537 Salzburg	Salzburger Becken	Anschüttung	A,s,g,x	-0,8	XY	fS,g	-3	XY	S,g,x	-5,8
14001	RaiffeisenNVZ	14001_CPTu_25_14	14001_KB_1_14	56524 Itzling	Salzburger Becken	Anschüttung	A,G,s,u-	-1	alzachschotte	G,s,u-	-2,4	Seeton	U,t,g,x	-2,9
14001	RaiffeisenNVZ	14001_CPTu_19_14	14001_KB_2_14	56524 Itzling	Salzburger Becken	Anschüttung	A,G,s,u-	-2	Moräne	U,T,S,G,x,y	-4,5	ysch verwitte	Tst,u	-12,5
14003	Wolfsgartenweg	14003_CPTu_1_14	14003_KB_2_13	56501 Aigen I	Salzburger Becken	Anschüttung	A,G,s	-0,5	Torf	H	-3,9	Seeton	U,t	-4,3
14003	Wolfsgartenweg	14003_CPTu_2_14	14003_KB_1_13	56501 Aigen I	Salzburger Becken	Anschüttung	A,G,s,u-	-0,7	Ausand	U,s	-1,3	Torf	H	-3,3
14003	Wolfsgartenweg	14003_CPTu_3_14	14003_KB_1_13	56501 Aigen I	Salzburger Becken	Anschüttung	A,G,s,u-	-0,7	Ausand	U,s	-1,3	Torf	H	-3,3
14013	SebastianKneippstraße	14013_CPT_1_15	14013_KB_1_16	56531 Maxglan	Salzburger Becken	Ton	T,U	-1,1	einsand, Schlu	fS,U	-2,5	Ton, Schluff	T,U	-3,5
14013	SebastianKneippstraße	14013_CPT_6_15	14013_KB_1_16	56531 Maxglan	Salzburger Becken	Ton	T,U	-1,5	einsand, Schlu	fS,U	-4,3	Ton, Schluff	T,U	-4,8
14013	SebastianKneippstraße	14013_CPT_10_15	14013_KB_2_16	56531 Maxglan	Salzburger Becken	in- bis Grobsa	fS,mS,gS	-10						
14013	SebastianKneippstraße	14013_CPT_14_15	14013_KB_2_16	56531 Maxglan	Salzburger Becken	in- bis Grobsa	fS,mS,gS	-10						
14013	SebastianKneippstraße	14013_CPT_15_15	14013_KB_2_16	56531 Maxglan	Salzburger Becken	in- bis Grobsa	fS,mS,gS	-10						
14013	SebastianKneippstraße	14013_CPT_2_15	14013_KB_1_12	56531 Maxglan	Salzburger Becken	Mutterboden	M	-2	bkies, Mittelk	gG,mG	-9,5	insand, Feinki	fS,fG	-20
14013	SebastianKneippstraße	14013_CPT_3_15	14013_KB_1_12	56531 Maxglan	Salzburger Becken	Mutterboden	M	-1,8	bkies, Mittelk	gG,mG	-11	insand, Feinki	fS,fG	-20

Appendix B:

Python codes of data base analysis, chapter 4.3

Python Code: Fig. 18

```
# -*- coding: utf-8 -*-
"""
Created on Wed Aug 14 14:44:06 2019

@author: angollo
"""

import os
import numpy as np
import pandas as pd
import matplotlib.pyplot as plt
plt.rcParams["font.family"] = "Times New Roman"


""" PART 1: CREATING DATAFRAME WITH WHOLE INFORMATION ------------"""

print(os.getcwd()) #show current working directory
os.chdir(r'E:\MA\Task 3\Daten_Attributtabelle')
print(os.getcwd())

""" loading data files """
path = r'E:\MA\Task 3\Daten_Attributtabelle'
files = os.listdir(path) #lists all files in folder where path is
print(files)

"""get information from Attributtabellen and store it to a single
dataframe"""
df = pd.DataFrame()
for i,f in enumerate(files):
    data = pd.read_excel(f, usecols=['Becken', 'Bundesland', 'Kat.
Gem.', 'Kernbohrun', 'Feinsedime'])
    data['TestType']=i
    df = df.append(data)


""" PART 2: CREATING DATAFRAMES WITH SEPARATED INFORMATION --------"""

CPT_data = df[df['TestType']== 0]
CPTu_data = df[df['TestType']== 1]
DMT_data = df[df['TestType']== 2]
Seismik_data = df[df['TestType']== 3]

Total = len(CPT_data)+len(CPTu_data)+len(DMT_data)+len(Seismik_data)

""" PART 3: PLOTTING ---------------------------------------------"""

'Pie Chart for total amount of tests '
labels = 'CPT', 'CPTu', 'DMT', 'SCPT\nSCPTu\nSDMT'
colors = 'firebrick', 'tab:blue', 'black', 'forestgreen'
sizes = [len(CPT_data), len(CPTu_data), len(DMT_data),
len(Seismik_data)]
explode = [0.0,0.1,0.3,0.2]

fig1, ax1 = plt.subplots(dpi=300)
```

```
ax1.pie(sizes, labels = sizes, labeldistance = 0.6, colors = colors,
explode=explode)
ax1.axis('equal')
ax1.set_title(f'Total amount of available tests: {Total}')
ax1.legend(labels, loc = 'upper left', title='type of test')
plt.show
fig1.savefig(r'E:\MA\Task
3\Output\Figure1_PieChart_TimesNewRoman.png', bbox_inches="tight")


'Bar Chart for total amount of tests '
fig2, ax2 = plt.subplots()
y = range(4)
x = [len(CPT_data), len(CPTu_data), len(DMT_data), len(Seismik_data)]
colors = 'firebrick', 'tab:blue', 'black', 'forestgreen'

ax2.barh(y, x, align= 'center', color = colors, tick_label = labels)
ax2.invert_yaxis()

datagesamt = df.groupby('TestType').size().reset_index(name= 'Anzahl
der Tests')
for i, v in enumerate(datagesamt.iloc[:,1]):
    if v == 0:
        continue
    ax2.text(v+8, i+0.05, str(v))

ax2.set_ylabel('Test Type')
ax2.set_title('Amount of available tests')
ax2.set_xlim(0, 850)
plt.tight_layout()
fig2.savefig(r'E:\MA\Task
3\Output\Figure1_BarChart_TimesNewRoman.png', bbox_inches="tight")
```

Python Code: Fig. 22, Fig. 23 and Fig. 32

```
# -*- coding: utf-8 -*-
"""
Created on Wed Aug 14 14:44:06 2019

@author: angollo
"""
import os
import numpy as np
import pandas as pd
import matplotlib.pyplot as plt
plt.rcParams["font.family"] = "Times New Roman"


print(os.getcwd()) #show current working directory
os.chdir(r'E:\MA\Task 3\Daten_Attributtabelle')
print(os.getcwd())


""" loading data files ------------------------------------------"""
path = r'E:\MA\Task 3\Daten_Attributtabelle'
files = os.listdir(path) #lists all files in folder where path is

print(files)
```

```
"""get information from excel files and store them into a single
dataframe"""
df = pd.DataFrame()

for i,f in enumerate(files):
    data = pd.read_excel(f, usecols=['Becken', 'Bundesland', 'Kat.
Gem.', 'Kernbohrun', 'Bezeichnun', 'Feinsedime'])
    data['TestType']=i
    data['Bezeichnun']= data['Bezeichnun']+'.xlsx'
    df = df.append(data)


Becken = df.groupby(['Becken',
'TestType']).size().reset_index(name='Anzahl der Tests')
            #.size() returns a series #.reset_index()returns a
dataframe
Bundesland = df.groupby(['Bundesland',
'TestType']).size().reset_index(name= 'Anzahl der Tests')

Katastralgemeinde = df.groupby(['Kat. Gem.',
'TestType']).size().reset_index(name= 'Anzahl der Tests')

Kernbohrungen = df.groupby(['Kernbohrun',
'TestType']).size().reset_index(name= 'Anzahl der Tests')

dfnew = pd.concat([Becken, Bundesland, Katastralgemeinde,
Kernbohrungen], axis = 1)

print(dfnew)

groupedBecken = Becken.groupby(['Becken']).size().reset_index(name=
'Testarten pro Becken')
groupedBundesland =
Bundesland.groupby(['Bundesland']).size().reset_index(name= 'Testarten
pro Bundesland')
groupedKatastralgemeinde = Katastralgemeinde.groupby([
        'Kat. Gem.']).size().reset_index(name= 'Testarten pro
Katastralgemeinde')


""" DATA PROCESSING ----------------------------------------------"""

#data function
def dataframecreation(df, Kategorie):
    previousrow = df.iloc[0,0]
    num0 = 0
    num1 = 0
    num2 = 0
    num3 = 0
    completelist = []

    for row in range(len(df)):
        if previousrow == df.iloc[row, 0]:
            if df.iloc[row,1] == 0:
                num0 = df.iloc[row,2] #Zwischenspeicherung von Anzahl
der Tests
            elif df.iloc[row,1] == 1:
                num1 = df.iloc[row,2]
            elif df.iloc[row,1] == 2:
                num2 = df.iloc[row,2]
            elif df.iloc[row,1] == 3:
                num3 = df.iloc[row,2]
        elif previousrow != df.iloc[row, 0]:
```

```
            newlist = [previousrow, num0, num1, num2, num3]
            completelist.append(newlist)
            num0=0
            num1=0
            num2=0
            num3=0
            if df.iloc[row,1] == 0:
                num0 = df.iloc[row,2] #Zwischenspeicherung von Anzahl
der Tests
            elif df.iloc[row,1] == 1:
                num1 = df.iloc[row,2]
            elif df.iloc[row,1] == 2:
                num2 = df.iloc[row,2]
            elif df.iloc[row,1] == 3:
                num3 = df.iloc[row,2]
        else:
            print('There must be an errror!')

        previousrow = df.iloc[row,0]

        if row == len(df)-1:
            newlist = [previousrow, num0, num1, num2, num3]
            completelist.append(newlist)

    dfcompletelist = pd.DataFrame(completelist,
columns=[f'{Kategorie}', 'CPT',
                                                'CPTu',
'DMT','SCPT,SCPTu,SDMT'])
    dfcompletelist['Total'] = dfcompletelist.sum(axis = 1)
    return(dfcompletelist)

#plot function
def dataframeplot(df, Kategorie):

    colors = 'firebrick', 'tab:blue', 'black', 'forestgreen'
    fig, ax = plt.subplots(figsize=(6.4,3.5), dpi=300)

    y = df.iloc[:,0]
    columns = list(df.iloc[:,1:5].columns.tolist())
    left = 0

    for n, color in zip(columns, colors):
        ax.barh(y, df[n], left = left, color= color, label= f'{n}')
        left = left+df[n]

    for i, v in enumerate(df.iloc[:,5]):
        ax.text(v+5, i+0.17, str(v), fontsize =9, fontstyle=
'oblique')
    ax.set_xlabel('Amount of Tests')
    ax.set_ylabel(f'{Kategorie}')
    plt.xticks(fontsize = 8)
    ax.set_yticklabels(labels = df.iloc[:,0], fontsize = 8)
    ax.invert_yaxis()
    ax.set_ylim(len(df), -1)
 #   plt.title(f'Test type distribution in {Kategorie}')
    ax.legend(title='Type of Test:', fontsize = 7, title_fontsize = 7)
    plt.tight_layout()
    plt.show()
    return(fig, ax)

" Gruppierung nach Becken "

dfBeckengesamt = dataframecreation(Becken, 'Becken')
```

```
fig1, ax1 = dataframeplot(dfBeckengesamt, 'Basins')
ax1.set_xlim(0,620)
fig1.savefig(r'E:\MA\Task 3\Output\Figure2_Basins.png',
             bbox_inches = 'tight')

" Gruppierung nach Becken - nur wo Feinsedimente aufgetreten sind "

Becken_nurFeinsedimente = df.groupby(['Becken', 'Feinsedime',

'TestType']).size().reset_index(name='Anzahl der Tests')
indexNames =
Becken_nurFeinsedimente[Becken_nurFeinsedimente['Feinsedime']==
'Nein'].index
Becken_nurFeinsedimente.drop(indexNames, inplace=True)
Becken_nurFeinsedimente.drop('Feinsedime', axis = 1, inplace=True)

dfBecken_nurFeinsedimente = dataframecreation(Becken_nurFeinsedimente,
'Becken')

fig2, ax2 = dataframeplot(dfBecken_nurFeinsedimente, 'Basins with fine
sediments')
ax2.set_xlim(0,550)
fig2.savefig(r'E:\MA\Task
3\Output\Figure2_Basinswithfinesediments.png',
             bbox_inches = 'tight')

" Gruppierung nach Bundesländern "

dfBundeslandgesamt = dataframecreation(Bundesland, 'Bundesland')

fig3, ax3 = dataframeplot(dfBundeslandgesamt, 'States')
ax3.set_xlim(0,1400)
fig3.savefig(r'E:\MA\Task 3\Output\Figure2_Bundesland.png',
             bbox_inches = 'tight')
```

Appendix C:

q_c, f_s, R_f, and V_s over depth for all basins – chapter 6.1

All basins are in alphabetical order depending on their location. The exact in-situ measured values at each depth can be found in Excel files on the attached CD in the back of this thesis.

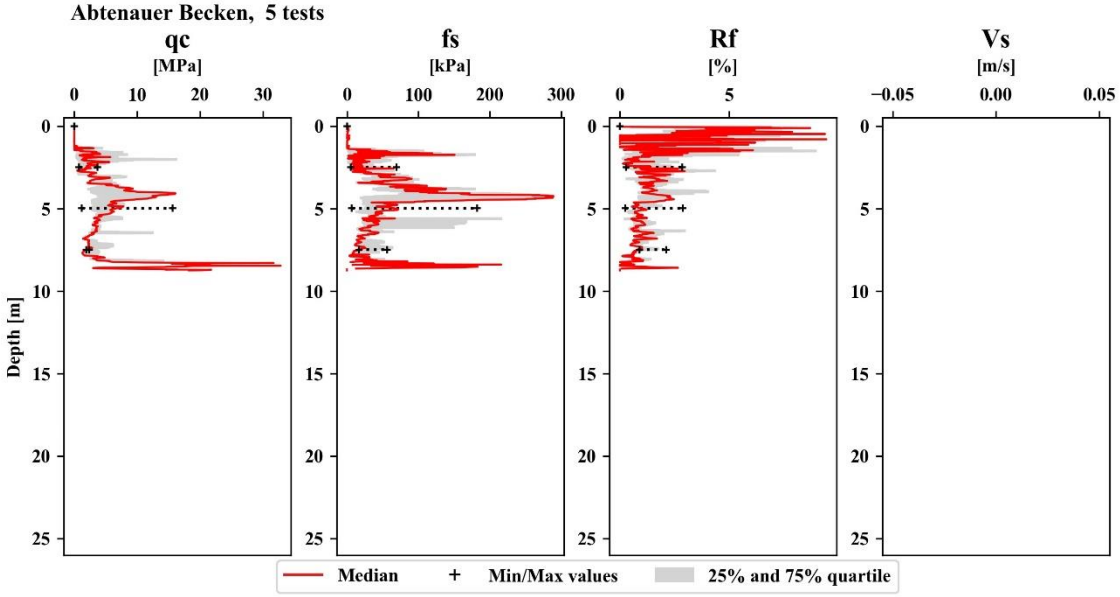

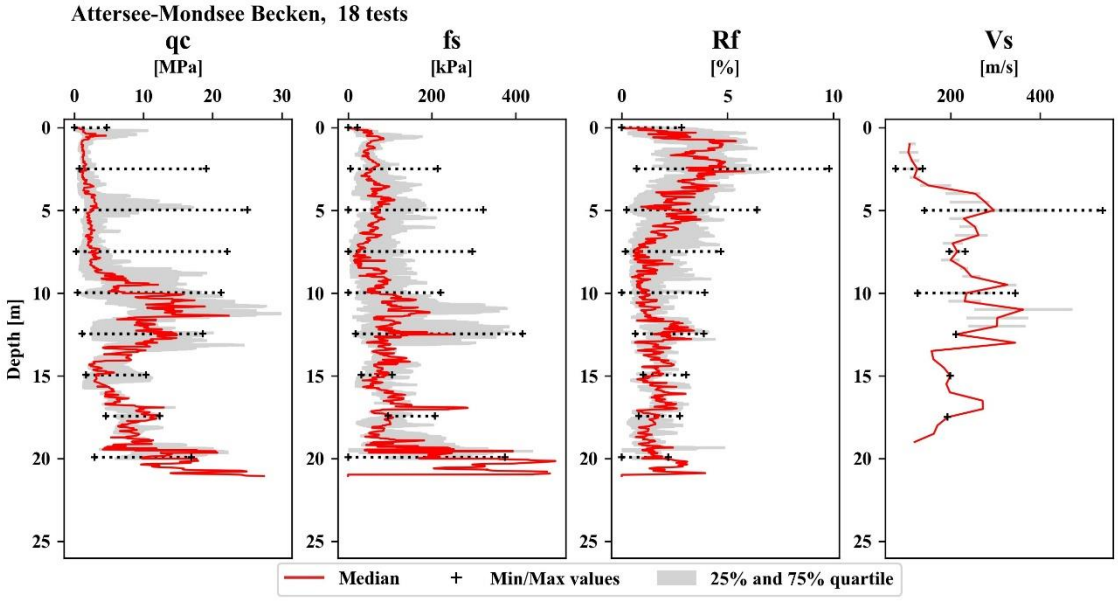

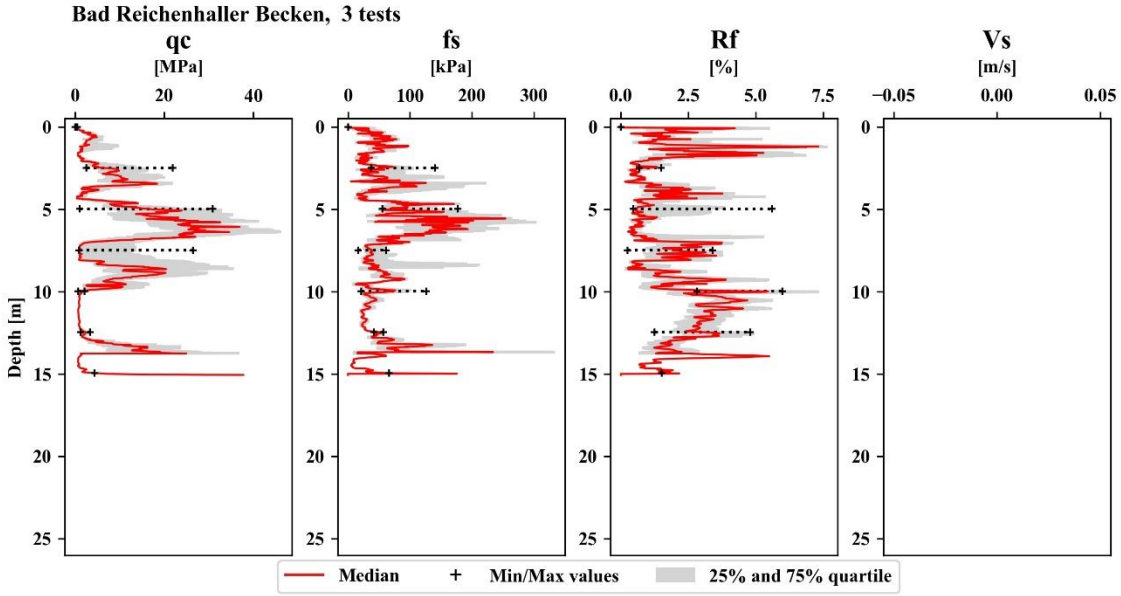
Bad Reichenhaller Becken, 3 tests
qc
[MPa]
fs
[kPa]
Rf
[%]
Vs
[m/s]
Depth [m]
Median
Min/Max values
25% and 75% quartile

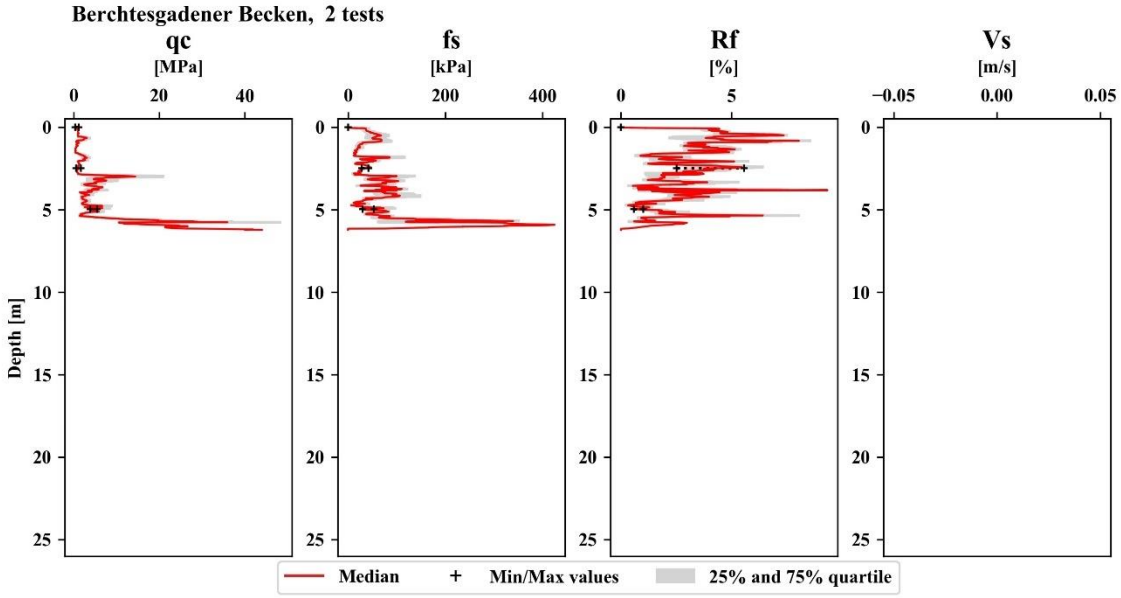
Berchtesgadener Becken, 2 tests
qc
[MPa]
fs
[kPa]
Rf
[%]
Vs
[m/s]
Depth [m]
Median
Min/Max values
25% and 75% quartile

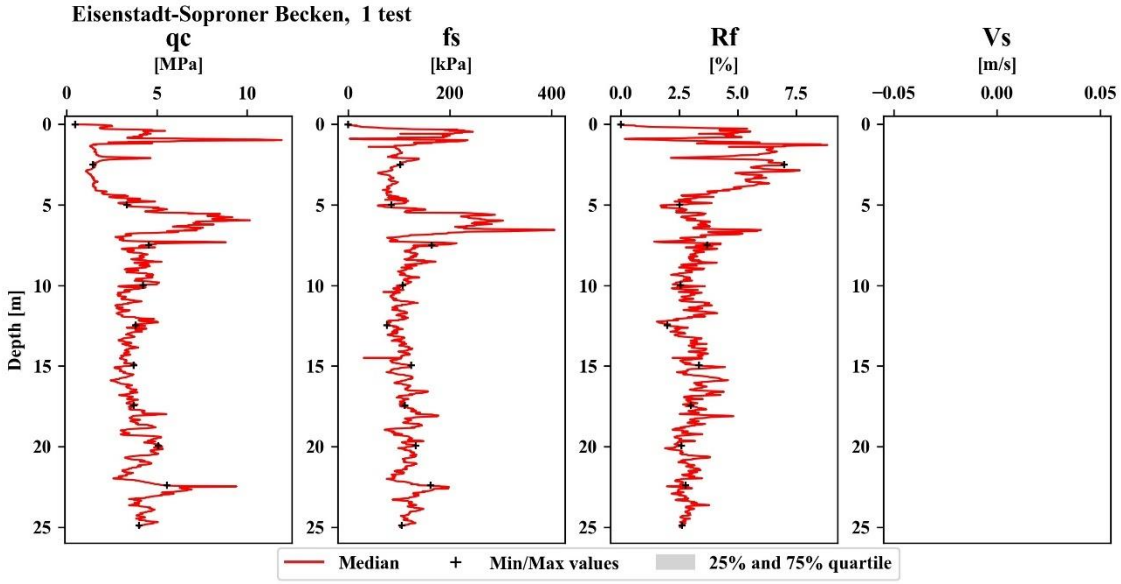
Eisenstadt-Soproner Becken, 1 test
qc
[MPa]
fs
[kPa]
Rf
[%]
Vs
[m/s]
Depth [m]
Median
Min/Max values
25% and 75% quartile

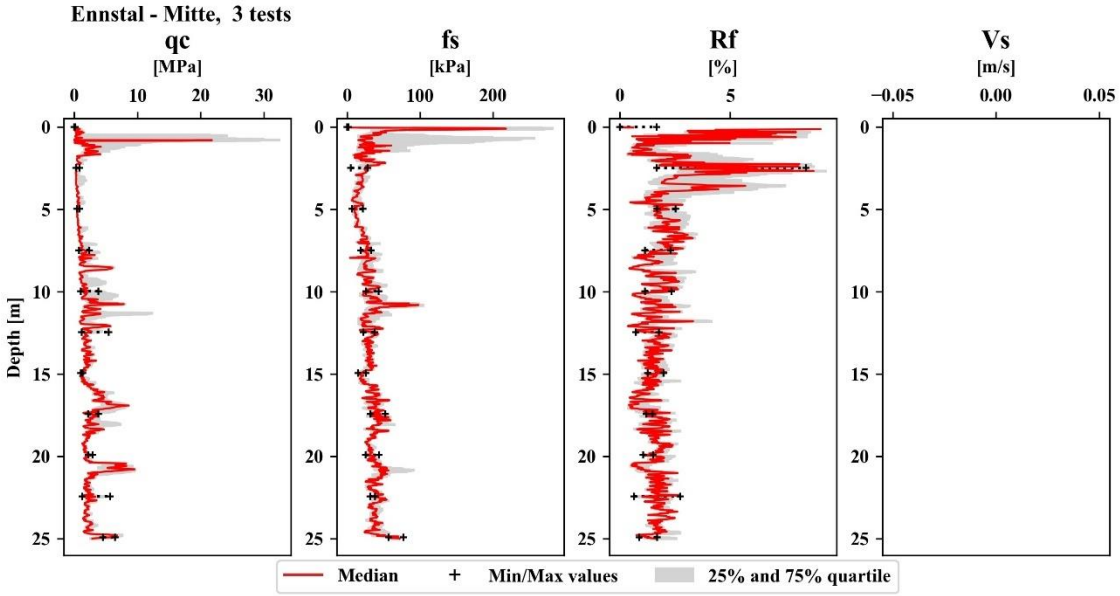
Ennstal - Mitte, 3 tests
qc
[MPa]
fs
[kPa]
Rf
[%]
Vs
[m/s]
Depth [m]
Median
Min/Max values
25% and 75% quartile

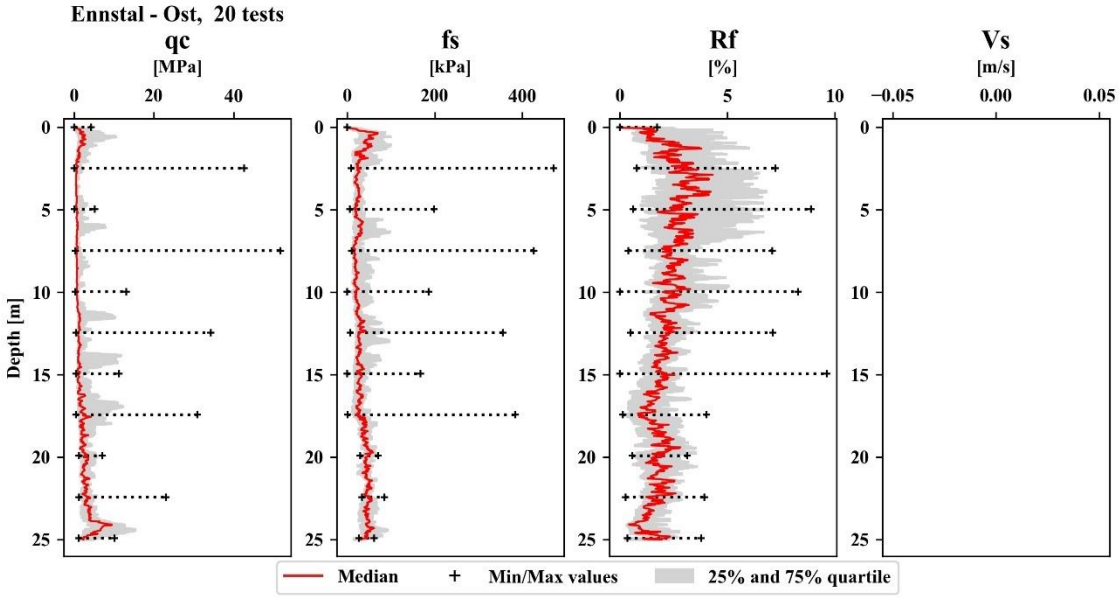
Ennstal - Ost, 20 tests
qc
[MPa]
fs
[kPa]
Rf
[%]
Vs
[m/s]
Depth [m]
Median
Min/Max values
25% and 75% quartile

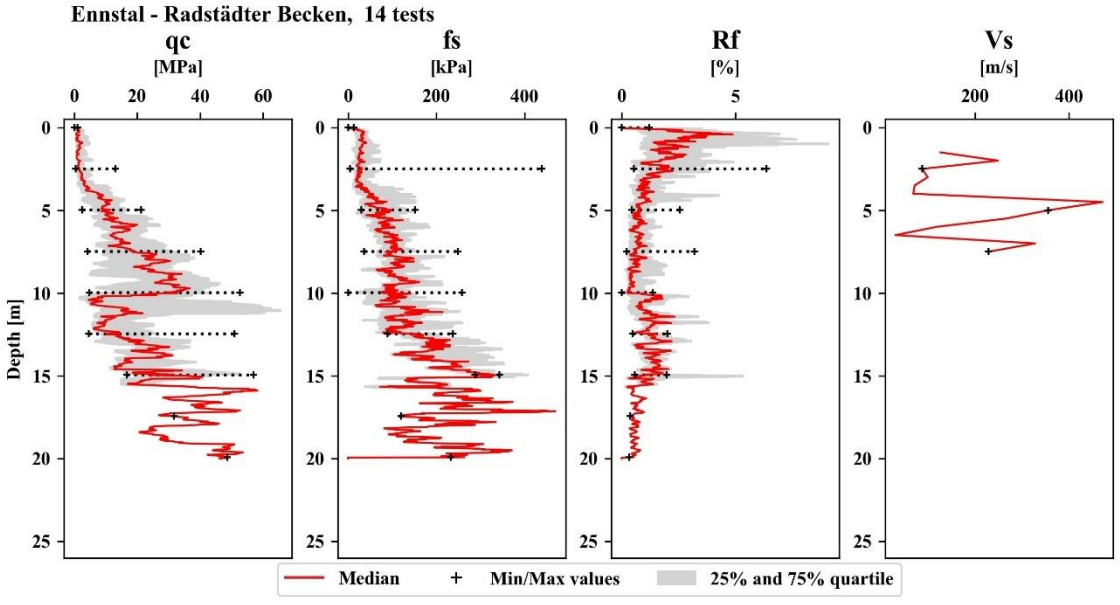
Ennstal - Radstädter Becken, 14 tests
qc
[MPa]
fs
[kPa]
Rf
[%]
Vs
[m/s]
Depth [m]
Median
Min/Max values
25% and 75% quartile

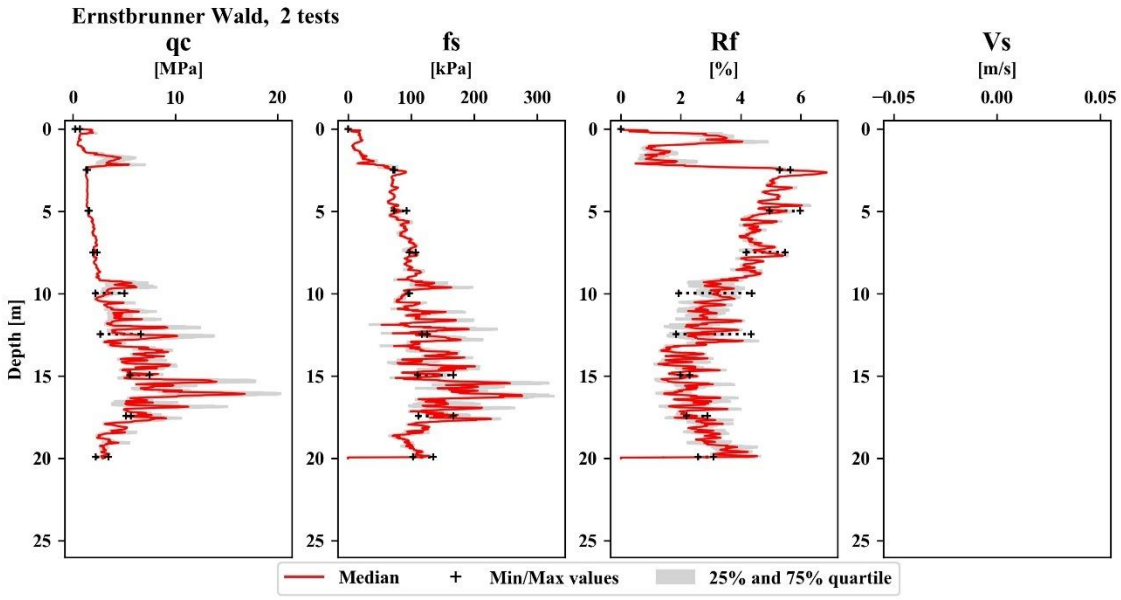
Ernstbrunner Wald, 2 tests
qc
[MPa]
fs
[kPa]
Rf
[%]
Vs
[m/s]
Depth [m]
Median
Min/Max values
25% and 75% quartile

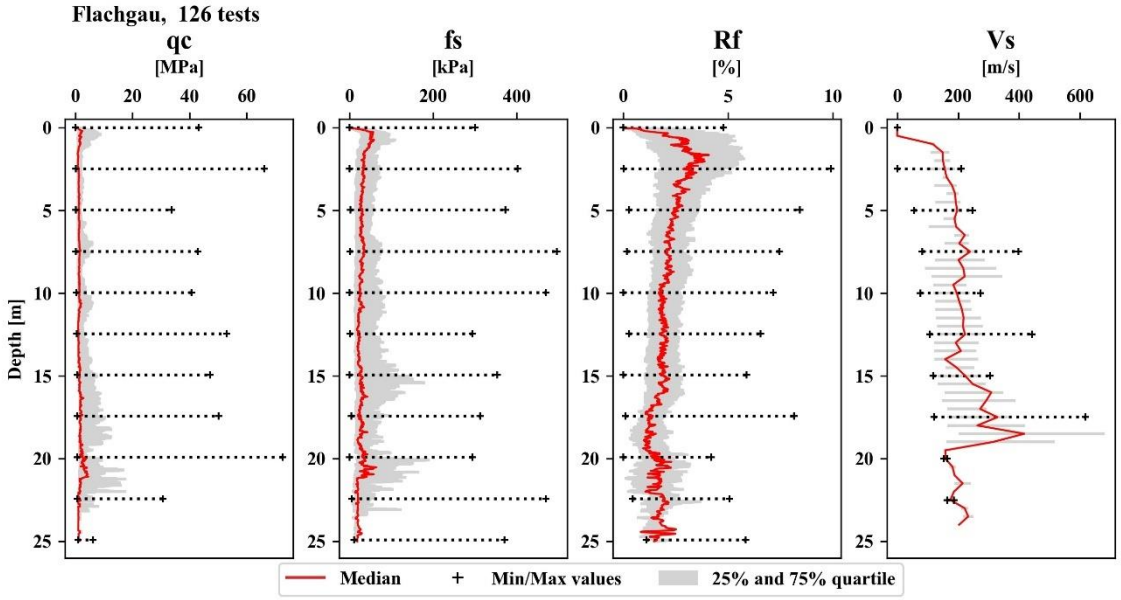
Flachgau, 126 tests
qc
[MPa]
fs
[kPa]
Rf
[%]
Vs
[m/s]
Depth [m]
Median
Min/Max values
25% and 75% quartile

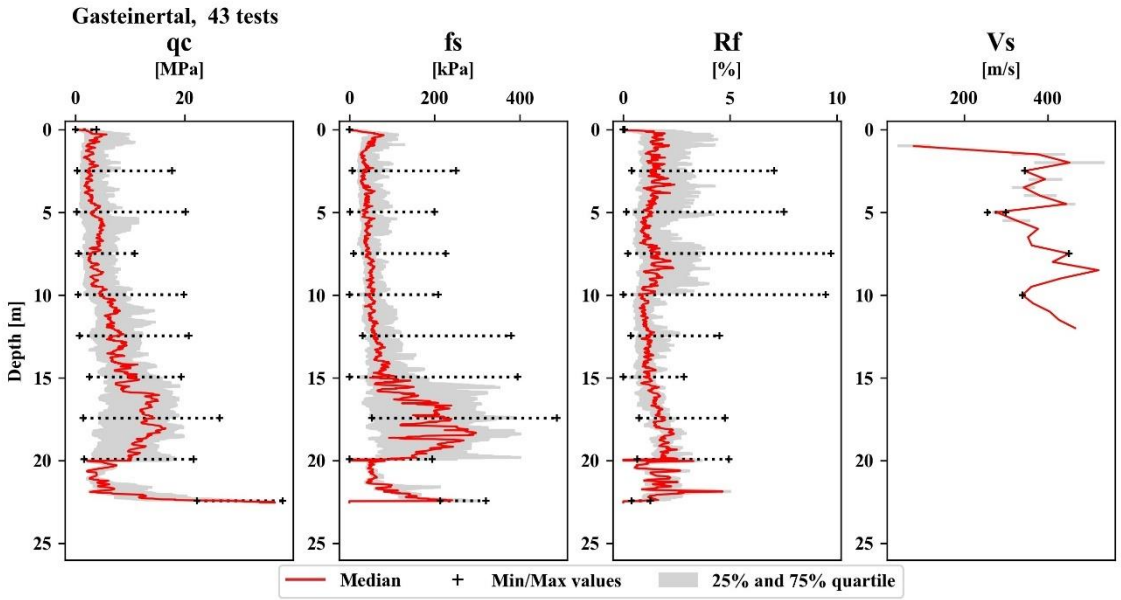
Gasteinertal, 43 tests
qc
[MPa]
fs
[kPa]
Rf
[%]
Vs
[m/s]
Depth [m]
Median
Min/Max values
25% and 75% quartile

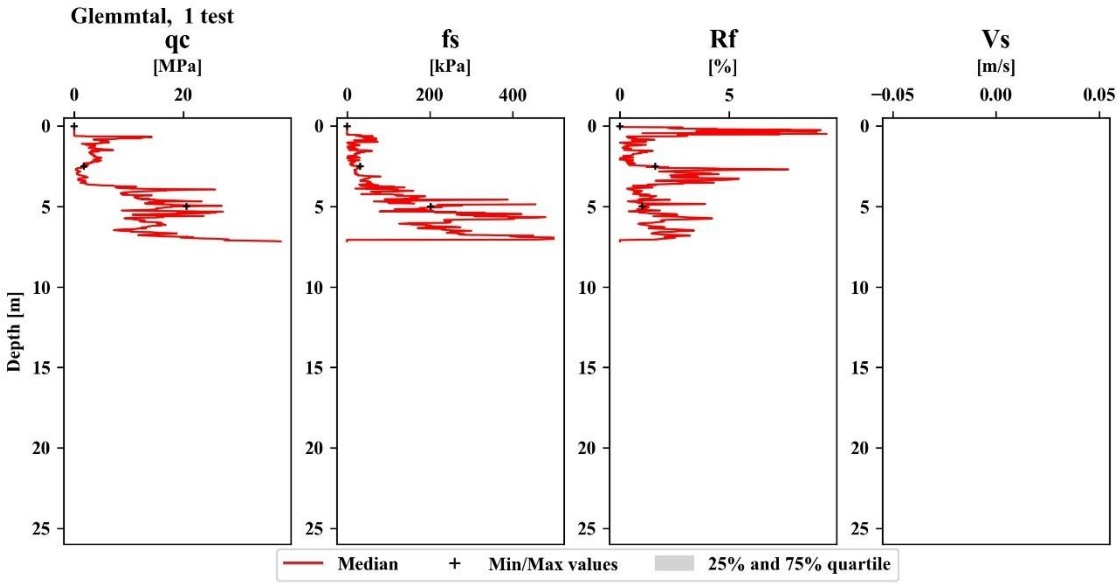
Glemmtal, 1 test
qc
[MPa]
fs
[kPa]
Rf
[%]
Vs
[m/s]
Depth [m]
Median
Min/Max values
25% and 75% quartile

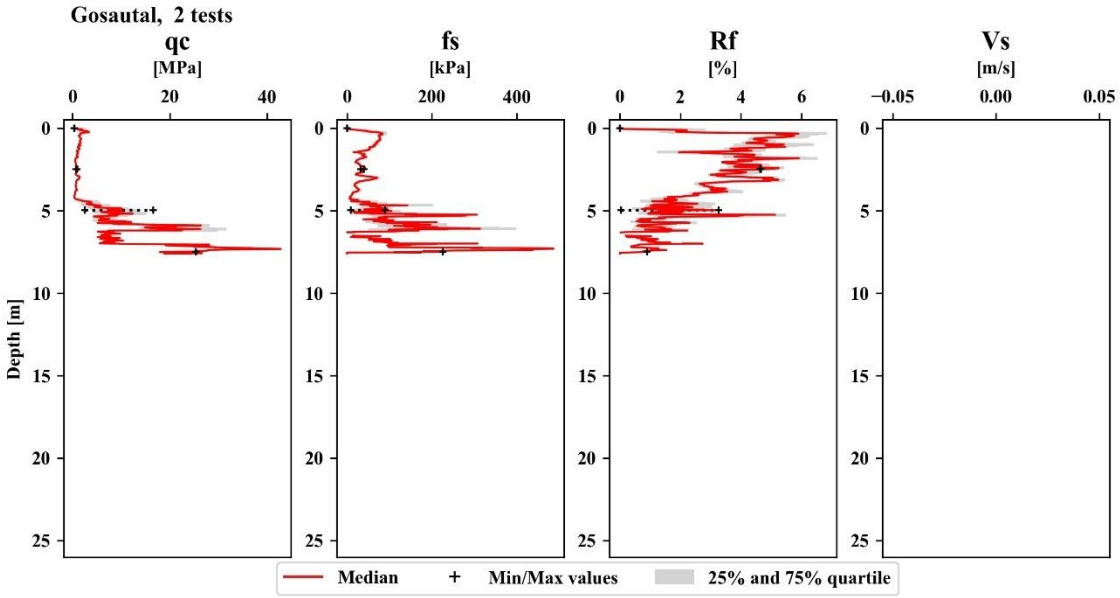
Gosautal, 2 tests
qc
[MPa]
fs
[kPa]
Rf
[%]
Vs
[m/s]
Depth [m]
Median
Min/Max values
25% and 75% quartile

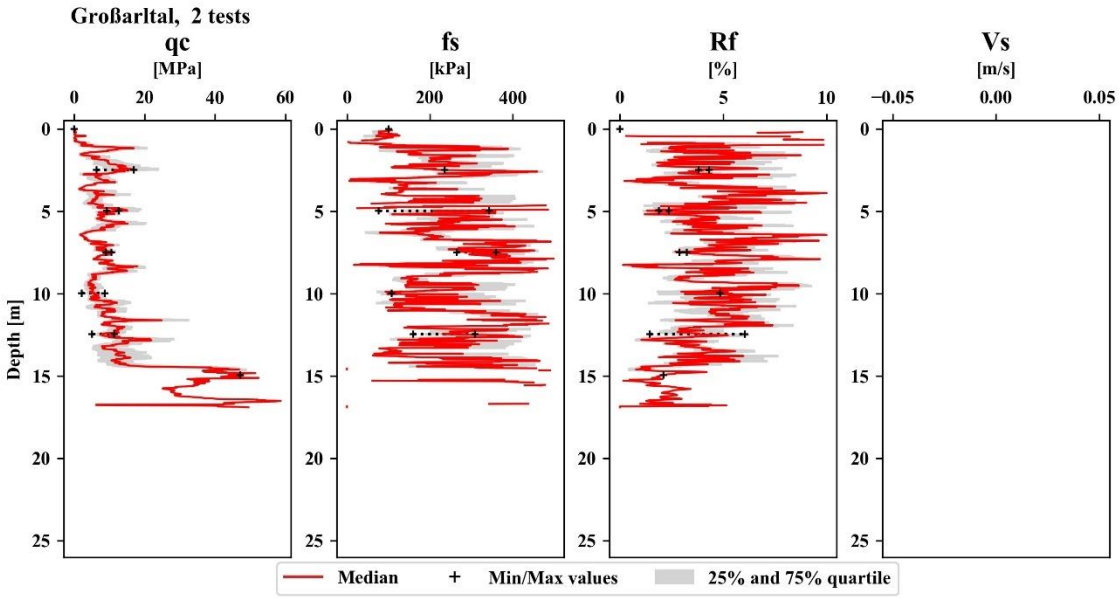
Großarltal, 2 tests
qc
[MPa]
fs
[kPa]
Rf
[%]
Vs
[m/s]
Depth [m]
Median
Min/Max values
25% and 75% quartile

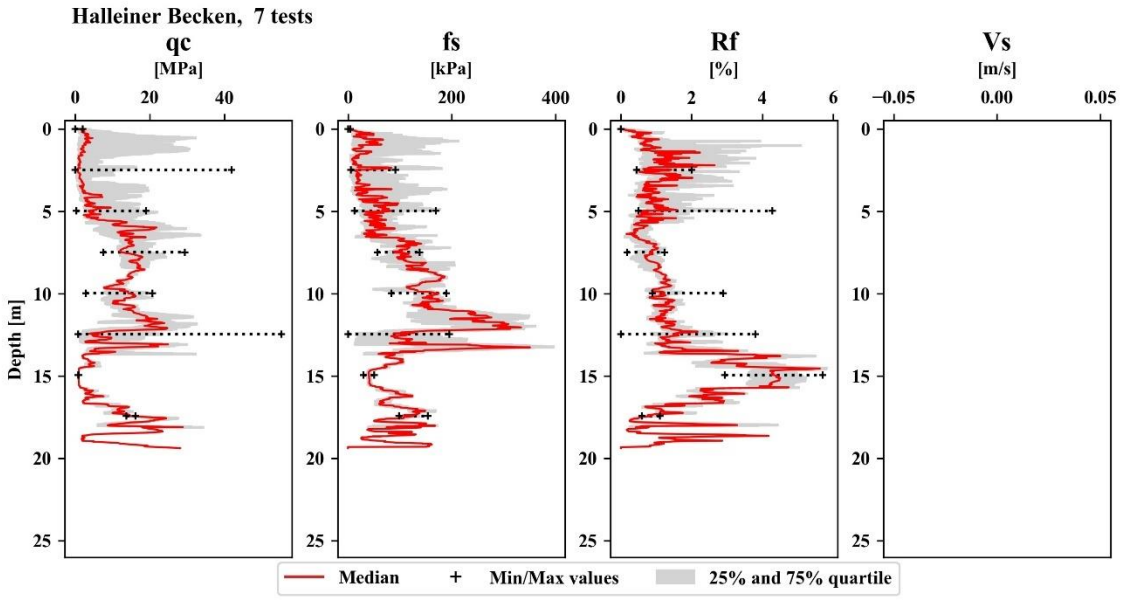
Halleiner Becken, 7 tests
qc
[MPa]
fs
[kPa]
Rf
[%]
Vs
[m/s]
Depth [m]
Median
Min/Max values
25% and 75% quartile

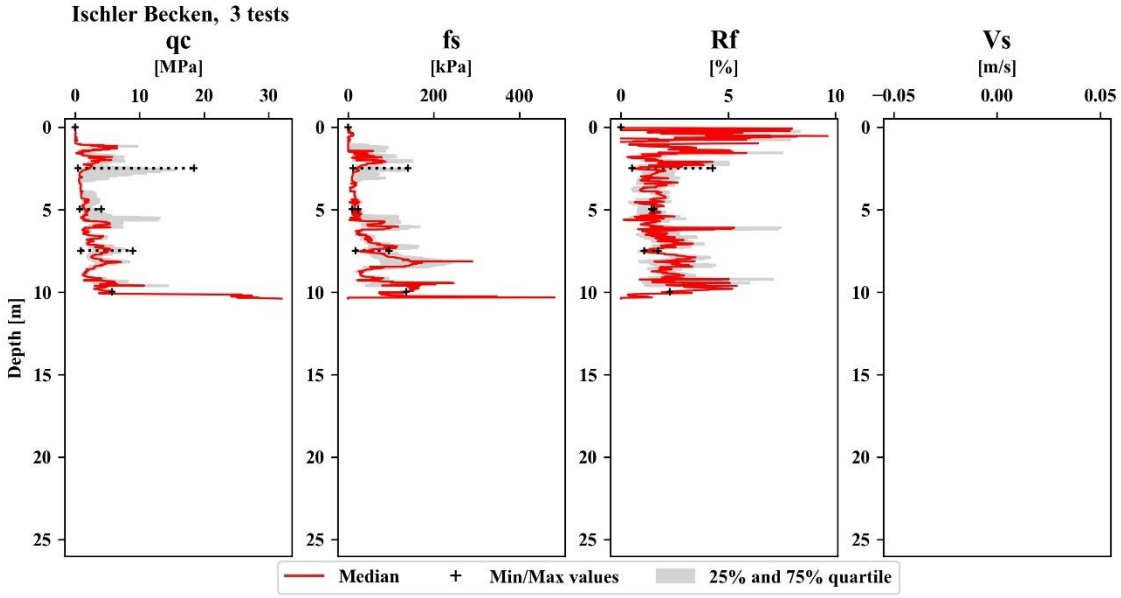
Ischler Becken, 3 tests
qc
[MPa]
fs
[kPa]
Rf
[%]
Vs
[m/s]
Depth [m]
Median
Min/Max values
25% and 75% quartile

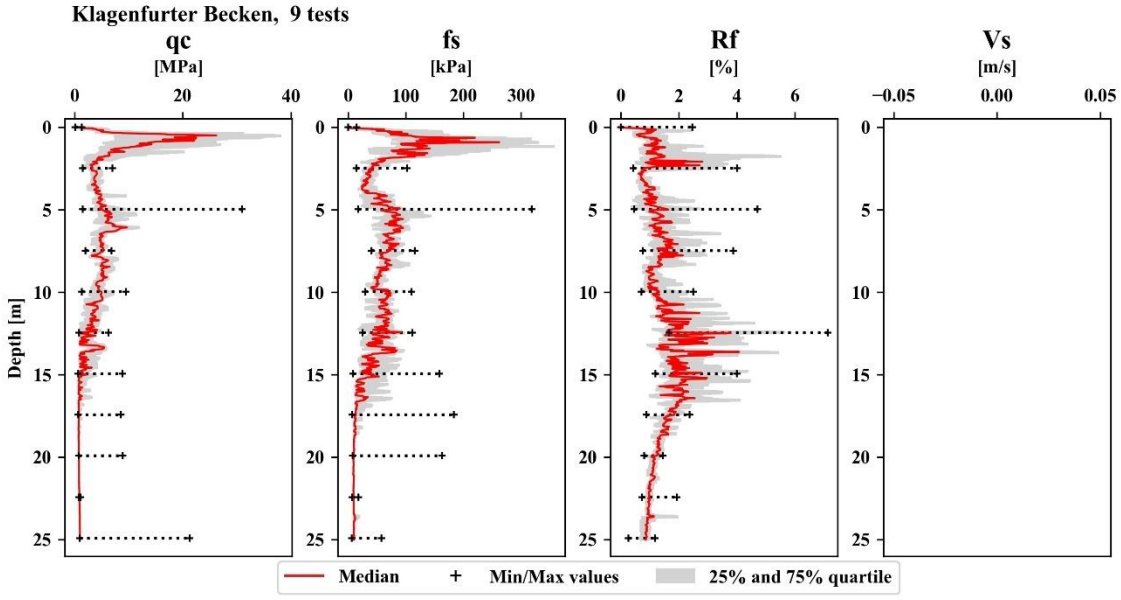
Klagenfurter Becken, 9 tests
qc
[MPa]
fs
[kPa]
Rf
[%]
Vs
[m/s]
Depth [m]
Median
Min/Max values
25% and 75% quartile

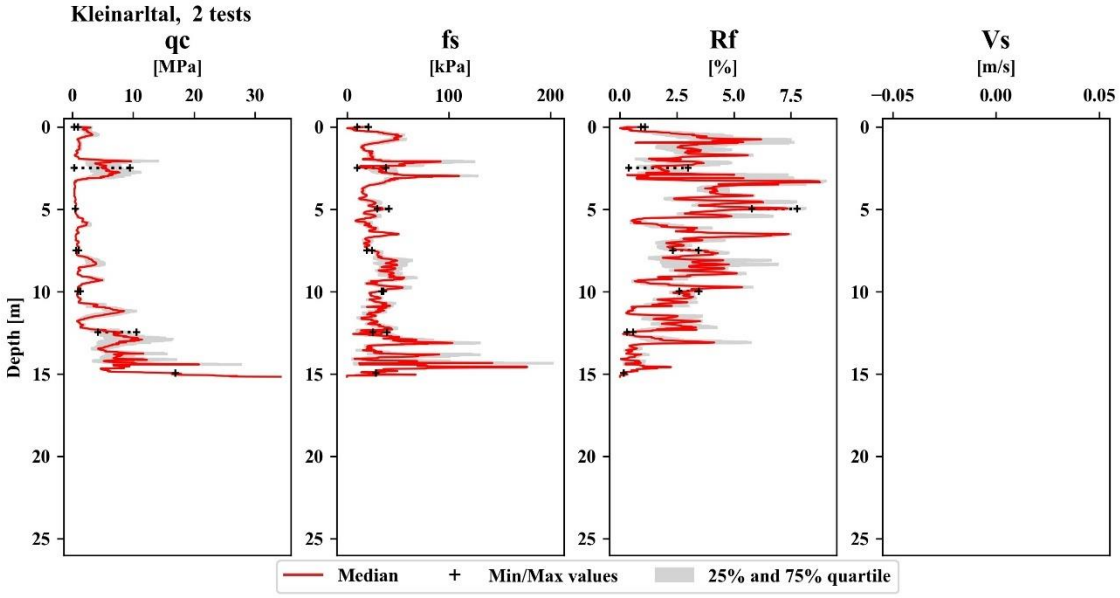
Kleinarltal, 2 tests
qc
[MPa]
fs
[kPa]
Rf
[%]
Vs
[m/s]
Depth [m]
Median
Min/Max values
25% and 75% quartile

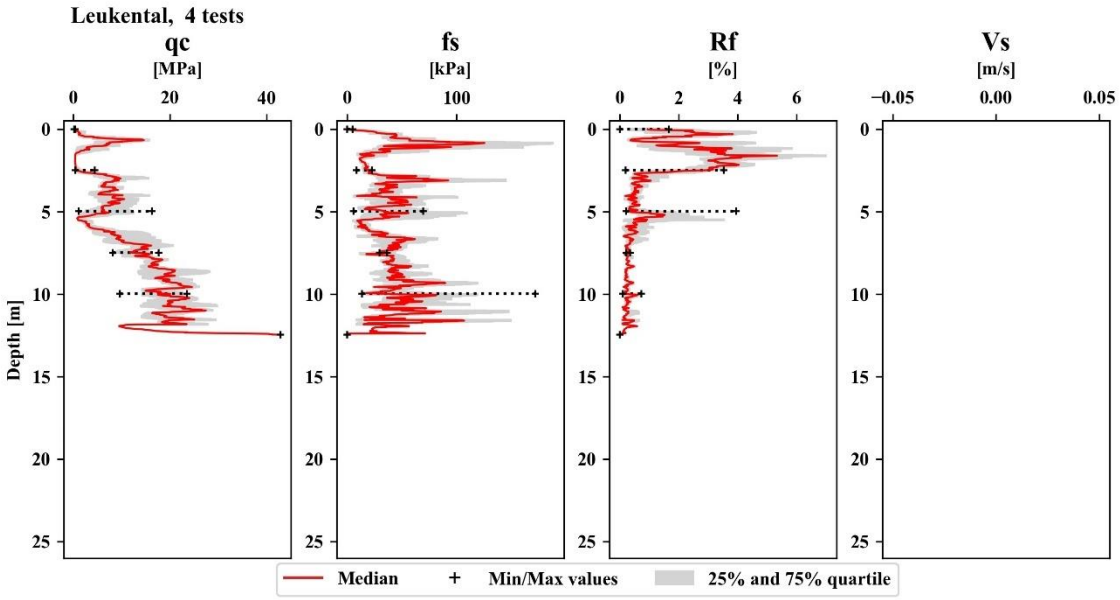
Leukental, 4 tests
qc
[MPa]
fs
[kPa]
Rf
[%]
Vs
[m/s]
Depth [m]
Median
Min/Max values
25% and 75% quartile

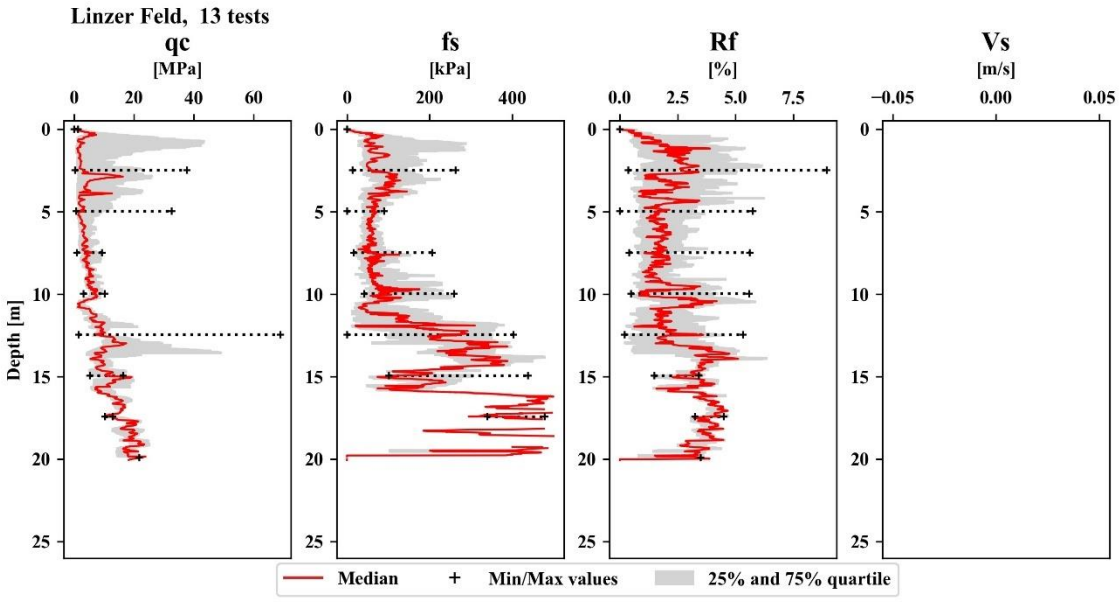
Linzer Feld, 13 tests
qc
[MPa]
fs
[kPa]
Rf
[%]
Vs
[m/s]
Depth [m]
Median
Min/Max values
25% and 75% quartile

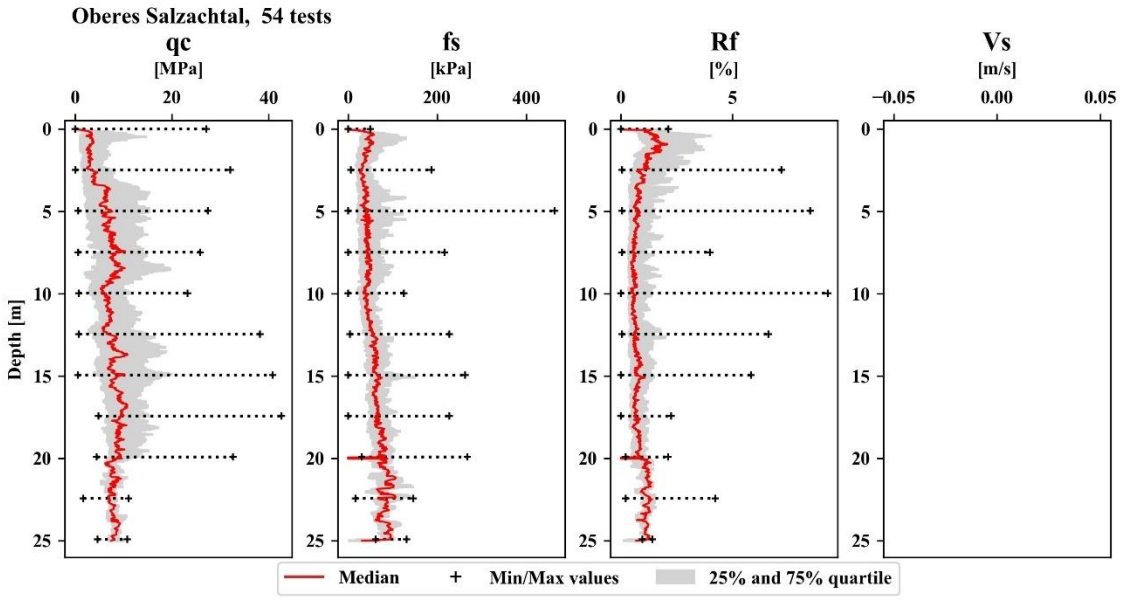
Oberes Salzachtal, 54 tests
qc
[MPa]
fs
[kPa]
Rf
[%]
Vs
[m/s]
Depth [m]
Median
Min/Max values
25% and 75% quartile

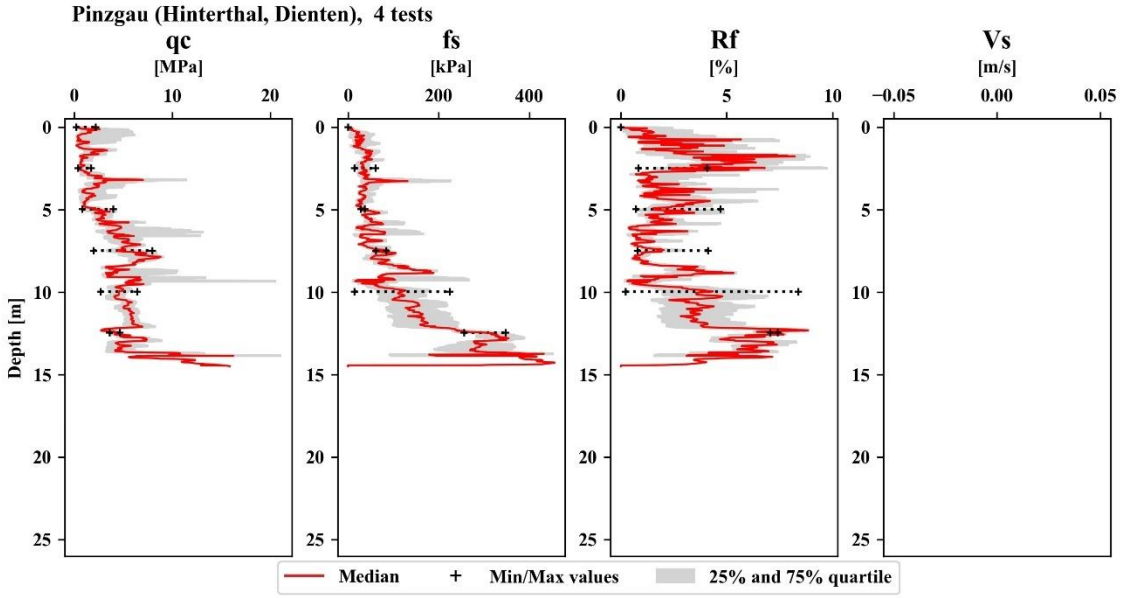
Pinzgau (Hinterthal, Dienten), 4 tests
qc
[MPa]
fs
[kPa]
Rf
[%]
Vs
[m/s]
Depth [m]
Median
Min/Max values
25% and 75% quartile

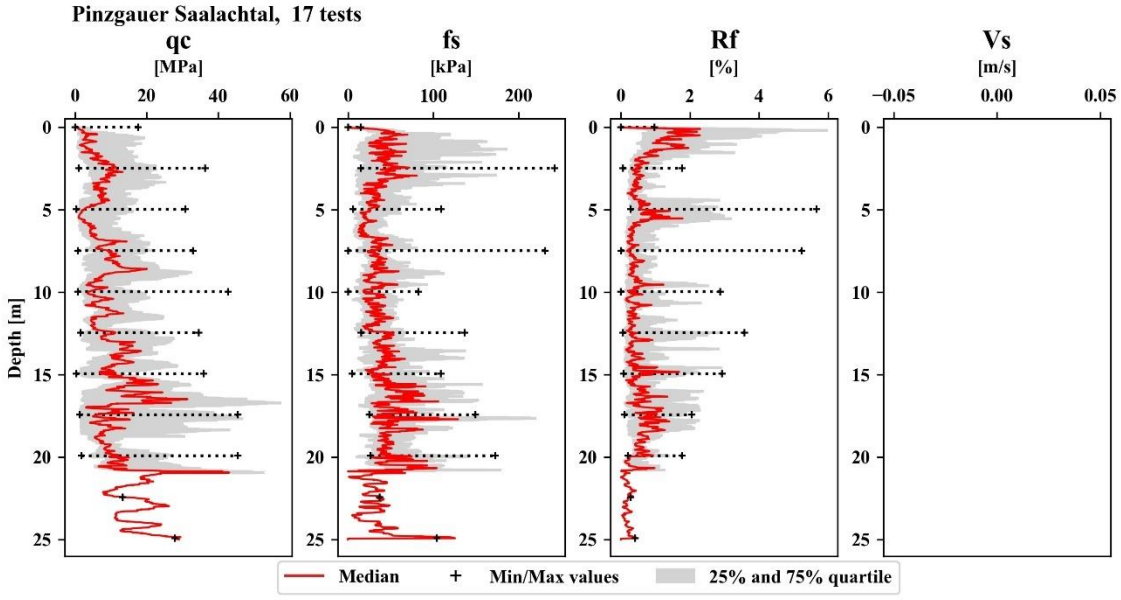
Pinzgauer Saalachtal, 17 tests
qc
[MPa]
fs
[kPa]
Rf
[%]
Vs
[m/s]
Depth [m]
Median
Min/Max values
25% and 75% quartile

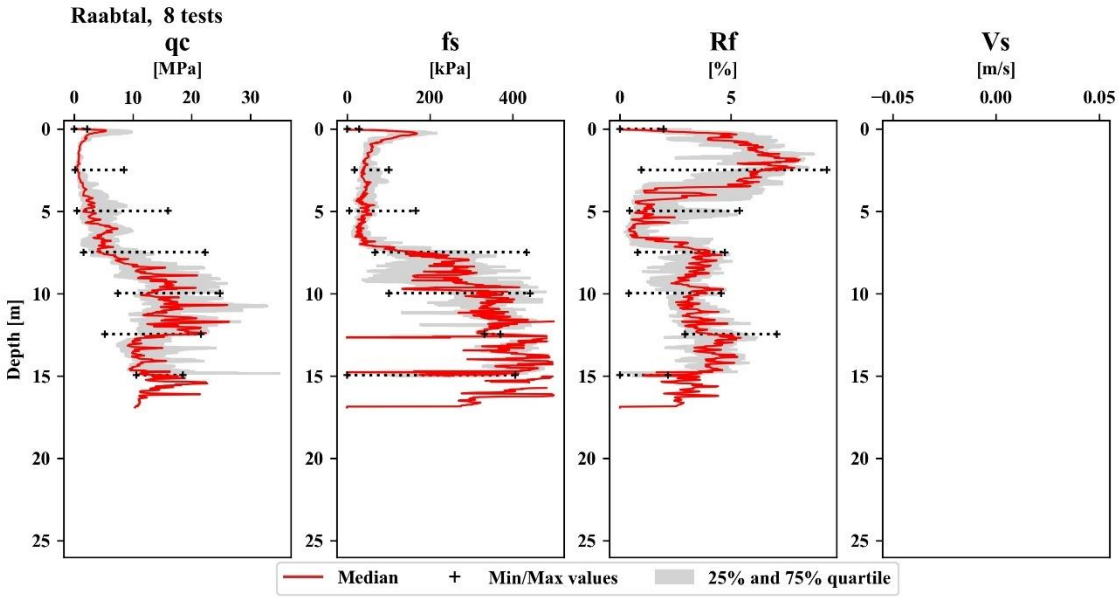
Raabtal, 8 tests
qc
[MPa]
fs
[kPa]
Rf
[%]
Vs
[m/s]
Depth [m]
Median
Min/Max values
25% and 75% quartile

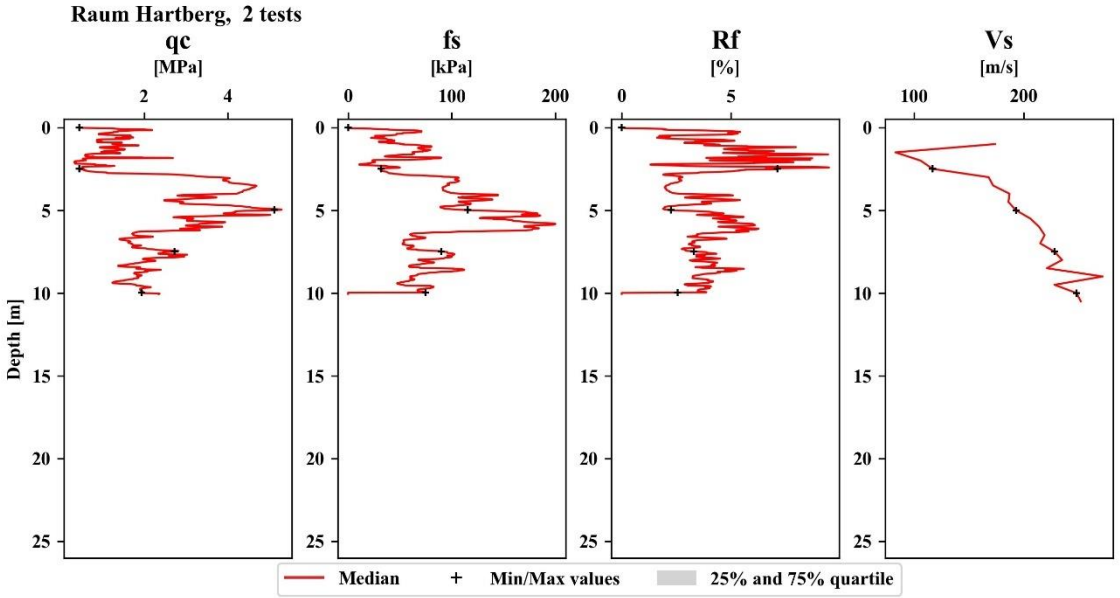
Raum Hartberg, 2 tests
qc
[MPa]
fs
[kPa]
Rf
[%]
Vs
[m/s]
Depth [m]
Median
Min/Max values
25% and 75% quartile

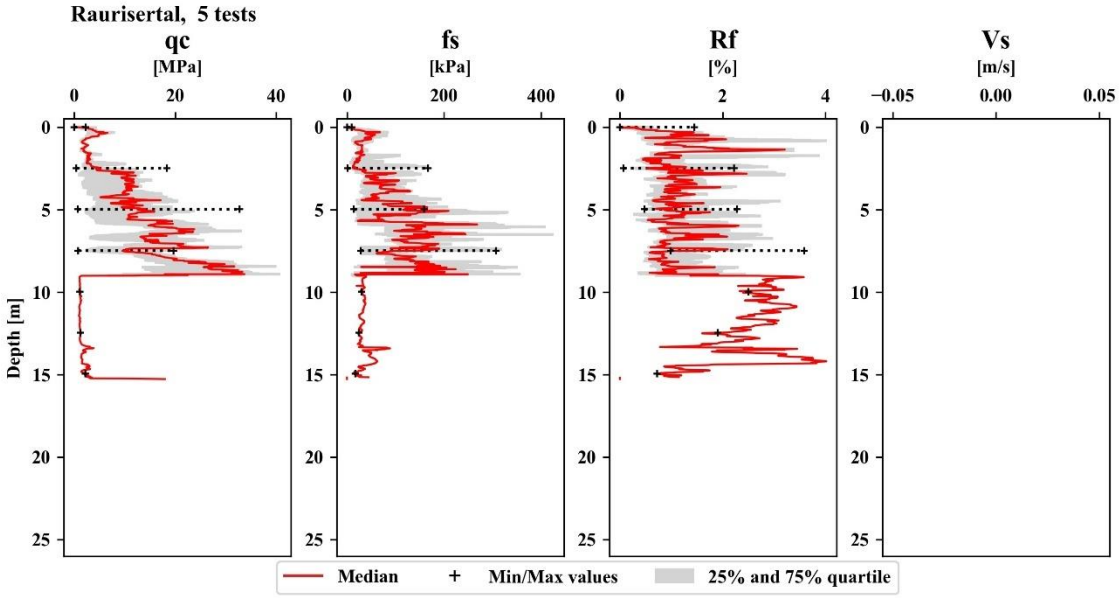
Raurisertal, 5 tests
qc
[MPa]
fs
[kPa]
Rf
[%]
Vs
[m/s]
Depth [m]
Median
Min/Max values
25% and 75% quartile

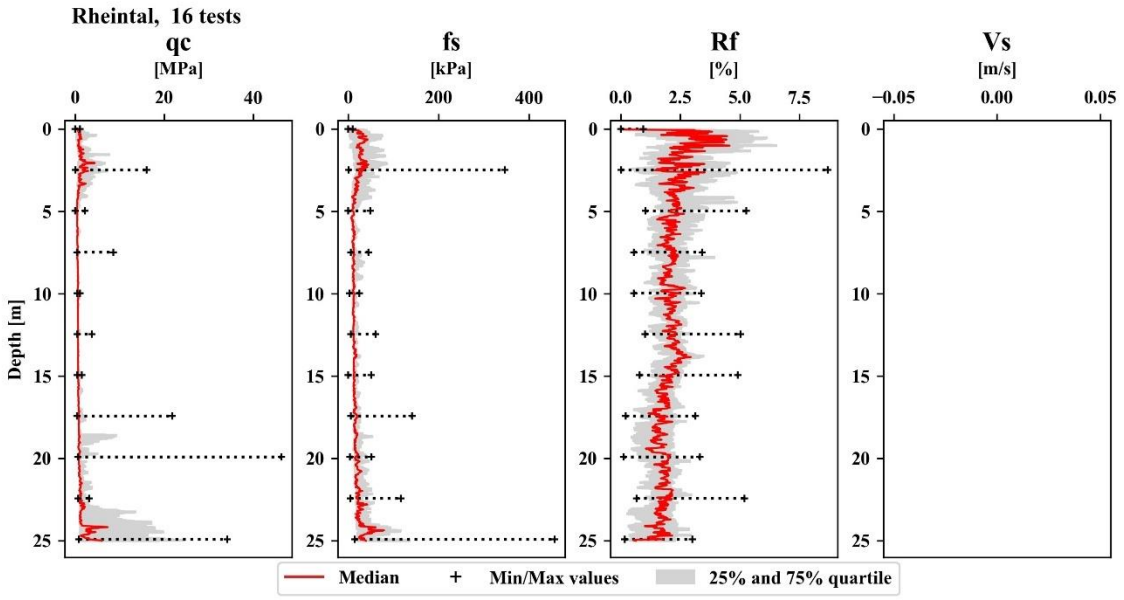
Rheintal, 16 tests
qc
[MPa]
fs
[kPa]
Rf
[%]
Vs
[m/s]
Depth [m]
Median
Min/Max values
25% and 75% quartile

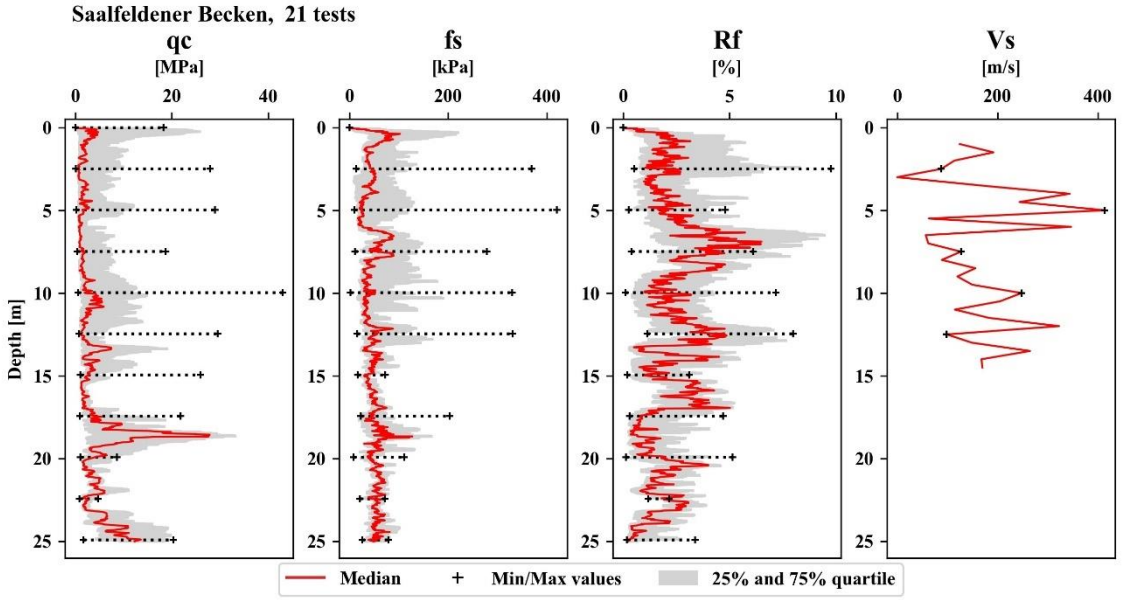
Saalfeldener Becken, 21 tests
qc
[MPa]
fs
[kPa]
Rf
[%]
Vs
[m/s]
Depth [m]
Median
Min/Max values
25% and 75% quartile

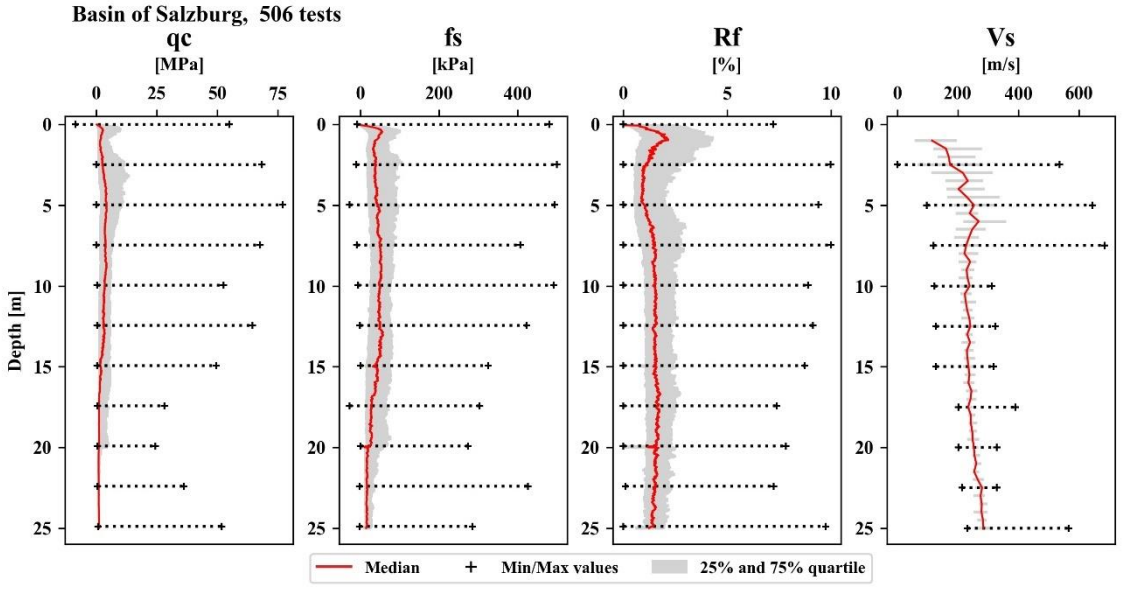
Basin of Salzburg, 506 tests
qc
[MPa]
fs
[kPa]
Rf
[%]
Vs
[m/s]
Depth [m]
Median
Min/Max values
25% and 75% quartile

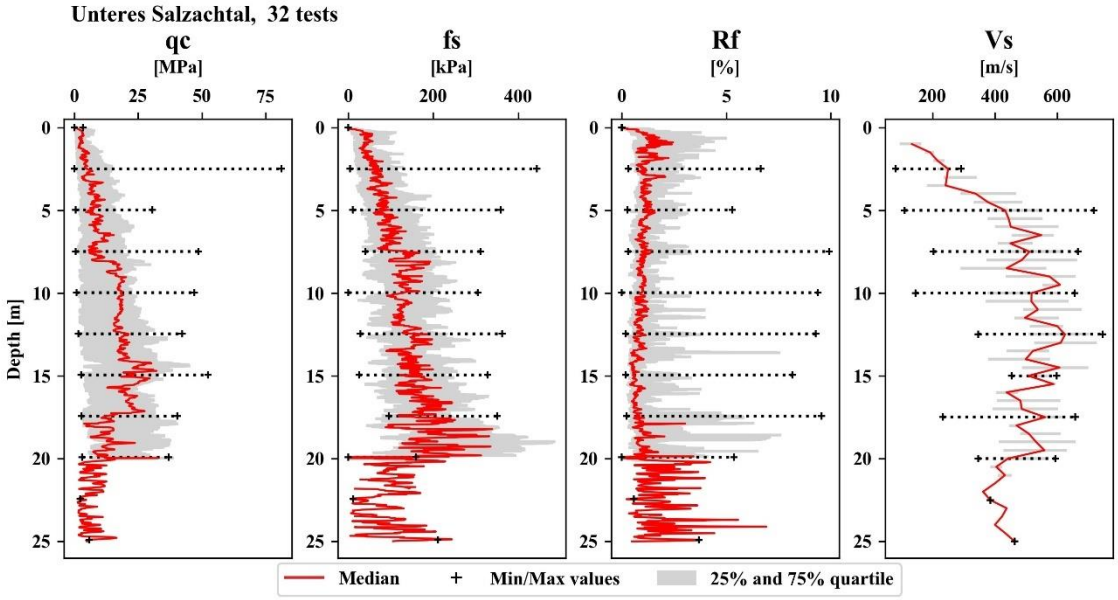
Unteres Salzachtal, 32 tests
qc
[MPa]
fs
[kPa]
Rf
[%]
Vs
[m/s]
Depth [m]
Median
Min/Max values
25% and 75% quartile

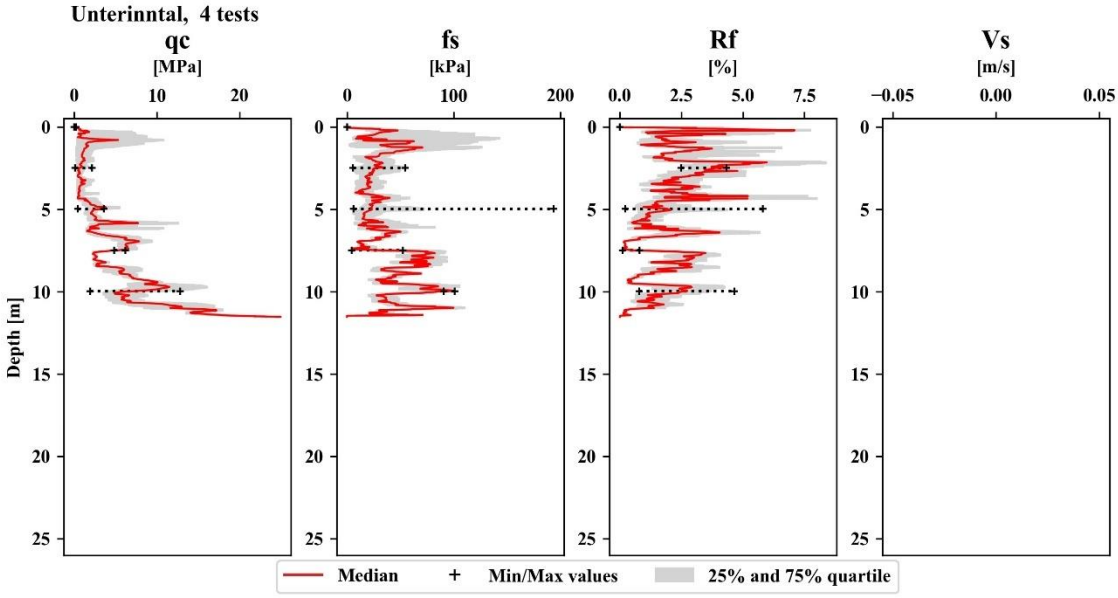
Unterinntal, 4 tests
qc
[MPa]
fs
[kPa]
Rf
[%]
Vs
[m/s]
Depth [m]
Median
Min/Max values
25% and 75% quartile

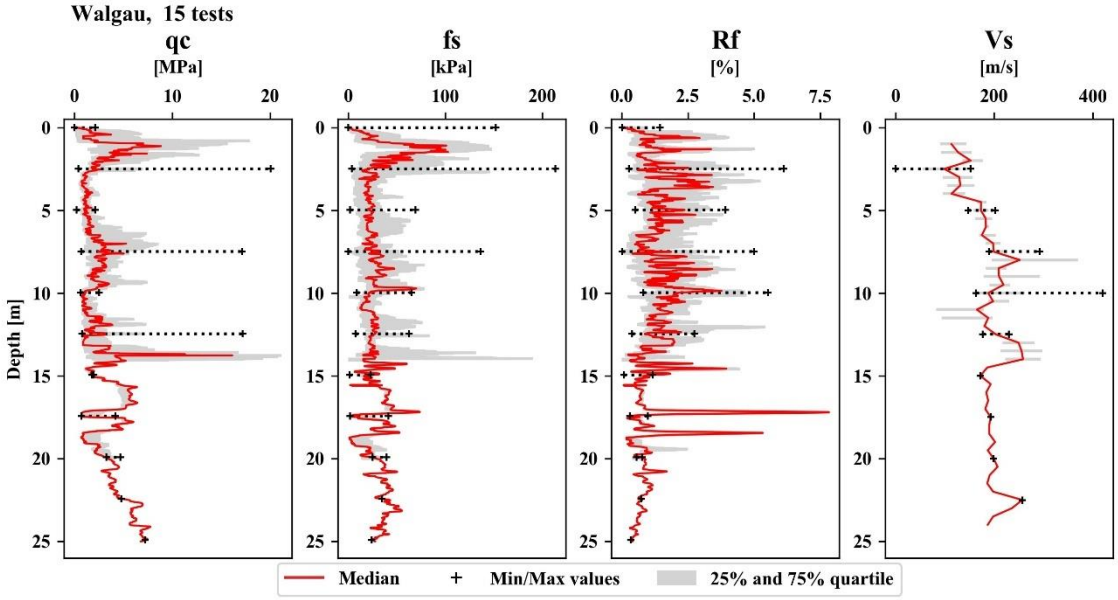
Walgau, 15 tests
qc
[MPa]
fs
[kPa]
Rf
[%]
Vs
[m/s]
Depth [m]
Median
Min/Max values
25% and 75% quartile

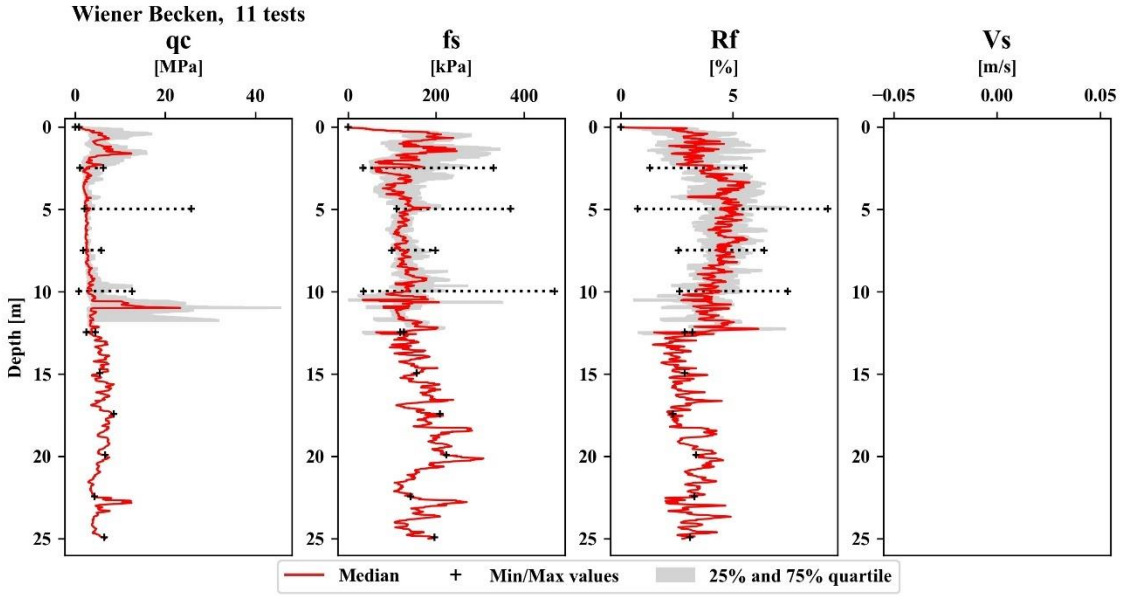
Wiener Becken, 11 tests
qc
[MPa]
fs
[kPa]
Rf
[%]
Vs
[m/s]
Depth [m]
Median
Min/Max values
25% and 75% quartile

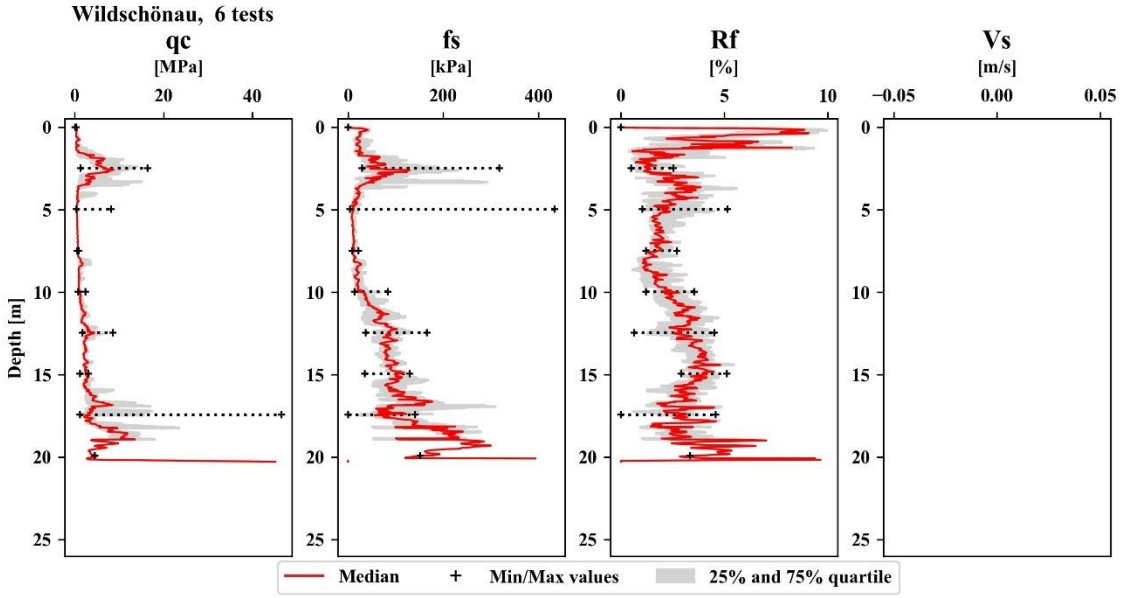
Wildschönau, 6 tests
qc
[MPa]
fs
[kPa]
Rf
[%]
Vs
[m/s]
Depth [m]
Median
Min/Max values
25% and 75% quartile

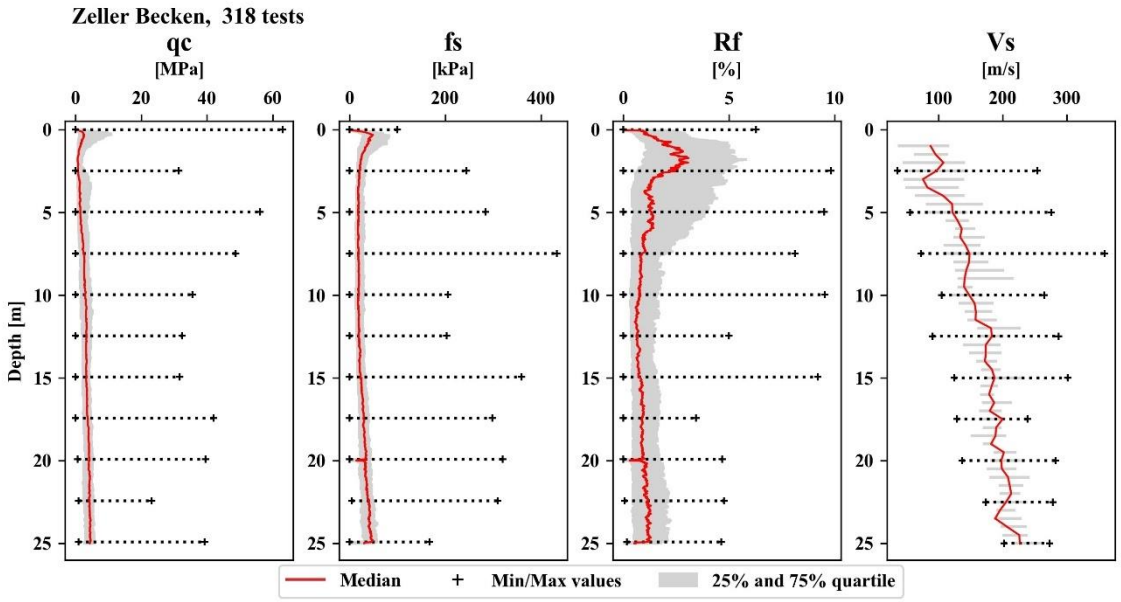
Zeller Becken, 318 tests
qc
[MPa]
fs
[kPa]
Rf
[%]
Vs
[m/s]
Depth [m]
Median
Min/Max values
25% and 75% quartile

Appendix D:

Soil group classification for Salzburg, Zell and Flachgau

A-Tab. 2: Soil group classification for the basin of Salzburg

Basin of Salzburg					
Soil group 1: gS → G	Soil group 2: Peat	Soil group 3: fS → gS	Soil group 4: U,fs → fS,u	Soil group 5: U,t → U,fs-	Soil group 6: U,t → U,T
G	U,h	S,fg,mg	S,u	U,fs-	U
G,S	U,h-	S,g,u	S,u+,g-	U,fs-,fs	U,gt
G,S,U	H	S,g,u-	S,u,fg	gU,fs,t-	U,t
G,S,u-	H,U	fS,fG	S,u,g	U,fs-,t	T,U
G,U	H,u	fS,g	S,u-	U,fs-,t-	T,s-,u
G,s	H,u-	fS,mS,u, fg+, mg+	fS,U,mS	U,t,fg-	T,u
G,s+	S,H	fS,ms,fg	fS,gU	U,t,fs	U,T
G,s+,u	S,h	gS	fS,gu	U,t,fs-	
G,s+,u-		gS,fS,g	fS,mS,u+	U,t,s-	
G,s,u		mS,gS,u-,mg-,gg-	fS,mS,u-	T,U,fs	
G,s,u+		mS,mg,gg	fS,mS,u-,u	T,fs-	
G,s,u-		fS	fS,mSmu+,t	T,u,g-	
G,u		fS, ms, gs	fS,s,u-	U,T,fS	
S,G, x-		fS,mS	fS,u	U,T,g	
fG		fS,ms	fS,u+		
fG,S		fS,t-	fS,u+,t-		
fG,gG,s+		mS,fS	fS,u,t		
fG,mG		mS,fS,u--	fS,u-		
fG,mG,gg-,u+		mS,fS,fg++,gs+	fS,u-,ms-		
fG,mG,s+			fS,u-,u		
fG,mG,u			mS, u		
fG,mg,s			S,U,g-		
fG,s+			U,G,s		
gG,fG,gS,fS			U,S		
mG			U,S,G		
mG,fg,gg			U,fS		
mG,gG,u			U,fS,mS		
mG,gG,u+,s			U,fs		
mG,gS			U,fs,fs+		
mG,s			U,s		
mG,s+			U,s,t-		
mG,s-			U,s-		
S,fG			fS,U		
S,fG,mG			fS,U,t-		
S,g					
S,g,x					

A-Tab. 3: Soil group classification for the basin of Zell

Basin of Zell					
Soil group 1: gS → G	**Soil group 2: Peat**	**Soil group 3: fS → gS**	**Soil group 4: U,fs → fS,u**	**Soil group 5: U,t → U,fs-**	**Soil group 6: U,t → U,T**
A,G,S	G,s,u,h	S	U,fs	U,fs,t	T
G,s	H	S,U,fg	U,fs+	U,fs,t-	T,u
G,s+,u	H,U	S,U,g	U,fs+,s	U,fs-	U,t
G,s,u	H,u,t	S,fg,u	U,fs,g-	U,fs-,t	U,t-
G,s,u+	fS,u,h	S,fg,u-	U,ms,gs-	fS,U	U,fS,t
G,s,u-		S,fg-	U,s		
G,s,x-		S,fs,u	fS,U,t-		
S,fg		S,fs,u-,fg-,mg-	fS,U,t--		
S,fg,mg		S,g,u-	fS,s,u		
fG,fS		S,u	fS,s-,u		
fG,gG,fs		S,u-	fS,u		
fG,gs		S,u-,fg-	fS,u+		
fG,mG,S		fG,S,u	fS,u,t		
fG,mG,gs		fS	fS,u-		
fG,mG,s		fS,fg-			
fG,mG,s+,u-		fS,gS			
fS,fG		fS,gS,u			
gS,fg+		fS,mS			
mG,fG,s+		fS,mS,u			
mG,fG,s,u-		fS,mS,u+,gs			
mG,fG,u-		fS,ms,fg-			
mG,gg-,fg+,s		fS,s,u-,fg-			
		gS,fg,u--			
		gS,u--			
		mS,gS,fg-,u-			
		mS,gs+			
		S,fg,mg,gg-			
		S,g			
		S,g-			
		fG,u			
		U,fs,gs,fg-,x-			

A-Tab. 4: Soil group classification for the region of Flachgau

Region of Flachgau					
Soil group 1: gS → G	**Soil group 2: Peat**	**Soil group 3: fS → gS**	**Soil group 4: U,fs → fS,u**	**Soil group 5: U,t → U,fs-**	**Soil group 6: U,t → U,T**
G	H	G,fs,u	U,S,g	T,u,fs	T
G,s	H,U,s-	S	U,g,s,t	T,u,s	T,u
G,s+	U,fs,h	S,g,u	U,g-,fs	U	U,t
G,s+,x	U,h	S,u,g-	U,s+,g+	U,fs,t-	T,S
G,s,t	U,t,h	fS,u,g,x	U,s,g	U,s-	T,fg-
G,s,t-	fS,U,h		U,s,g-	U,t,s	T,fs
G,s,u			fS,U		T,g-
G,s,x			fS,u		T,mg
G,u,s+			fS,u+,t-		U,t,s-
G,u,s+,x			fS,u,g--		
S,g					
S,g+,x					
gG,u					
gG,x,u++,s++					
mG,gG					
mG,gG,t+					
G,T,S					

Appendix E:

Python codes of chapter 6

Only selected codes for chapter 6 are presented in this Appendix. A complete collection of all Python codes is included on the CD.

Python Code: Fig. 33

```
# -*- coding: utf-8 -*-
"""
Created on Thu Aug 29 08:27:38 2019

@author: angollo
"""
import time
import os
import numpy as np
import pandas as pd
import matplotlib.pyplot as plt
import matplotlib.patches as mpatches
plt.rcParams["font.family"] = "Times New Roman"

start_time = time.time()

print(os.getcwd()) #show current working directory
os.chdir(r'E:\MA\Task 5\Daten_Attributtabelle')
print(os.getcwd())


""" loading information about files ------------------------------"""
path = r"E:\MA\Task 5\Daten_Attributtabelle"
files = os.listdir(path) #lists all files in folder where path is
print(files)

df_information = pd.DataFrame()
for f in files:
    information = pd.read_excel(f,
usecols=['Becken','Bezeichnun','Feinsedime', 'Kat. Gem.'])
    information['Bezeichnun'] = information['Bezeichnun']+'.xls'
    df_information = df_information.append(information)

df_information.reset_index(drop= True, inplace=True)

indexNames = df_information[df_information['Feinsedime'] ==
'Nein'].index
df_information.drop(indexNames , inplace=True)
df_information.reset_index(drop= True, inplace = True)

df_information= df_information[df_information['Becken']=='Salzburger
Becken']
df_information.reset_index(drop = True, inplace =True)

indexNames =
df_information[df_information.Bezeichnun.str.contains('DMT')].index
df_information.drop(indexNames, inplace = True)
df_information.reset_index(drop = True, inplace =True)

""" loading data files from whole Salzburger Becken----------"""
```

```
one_to_twentyfive = pd.Series(np.arange(0.01,25.01,0.01))
one_to_twentyfive_Vs = pd.Series(np.arange(0.0,25.01,0.5))
df_qc_raw = pd.DataFrame()
df_qc_raw.insert(0, 'Depth (m)', one_to_twentyfive)
df_fs_raw = pd.DataFrame()
df_fs_raw.insert(0, 'Depth (m)', one_to_twentyfive)
df_Rf_raw = pd.DataFrame()
df_Rf_raw.insert(0, 'Depth (m)', one_to_twentyfive)
df_Vs_raw = pd.DataFrame()
df_Vs_raw.insert(0, 'Depth (m)', one_to_twentyfive_Vs)
df_G0_raw = pd.DataFrame()
df_G0_raw.insert(0, 'Depth (m)', one_to_twentyfive_Vs)


list_filenames= df_information.iloc[:, 1]
print(list_filenames)

os.chdir(r'E:\MA\Task 5\Daten_Excel_SalzburgerBecken')
print(os.getcwd())

list_filenames_Seismik =[]

for row in list_filenames:
    found = False
    if 'S' in row:
        list_filenames_Seismik.append(row)
    for file in os.listdir(os.getcwd()):
        if file.endswith(row):
            rawdata = pd.read_excel(row, sheet_name='Basic results',
header = 1, usecols = ['Depth (m)','qc (MPa)', 'fs (kPa)', 'Rf (%)'])
            found = True
            df_qc_raw ['qc ' + file] = rawdata.iloc[:,1]
            df_fs_raw ['fs ' + file] = rawdata.iloc[:,2]
            df_Rf_raw ['Rf ' + file] = rawdata.iloc[:,3]
            break
    if found == False:
        print ( f'file not found: {row}')

for row in list_filenames_Seismik:
    for file in os.listdir(os.getcwd()):
        if file.endswith(row):
                rawdata = pd.read_excel(row, sheet_name='Tabelle1',
header = 4, skiprows = [5,6], usecols = ['Z', 'Vs','Go'])
                found = True
                start = rawdata.iloc[0,0]
                list_dataVs = np.full(len(one_to_twentyfive_Vs),
np.nan)
                list_dataG0 = np.full(len(one_to_twentyfive_Vs),
np.nan)
                for x in range(len(one_to_twentyfive_Vs)):
                    for y in range(len(rawdata.iloc[:,0])):
                        if one_to_twentyfive_Vs.loc[x] ==
rawdata.iloc[y,0]:
                            list_dataVs[x] = rawdata.iloc[y,1]
                            list_dataG0[x] = rawdata.iloc[y,2]
                            break
                        else:
                            continue
                df_Vs_raw [file] = list_dataVs
                df_G0_raw [file] = list_dataG0
                break
    if found == False:
```

```
        print ( f'file not found: {row}')


""" data processing ---------------------------------------------"""

df_qc_raw = df_qc_raw.iloc[:2500]
df_fs_raw = df_fs_raw.iloc[:2500]
df_Rf_raw = df_Rf_raw.iloc[:2500]

df_qc_raw.iloc[:,:] = np.where(df_qc_raw.iloc[:,:]<-500, np.nan,
df_qc_raw.iloc[:,:])
df_fs_raw.iloc[:,:] = np.where(df_fs_raw.iloc[:,:]<-500, np.nan,
df_fs_raw.iloc[:,:])
df_Rf_raw.iloc[:,:] = np.where(df_Rf_raw.iloc[:,:]<0, np.nan,
df_Rf_raw.iloc[:,:])

df_qc_raw.iloc[:,:] = np.where(df_qc_raw.iloc[:,:]>500, np.nan,
df_qc_raw.iloc[:,:])
df_fs_raw.iloc[:,:] = np.where(df_fs_raw.iloc[:,:]>500, np.nan,
df_fs_raw.iloc[:,:])
df_Rf_raw.iloc[:,:] = np.where(df_Rf_raw.iloc[:,:]>10, np.nan,
df_Rf_raw.iloc[:,:])
df_Vs_raw.iloc[:,:] = np.where(df_Vs_raw.iloc[:,:]>750, np.nan,
df_Vs_raw.iloc[:,:])

def create_df(df_raw, depth_series):
    df = pd.DataFrame()
    df.insert(0, 'Depth (m)', depth_series)
    df.insert(1, 'Median Value (MPa)', df_raw.drop('Depth (m)',
axis=1).median(axis = 1, skipna=True))
    df.insert(2, 'Lower Quartile', df_raw.drop('Depth (m)',
axis=1).quantile(q=0.25, axis=1))
    df.insert(3, 'Upper Quartile', df_raw.drop('Depth (m)',
axis=1).quantile(q=0.75, axis=1))
    df.insert(4, 'Min Value (MPa)', df_raw.drop('Depth (m)',
axis=1).min(axis=1))
    df.insert(5, 'Max Value (MPa)', df_raw.drop('Depth (m)',
axis=1).max(axis=1))
    return(df)

df_qc = create_df(df_qc_raw, one_to_twentyfive)
df_fs = create_df(df_fs_raw, one_to_twentyfive)
df_Rf = create_df(df_Rf_raw, one_to_twentyfive)

df_Vs = create_df(df_Vs_raw, one_to_twentyfive_Vs)
df_G0 = create_df(df_G0_raw, one_to_twentyfive_Vs)

""" save results to Excel ---------------------------------------"""
writer = pd.ExcelWriter(r'E:\MA\Task 5\Output\Grafik4_Tabellarische
Auflistung_Salzburger Becken.xlsx') #create the excel file
df_qc.to_excel(writer, 'Sheet1 - qc') #write data into the file
df_fs.to_excel(writer, 'Sheet2 - fs') #write data into the file
df_Rf.to_excel(writer, 'Sheet3 - Rf') #write data into the file
df_Vs.to_excel(writer, 'Sheet1 - Vs') #write data into the file
writer.save()

""" Plot all subplots in one figure ----------------------------"""

fig, (ax1, ax2, ax3, ax4) = plt.subplots(1,4, figsize = (10,4.8), dpi
= 300)
fig.suptitle('Basin of Salzburg', fontweight='bold', x=0.13, y = 1.08,
ha = 'left')
```

```
'------ qc --------'
ax1.set_title('qc', loc = 'center', fontweight='bold', fontsize=14)
ax1.set_xlabel('[MPa]', labelpad = 9)
ax1.set_ylabel('Depth [m]', fontsize=10)

x = df_qc.iloc[:,1] #median value
y = df_qc.iloc[:,0] #depth
z = df_qc.iloc[:, 2] #lower quartile
w = df_qc.iloc[:, 3] #upper quartile
a = df_qc.iloc[::249, 4] # minValue (only every 250th value)/all
2.5meters
b = df_qc.iloc[::249, 5] # maxValue (only every 250th value)
c = df_qc.iloc[::249, 0] # depth (only every 250th value --> need axis
values in same range)
#d = average_values_qc.iloc[:,2] # average qc value each 5meters
#e = average_values_qc.iloc[:,0]

ax1.plot(x,y, 'r', label = 'median', linewidth=1)
ax1.plot(a,c, 'k+', label='min values', linewidth=2, markersize=4)
ax1.plot(b,c, 'k+', label='max values', linewidth=2, markersize=4)
#ax1.plot(d,e, ',')
#for i,j in zip(d,e):
#    ax1.annotate(str(e),xy=(d,e))
ax1.invert_yaxis()
ax1.set_ylim(ymax=-0.5, ymin=26)
ax1.xaxis.tick_top()
ax1.xaxis.set_label_position('top')
#ax1.set_xticks(np.arange(0,70,10))
ax1.hlines(y, z,w, 'lightgrey', 'solid')
ax1.hlines(c, a,b, 'k', 'dotted')

'------ fs --------'

ax2.set_title('fs', loc = 'center', fontweight='bold', fontsize=14)
ax2.set_xlabel('[kPa]', labelpad = 9)

x = df_fs.iloc[:,1]
y = df_fs.iloc[:,0]
z = df_fs.iloc[:,2]
w = df_fs.iloc[:,3]
a = df_fs.iloc[::249, 4]
b = df_fs.iloc[::249, 5]
c = df_fs.iloc[::249, 0]

ax2.plot(x,y, 'r', label = 'median', linewidth=1)
ax2.plot(a,c, 'k+', label='min values', markersize=4)
ax2.plot(b,c, 'k+', label='max values', markersize=4)
ax2.invert_yaxis()
ax2.set_ylim(top = -0.5, ymin=26)
ax2.xaxis.tick_top()
ax2.xaxis.set_label_position('top')
#ax2.set_xticks(np.arange(0,400,50))
ax2.hlines(y, z,w, 'lightgrey', 'solid')
ax2.hlines(c, a,b, 'k', 'dotted')

'------ Rf --------'

ax3.set_title('Rf', loc = 'center', fontweight='bold', fontsize=14)
ax3.set_xlabel('[%]' , labelpad = 9)

x = df_Rf.iloc[:,1]
y = df_Rf.iloc[:,0]
z = df_Rf.iloc[:,2]
```

```
w = df_Rf.iloc[:,3]
a = df_Rf.iloc[::249, 4]
b = df_Rf.iloc[::249, 5]
c = df_Rf.iloc[::249, 0]

ax3.plot(x,y, 'r', label = 'median', linewidth=1)
ax3.plot(a,c, 'k+', label='min values', markersize=4)
ax3.plot(b,c, 'k+', label='max values', markersize=4)
ax3.invert_yaxis()
ax3.set_ylim(ymax=-0.5, ymin=26)
ax3.xaxis.tick_top()
ax3.xaxis.set_label_position('top')
#ax3.set_xticks(np.arange(0,400,50))
ax3.hlines(y, z,w, 'lightgrey', 'solid')
ax3.hlines(c, a,b, 'k', 'dotted')

'------ Vs --------'

ax4.set_title('Vs', loc = 'center', fontweight='bold', fontsize=14)
ax4.set_xlabel('[m/s]', labelpad = 9)

x = df_Vs.iloc[:,1] #mean value
y = df_Vs.iloc[:,0] #depth
z = df_Vs.iloc[:,2] #minStd
w = df_Vs.iloc[:,3] #maxStd
a = df_Vs.iloc[::5, 4] #minValue (only every fifth value)/every 2.5m
b = df_Vs.iloc[::5, 5] #maxValue
c = df_Vs.iloc[::5, 0]

ax4.plot(x,y, 'r', label = 'median', linewidth=1)
ax4.plot(a,c, 'k+', label='Min values', markersize=4)
ax4.plot(b,c, 'k+', label='Max values', markersize=4)
ax4.invert_yaxis()
ax4.set_ylim(ymax=-0.5, ymin=26)
ax4.xaxis.tick_top()
ax4.xaxis.set_label_position('top')
ax4.hlines(y, z,w, 'lightgrey', 'solid')
ax4.hlines(c, a,b, 'k', 'dotted')


#legend
import matplotlib.lines as mlines

h =[mlines.Line2D([], [], color='tab:red'),
    mlines.Line2D([], [], color='black', marker='+', linestyle='None',
markersize=6),
    mpatches.Patch(color='lightgrey')]
l=['Median', 'Min/Max values', '25% and 75% quartile']
fig.legend(h,l, loc = 'lower center', ncol=4, fontsize=9,
           bbox_to_anchor=(0.44, 0.0235))

#save figure
plt.savefig(f'E:\MA\Task 5\Output\Grafik4_Basin of Salzburg.jpg',
bbox_inches='tight')


end_time = time.time()
print("--- %s seconds ---" % (end_time - start_time))
print(len(list_filenames))
```

Python Code: Fig. 50

```
# -*- coding: utf-8 -*-
"""
Created on Thu Aug 29 08:27:38 2019

@author: angollo
"""
import time
import os
import numpy as np
import pandas as pd
import matplotlib.pyplot as plt
plt.rcParams["font.family"] = "Times New Roman"

start_time = time.time()

print(os.getcwd()) #show current working directory
os.chdir(r'E:\MA\Alle Becken\Task 7\Daten_Attributtabelle')
print(os.getcwd())


""" loading information about files ------------------------------"""
path = r"E:\MA\Alle Becken\Task 7\Daten_Attributtabelle"
files = os.listdir(path) #lists all files in folder where path is
print(files)

df_information = pd.DataFrame()
for f in files:
    information = pd.read_excel(f,
                usecols=['Becken','Bezeichnun','Feinsedime', 'Kat.
Gem.'])
    information['Bezeichnun'] = information['Bezeichnun']+'.xlsx'
    df_information = df_information.append(information)

df_information.reset_index(drop= True, inplace=True)

indexNames = df_information[df_information['Feinsedime'] ==
'Nein'].index
df_information.drop(indexNames , inplace=True)
df_information.reset_index(drop= True, inplace = True)

""" loading data files - rawdata for Flachgau------------"""

list_filenames = df_information.iloc[:,1]

list_filenames_used = []
list_filenames_Seismik =[]
list_filenames_Seismik_used =[]

whole_rawdata = pd.DataFrame()
whole_rawdata_Seismik = pd.DataFrame()

os.chdir(r'E:\MA\Alle Becken\Task 7\Daten_Excel_Alle Becken mit
Bodenansprache')

for row in list_filenames:
    if 'S' in row:
        list_filenames_Seismik.append(row)
    for file in os.listdir(os.getcwd()):
            if file.endswith(row):
```

```
                rawdata = pd.read_excel(row, sheet_name='Basic
results',
                        header = 1, usecols = ['Depth (m)','qc (MPa)',
                                               'fs (kPa)', 'Rf (%)',
'Bodenansprache'])
                whole_rawdata = whole_rawdata.append(rawdata)
                list_filenames_used.append(row)
                try:
                    rawdata_Seismik = pd.read_excel(row,
sheet_name='Tabelle1',
                                    header = 4, skiprows= [5,6],
                                    usecols = ['Z','Vs','Go',
'Bodenansprache'])
                    whole_rawdata_Seismik =
whole_rawdata_Seismik.append(rawdata_Seismik)
                    list_filenames_Seismik_used.append(row)
                except:
                    pass
                break

whole_rawdata.iloc[:,1:4] = np.where(whole_rawdata.iloc[:,1:4]<0,
                  np.nan, whole_rawdata.iloc[:,1:4])
whole_rawdata.iloc[:,1:4] = np.where(whole_rawdata.iloc[:,1:4]>500,
                  np.nan, whole_rawdata.iloc[:,1:4])

whole_rawdata_Seismik.iloc[:,1:3] =
np.where(whole_rawdata_Seismik.iloc[:,1:3]<0,
                  np.nan, whole_rawdata_Seismik.iloc[:,1:2])
whole_rawdata_Seismik.iloc[:,1:3] =
np.where(whole_rawdata_Seismik.iloc[:,1:3]>500,
                  np.nan, whole_rawdata_Seismik.iloc[:,1:2])

whole_rawdata.reset_index(drop = True, inplace =True) #resets index
whole_rawdata.drop('Depth (m)', axis=1, inplace = True) #drop detph
column
whole_rawdata.dropna(subset = ['Bodenansprache'],axis=0,inplace =
True) #drop all rows where Bodenansprache is not given
whole_rawdata.reset_index(drop = True, inplace =True)

whole_rawdata_Seismik.drop('Z', axis=1, inplace = True)
whole_rawdata_Seismik.dropna(subset =
['Bodenansprache'],axis=0,inplace = True) #drop all rows where
Bodenansprache is not given
whole_rawdata_Seismik.reset_index(drop = True, inplace =True)


Bodenansprachen_size =
whole_rawdata.groupby(['Bodenansprache']).size()
Bodenansprachen_Seismik_size =
whole_rawdata_Seismik.groupby(['Bodenansprache']).size()


""" data processing ------------------------------------------------"""
#lists of soil groups:
print(os.getcwd()) #show current working directory
os.chdir(r'E:\MA\Alle Becken\Task 7')
print(os.getcwd())

file = r"E:\MA\Alle Becken\Task 7\Sortierung Bodenansprachen.xlsx"
#lists file
print(file)
```

```
Bodenansprachen_Alle_Becken = pd.read_excel(file, sheet_name='Alle
Becken',
                                  skiprows= [1,2,3])

Bodenansprachen_Alle_Becken.drop(Bodenansprachen_Alle_Becken.columns

[Bodenansprachen_Alle_Becken.columns.str.contains('Unnamed')],
                axis=1, inplace=True)

BodenanspracheSoil1 = Bodenansprachen_Alle_Becken['Soil 1'].tolist()
BodenanspracheSoil2 = Bodenansprachen_Alle_Becken['Soil 2'].tolist()
BodenanspracheSoil3 = Bodenansprachen_Alle_Becken['Soil 3'].tolist()
BodenanspracheSoil4 = Bodenansprachen_Alle_Becken['Soil 4'].tolist()
BodenanspracheSoil5 = Bodenansprachen_Alle_Becken['Soil 5'].tolist()
BodenanspracheSoil6 = Bodenansprachen_Alle_Becken['Soil 6'].tolist()

Boden1 = list(set(BodenanspracheSoil1))
Boden2 = list(set(BodenanspracheSoil2))
Boden3 = list(set(BodenanspracheSoil3))
Boden4 = list(set(BodenanspracheSoil4))
Boden5 = list(set(BodenanspracheSoil5))
Boden6 = list(set(BodenanspracheSoil6))

Boden1 = [x for x in Boden1 if str(x) != 'nan']
Boden2 = [x for x in Boden2 if str(x) != 'nan']
Boden3 = [x for x in Boden3 if str(x) != 'nan']
Boden4 = [x for x in Boden4 if str(x) != 'nan']
Boden5 = [x for x in Boden5 if str(x) != 'nan']
Boden6 = [x for x in Boden6 if str(x) != 'nan']


#collect data for one soil group:only qc, fs, Rf because too little
values for Vs
def getwholedata(Boden, dataframe1, dataframe2):
    wholedata = pd.DataFrame()
#     wholedata_y = pd.DataFrame()
    for i in Boden:
        x = dataframe1[dataframe1['Bodenansprache'] == f'{i}']
        wholedata = wholedata.append(x)
        wholedata.reset_index(drop = True, inplace = True)
        wholedata.dropna(axis=0, inplace=True)
#         y = dataframe2[dataframe2['Bodenansprache'] == f'{i}']
#         wholedata_y = wholedata_y.append(y)
#         wholedata_y.reset_index(drop = True, inplace = True)
#         wholedata_y.dropna(axis=0, inplace=True) #drop rows with NaN
#     wholedata['Vs'] = wholedata_y['Vs']
#     wholedata['G0'] = wholedata_y['Go']
    return(wholedata)

df_Group1 = getwholedata(Boden1, whole_rawdata, whole_rawdata_Seismik)
df_Group2 = getwholedata(Boden2, whole_rawdata, whole_rawdata_Seismik)
df_Group3 = getwholedata(Boden3, whole_rawdata, whole_rawdata_Seismik)
df_Group4 = getwholedata(Boden4, whole_rawdata, whole_rawdata_Seismik)
df_Group5 = getwholedata(Boden5, whole_rawdata, whole_rawdata_Seismik)
df_Group6 = getwholedata(Boden6, whole_rawdata, whole_rawdata_Seismik)


df_Group1.reset_index(drop=True, inplace =True)
df_Group2.reset_index(drop=True, inplace =True)
df_Group3.reset_index(drop=True, inplace =True)
df_Group4.reset_index(drop=True, inplace =True)
df_Group5.reset_index(drop=True, inplace =True)
df_Group6.reset_index(drop=True, inplace =True)
```

```
#calculate data for plotting
def createdataforplot(dataframe):
    lower = dataframe.quantile(0.25, axis = 0) #calculate 25% quartile
    median = dataframe.quantile(0.5, axis = 0) #calculate median (50%
quartile)
    upper = dataframe.quantile(0.75, axis = 0) #calculate 25% quartile
    mean = dataframe.mean(axis=0) # calculate mean
    modus = dataframe.drop(['Bodenansprache'], axis =1).mode(axis=0)
    df = pd.concat([lower, median, upper, mean], axis = 1)
    df = df.transpose()
    df = df.append(modus)
    df.reset_index(drop=True, inplace = True)
    return(df)

data_for_plot_Group_1 = createdataforplot(df_Group1)
data_for_plot_Group_2 = createdataforplot(df_Group2)
data_for_plot_Group_3 = createdataforplot(df_Group3)
data_for_plot_Group_4 = createdataforplot(df_Group4)
data_for_plot_Group_5 = createdataforplot(df_Group5)
data_for_plot_Group_6 = createdataforplot(df_Group6)


#CUT OFF CRITERIA
#qc
df_Group1.iloc[:,0] = np.where(df_Group1.iloc[:,0]>20,
                    np.nan, df_Group1.iloc[:,0])
df_Group2.iloc[:,0] = np.where(df_Group2.iloc[:,0]>5,
                    np.nan, df_Group2.iloc[:,0])
df_Group3.iloc[:,0] = np.where(df_Group3.iloc[:,0]>20,
                    np.nan, df_Group3.iloc[:,0])
df_Group4.iloc[:,0] = np.where(df_Group4.iloc[:,0]>20,
                    np.nan, df_Group4.iloc[:,0])
df_Group5.iloc[:,0] = np.where(df_Group5.iloc[:,0]>4,
                    np.nan, df_Group5.iloc[:,0])
df_Group6.iloc[:,0] = np.where(df_Group6.iloc[:,0]>4,
                    np.nan, df_Group6.iloc[:,0])
#fs
df_Group1.iloc[:,1] = np.where(df_Group1.iloc[:,1]>200,
                    np.nan, df_Group1.iloc[:,1])
df_Group2.iloc[:,1] = np.where(df_Group2.iloc[:,1]>150,
                    np.nan, df_Group2.iloc[:,1])
df_Group3.iloc[:,1] = np.where(df_Group3.iloc[:,1]>160,
                    np.nan, df_Group3.iloc[:,1])
df_Group4.iloc[:,1] = np.where(df_Group4.iloc[:,1]>100,
                    np.nan, df_Group4.iloc[:,1])
df_Group5.iloc[:,1] = np.where(df_Group5.iloc[:,1]>80,
                    np.nan, df_Group5.iloc[:,1])
df_Group6.iloc[:,1] = np.where(df_Group6.iloc[:,1]>85,
                    np.nan, df_Group6.iloc[:,1])

#Rf
df_Group1.iloc[:,2] = np.where(df_Group1.iloc[:,2]>4,
                    np.nan, df_Group1.iloc[:,2])
df_Group2.iloc[:,2] = np.where(df_Group2.iloc[:,2]>10,
                    np.nan, df_Group2.iloc[:,2])
df_Group3.iloc[:,2] = np.where(df_Group3.iloc[:,2]>5,
                    np.nan, df_Group3.iloc[:,2])
df_Group4.iloc[:,2] = np.where(df_Group4.iloc[:,2]>7,
                    np.nan, df_Group4.iloc[:,2])
df_Group5.iloc[:,2] = np.where(df_Group5.iloc[:,2]>6,
                    np.nan, df_Group5.iloc[:,2])
df_Group6.iloc[:,2] = np.where(df_Group6.iloc[:,2]>6,
```

```
                np.nan, df_Group6.iloc[:,2])

df_Group1.dropna(axis=0, inplace = True)
df_Group2.dropna(axis=0, inplace = True)
df_Group3.dropna(axis=0, inplace = True)
df_Group4.dropna(axis=0, inplace = True)
df_Group5.dropna(axis=0, inplace = True)
df_Group6.dropna(axis=0, inplace = True)

df_Group1.reset_index(drop=True, inplace =True)
df_Group2.reset_index(drop=True, inplace =True)
df_Group3.reset_index(drop=True, inplace =True)
df_Group4.reset_index(drop=True, inplace =True)
df_Group5.reset_index(drop=True, inplace =True)
df_Group6.reset_index(drop=True, inplace =True)

#create dataframes for violinplot
data_violinplot_qc = [df_Group1.iloc[:,0], df_Group2.iloc[:,0],
                      df_Group3.iloc[:,0], df_Group4.iloc[:,0],
                      df_Group5.iloc[:,0], df_Group6.iloc[:,0]]

data_violinplot_fs = [df_Group1.iloc[:,1], df_Group2.iloc[:,1],
                      df_Group3.iloc[:,1], df_Group4.iloc[:,1],
                      df_Group5.iloc[:,1], df_Group6.iloc[:,1]]


data_violinplot_Rf = [df_Group1.iloc[:,2], df_Group2.iloc[:,2],
                      df_Group3.iloc[:,2], df_Group4.iloc[:,2],
                      df_Group5.iloc[:,2], df_Group6.iloc[:,2]]


medians_qc = [data_for_plot_Group_1.iloc[1,0],
data_for_plot_Group_2.iloc[1,0],
              data_for_plot_Group_3.iloc[1,0],
data_for_plot_Group_4.iloc[1,0],
              data_for_plot_Group_5.iloc[1,0],
data_for_plot_Group_6.iloc[1,0]]

quartile1_qc = [data_for_plot_Group_1.iloc[0,0],
data_for_plot_Group_2.iloc[0,0],
              data_for_plot_Group_3.iloc[0,0],
data_for_plot_Group_4.iloc[0,0],
              data_for_plot_Group_5.iloc[0,0],
data_for_plot_Group_6.iloc[0,0]]

quartile3_qc = [data_for_plot_Group_1.iloc[2,0],
data_for_plot_Group_2.iloc[2,0],
              data_for_plot_Group_3.iloc[2,0],
data_for_plot_Group_4.iloc[2,0],
              data_for_plot_Group_5.iloc[2,0],
data_for_plot_Group_6.iloc[2,0]]

medians_fs = [data_for_plot_Group_1.iloc[1,1],
data_for_plot_Group_2.iloc[1,1],
              data_for_plot_Group_3.iloc[1,1],
data_for_plot_Group_4.iloc[1,1],
              data_for_plot_Group_5.iloc[1,1],
data_for_plot_Group_6.iloc[1,1]]

quartile1_fs = [data_for_plot_Group_1.iloc[0,1],
data_for_plot_Group_2.iloc[0,1],
              data_for_plot_Group_3.iloc[0,1],
data_for_plot_Group_4.iloc[0,1],
```

```
                data_for_plot_Group_5.iloc[0,1],
data_for_plot_Group_6.iloc[0,1]]

quartile3_fs = [data_for_plot_Group_1.iloc[2,1],
data_for_plot_Group_2.iloc[2,1],
                data_for_plot_Group_3.iloc[2,1],
data_for_plot_Group_4.iloc[2,1],
                data_for_plot_Group_5.iloc[2,1],
data_for_plot_Group_6.iloc[2,1]]

medians_Rf = [data_for_plot_Group_1.iloc[1,2],
data_for_plot_Group_2.iloc[1,2],
                data_for_plot_Group_3.iloc[1,2],
data_for_plot_Group_4.iloc[1,2],
                data_for_plot_Group_5.iloc[1,2],
data_for_plot_Group_6.iloc[1,2]]

quartile1_Rf = [data_for_plot_Group_1.iloc[0,2],
data_for_plot_Group_2.iloc[0,2],
                data_for_plot_Group_3.iloc[0,2],
data_for_plot_Group_4.iloc[0,2],
                data_for_plot_Group_5.iloc[0,2],
data_for_plot_Group_6.iloc[0,2]]

quartile3_Rf = [data_for_plot_Group_1.iloc[2,2],
data_for_plot_Group_2.iloc[2,2],
                data_for_plot_Group_3.iloc[2,2],
data_for_plot_Group_4.iloc[2,2],
                data_for_plot_Group_5.iloc[2,2],
data_for_plot_Group_6.iloc[2,2]]

""" data plotting-- ------------------------------------------------"""

fig, (ax1, ax2, ax3) = plt.subplots(1,3, figsize = (10,4.8), dpi =
300)

color = ['tab:red', 'tab:orange', 'forestgreen', 'olivedrab',
'midnightblue',
             'rebeccapurple']


violin_parts1 = ax1.violinplot(data_violinplot_qc, showmedians=True,
showextrema=False)
violin_parts2 = ax2.violinplot(data_violinplot_fs, showmedians=True,
showextrema=False)
violin_parts3 = ax3.violinplot(data_violinplot_Rf, showmedians=True,
showextrema=False)

xaxis = pd.Series(np.arange(1,7,1))
labels =['Group1', 'Group2', 'Group3', 'Group4', 'Group5', 'Group6']
ax1.set_xticks(xaxis)
ax1.set_xticklabels(labels, rotation=90, fontsize=12)
ax2.set_xticks(xaxis)
ax2.set_xticklabels(labels, rotation=90, fontsize=12)
ax3.set_xticks(xaxis)
ax3.set_xticklabels(labels, rotation=90, fontsize=12)

for vp, n in zip(violin_parts1['bodies'], color):
    vp.set_facecolor(n)
    vp.set_edgecolor(n)
    vp.set_alpha(0.5)
```

```
for vp, n in zip(violin_parts2['bodies'], color):
    vp.set_facecolor(n)
    vp.set_edgecolor(n)
    vp.set_alpha(0.5)

for vp, n in zip(violin_parts3['bodies'], color):
    vp.set_facecolor(n)
    vp.set_edgecolor(n)
    vp.set_alpha(0.5)

inds = np.arange(1,7)

ax1.scatter(inds, medians_qc, marker='s', color='k', s=7, zorder=3)
ax2.scatter(inds, medians_fs, marker='s', color='k', s=7, zorder=3)
ax3.scatter(inds, medians_Rf, marker='s', color='k', s=7, zorder=3)
ax1.vlines(inds, quartile1_qc, quartile3_qc, color='k', linestyle='--
', lw=0.8)
ax2.vlines(inds, quartile1_fs, quartile3_fs, color='k', linestyle='--
', lw=0.8)
ax3.vlines(inds, quartile1_Rf, quartile3_Rf, color='k', linestyle='--
', lw=0.8)

ax1.set_ylim(ymin=0, ymax=20)
ax2.set_ylim(ymin=0, ymax=200)
ax3.set_ylim(ymin=0, ymax=10)

#ax1 --- qc
ax1.set_ylabel('(MPa)', fontweight='bold', fontsize=14, labelpad=9)
ax1.set_title('qc', fontweight='bold', fontsize=17, loc = 'left',
pad=9)

#ax2 --- fs
ax2.set_ylabel('(kPa)', fontweight='bold', fontsize=14, labelpad=9)
ax2.set_title('fs', fontweight='bold', fontsize=17, loc = 'left',
pad=9)

#ax3 --- Rf
ax3.set_ylabel('(%)', fontweight='bold', fontsize=14, labelpad=9)
ax3.set_title('Rf', fontweight='bold', fontsize=17, loc = 'left',
pad=9)

#save figure
plt.tight_layout()
plt.savefig('E:\MA\Alle Becken\Task 7\Output\Grafik6_Violinplot_alle
Becken.jpg', bbox_inches='tight')

print('Total amount of Tests:', len(list_filenames))
print('Usable Tests (Bodenansprache available):',
len(list_filenames_used))
print('Available Seismik Tests:', len(list_filenames_Seismik))
print('Usable Seismik Tests (Bodenansprachen available):',
len(list_filenames_Seismik_used), list_filenames_Seismik_used)

from statistics import median
for i in range(0,6,1):
    print(median(data_violinplot_qc[i]))
for i in range(0,6,1):
    print(median(data_violinplot_fs[i]))
for i in range(0,6,1):
    print(median(data_violinplot_Rf[i]))

end_time = time.time()
print("--- %s seconds ---" % (end_time - start_time))
```

Appendix F:

Python codes of chapter 7

Only selected codes for chapter 7 are presented in this Appendix. A complete collection of all Python codes is included on the CD.

Python Code: Fig. 63 and Fig. 64

```
# -*- coding: utf-8 -*-
"""
Created on Fri Oct 11 10:27:10 2019

@author: angollo
"""

import time
import os
import numpy as np
import pandas as pd
import matplotlib.pyplot as plt

plt.rcParams["font.family"] = "Times New Roman"

start_time = time.time()

print(os.getcwd()) #show current working directory
os.chdir(r'E:\MA\Alle Becken\Task 7\Daten_Attributtabelle')
print(os.getcwd())


""" loading information about files ------------------------------"""
path = r"E:\MA\Alle Becken\Task 7\Daten_Attributtabelle"
files = os.listdir(path) #lists all files in folder where path is
print(files)

df_information = pd.DataFrame()
for f in files:
    information = pd.read_excel(f,
usecols=['Becken','Bezeichnun','Feinsedime', 'Kat. Gem.'])
#    information['Bezeichnun'] = information['Bezeichnun']+'.xlsx'
    df_information = df_information.append(information)

df_information.reset_index(drop= True, inplace=True)

indexNames = df_information[df_information['Feinsedime'] ==
'Nein'].index
df_information.drop(indexNames , inplace=True)
df_information.reset_index(drop= True, inplace = True)

""" loading data files - all basins ------------------------------"""

list_allfilenames = df_information.iloc[:,1] #list of all files
list_filenames_Seismik =[]
list_filenames_used = []

list_filenames = []
list_Mfilenames = []
```

```
os.chdir(r'E:\MA\Alle Becken\Task 7\Daten_Excel_Alle Becken mit
Bodenansprache')

for row in list_allfilenames:
    for file in os.listdir(os.getcwd()):
        if row+'_M.xlsx' == file: #search for _MFiles and append to
list
            list_Mfilenames.append(row+'_M')
        elif file.endswith(row+'.xlsx'): #append all other files to
other list
            list_filenames.append(row)

for i,row in enumerate(list_filenames): #replace with _MFiles
    for elem in list_Mfilenames:
        if row in elem:
            list_filenames[i] = elem

for i, row in enumerate(list_filenames): #append .xlsx
    list_filenames[i]= row +'.xlsx'

""" data processing --------------------------------------------"""

#lists of soil groups:

print(os.getcwd()) #show current working directory
os.chdir(r'E:\MA\Alle Becken\Task 7')
print(os.getcwd())



file = r"E:\MA\Alle Becken\Task 7\Sortierung Bodenansprachen.xlsx"
#lists file
print(file)


Bodenansprachen_Alle_Becken = pd.read_excel(file, sheet_name='Alle
Becken',
                                skiprows= [1,2,3])

Bodenansprachen_Alle_Becken.drop(Bodenansprachen_Alle_Becken.columns

[Bodenansprachen_Alle_Becken.columns.str.contains('Unnamed')],
               axis=1, inplace=True)


BodenanspracheSoil1 = Bodenansprachen_Alle_Becken['Soil 1'].tolist()
BodenanspracheSoil2 = Bodenansprachen_Alle_Becken['Soil 2'].tolist()
BodenanspracheSoil3 = Bodenansprachen_Alle_Becken['Soil 3'].tolist()
BodenanspracheSoil4 = Bodenansprachen_Alle_Becken['Soil 4'].tolist()
BodenanspracheSoil5 = Bodenansprachen_Alle_Becken['Soil 5'].tolist()
BodenanspracheSoil6 = Bodenansprachen_Alle_Becken['Soil 6'].tolist()

Boden1 = list(set(BodenanspracheSoil1))
Boden2 = list(set(BodenanspracheSoil2))
Boden3 = list(set(BodenanspracheSoil3))
Boden4 = list(set(BodenanspracheSoil4))
Boden5 = list(set(BodenanspracheSoil5))
Boden6 = list(set(BodenanspracheSoil6))

Boden1 = [x for x in Boden1 if str(x) != 'nan']
Boden2 = [x for x in Boden2 if str(x) != 'nan']
Boden3 = [x for x in Boden3 if str(x) != 'nan']
Boden4 = [x for x in Boden4 if str(x) != 'nan']
```

```
Boden5 = [x for x in Boden5 if str(x) != 'nan']
Boden6 = [x for x in Boden6 if str(x) != 'nan']

whole_rawdata_SBTchart = pd.DataFrame()

os.chdir(r'E:\MA\Alle Becken\Task 7\Daten_Excel_Alle Becken mit
Bodenansprache')

for row in list_filenames:
    for file in os.listdir(os.getcwd()):
            if file.endswith(row):
                rawdata_SBTchart = pd.read_excel(row,
sheet_name='Basic results',
                                 header = 1, usecols = ['Fr (%)', 'Qtn',
'Bodenansprache'])
                whole_rawdata_SBTchart =
whole_rawdata_SBTchart.append(rawdata_SBTchart)
                list_filenames_used.append(row)
                break

whole_rawdata_SBTchart.iloc[:,1] =
np.where(whole_rawdata_SBTchart['Qtn'] == '>1,000',
                            np.nan, whole_rawdata_SBTchart.iloc[:,1])
whole_rawdata_SBTchart.dropna(axis = 0, inplace=True) #drop rows with
NaN
whole_rawdata_SBTchart.reset_index(drop = True, inplace =True) #resets
index
whole_rawdata_SBTchart['Qtn'] =
whole_rawdata_SBTchart['Qtn'].astype(float)

whole_rawdata_SBTchart_mean =
whole_rawdata_SBTchart.groupby(['Bodenansprache']).mean()
whole_rawdata_SBTchart_size =
whole_rawdata_SBTchart.groupby(['Bodenansprache']).size()


def selectdataSBT(Boden, data):
    selected_data_Boden = pd.DataFrame()
    for i in Boden:
        df = data[data['Bodenansprache'] == i]
        selected_data_Boden = selected_data_Boden.append(df)
        selected_data_Boden.reset_index(drop = True, inplace =True)
    return(selected_data_Boden)


#select data for plotting
selected_data_SBT_Boden1 = selectdataSBT(Boden1,
whole_rawdata_SBTchart)
selected_data_SBT_Boden2 = selectdataSBT(Boden2,
whole_rawdata_SBTchart)
selected_data_SBT_Boden3 = selectdataSBT(Boden3,
whole_rawdata_SBTchart)
selected_data_SBT_Boden4 = selectdataSBT(Boden4,
whole_rawdata_SBTchart)
selected_data_SBT_Boden5 = selectdataSBT(Boden5,
whole_rawdata_SBTchart)
selected_data_SBT_Boden6 = selectdataSBT(Boden6,
whole_rawdata_SBTchart)


""" data plotting ------------ SCATTER PLOT: SBT ---------------"""

'plot all in one graph'
```

```
fig, ax = plt.subplots(figsize=(8, 8), dpi=2000)
color = ['tab:red', 'tab:orange',
         'forestgreen', 'olivedrab', 'midnightblue', 'rebeccapurple']
Boden = [selected_data_SBT_Boden1, selected_data_SBT_Boden2,
         selected_data_SBT_Boden3, selected_data_SBT_Boden4,
         selected_data_SBT_Boden5, selected_data_SBT_Boden6]

for i, n in zip(Boden, color): #plot all 6 soil groups in loop
    x = i.iloc[:,0]
    y = i.iloc[:,1]
    ax.scatter(x,y, s=1, alpha =0.15, c = n)

ax.set_xscale('log')  # logarithmic scale
ax.set_yscale('log')  # logarithmic scale
ax.set_xlim(left=0.1, right=10)  # set limits of plot
ax.set_ylim(bottom=1, top=1000)
#ax.grid(alpha=0.4, which='both')  # less well visible grid in
background
#ax.grid(alpha=1)  # "bolder" grid in the foreground of the plot
#ax.set_xlabel('Fr (%)')
#ax.set_ylabel('Qtn')
ax.get_xaxis().set_ticks([]) #turn off ticks
ax.get_yaxis().set_ticks([])
ax.get_xaxis().set_ticklabels([]) # turn off ticklabels
ax.get_yaxis().set_ticklabels([])


#legend
#l = ['Group 1: CSa ?' Gr', 'Group 2: Peat',
#     'Group 3: FSa ?' CSa', 'Group 4: Si,fsa ?' FSa,si',
#     'Group 5: Si,cl- ?' Si,fsa-', 'Group 6: Si,Cl ?' Si,cl']
#fig.legend(labels=l, loc = 'upper center', ncol=2, markerscale = 8)


#plt.tight_layout()
#save figure
plt.savefig(r'E:\MA\Alle Becken\Task 7\Output\Grafik7.jpg',
bbox_inches='tight',
            transparent = True)

'plot all separately'
def scatplot(n, Boden, color):
    fig_n, ax_n = plt.subplots(figsize=(8,8), dpi=1200)
    a = Boden.iloc[:,0]
    b = Boden.iloc[:,1]
    ax_n.scatter(a,b, s=1, alpha=0.3, c = color)
    ax_n.set_xscale('log')  # logarithmic scale
    ax_n.set_yscale('log')  # logarithmic scale
    ax_n.set_xlim(left=0.1, right=10)  # set limits of plot
    ax_n.set_ylim(bottom=1, top=1000)
#    ax_n.grid(alpha=0.4, which='both')  # less well visible grid in
background
#    ax_n.grid(alpha=1)  # "bolder" grid in the foreground of the plot
#    ax_n.set_xlabel('Fr (%)')
#    ax_n.set_ylabel('Qtn')
    ax_n.get_xaxis().set_ticks([])
    ax_n.get_yaxis().set_ticks([])
    ax_n.get_xaxis().set_ticklabels([])
    ax_n.get_yaxis().set_ticklabels([])
    plt.savefig(rf'E:\MA\Alle Becken\Task
7\Output\Grafik7_Boden{n}.jpg',
                bbox_inches='tight', transparent = True)
```

```
    return(fig_n, ax_n)

fig1 = scatplot(1, selected_data_SBT_Boden1, 'tab:red')
fig2 = scatplot(2, selected_data_SBT_Boden2, 'tab:orange')
fig3 = scatplot(3, selected_data_SBT_Boden3, 'forestgreen')
fig4 = scatplot(4, selected_data_SBT_Boden4, 'olivedrab')
fig5 = scatplot(5, selected_data_SBT_Boden5, 'midnightblue')
fig6 = scatplot(6, selected_data_SBT_Boden6, 'rebeccapurple')


end_time = time.time()
print("--- %s seconds ---" % (end_time - start_time))
```

Python Code: Fig. 75

```
# -*- coding: utf-8 -*-
"""
Created on Fri Oct 11 10:27:10 2019

@author: angollo
"""

import time
import os
import numpy as np
import pandas as pd
import matplotlib.pyplot as plt
plt.rcParams["font.family"] = "Times New Roman"

start_time = time.time()

print(os.getcwd()) #show current working directory
os.chdir(r'E:\MA\Alle Becken\Task 7\Daten_Attributtabelle')
print(os.getcwd())


""" loading information about files ------------------------------"""
path = r"E:\MA\Alle Becken\Task 7\Daten_Attributtabelle"
files = os.listdir(path) #lists all files in folder where path is
print(files)

df_information = pd.DataFrame()
for f in files:
    information = pd.read_excel(f,
usecols=['Becken','Bezeichnun','Feinsedime', 'Kat. Gem.'])
    information['Bezeichnun'] = information['Bezeichnun']+'.xlsx'
    df_information = df_information.append(information)

df_information.reset_index(drop= True, inplace=True)

indexNames = df_information[df_information['Feinsedime'] ==
'Nein'].index
df_information.drop(indexNames , inplace=True)
df_information.reset_index(drop= True, inplace = True)

""" loading data files - Alle Becken ---------------------------"""

list_allfilenames = df_information.iloc[:,1]
list_filenames_Seismik =[]
data= pd.DataFrame()
```

```
for row in list_allfilenames:
    if 'S' in row:
        list_filenames_Seismik.append(row)

os.chdir(r'E:\MA\Alle Becken\Task 7\Daten_Excel_Alle Becken mit
Bodenansprache')
cwd = os.getcwd()
files = os.listdir(cwd)
print(f'files in {cwd}: {files}')

for row in list_filenames_Seismik:
    for file in files:
        if file.endswith(row):
            rawdata1 = pd.read_excel(row, sheet_name='Basic results',
header = 1,
                usecols = ['Depth (m)','qt (MPa)', 'σ,v (kPa)', 'Qtn',
'Bodenansprache'])
            rawdata2 = pd.read_excel(row, sheet_name='Tabelle1',
header = 4,
                skiprows =[5,6], usecols = ['Z', 'Vs', 'Go',
'Bodenansprache'])

            rawdata1['G0']= np.full(len(rawdata1), np.nan)

            for elem in range(len(rawdata2)): #insert G0 in rawdata2
                for row in range(len(rawdata1)):
                    if rawdata2.iloc[elem,0] == rawdata1.iloc[row,0]:
                        rawdata1.iloc[row,5] = rawdata2.iloc[elem, 2]
                        break

            data = data.append(rawdata1)
            break

data.iloc[:,3] = np.where(data['Qtn'] == '>1,000', np.nan,
data.iloc[:,3])
data.dropna(axis=0, inplace= True) #drop NaN
data.reset_index(drop=True, inplace=True)

data['qn'] = data['qt (MPa)'] - (data['σ,v (kPa)']/1000) #calculate qn

data['IG'] = data['G0']/ data['qn']  #calculate IG


""" data processing ------------------------------------------------"""

#lists of soil groups:
print(os.getcwd()) #show current working directory
os.chdir(r'E:\MA\Alle Becken\Task 7')
print(os.getcwd())

file = r"E:\MA\Alle Becken\Task 7\Sortierung Bodenansprachen.xlsx"
#lists file
print(file)

Bodenansprachen_Alle_Becken = pd.read_excel(file, sheet_name='Alle
Becken', skiprows= [1,2,3])

Bodenansprachen_Alle_Becken.drop(Bodenansprachen_Alle_Becken.columns

[Bodenansprachen_Alle_Becken.columns.str.contains('Unnamed')],
                axis=1, inplace=True)

BodenanspracheSoil1 = Bodenansprachen_Alle_Becken['Soil 1'].tolist()
```

```
BodenanspracheSoil2 = Bodenansprachen_Alle_Becken['Soil 2'].tolist()
BodenanspracheSoil3 = Bodenansprachen_Alle_Becken['Soil 3'].tolist()
BodenanspracheSoil4 = Bodenansprachen_Alle_Becken['Soil 4'].tolist()
BodenanspracheSoil5 = Bodenansprachen_Alle_Becken['Soil 5'].tolist()
BodenanspracheSoil6 = Bodenansprachen_Alle_Becken['Soil 6'].tolist()

Boden1 = list(set(BodenanspracheSoil1))
Boden2 = list(set(BodenanspracheSoil2))
Boden3 = list(set(BodenanspracheSoil3))
Boden4 = list(set(BodenanspracheSoil4))
Boden5 = list(set(BodenanspracheSoil5))
Boden6 = list(set(BodenanspracheSoil6))

Boden1 = [x for x in Boden1 if str(x) != 'nan']
Boden2 = [x for x in Boden2 if str(x) != 'nan']
Boden3 = [x for x in Boden3 if str(x) != 'nan']
Boden4 = [x for x in Boden4 if str(x) != 'nan']
Boden5 = [x for x in Boden5 if str(x) != 'nan']
Boden6 = [x for x in Boden6 if str(x) != 'nan']


def selectdata(Boden, data):
    selected_data_Boden = pd.DataFrame()
    for i in Boden:
        df = data[data['Bodenansprache'] == i]
        selected_data_Boden = selected_data_Boden.append(df)
        selected_data_Boden.reset_index(drop = True, inplace =True)
    return(selected_data_Boden)


selected_data_Boden1 = selectdata(Boden1, data)
selected_data_Boden2 = selectdata(Boden2, data)
selected_data_Boden3 = selectdata(Boden3, data)
selected_data_Boden4 = selectdata(Boden4, data)
selected_data_Boden5 = selectdata(Boden5, data)
selected_data_Boden6 = selectdata(Boden6, data)


""" data plotting ---------- SCATTER PLOT: Qtn/IG -----------------"""

'plot all in one graph'
fig, ax = plt.subplots(figsize=(8, 8), dpi = 2000
                       )
color = [#'tab:red', 'tab:orange',
         'forestgreen', 'olivedrab', 'midnightblue', 'rebeccapurple']
Boden = [#selected_data_Boden1, selected_data_Boden2,
        selected_data_Boden3, selected_data_Boden4,
        selected_data_Boden5, selected_data_Boden6]

for i, n in zip(Boden, color):
    x = i.iloc[:,7]
    y = i.iloc[:,3]
    ax.scatter(x,y, s=8, alpha=0.8, c = n)

ax.set_xscale('log')  # logarithmic scale
ax.set_yscale('log')  # logarithmic scale
ax.set_xlim(left=1, right=1000)  # set limits of plot
ax.set_ylim(bottom=1, top=1000)
#ax.grid(alpha=0.4, which='both')  # less well visible grid in
background
#ax.grid(alpha=1)  # "bolder" grid in the foreground of the plot
#ax.set_xlabel('IG = G0/qn')
#ax.set_ylabel('Qtn')
```

```
ax.get_xaxis().set_ticks([]) #turn off ticks
ax.get_yaxis().set_ticks([])
ax.get_xaxis().set_ticklabels([]) # turn off ticklabels
ax.get_yaxis().set_ticklabels([])

#legend
l = [#'Soil group 1: CSa →' Gr', 'Soil group 2: Peat',
     'Soil group 3: FSa →' CSa', 'Soil group 4: Si,fsa →' FSa,si',
     'Soil group 5: Si,cl- →' Si,fsa-', 'Soil group 6: Si,Cl →'
Si,cl']
fig.legend(labels=l, loc = 'upper center', ncol=2, markerscale = 4)

#ax.spines['top'].set_visible(False)

#plt.tight_layout()
plt.savefig('E:\MA\Alle Becken\Task
7\Output\Grafik8_QtnIG_Diagram.jpg',
            bbox_inches='tight', transparent = True)

end_time = time.time()
print("--- %s seconds ---" % (end_time - start_time))
```